STARCH 1500

submitted by
David Bradley Brook Simpson B.Pharm. (Hons), M.R.Pharm.S.
for the degree of Doctor of Philosophy
of the University of Bath, December 2000.

ProQuest LLC
789 East Eisenhower Parkway
P.O. Box 1346
Ann Arbor, MI 48106-1346

Acknowledgements

I would like to thank both of my supervisors, Mike Tobyn and John Staniforth for their guidance and support throughout my project.

I would also like to thank the following: Stephen Edge for his help and advice on the compaction studies, Fraser Steele for his encyclopaedic knowledge, Marina Levina for the rotary tablet press studies, Ian Blagborough for the use of his lab and students (Simon Carrington, Andy Geall and Adrian Neal) for their help with the extract analysis, Don Perry for providing an infinite supply of suitable apparatus for Soxhlet extraction, Kara Brennan and all at Phasex Corp. for the supercritical fluid extraction technique, Kevin Smith for his help using the GC/MS apparatus, everyone at the Department of Pharmacy, Queens University Belfast for their help using the Modulated Temperature DSC, David Apperly at Durham University for performing the Solid State NMR studies, Steve Newman at Cambridge University for performing the TG/MS study, everyone at electron optics for their help with the electron microscopy studies and to all my friends at the University of Bath.

Finally I would like to thank my parents and my beautiful wife Kathryn for all their love and support. I dedicate this work to them

Abstract

Starch 1500 is a partially pregelatinised maize starch. It is a widely used multipurpose excipient in direct compression and wet granulation tableting operations. Tableting formulation requires that an excipient has good compressibility characteristics. Although the properties of Starch 1500 are not poor in this regard, they do not approach the advantageous characteristics of a material such as microcrystalline cellulose.

The predominant mechanism by which Starch 1500 forms coherent compacts is through the formation of hydrogen bonds. The relatively poor compressibility of Starch 1500 has been primarily attributed to lubricant sensitivity and elasticity (combined with strain rate sensitivity). Few improvements of Starch 1500, related to improving its compressibility, have been made since its invention.

It is well documented that lipids are minor constituent of starches. They are located both within the granule and on its surface and may be removed using so-called 'defatting' techniques. It was discovered that defatting Starch 1500, by means of solvent extraction, produced a material with considerably enhanced pharmaceutical performance. This effect may be explained by the possibility that the extracted lipids were preventing the formation of the hydrogen bonds (in exactly the same was as hydrophobic lubricants), which normally strengthen the system.

A range of compression test techniques demonstrated that, under all conditions tested, defatted Starch 1500 produced stronger compacts than the parent material. The use of various solvent systems led to further improvements in performance. In some tests the optimised material performed in an almost equivalent manner to microcrystalline cellulose.

An extensive battery of additional tests demonstrated that these benefits came without detectable changes in the chemical constitution of the starch. Limited changes to the bulk physical characteristics (apart from the improved functionality) could be detected using very sensitive techniques.

Acknowledgements

Abstract

Table of Contents

CHAPTER 1

GENERAL INTRODUCTION

1.1 Tablet formulation and manufacturing

The compressed tablet is widely used for the administration of drugs via the oral route. Tablets provide a simple means of administering an accurate, unit dose of drug in a safe and effective manner (Banker and Peck, 1980). In order to meet this and other requirements the tablets must exhibit sufficient weight and content uniformity along with suitable dissolution characteristics following administration. The active drug component must possess adequate chemical stability within the dosage form. In addition, the tablets should be sufficiently robust to ensure product integrity prior to administration and the formulation should allow production on an industrial scale to an appropriate level of product quality (York, 1988).

In the majority of cases, such tablet characteristics cannot be achieved simply by the compression of the active alone. It is usually necessary to incorporate additional pharmacologically inert compounds known as excipients prior to compaction. One of the main class of excipient is the "filler" or "diluent", which is added to the formulation to improve, for example, its compactibilty and increase the bulk of the tablet.

1.2 Powder processing techniques prior to compaction.

Tablets are produced by the compaction of either granules or dry powder blends of the formulation. Wet granulation involves the agglomeration of the components of the formulation using binding fluid (Führer, 1996). The discrete granules resist segregation and may show improved powder flow and compressibility. As a consequence of the introduction of moisture into the formulation and the necessary drying stage the chemical stability of the active component may be affected.

Direct compression is the simplest method by which tablets are manufactured. This process involves firstly dry blending the active drug compound with the other components of the formulation prior to the compaction of the blend into a coherent tablet. The advantages conferred by direct compression have been reviewed elsewhere (Bolhuis and Chowhan, 1996; Armstrong, 1988). These include process simplicity and reduced production costs in addition to potentially greater chemical stability of the drug. Excipient characteristics are more critical in direct compression formulations as the characteristics of the blend cannot be easily altered or enhanced by process manipulation. For this reason it is desirable for a direct compression formulation to resist segregation, be free flowing and compressible.

1.3 Native Starch – An introduction and description

After cellulose, starch is the second most abundant naturally occurring biopolymer in nature. Starch is found in the form of small granules at various sites in all forms of green leafed plant, where it serves as an energy reserve during dormancy and germination (Zobel, 1988). In 1985 the total annual world production of commercial starches was estimated at approximately 17 million tones of which nearly 60% was obtained from maize (Swinkels, 1985). Other sources of starch that are used for commercial purposes are wheat, potato and rice. The physical properties and chemical composition of starches obtained from different botanical sources show considerable variation. Factors such as granule morphology, the degree of polymerization and ratio of amylose and amylopectin and gelatinisation temperature have been used to distinguish the origin of the starch (Swinkels, 1985).

1.3.1 Major components

Starch is primarily a mixture of two polysaccharides, amylose and amylopectin, the building blocks of which are α-D-glucose units. Amylose is essentially a linear glucan that naturally adopts a helical conformation as a consequence of its α(1,4)-linkage. Amylose may adopt either an extended or collapsed helical conformation, both of which possess six glucosyl units per turn. The extended form repeats in a distance of 21 Ångströms (Å) and the collapsed form in 8Å (Zobel, 1988). The collapsed amylose helix has a hydrophobic core comprised of hydrogen and carbon atoms. This allows complexation to occur with hydrophobic compounds such as lipids, surfactants and iodine.

Amylopectin is a linear α(1,4)-linked glucan, with α(1,6)glycosidic linkages approximately every 20 to 25 glucose units (Ring, 1995). The linear portions of amylopectin possess the same helical conformation as amylose. The currently accepted model of the structure of amylopectin is pivotal to the general model of native starch granule ultrastructure. The cluster model was proposed by both French (1972) and Nikuni (1978). In this model, the high degree of ordering observed in starch granules is attributed to amylopectin through the association of inter-adjacent linear sections of the molecule as double helices (French, 1984; Imberty et al, 1988). The granule is composed of alternating amorphous and crystalline growth rings that spread radially through the granule (Jenkins et al , 1993). Native starches show a limited level of swelling in cold water. The degree of granule swelling seen is proportional to the level of crystallinity within the granule.

Here the crystalline regions maintain the structural integrity of the granule, thus limiting the degree of swelling (Collinson, 1968). Conversely this may also influence the material's compaction properties, in that the crystalline regions may contribute to the elastic component of native starch. This suggestion is supported by the findings that where the native structure has been destroyed or modified, e.g. in pregelatinised starch, the material is more compressible (Manudhane et al, 1969).

Upon heating hydrated starch granules a critical temperature is reached where the ultrastructure of the granule is irreversible changed. This process is known as gelatinisation and involves water absorption into the granule followed by granular swelling, amylose leaching and the dissociation of the amylose double helices (Tester and Morrison, 1990). The loss of molecular order which accompanies the process of gelatinisation has been widely studied using differential scanning calorimetry and is greatly influenced by the water content of the system (Liu and Lelievre, 1993; Lund, 1983).

The crystalline regions of the granule are further comprised of alternating crystalline and amorphous lamellae (Zobel, 1988; Manners, 1989). Here, the double helices are located in the crystalline regions whereas the α(1,6)-branch points lie in the amorphous lamellae. This structure is illustrated in figure 1.1 (Jenkins et al, 1994).

Studies performed using ^{13}C Cross Polarisation Magic Angle Spinning Nuclear Magnetic Resonance (CPMAS-NMR) spectroscopy identified 3 separate regions within the starch granule: a highly crystalline region comprised of amylopectin double helices, a "solid-like" region arising from lipid-amylose complexes and an amorphous region that was attributed to the α(1,6)-branch points of amylopectin and the lipid free growth rings of amylose (Morgan et al, 1995).

1.3.2 Minor Components

In addition to amylose and amylopectin starch also contains trace levels of several other components (e.g. proteins, lipids, phosphorus, silica). Of these components, the presence of proteins and lipids are regarded as the most significant. Although they constitute only a minor proportion of the granule, their presence has been demonstrated to elicit significant effects on its properties (Cauvain et al, 1977).

Figure 1.1: Diagram showing the ultrastructure of a native maize starch granule

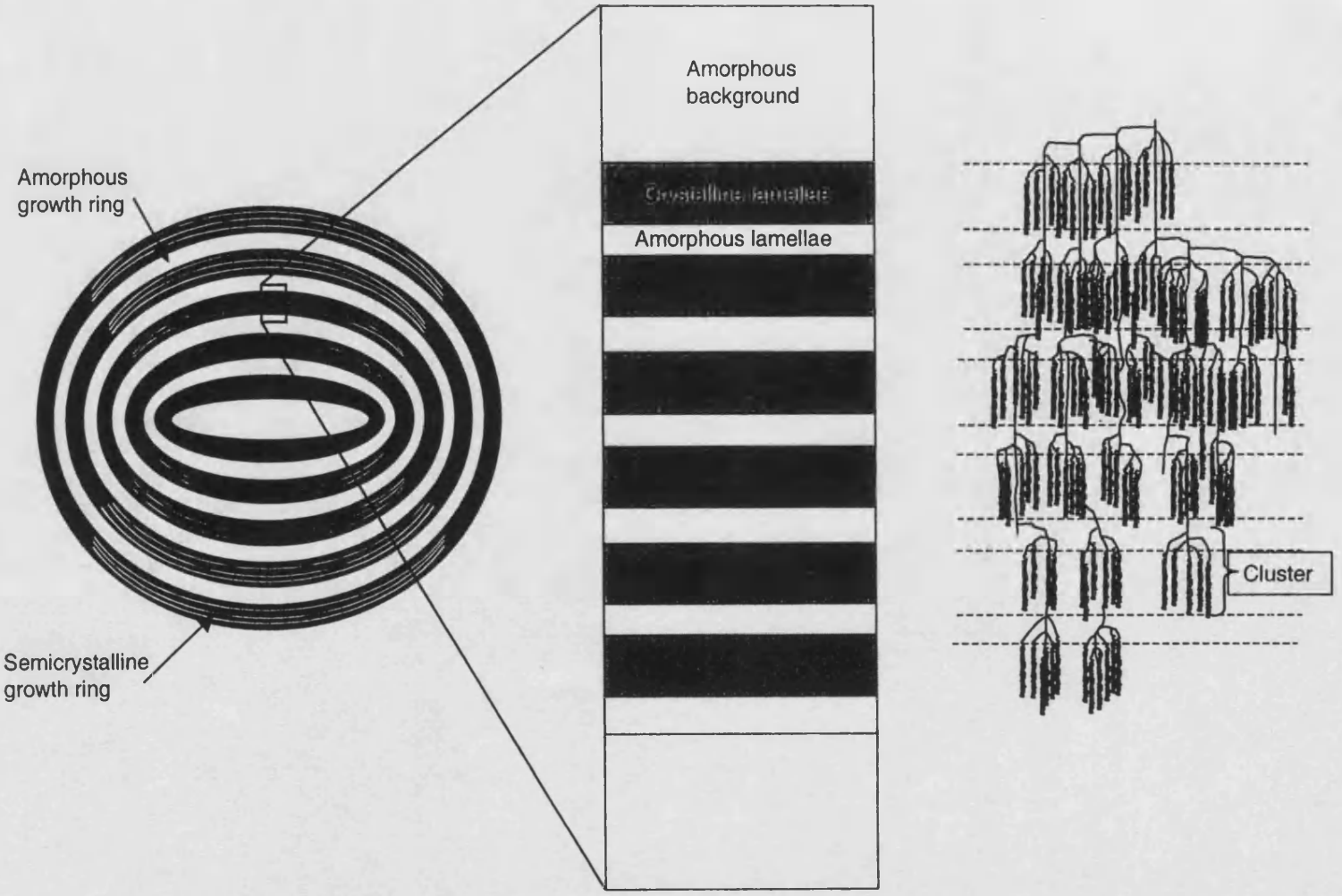

Cereal starches such as those from maize and rice contain a high percentage of lipids (0.6 – 1.0%$^{w}/_{w}$) when compared to, for example, potato starch (0.05%$^{w}/_{w}$) (Swinkels, 1985). These lipids are present both on the surface of the starch granule as well as internally (Morrison, 1981). The surface lipids can be further classified into "starch lipids" and "non-starch lipids", the latter occurring in plant tissue and becoming absorbed onto the surface of the starch granules during their isolation (Morrison, 1981; Galliard and Bowler, 1987).

In maize starch the internal lipids are mainly monoacyl lipids, present as lysophospholipids and free fatty acids (Hargin and Morrison, 1980; Morrison, 1981) some of which may be bound as amylose-lipid inclusion complexes (Acker, 1977) within the granule. Furthermore lipids may be bound either by ionic or hydrogen bonding to the hydroxyl groups of amylose and amylopectin. Oostergetel and van Bruggen (1993) proposed in the crystalline lamellae of starch, the amylopectin double helices are further organized into superhelices. Morgan et al (1995) suggested that the centre of these superhelices may be a site of enzymatic attack. Furthermore it was proposed that amylose-lipid complexes plug the core of the superhelicies thus preventing enzymatic degradation. Vasanthan and Hoover (1992) have also suggested that amylose becomes more susceptible to enzymatic attack by alpha amylase hydrolysis after lipid removal. It is thought that this is due to a change in the amylose conformation, from helix to random coil. It has been demonstrated that amylose-lipid complexes are less susceptible to alpha amylase attack, than free amylose (Schweizer et al, 1986; Holm et al, 1983). However increased alpha amylase activity has been observed in defatted starches with only trace quantities of complexed lipids (Sair, 1964). It has been suggested that in such cases the thermal energy provided by defatting allows the mobilisation of amylose chains into the amorphous regions of the granule and hence they become more accessible for enzymatic hydrolysis.

Cereal starches contain approximately 0.25 – 0.5%$^{w}/_{w}$ of proteins. It is generally accepted that the majority of these proteins are biosynthetic and degredative enzymes associated with the granule (Imam, 1989). It has been suggested that internal starch proteins occur as a consequence of residual material being trapped during the synthesis of the granule (Stark and Lynn, 1991). Proteins have been demonstrated to affect starch properties such as flavour and colour (Swinkels, 1985) and paste viscosities (Miller et al, 1973). One of the main components present in the granule is a 15-kDa protein called friabilin, which is involved in

determining the hardness of the endosperm (Greenwell and Schofield, 1986). The nature of starch surface proteins has been reviewed elsewhere (Greenwell et al, 1985; Sulaiman and Morrison 1990).

1.4 Starch 1500 – an introduction and description

Pregelatinisation involves the disruption of native starch granules by chemical, thermal or mechnical processes at high moisture levels (Lordi, 1994). Such a treatment may result in the partial or total gelatinisation of the granules, which are then dried. In the case of partially pregelatinised starches, such as Starch 1500, the finished product contains aggregates of unmodified granules in a matrix of pregelatinised starch (Colorcon Product Literature).

Starch 1500 production involves thermal modification of 20% of the starch through a process of continuous extrusion of native starch granules. The granules are presheared at a constant rate in a pellet mill. This fracturing allows gelatinisation to occur more readily through reduced granule integrity. The process of Starch 1500 production is summarised in figure 1.2 (supplied by Colorcon).

The main stages of the process involve firstly mixing the native maize starch with water prior to extrusion. It is necessary to moisten the starch in this way to prevent charring through the high shear conditions of extrusion. As the starch exits the extruder it is partially pregelatinised and in the form of dense pellets, which are approximately 1cm in diameter. The extruded material is subsequently dried and the pellets broken down into smaller fragments. The starch material which is now in the form of a coarse powder is then fed through a cyclone which removes from it fine particles (<5 μm). The coarse material, prior to being screened, is exposed to a high humidity conditioning process. The final product is then blended with product from additional lines before being packaged and "hot-roomed" (for microbiological purposes). Material that does not pass physical quality control tests is returned to the extruder for further processing with native starch. Points of interest relating to Starch 1500 production include the fact that only 20% of the native starch which passes through the extruder is pregelatinised. Regarding the high degree of shearing and milling that the material is exposed to it seems unlikely that the remaining 80% of native starch remains unaffected by the processing.

Figure 1.2: Flow diagram describing the stages of Starch 1500 production

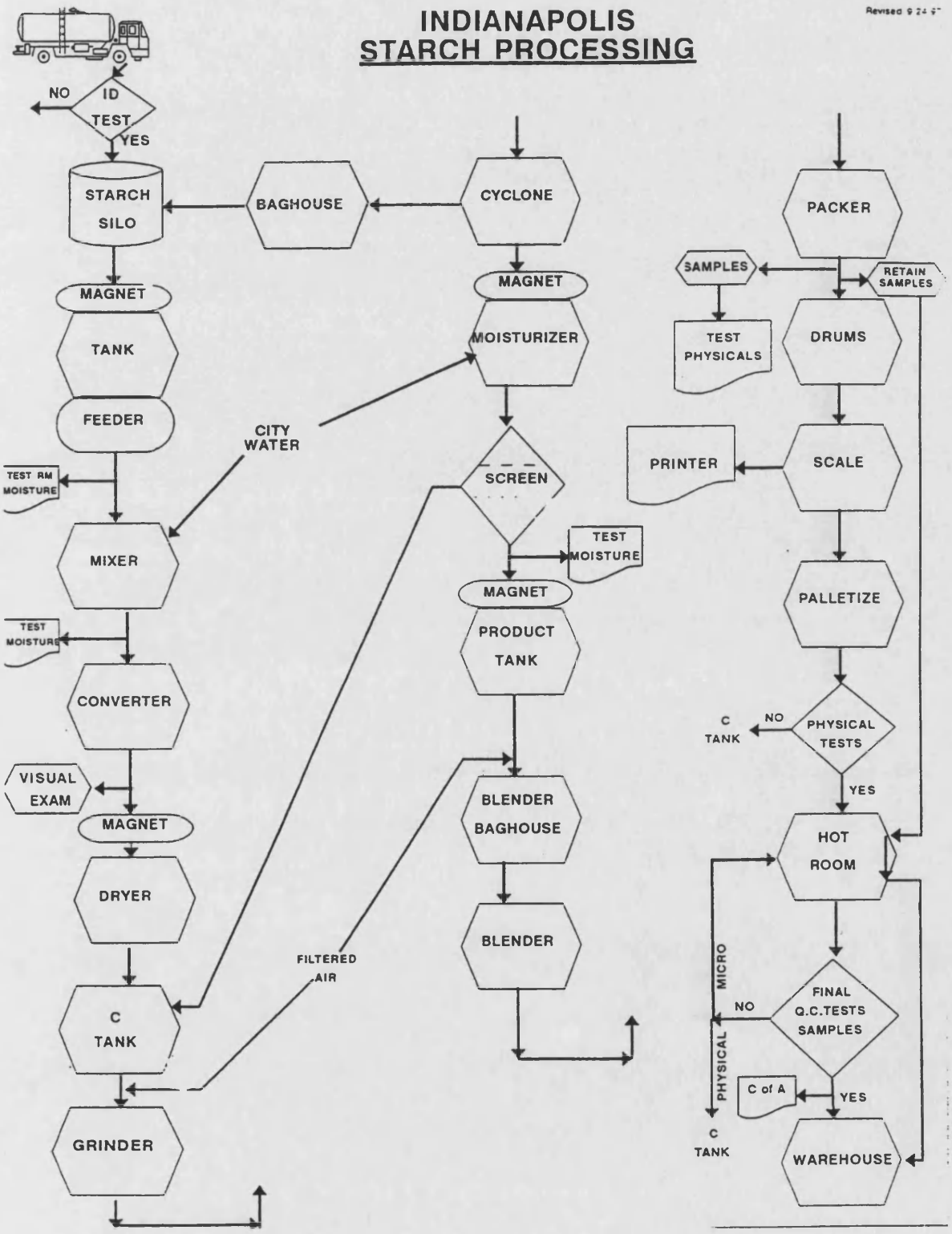

The degree of pregelatinisation is dependent on the starch bleaching process used by the native starch supplier. High bleaching levels will result in higher levels of cold-water soluble (CWS) starch. The degree of pregelatinisation is assessed through the CWS levels. Any changes in the CWS levels are rectified by altering the level of bleaching of the native starch.

Studies suggest that the bleaching of native starch affects the lipid component of the material (Youngquist et al, 1969). This particular study demonstrated that the gelatinisation properties of unmodified starch were affected by chlorination, however defatted starch demonstrated no such change on bleaching. Such a result may suggest that the lipid and protein present on the surface of the granules acts as a protective barrier that can limit gelatinisation. Studies by Seguchi (1984, 1985) suggest that chlorination results in the hydrophobic modification of the surface proteins of the starch granules. The level of bleaching required to obtain the desired level of pregelatinisation is known to demonstrate seasonal variation. This may be attributed to variation in the level of protein and lipid deposition on the granule surface throughout the season.

Conflicting evidence was provided by another study (Telloke, 1985), which suggested that with increased chlorination levels there was a proportional increase in amylose leaching from the granules. This effect was attributed to chlorine-induced depolymerisation. In addition this study revealed no evidence of a non-carbohydrate (i.e. protein and lipid) involvement.

Cold-water soluble starch can be liberated by mechanically damaging starch granules by milling. It has been demonstrated that amylopectin is preferentially released into solution from mildly damaged starch granules (Craig and Stark, 1984). It was suggested that mild damage resulted in the cleaving of protruding amylopectin clusters from the surface of the granules (Stark and Yin, 1986). In the case of more severe damage, as would be expected to occur in the high shear processing of Starch 1500, both amylose and amylopectin are released as cold water soluble fractions of starch (Glennie et al, 1987). In wet granulation systems native starches are gelatinised and used as binding agents (Khankari and Hontz, 1997). The cold water solubility of Starch 1500 conferred by pregelatinisation negates this initial heating stage, this improving the efficiency of the granulation process.

The use of native starch as a tablet disintegrant is well recognized (Ingram and Lowenthal, 1966; Patel and Hopponen, 1966). As a consequence of partial pregelatinisation, Starch 1500 retains the disintegrant properties of native maize starch but with the additional disintegrant action of liberated free amylose (Colorcon Product Literature). Although the moisture content of Starch 1500 is over twice that of microcrystalline cellulose (approximately 10 – 12%$^{w}/_{w}$ and 5%$^{w}/_{w}$ respectively), the former has been demonstrated to have no effect on the stability of moisture sensitive materials such as aspirin (Manudhane, 1969). It is suggested that the water in Starch 1500 is highly bound and therefore does not attack such materials. From this evidence it may be seen that Starch 1500 provides the potential for use as an economical, multi-purpose, direct compression excipient and for these reasons it is widely used. However if compared to other materials currently available, such as microcrystalline cellulose, it exhibits both poorer flow and compressibility.

1.4.1 Tabletting properties

It has been demonstrated that Starch 1500 shows a higher compressibility (Manudhane et al, 1969) and flowability (Sakr et al, 1973) than native maize starch as a consequence of the agglomeration native granule in a matrix of pregelatinised starch. Further details of the properties of Starch 1500 have been reviewed elsewhere (Bolhuis and Chowhan, 1996)

Scanning electron microscopy of Starch 1500 particles both before and after compaction failed to identify any significant degree of fragmentation, although a slight change in particle shape was observed (Duberg and Nystrom, 1982). It has suggested that the apparent resistance to aggregate shearing, may be responsible for the high degree of lubricant sensitivity observed with Starch 1500 (Shangraw et al, 1981). It has been demonstrated that the tensile strength of Starch 1500 compacts is dependent on the particle size (Alderborn and Nyström, 1982a). Due to the lack of fragmentation of the material on compaction, factors such as particle shape (Alderborn and Nyström, 1982b) have a great influence on tensile strength.

Starch 1500 has an inherent lubricity, resulting from slow initial, post-compaction relaxation that exerts minimal pressure on the die wall during compact ejection (Travers and Cox, 1978). On blending with a hydrophobic lubricant such as magnesium stearate, Starch 1500 produces significantly weaker compacts (Sakr et al, 1973; Manudhane et al, 1969).

1.4.2 Lubricant Sensitivity

It is widely recognized that blends of hydrophobic lubricants and plastically deforming excipients such as starch and microcrystalline cellulose form much weaker compacts than unlubricated material (Bolhuis et al, 1975; Jarosz and Parrott, 1984). It is thought that such hydrophobic materials form a film around the individual particles (Strickland et al, 1956) that inhibits the formation of interparticulate hydrogen bonds (De Boer et al, 1978). Studies performed using microcrystalline cellulose demonstrated that the in-die porosity of lubricated and unlubricated compacts was that same, however the lubricated compacts displayed a greater degree of relaxation resulting from the inhibition of the interparticulate bonds (Zuurman et al, 1999).

A comparison of the compaction characteristics and lubricant sensitivity of native starches from various botanical sources demonstrated that rice starch had the highest compactibility and the lowest lubricant sensitivity (Bos et al, 1987). This was attributed to the fine particle size of native rice starch that resulted in a higher surface area for bonding and hence stronger compacts. The lower lubricant sensitivity was thought to arise from the poor flowability of the material, which was thought to restrict the distribution of the lubricant. On granulating native rice starch, both the compactibilty and flowabilty of the material was increased yet so was the lubricant sensitivity.

Heckel analysis of Starch 1500 has demonstrated that it undergoes a high degree of plastic deformation and that dwell time greatly affects the strength of the compact produced (Armstrong and Palfrey, 1989; Rees and Rue, 1978; Duberg and Nystrom, 1982; Humbert-Droz et al, 1982). It has been suggested that the low strength of Starch 1500 compacts results from plastic deformation occurring too slowly to form sufficient interparticulate bonds (Rees and Rue, 1978). Compared to other plastically deforming materials, Starch 1500 produces weak tablets, in addition it displays high lubricant sensitivity (Lerk et al, 1977; Bolhuis et al, 1985). The deleterious effect on tablet strength of hydrophobic lubricants can be somewhat overcome by blending with colloidal silica prior to the addition of magnesium stearate (Schrank-Junghäni et al, 1984). The addition of colloidal silica acts to prevent the lubricant film formation around the Starch 1500 particles.

1.5 Other starch-based excipients

Numerous attempts have been made to produce a directly compressible starch based excipient. Several investigations have concentrated on using modified potato starches as hydrophilic matrices to control drug release (Herman et al, 1989). Maltodextrins such as maize starch-based Soludex™ 15 (Penford Products Co., IA, USA) are obtained by the hydrolysis of starch in acidic or enzymatic conditions. Soludex™ 15 demonstrated better flow than microcrystalline cellulose but its compressibility was lower and also exhibited lubricant sensitivity (Parrott, 1989).

Sepistab® St200 (Seppic Co., Paris, France) is a directly compressible starch based excipient derived from maize starch. It has been demonstrated that Sepistab® St200 shows improved flowability and is a more effective disintegrant than Starch 1500 (Mondero Perales et al, 1996) however this material is only minimally stronger than Starch 1500 and the addtion of hydrophobic lubricants has a similarly deleterious effect on tablet strength (Bolhuis and Chowhan, 1996).

Era-Tab® (Erawan Pharmaceutical Research and Laboratory Co., Ltd., Bangkok, Thailand) is a spray-dried rice starch comprised of near-spherical agglomerates of native granules (Mitrevej and Varavinit, 1988) of higher flowability than Starch 1500 (Mitrevej et al, 1996). It has been suggested that Era-Tab® can form stronger compacts than Starch 1500 but is also weakened by the addition of magnesium stearate (Mitrevej et al, 1996). An extensive literature review failed to reveal any further information on this material, which seems not be widely used (Levina, personal communication).

1.6 Aims of the study

Starch 1500 is a partially pregelatinised maize starch that is utilised as a multipurpose excipient both in direct compression and wet granulation tablet formulations. A tablet is only as strong as the weakest component of the formulation, for this reason, where used Starch 1500 comprises approximately 10%$^{w}/_{w}$ of the formulation. It is widely accepted that the tensile strength of Starch 1500 is below that required for direct compression formulations and therefore the proportion used is limited. If the tabletting properties of Starch 1500 could be improved then greater proportions could be included in formulations.

There exists a trend towards the simplification of formulations by the rationalisation of the number of components. Therefore multifunctional excipients such as Starch 1500 are prime candidates for property optimisation. A wealth of literature exists describing the compression characteristics of Starch 1500 and other plastically deforming materials, however no progress has been made in improving this material's compression properties. Therefore attempts were made to identify the factors affecting the mechanical properties of Starch 1500 starting with an in depth study of the raw material native maize starch.

Very few electron micrographs of Starch 1500 exist in the literature (Shangraw et al, 1981; Alderborn and Nyström; Bolhuis and Chowhan, 1996). Such qualifying information is regarded as fundamental to the characterisation of a material. It is known that starches have high moisture contents. Such materials are typically complex to characterise by conventional scanning electron microscopy techniques. It was therefore considered essential to develop alternative microscopic techniques to elucidate the structure of Starch 1500 and to allow a greater understanding of the material's functionality.

Several approaches have been taken to enhance the physical properties of starch by chemical modification. These include the development of the super-disintegrant, sodium starch glycolate in which the natural swelling properties of the granule are enhanced by chemical substitution at the surface of the material. However the enhanced disintegration properties of this material are still accompanied by poor flow and compressibility. High amylose cross-linked starches have been investigated as potential excipients for use in controlled-release preparations (Lenaerts et al, 1998). Cross-linked starches exhibit gel formation on wetting with

minimal swelling or erosion and increased water uptake, thus providing a hydrophilic matrix for controlled drug release.

In addition to the failure to improve the compressibility of starch, chemical modification also incurs further expense of material processing and production of a new chemical entity. The aim of this study was, with an in-depth knowledge of the chemical and physical composition of the material, to determine whether the compactibility and flowabilty of Starch 1500 could be improved by physical rather than chemical modification.

CHAPTER 2

ASSESSMENT OF THE PHYSICAL AND MECHANICAL PROPERTIES OF UNMODIFIED AND DEFATTED STARCH 1500 COMPACTS

2.1 GENERAL INTRODUCTION

As has previously been reported, the predominant mechanism by which Starch 1500 forms coherent compacts is through the formation of hydrogen bonds (Karehill et al, 1993). It has been demonstrated that plastically deforming materials exhibit lower crushing strengths on mixing with lubricants (Bolhuis et al, 1985). This phenomenon results from the formation of a hydrophobic film around the particles, which interferes with the hydrogen bonding process. This effect has been attributed to the presence of weak lubricant-lubricant bonds at the interface of particles covered in such a hydrophobic film (De Boer et al, 1978). The presence of lipids that are associated with starch granules has been well documented (Whistler et al, 1965). Attempts have been made to classify these lipids as either "starch surface lipids" or "internal starch lipids" (Morrison, 1981) and as a result selective extraction techniques have been developed for each category (Morrison, 1981; Vasanthan and Hoover, 1992).

The aim of this study was to investigate the mechanical properties of compacts prepared from Starch 1500 defatted using various solvent systems. Assessment of the peak tensile strength and the pore size distribution of these compacts will be discussed.

2.2 GENERAL METHODS

2.2.1 Compact Preparation

(i) *Using the compaction simulator*

The majority of starch compacts were prepared using a compaction simulator (ESH Testing Ltd., Machine No. 4287, Brierly Hill, U.K.), which enabled force and speed of compaction to be accurately controlled. The compaction simulator was equipped with a 100kN load cell and fitted with 10mm flat-faced F tooling. Linear variable differential transformers (LVDT) that were attached to the upper and lower punches of the simulator were used to monitor the displacement of the punch tips from a reference position (designated as zero). This allowed determination of the separation of the punch faces at any point in time. A saw-tooth displacement time profile was employed at a compaction speed of 16mm s^{-1}. Compaction force was determined by adjusting the penetration distance of the upper punch into the die. Compact weight was selected by determining the weight of material that would be required to produce a 3.5 X 10mm compact at zero porosity. For this calculation the true density of Starch 1500 determined in section 4.3.4 was used. The target compact weight was calculated to be 0.412 g. Accurately weighed samples were

measured into the die cavity and compacted at upper punch forces of approximately 4, 8, 12, 16 and 20kN. Sixteen compacts were prepared at each compaction force, of which 10 were used to determine the tensile strength of the material (section 2.2.2) and 6 were subject to analysis by mercury intrusion porosimetry (section 2.2.3). The punches and die were not pre-lubricated prior to testing so that the ejection force of the formed compacts could be measured.

(ii) *Using the Instron tensile testing instrument.*

Compacts of starches were prepared using an Instron 1185 test machine (Instron, High Wycombe, U.K.) equipped with a 500 kN load cell and heat-treated silver steel die and flat-faced punches. Compacts were formed at various loads with either a 25 mm or a 10 mm diameter die for which 6 g or 0.412 g respectively of material were accurately measured prior to compaction. A compaction speed of 10 mm min^{-1} and a dwell time of 1 minute were used.

(iii) *Using the Piccola® instrumented rotary tablet press*

A Piccola PI-080, ten station instrumented tablet press (Riva S.A., Buenos Aires, Rep. Argentina) fitted with 10mm flat-faced "B" type tooling was used to prepare 20 - 30 compacts at upper punch forces of approximately 4, 8, 12, 16 and 20kN. Five stations were selected and turret speeds of 20 and 30 RPM were used. The tablet dies were filled via a paddle feeder. The tablet press was equipped with upper and lower pin load cells (Specialty Measurements Inc., NJ, U.S.A.) to measure upper punch forces and ejection forces respectively. The signals from the load cells were processed using "The Director" software (Specialty Measurements Inc., NJ, U.S.A.).

2.2.2 Diametric tensile testing of compacts

The tensile strength of the compacts was determined approximately 24 hours after compaction to allow for elastic recovery. Prior to testing, the compacts were stored in a controlled humidity chamber, maintained at 44% RH. Diametric tensile testing was performed using either a Schleuniger 2-E tensile tester (Dr. K. Schleuniger & Co., Switzerland) or an Instron 1122 test machine (Instron, High Wycombe, U.K.) equipped with a 100kN load cell and operating at a crosshead speed of 5 mm min^{-1}. Tensile strength was calculated as described by equation 2.1 (Fell and Newton, 1970).

$$\text{Tensile strength} = \frac{2P}{\pi Dt} \qquad \text{Equation 2.1}$$

Where: P = Peak force required to cause tensile failure.

D = Diameter of the compact

t = thickness of the compact.

2.2.3 Mercury intrusion porosimetry studies of material compacts

Mercury intrusion porosimetry was performed on compacts prepared at upper punch forces of approximately 4, 8, 12, 16 and 20kN using the method outlined in section 4.3.7. Three compacts were placed into one of two 5ml solid penetrometers which had stem volumes of 0.4120 and 0.3920 ml respectively. Analysis of the compacts was again performed at pressures equating to pore sizes between 0.0034 and 18.1μm.

2.3 RESULTS & DISCUSSION

2.3.1 Study of the effect of the removal of free surface lipids on the tensile strength of Starch 1500 compacts

Vasanthan and Hoover (1992) developed a relatively gentle extraction process by which free lipids may be removed from the surfaces of starch granules with minimal disturbance of the internal structure of the granule. This was achieved by adding 50g of Starch 1500 to a 2 litre, volumetric flask containing 1 litre solution of chloroform-methanol 2:1 $^{v}/_{v}$ (CM). This was vigorously agitated at ambient laboratory temperatures for 60 minutes. After this period the starch slurry was filtered and washed through with fresh CM solvent, to remove any residual extract remaining on the material. Tablets were produced from Starch 1500 and the CM treated material using the compaction simulator as described in section 2.2.1(i). The tensile strengths of the materials were determined as described in section 2.2.2. Figure 2.1 demonstrates that tablets prepared from Starch 1500 which had been exposed to this process, produced compacts of an apparent higher tensile strength than the unmodified material. It was only possible to acquire data points of 4 and 8kN for the CM treated material. This was because the tablets produced at higher compaction forces were too strong to break using the Schleuniger 2-E tensile tester.

The CM solvent system is thought to remove only free surface lipids as its penetration into the interior of granule and capacity to extract bound lipids will be

limited when used at ambient temperatures (Vasanthan and Hoover, 1992). However, it has been reported that starch lipids may also be bound to the surface of the granule by ionic or hydrogen bonding (Mikus, et al, 1946; Morrison, 1981; Galliard and Bowler, 1987). As such it may be necessary to use more powerful extraction techniques to ensure further removal of surface lipid. Hot solvent extraction, using the Soxhlet apparatus, is a well-documented means of removing bound lipid from starch granules (Whistler et al, 1965; Morrison, 1981). Thus experiments were undertaken to determine whether removal of free and bound lipid by Soxhlet extraction resulted in modification of the tensile strength of Starch 1500.

2.3.2 A study of the effect of lipid removal by hot ethanolic solvent extraction on the tensile strength and pore size distribution of Starch 1500 compacts

Bhatnagar and Hanna (1994 and 1997) attemped to remove uncomplexed lipids from extruded starch using the Soxhlet apparatus (figure 3.1) with petroleum ether at 37°C. Initial studies were performed using this method, however defatting for 24 hours failed to yield a material with improved tabletting properties. This was attributed to the failure of the solvent to remove any appreciable quantity of lipid from Starch 1500. In the studies by Bhatnagar and Hanna (1994 and 1997) no attempt was made to analyse the lipid extract and as such there is no evidence that petroleum ether is capable of lipid removal from starch. It was proposed that this was a result of the non-polar nature of the solvent used. To overcome this problem 96% ethanol was used as an alternative solvent for extraction. Starch 1500 was treated with 96% ethanol for 24 and 48 hours (referred to as DF24-96-01 and DF48-96-01 respectively) using the Soxhlet extraction apparatus. Figure 2.2 demonstrates that the defatted materials produced stronger tablets than Starch 1500 and were comparable in strength to CM treated Starch 1500. Again, data could only be collected for DF24-96-01 and DF48-96-01 at low compaction forces for the reason outlined above. For this reason diametric tensile testing was performed using an Instron 1122 test machine, on which it was possible to apply loads of up to 100 Kg and thus test much stronger compacts. The procedure for testing is outlined in section 2.2.2.

Figures 2.3 and 2.4 show the incremental mercury intrusion plots for Starch 1500 and DF48-96-01 compacts respectively, produced at upper punch forces of 4, 8, 12, 16 and 20kN. Incremental intrusion (ml/g) is presented on a linear scale and pore diameter (μm) is on a logarithmic scale. With increasing compaction force a

reduction in intra-particulate void space is observed in the distribution of pore sizes between 3 and 7μm in Starch 1500 and 1 to 3μm in DF48-96-01 as a shift in the maximum towards smaller pores. The densification of both materials also results in a reduction in the porosity, total pore volume and the median pore diameter (see table 2.1).

Table 2.1: Effect of compaction force on the pore parameters of compacts of Starch 1500 and DF48-96-01

Upper Punch Force (kN)	Porosity (%)		Median Pore Diameter (μm)		Total Pore Volume (ml g^{-1})	
	Starch 1500	DF48-96-01	Starch 1500	DF48-96-01	Starch 1500	DF48-96-01
4	37.16	15.92 23.51	2.71	2.22 5.37	0.342	0.129 0.207
8	30.17 30.03	17.44 21.80	5.06 3.11	2.17 2.41	0.267 0.261	0.129 0.166
12	25.19 22.67	13.60 15.69	3.58 3.12	1.26 1.86	0.202 0.173	0.095 0.113
16	22.88 22.93	11.35 14.89	3.34 3.30	1.14 1.42	0.178 0.178	0.077 0.104
20	21.69	11.68	2.97	0.77	0.166	0.079

The data in given in table 2.1 demonstrates such variability as to necessitate further experimental work before any firm conclusions can be drawn. However as can be seen from table 2.1 defatted Starch 1500 consistently produces compacts of a lower porosity than unmodified Starch 1500 at equivalent compaction forces.

2.3.3 A study of the effect of Soxhlet extraction on the tensile strength of Starch 1500 compacts prepared using solvents of varying polarities

Initial studies had shown that defatting Starch 1500, using a polar solvent such as ethanol, yielded a material capable of forming tablets, which were apparently stronger than the commercially available product. Numerous schemes allow the classification of solvent polarity, (Ho, 1991) one of which is the Hildebrand Solubility Parameter (δ). The solubility parameter is a numerical value that indicates the relative solvency behavior of a specific solvent. It is derived from the cohesive energy density of the solvent, which in turn is derived from the heat of vaporization.

From the heat of vaporization, in calories per cubic centimeter of liquid, we can derive the cohesive energy density (c) by the following expression

where: $\delta = c^{0.5} = \left[\frac{\Delta H - RT}{V_m}\right]^{0.5}$ Equation 2.2

c=Cohesive energy density

ΔH=Heat of vaporization

R=Gas constant

T=Temperature

V_m=Molar volume

Hildebrand proposed that the square root of the cohesive energy density (c) could be taken as a value indicating the solvency behavior of a specific solvent. Thus a range of values will be seen for polar (high values) and non-polar (low values) solvents. Furthermore it is noteworthy that the Hildebrand value of a solvent mixture can be determined by averaging the Hildebrand values of the individual solvents by volume. Theoretically, this would allow the prediction of the solubility of a mixture using only the properties of its components.

Table 2.2 shows δ values for a range of solvent systems, which were used to defat Starch 1500 by means of soxhlet extraction, as detailed in section 3.2.1.1.

Table 2.2: SI Hildebrand Solubilty Parameter (δ) values (Barton, 1983).

Pure Solvent	δ/MPa$^{1/2}$	Ethanol Conc. (%$^{v}/_{v}$)	δ/MPa$^{1/2}$
Water	48	99.7 (absolute)	26.3
Methanol	29.7	96	27.1
Ethanol	26.2	85	29.5
n-propanol	24.9	70	32.7
n-butanol	23.1	60	34.9
n-hexane	14.9		

It is apparent from figure 2.5 that all of the defatted materials produced compacts of higher tensile strengths, than those of unmodified Starch 1500, at the compaction pressures tested. Some correlation between δ values for each solvent and tensile strength of the defatted material is observed. The hexane (DF48-He-03) and n-butanol (DF48-Bu-01) defatted materials produced the weakest tablets. Starch

1500 which had been defatted with methanol (DF48-Me-02), ethanol (DF48-96-01A) or n-propanol (DF48-Pr-04) produced tablets that were apparently stronger than DF48-Bu-01 and DF48-He-01.

No apparent difference could be found between the tensile strengths of DF48-Me-02, DF48-96-02A and DF48-Pr-04 compacts. Figure 3.2 demonstrates that the quantity of lipid extracted increases with the polarity of the solvent used. Thus maximal removal of surface lipid may be possible with n-propanol. Further lipid removal with methanol and ethanol may have little effect on the tensile strength of the material if further lipid removal occurs from the internal granule structure.

Further evidence to support this theory is given in figure 2.6, which illustrates the effect of ethanol concentration on the tensile strength of defatted Starch 1500 compacts. All of the ethanol defatted materials were apparently stronger than Starch 1500. There was no apparent difference in the tensile strength of Starch 1500 defatted with 85% (DF48-85-01), 70% (DF48-70-01) and 60% (DF48-60-01) ethanol.

2.3.4 A comparison of the tensile strengths of Starch 1500 compacts prepared from material defatted in the standard and giant Soxhlet extraction apparatus

For the purpose of preparing more material for additional testing, a giant Soxhlet apparatus, capable of defatting approximately 500g of Starch 1500 (figure 3.1) was run alongside the standard Soxhlet apparatus. Figures 2.7 and 2.8 illustrate the tensile strengths of Starch 1500 compacts, which were defatted in the standard and giant Soxhlet apparatus with hexane and propan-1-ol respectively. For both solvents, the materials defatted in the standard Soxhlet apparatus produce compacts of a higher tensile strength than those defatted in the giant Soxhlet extractor. This result correlates with the finding that less extract was obtained on defatting with the giant than with the standard Soxhlet apparatus (section 3.3.1.1).

Figure 2.9 illustrates the tensile strength of compacts prepared from DF48-96-01A, DF48-96-02A and Starch 1500. DF48-96-01A produced apparently stronger compacts than DF48-96-02A between 16 and 23kN. However, both of these materials produced compacts that were apparently stronger than those prepared from unmodified Starch 1500. The mass of extract per 100g of Starch 1500 obtained for DF48-96-01A and DF48-96-02A was 0.225g and 0.198g respectively.

Although the difference in the mass of extract for these two samples is small it is possible that residual lipid in DF48-96-02A prevents the formation of compacts of equivalent strengths to that of DF48-96-01.

2.3.5 A study of the tensile strength of Starch 1500 compacts defatted using Supercritical Fluid Extraction (SFE) techniques

Supercritical fluid extraction (SFE) techniques were investigated as an alternative to defatting Starch 1500 using the Soxhlet apparatus (section 3.1.2). As the results in section 3.3.1.1 indicate, SFE treatment failed to extract an appreciable quantity of material from Starch 1500. Loss on drying measurements were performed on the SEF treated material (SEF01) using the method described in section 4.3.3. After conditioning for 4 days at 44% RH the loss on drying measurement for SEF01 was 3.8%$^{w}/_{w}$. The low moisture content of SEF01 was attributed to extraction of water from the material on SEF treatment (Brennan, personal communication). As the moisture content of starch is known to affect its compressibility (Rees and Tsardaka, 1994), SEF01 was conditioned for a total of 5 months at 44% RH as a result the material tested had a moisture content of 9.6% $^{w}/_{w}$. As material was limited four, 10mm diameter compacts were prepared at 20kN using the method described in section 2.2.1 (ii). This material was tested alongside compacts of Starch 1500, DF48-99-04 and SEF01 that had been extracted with absolute ethanol using the Soxhlet apparatus (SEF99). The results for this study are summarised in table 2.3.

Table 2.3: Tensile strength of 20kN compacts prepared from defatted and unmodified Starch 1500 on the Instron tensile testing apparatus.

	Starch 1500	SEF01	SEF99	DF48-99-04
Tensile	2.95	3.26	10.48	10.93
Strength	2.98	3.33	9.70	10.79
(MPa)	3.21	3.47	9.93	10.20
	3.36	3.78	9.51	10.84
Mean	3.13	3.46	9.91	10.69
Std Deviation	0.20	0.23	0.42	0.33

One-way analysis of variance revealed that there was no apparent difference in the tensile strengths of compacts formed from either Starch 1500 and SEF01 or SEF99 and DF48-99-04. However compacts prepared from the materials that had been

defatted with absolute ethanol using the Soxhlet extraction apparatus (i.e. SEF99 and DF48-99-04) were apparently stronger than Starch 1500 and SEF01. Such a result adds further weight to the theory that the removal of lipid from Starch 1500 correlates well with the tensile strength of the resulting compact.

2.3.6 Tensile strength of Starch 1500 compacts defatted with both absolute ethanol and n-hexane

As is alluded to in section 4.3.9, the diluent theory proposes that it is possible to depress the glass transition point of a material by exposure to low-weight molecular solvents (Shen and Eisenberg, 1966). This study was performed to determine whether the increased crushing strength of defatted Starch 1500 compacts resulted from the incorporation of the defatting solvents into the material. This involved the further defatting of n-hexane treated material with absolute ethanol (DF48-He(99)-01) and absolute ethanol treated material with n-hexane (DF48-99(He)-02).

Figure 2.10 details the crushing strength of compacts of Starch 1500, DF48-He-03, DF48-99-03, DF48-He(99)-01 and DF48-99(He)-02. One-way analysis of variance revealed that there was no difference in the tensile strength of DF48-He-03 and DF48-99-03 compacts. According to the diluent theory the tensile strength of compacts formed from DF48-He(99)-01 and DF48-99(He)-02 should therefore be equivalent to those of DF48-He-03 and DF48-99-03. It is apparent from figure 2.10 that the compacts prepared from DF48-He(99)-01 and DF48-99(He)-02 were apparently stronger than the two materials that had undergone a single Soxhlet extraction.

2.3.7 Analysis of the lubricant sensitivity of unmodified and defatted Starch 1500 materials

Hydrophobic lubricants like magnesium stearate are widely recognised for their deleterious effects on the tensile strength of materials such as starch and microcrystalline cellulose. The lubricant sensitivity of these plastically deforming materials has been attributed the formation of a hydrophobic film around the particles which in turn prevents the formation of hydrogen bonds that hold the compacts together. Studies performed in section 3.2.2 identify the major constituents of the extract obtained from Starch 1500 using the Soxhlet apparatus to be C16 (palmitates) and C18 (stearates) fatty acid derivatives. The aim of this study was to assess the lubricant sensitivity of Starch 1500 samples that had high (DF48-96-01A), medium (DF48-Pr-01A) and low (DF48-He-01A) levels of their

native lipids removed. The lubricant sensitivity of unmodified Starch 1500 was also assessed alongside that of the defatted materials.

The lubricants chosen for this study were magnesium stearate (M.S: Colorcon, U.K.), stearic acid (S.A: Sigma Chemicals, U.K) and sodium stearyl fumarate (Pruv®, Mendell, Paterson, NY, U.S.A.). The lubricants and Starch 1500 samples were conditioned in a controlled relative humidity environment of 44% for 48 hours before use. Prior to blending, the lubricants were screened through a 22- and then a 40-mesh standard brass test sieve (Endecotts, London, U.K.) to break up powder agglomerates. The unmodified and defatted Starch 1500 samples were prepared in 100g batches containing 0.5%$^{w}/_{w}$ of lubricant. These batches were blended in a in a low shear turbulent tumbling mixer (Turbula T2C, Bachofen, Basel, Switzerland) at 20 rev min^{-1} for period of 2 and 10 minutes. Compacts were prepared from these materials immediately after blending using the method described in section 3.2.1(i) at compaction forces of approximately 8,12 and 16kN. To allow the measurement of compact ejection forces the punches and die were thoroughly cleaned with isopropyl alcohol between batches to remove any residual lubricant from the punch faces.

As a means of quantifying the reduction in the tensile strength of compacts of unmodified and defatted Starch 1500 blends the lubricant sensitivity ratio (equation 2.3) proposed by Bos et al (1991) was employed:

$$\text{Lubricant Sensitivity Ratio (LSR)} = S_0 - S_{lub} / S_0 \qquad \text{Equation 2.3}$$

Where S_0 and S_{lub} are the tensile strengths of compacts prepared with and without lubricant at a given compaction force. As the compaction force of each compact will vary, where one-way analysis of variance revealed no difference between the compaction forces of the lubricated and unlubricated blends the LSR was applied to the mean tensile strength of the compacts.

Figures 2.11, 2.12, 2.13 and 2.14 illustrate the tensile strengths of lubricated and non-lubricated compacts of Starch 1500, DF48-96-01A, DF48-Pr-01A and DF48-He-01A respectively. It may be observed from these figures that both unmodified and defatted Starch 1500 exhibit varying degrees of lubricant sensitivity. This can be studied more clearly in table 2.4, which details the lubricant sensitivity ratios for both unmodified and defatted Starch 1500 lubricant blends. It is evident from this

data that DF48-96-01A demonstrates the greatest lubricant sensitivity whereas Starch 1500 has the lowest LSR values. Such data infers that defatting Starch 1500 increases the lubricant sensitivity of the material. Whilst all three of the defatted samples exhibit higher lubricant sensitivity than Starch 1500 it is apparent from figure 3.2 that this correlation does not hold for the propan-1ol and n-hexane defatted samples (DF48-Pr-01A and DF48-He-01A respectively). It is noteworthy however that the tensile strength of the blend of DF48-96-01A showing the greatest lubricant sensitivity is still stronger than the unlubricated Starch 1500 compacts (figures 2.11 and 2.12).

Section 3.3 demonstrates that solvent choice influences only the mass rather than the composition of the extract removed from Starch 1500. In addition, this study failed to reveal any trend between choice of lubricant and LSR values for Starch 1500 and the different defatted materials. The negative LSR values observed for DF48-Pr-01A and Starch 1500 samples blended with sodium stearyl fumarate indicate that this lubricant did not weaken the compacts significantly.

Table 2.4: LSR values for Starch 1500, DF48-96-01A, DF48-Pr-01A and DF48-He-01A blended with several lubricants.

	Lubricant Sensitivity Ratio					
Material (Compaction Force / kN)	**Stearic Acid 2 min**	**Stearic Acid 10 min**	**Mag Stearate 2 min**	**Mag Stearate 10 min**	**Pruv ® 2 min**	**Pruv® 10 min**
DF48-96-01A						
(8)	0.57	0.64	0.37	0.70	0.44	0.43
(12)	0.55	0.63	0.29	0.75	0.37	0.40
(16)	0.66	0.71	0.41	0.77	0.52	0.53
DF48-Pr-01A						
(8)	0.16	0.47	0.18	0.50	-0.13	0.11
(12)	0.28	0.46	0.21	0.47	-0.05	0.12
(16)	0.36	0.49	0.29	0.50	0.03	0.21
DF48-He-01A						
(8)	0.47	0.62	0.48	0.59	0.14	0.17
(12)	0.48	0.55	0.32	0.51	0.10	0.13
(16)	0.51	0.56	0.34	0.54	0.16	0.18
S1500						
(8)	0.10	0.22	0.37	0.55	-0.17	-0.03
(12)	0.21	0.26	0.36	0.49	-0.15	-0.09
(16)	0.30	0.35	0.35	0.51	0.00	0.06

The ejection forces of unlubricated compacts of Starch 1500 and DF48-96-03A is discussed in section 2.3.8, using the measurements obtained for compacts prepared on the Piccola rotary tablet press.

2.3.8 Investigation of unmodified and defatted Starch 1500 compacts prepared on a rotary tablet press

Tablet production is usually classified as either single- or double-sided compaction facilitated by a single punch tablet machine or a rotary tablet press respectively. Single punch tablet machines are primarily used for development studies whereas rotary tablet presses are used in high-volume tablet production. As the rates (Fell and Newton, 1970; Armstrong and Palfrey, 1989) and methods (Muller and Augsburger, 1994) of compaction employed vary between the two types of tablet press, materials may produce compacts of different strengths on each machine.

The aim of this study was to determine whether compacts of defatted Starch 1500 prepared on an instrumented rotary tablet press would demonstrate the same increased tensile strength over unmodified Starch 1500 compacts, as was observed with compacts prepared using the compaction simulator. Compacts were prepared using the method outlined in section 2.2.1(iii) from Starch 1500, DF48-96-02A and DF48-96-03A and tested on the Instron tensile testing instrument using the method outlined in section 2.2.2. The materials that were used, were conditioned in a controlled humidity environment, maintained at 44%RH for a minimum of 48 hours prior to compaction. Compacts were prepared without the addition of an external lubricant so that the inherent lubricity of the compacts could be assessed.

Figures 2.15 and 2.16 illustrate the tensile strength of Starch 1500 and DF48-96-03A compacts prepared on the compaction similar and rotary tablet press. In both cases it can be seen that the compacts prepared on the rotary tablet press are stronger than those prepared using the compaction simulator. The data given in appendix 1 demonstrates that as punch speed increases, the tensile strength of compacts prepared from both unmodified and defatted Starch 1500 decreases. Such an effect is also evident in that the tensile strengths of unmodified and defatted Starch 1500 compacts prepared on the rotary tablet press at 20 RPM are higher than those prepared at 30 RPM.

Figures 2.17 and 2.18 illustrate the ejection forces for compacts prepared from Starch 1500 and DF48-96-03A on the rotary tablet press at 20 and 30RPM respectively. It is apparent from this data that the ejection forces for both materials are higher for compacts prepared at 30 than at 20RPM. Such an effect may be attributed to increased shear imparted on the die walls by the compact, resulting from the higher ejection rate used for the 30RPM tablets (Wray, 1992). At both compaction speeds the ejection forces of compacts of DF48-96-03A were lower than those for unmodified Starch 1500. Prior to measuring the ejection forces of the defatted material it was feared that the inherent lubricity would be adversely affected by the removal of its native lipids. Figure 2.19 illustrates that the defatted material has a higher relative density than unmodified Starch 1500. Therefore although the extract obtained by defatting Starch 1500 is similar in chemical composition to the lubricants routinely using in the pharmaceutical industry, the increased relative density of defatted Starch 1500 leads to reduces die wall friction on ejection of the compact.

2.4 GENERAL DISCUSSION

The data presented in this chapter shows that defatting Starch 1500 consistently produces a material, which on compaction is apparently stronger than unmodified Starch 1500. A degree of correlation could be demonstrated between the polarity of the defatting solvent and the tensile strength of the compacts formed. Furthermore correlation was observed between the tensile strengths of the compacts and the mass of extract obtained on defatting in the standard and giant Soxhlet extractors. This data, along with the higher lubricant sensitivity ratio exhibited by the defatted materials supports the theory that the increased strength of defatted Starch 1500 is due to the removal of native lipids that inhibit hydrogen bonding between particles.

Figure 2.1: Tensile Strength of compacts of unmodifed and CM treated Starch 1500

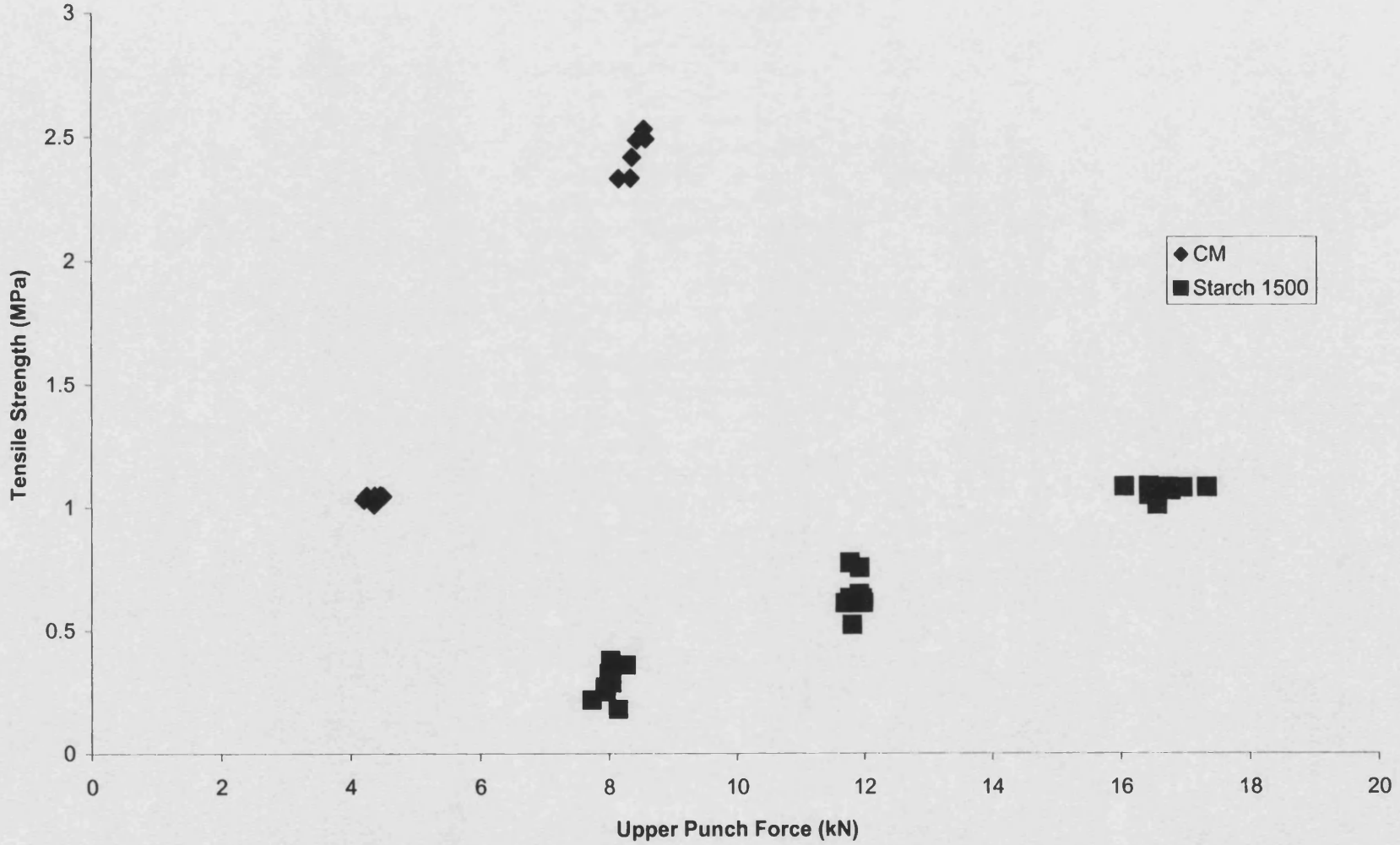

Figure 2.2: Tensile strength of Starch 1500 compacts defatted with 96% ethanol for 48 and 24 hours

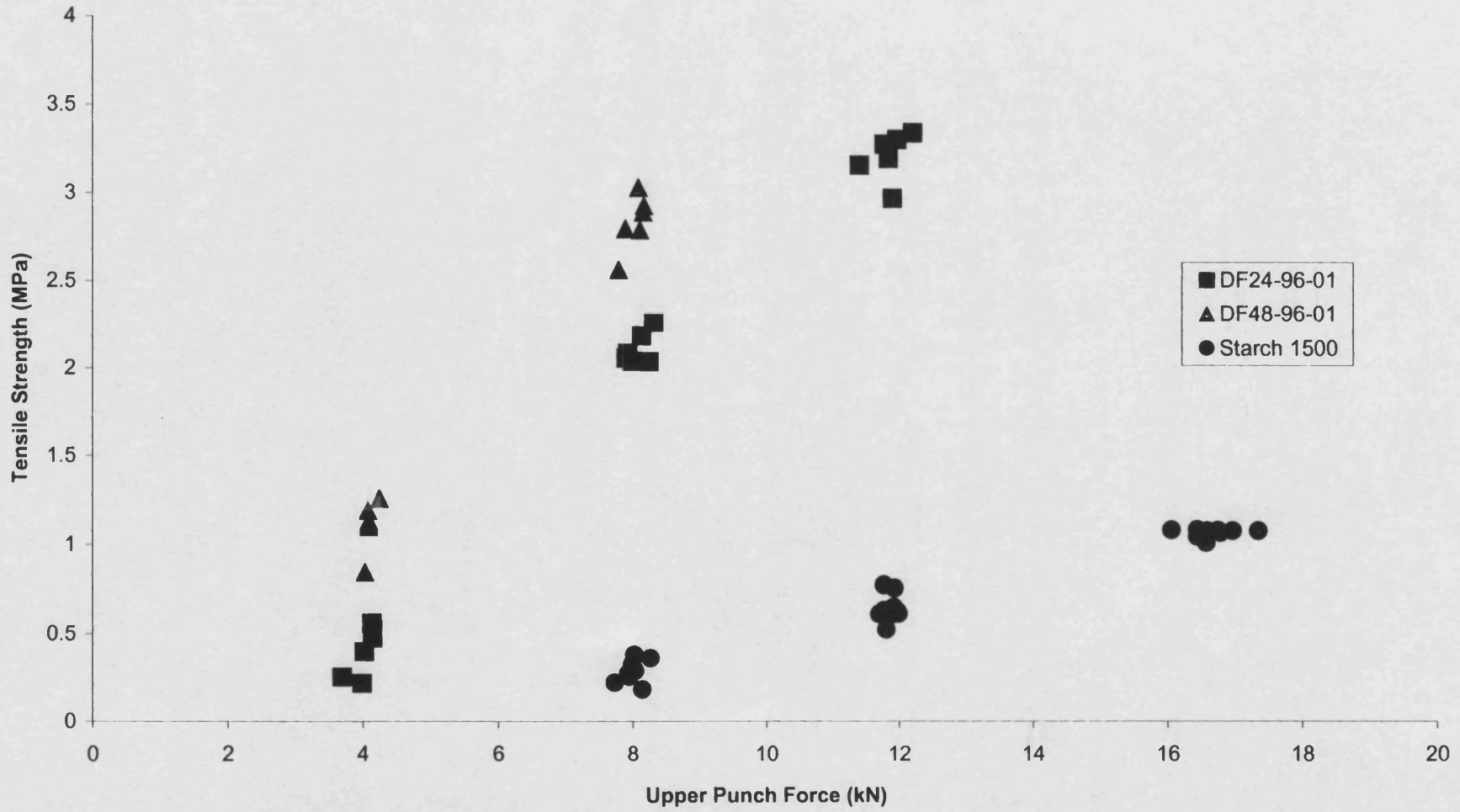

Figure 2.3 Effect of compaction force on the incremental mercury intrusion plot for Starch 1500 compacts

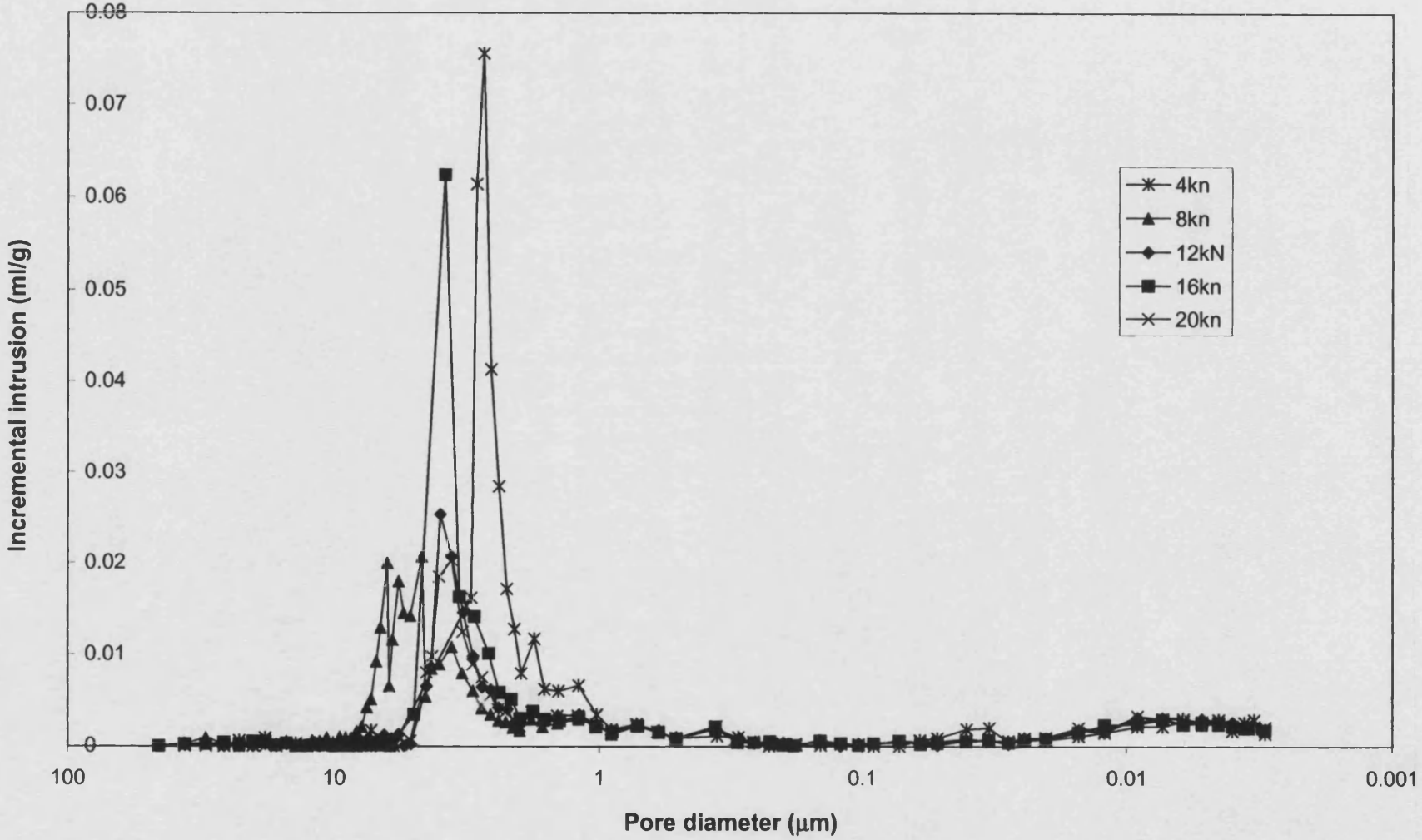

Figure 2.4 Effect of compaction force on the incremental mercury intrusion plot for DF48-96-01 compacts

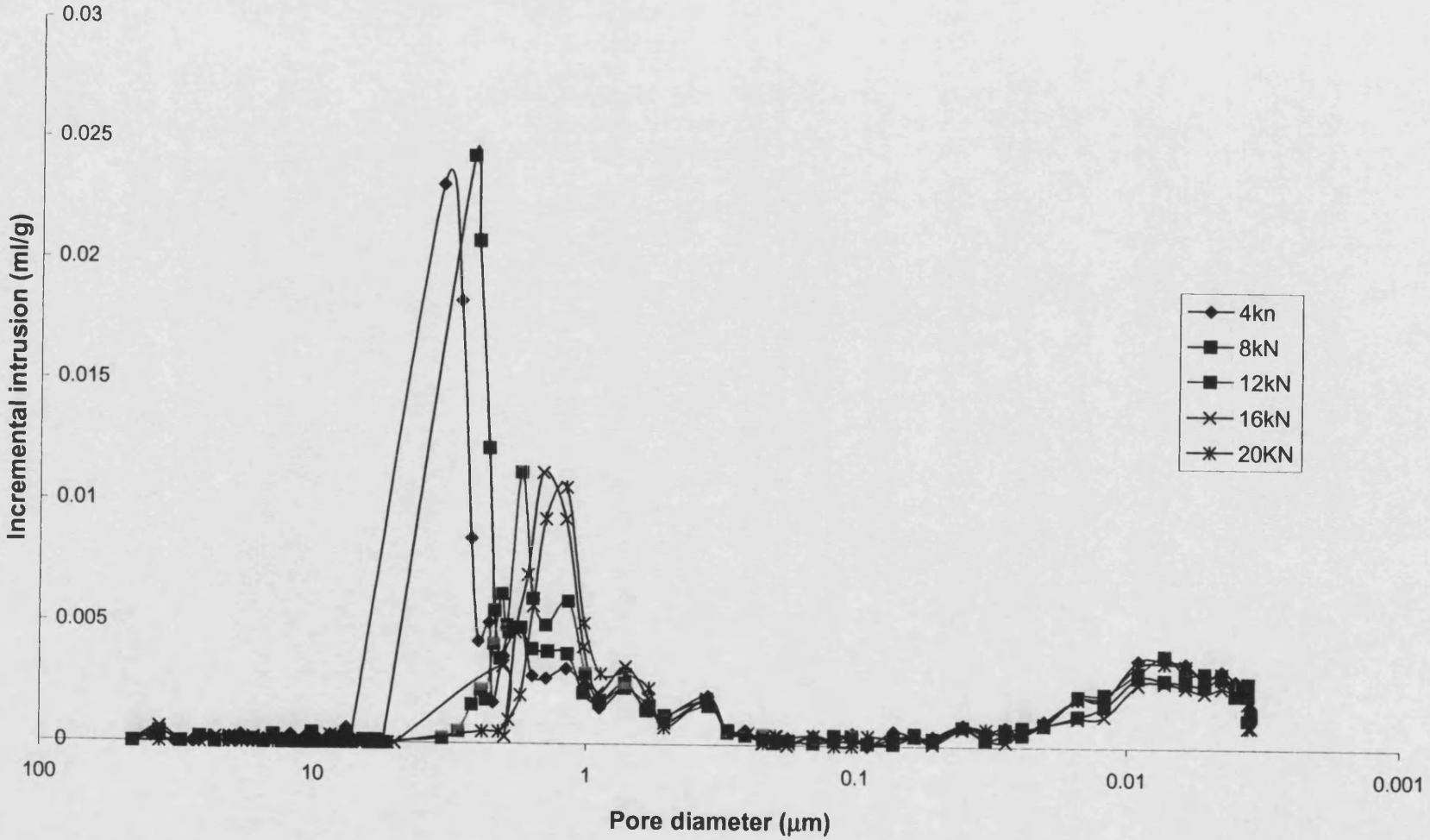

Figure 2.5 Tensile strength of Starch 1500 defatted with solvents of various polarities

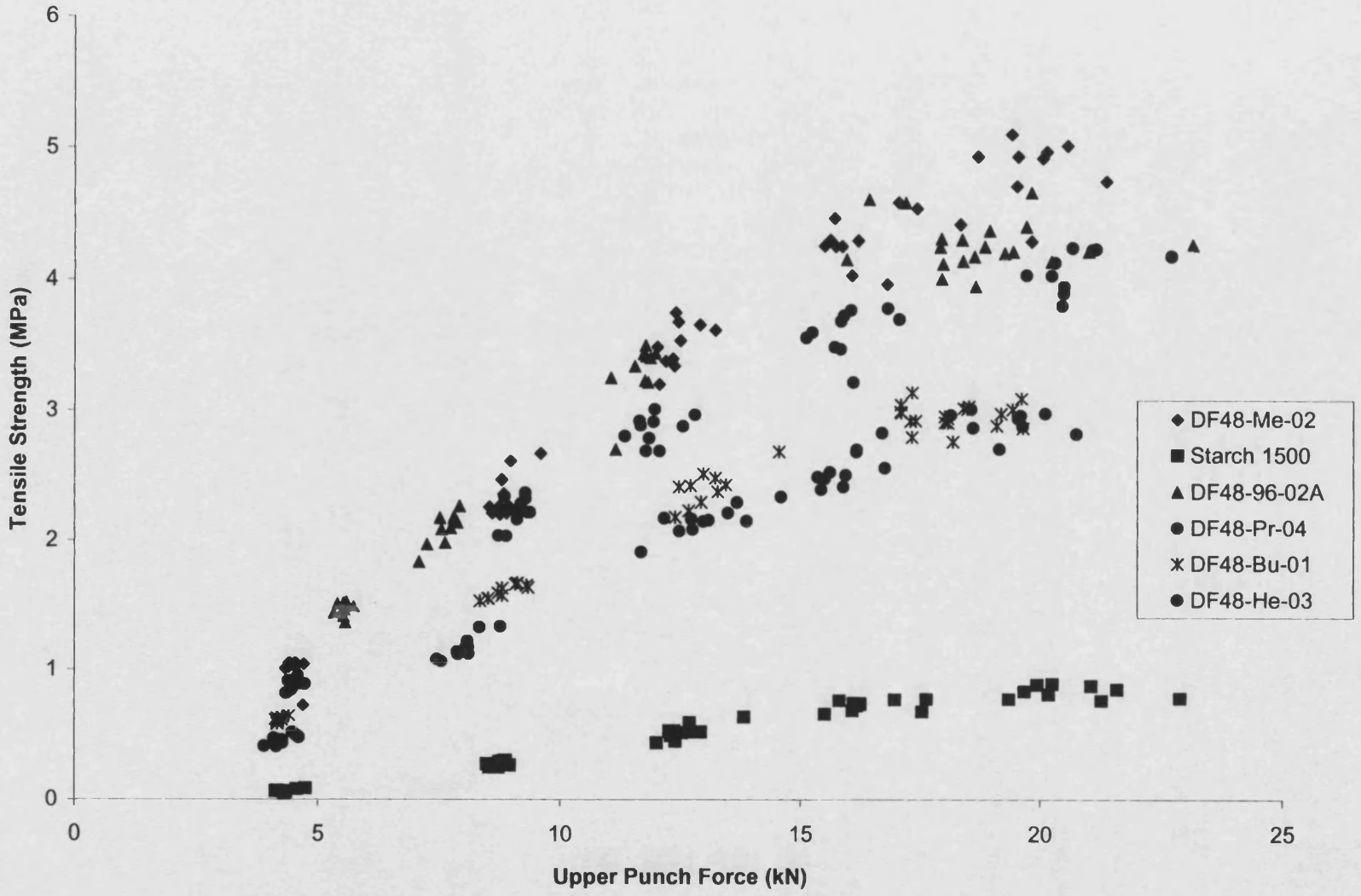

Figure 2.6: Comparison of tensile strength of Starch 1500 compacts defatted with different concentrations of ethanol

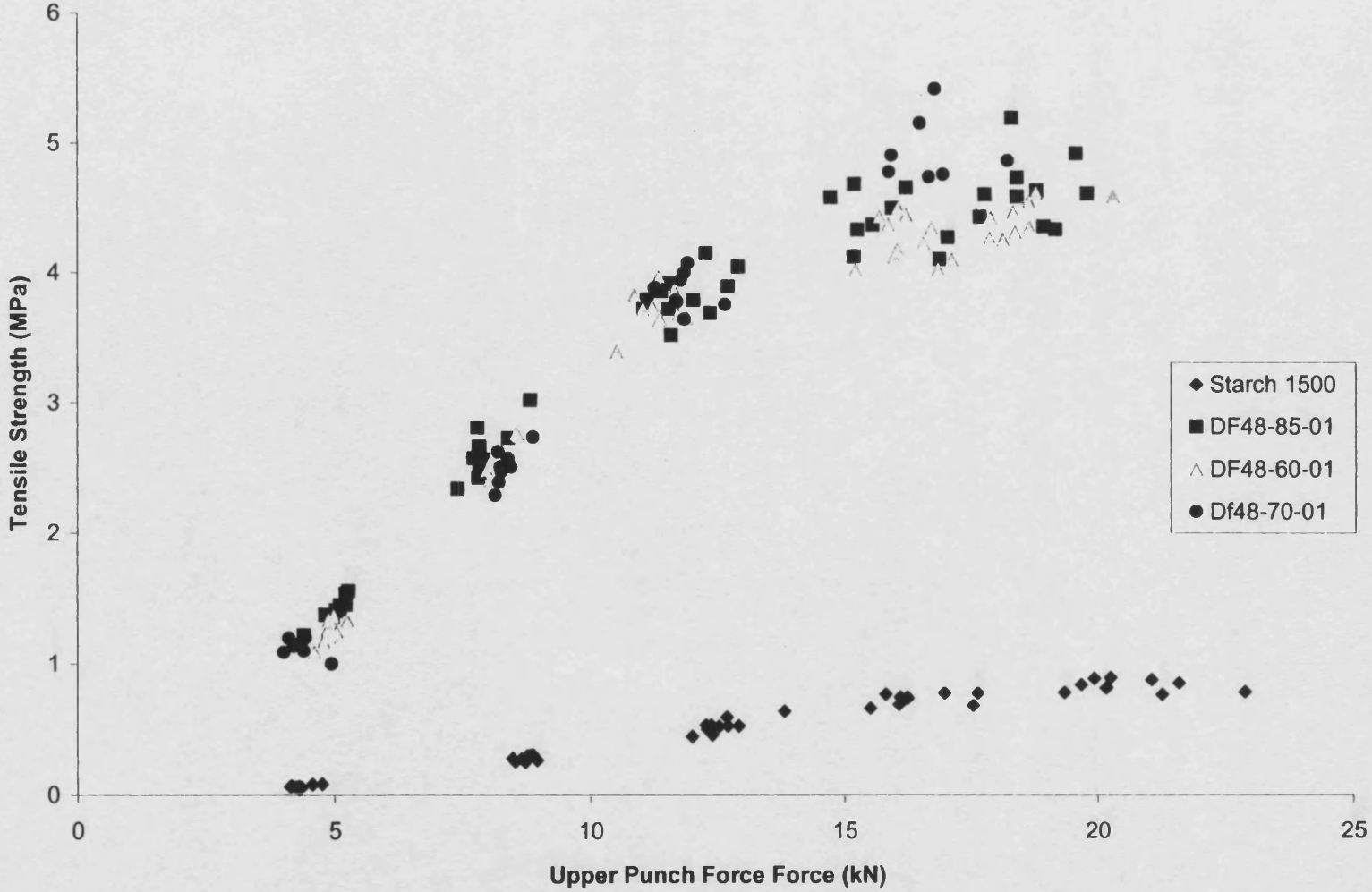

Figure 2.7: Comparison of the tensile strength of n-hexane defatted Starch 1500 using the standard and giant Soxhlet apparatus

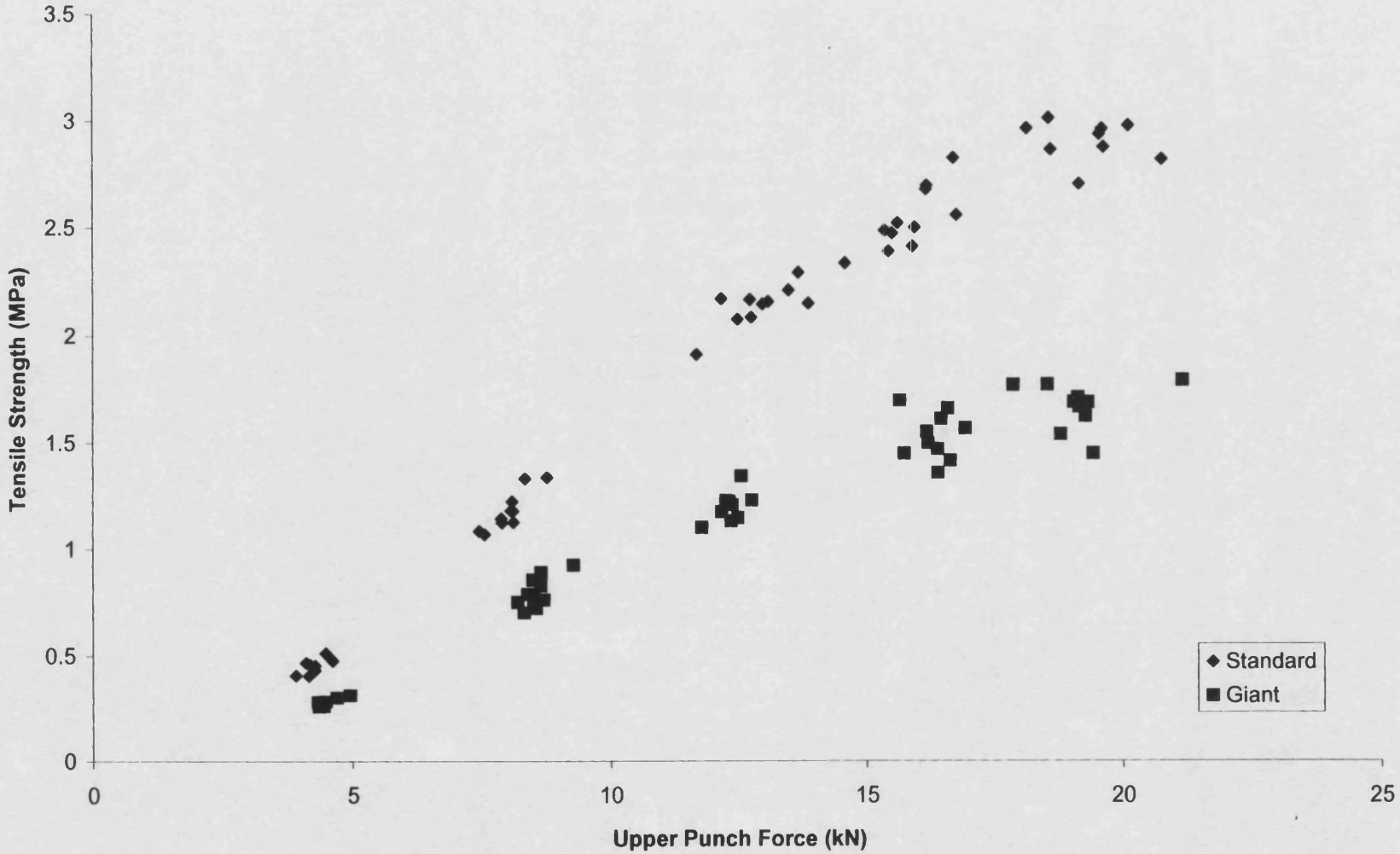

Figure 2.8: Comparison of the tensile strength of propan-1-ol defatted Starch 1500 using the standard and giant Soxhlet apparatus

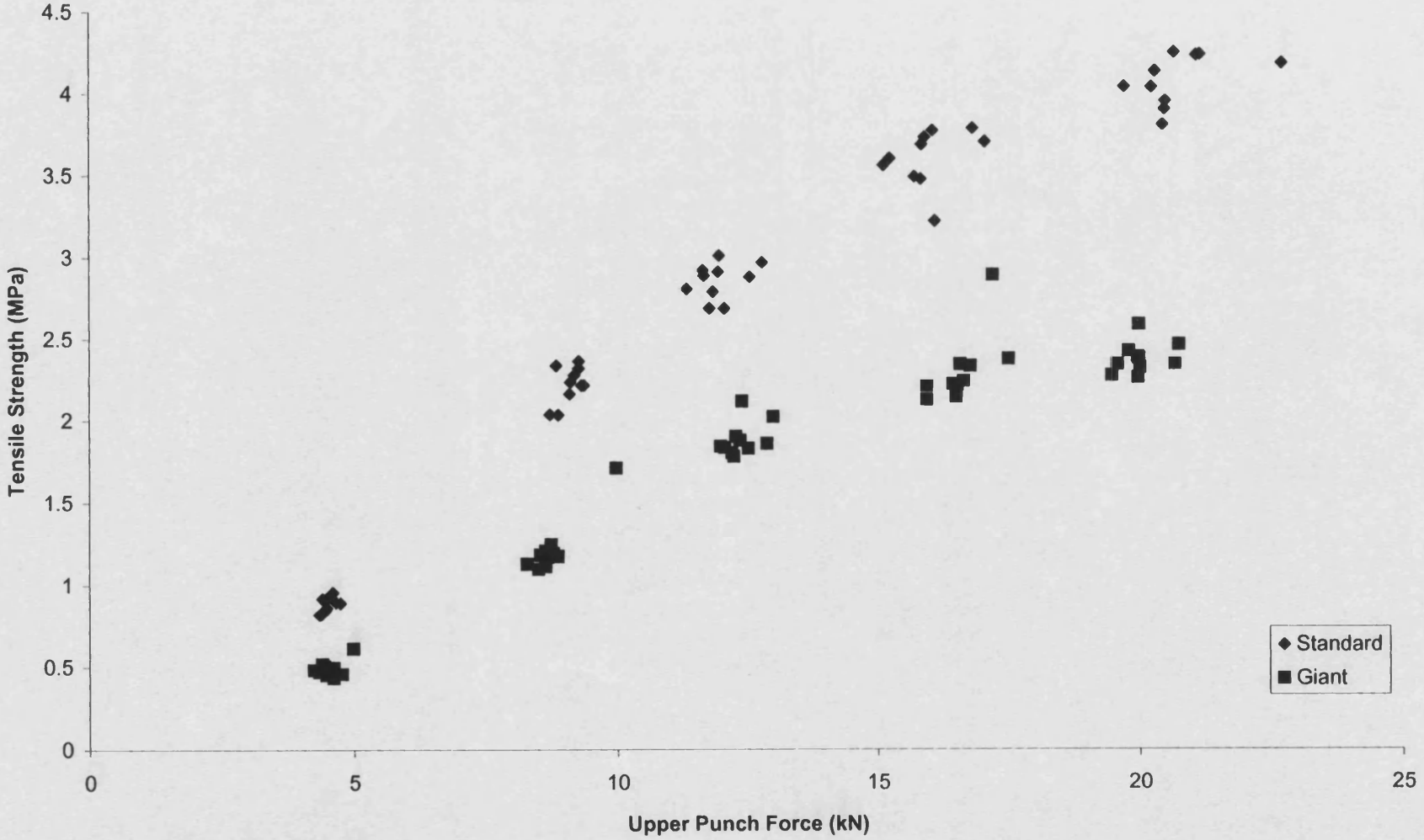

Figure 2.9: Comparison of the tensile strength of compacts of Starch 1500, DF48-96-01 and DF48-96-02A

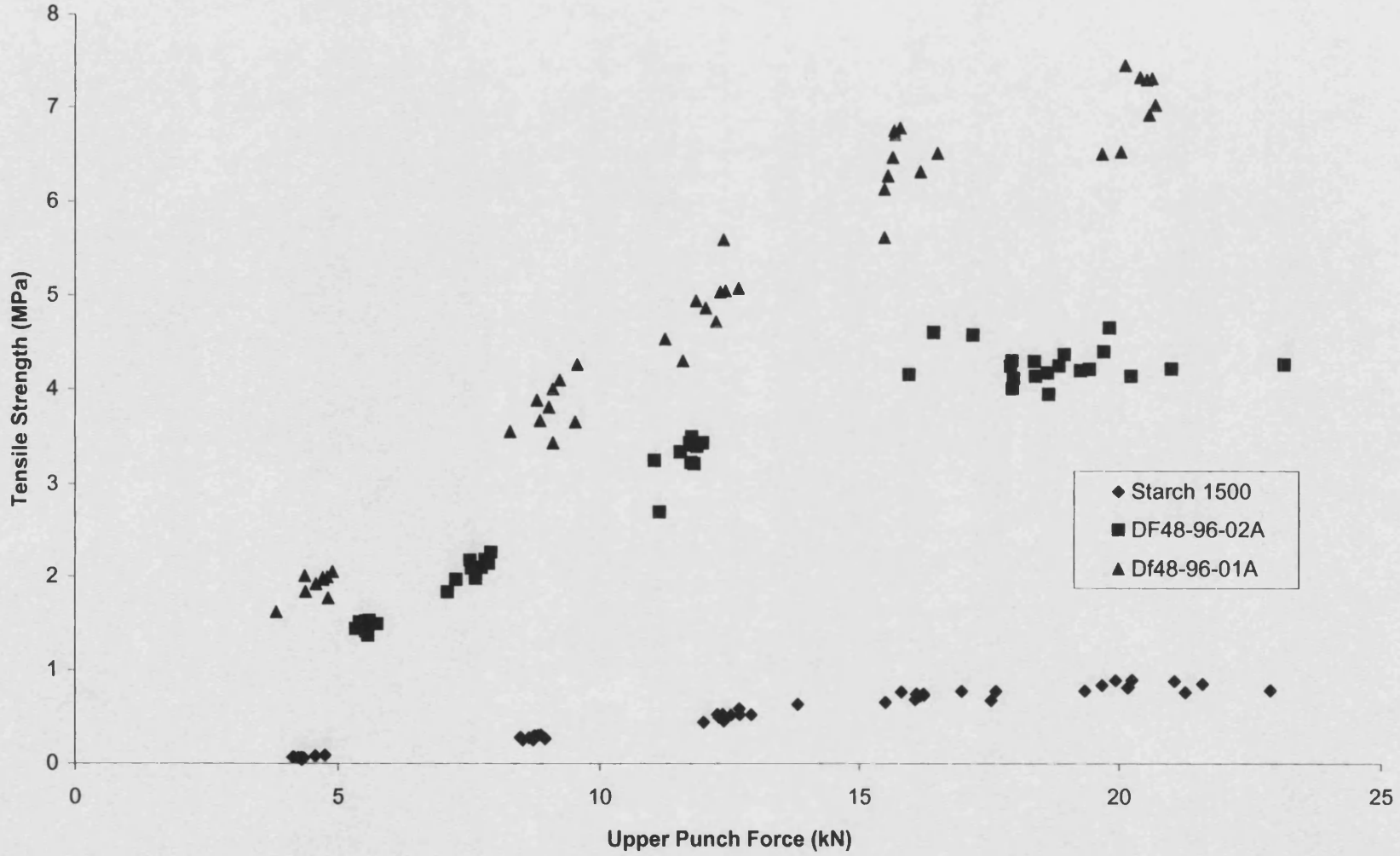

Figure 2.10: Tensile strength of Starch 1500 compacts defatted with Ethanol and Hexane

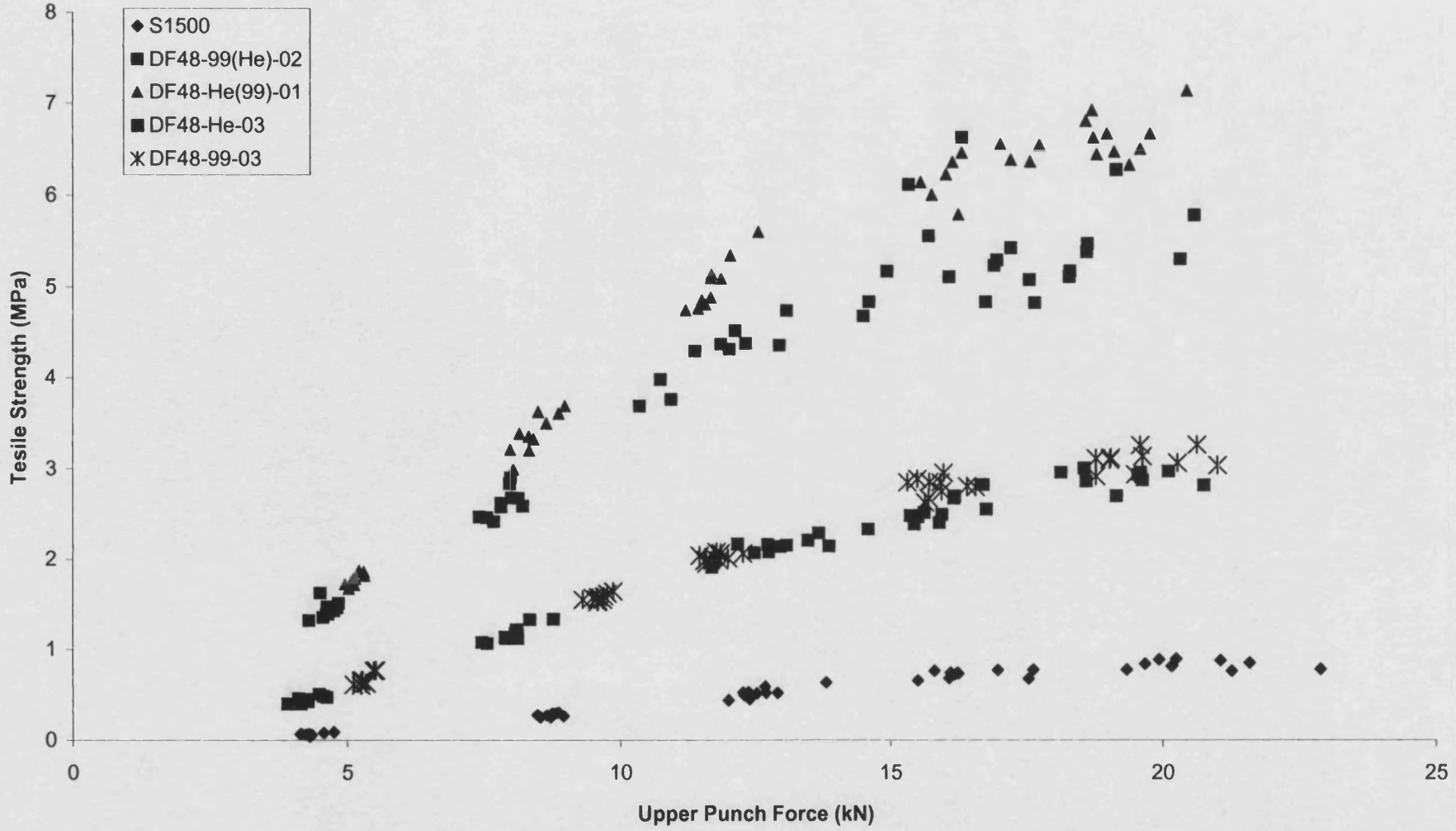

Figure 2.11: Effect of blend time and lubricant choice on the tensile strength of Starch 1500 compacts

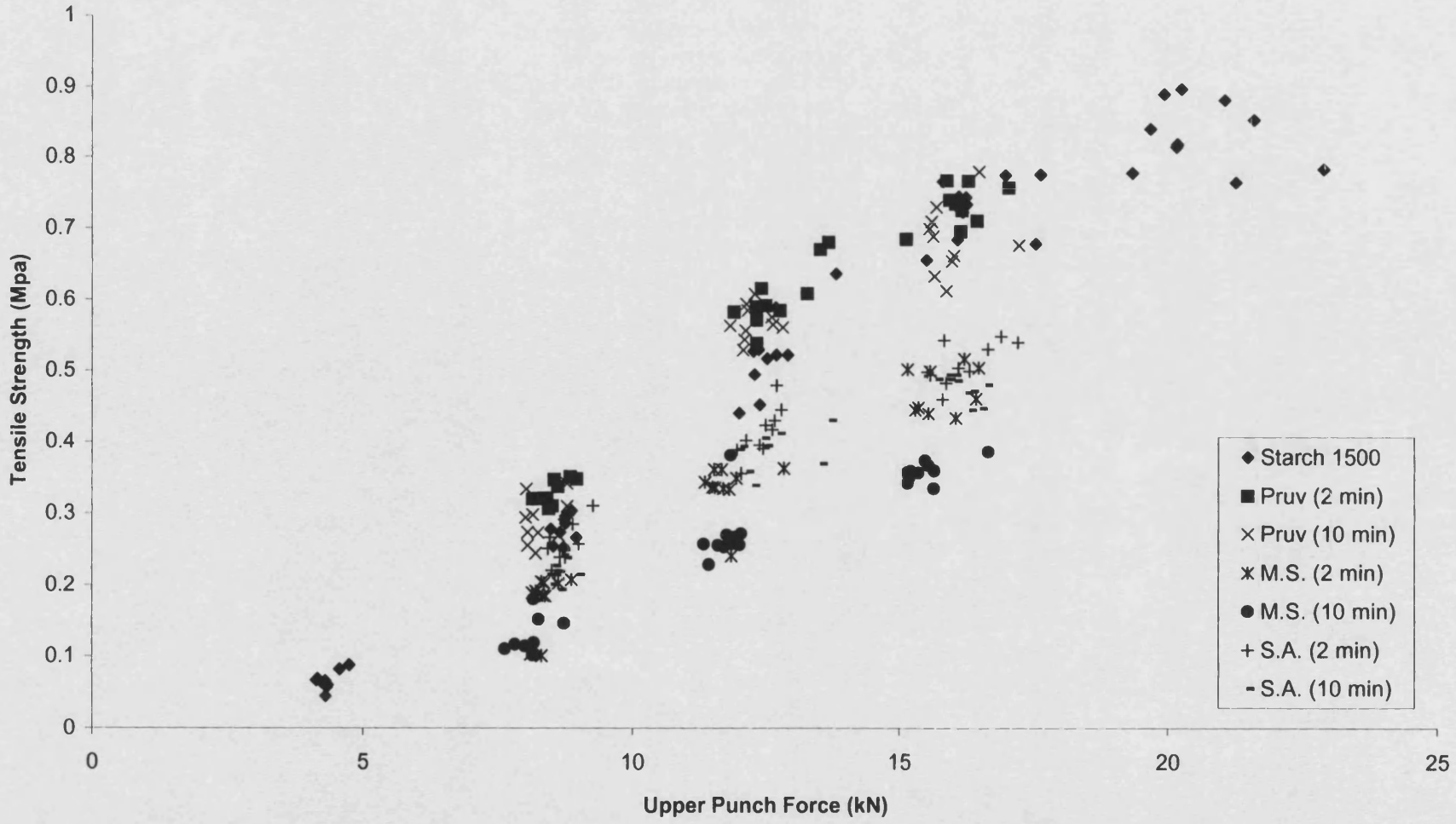

Figure 2.12: Effect of blend time and lubricant choice on the tensile strength of DF48-96-01A compacts

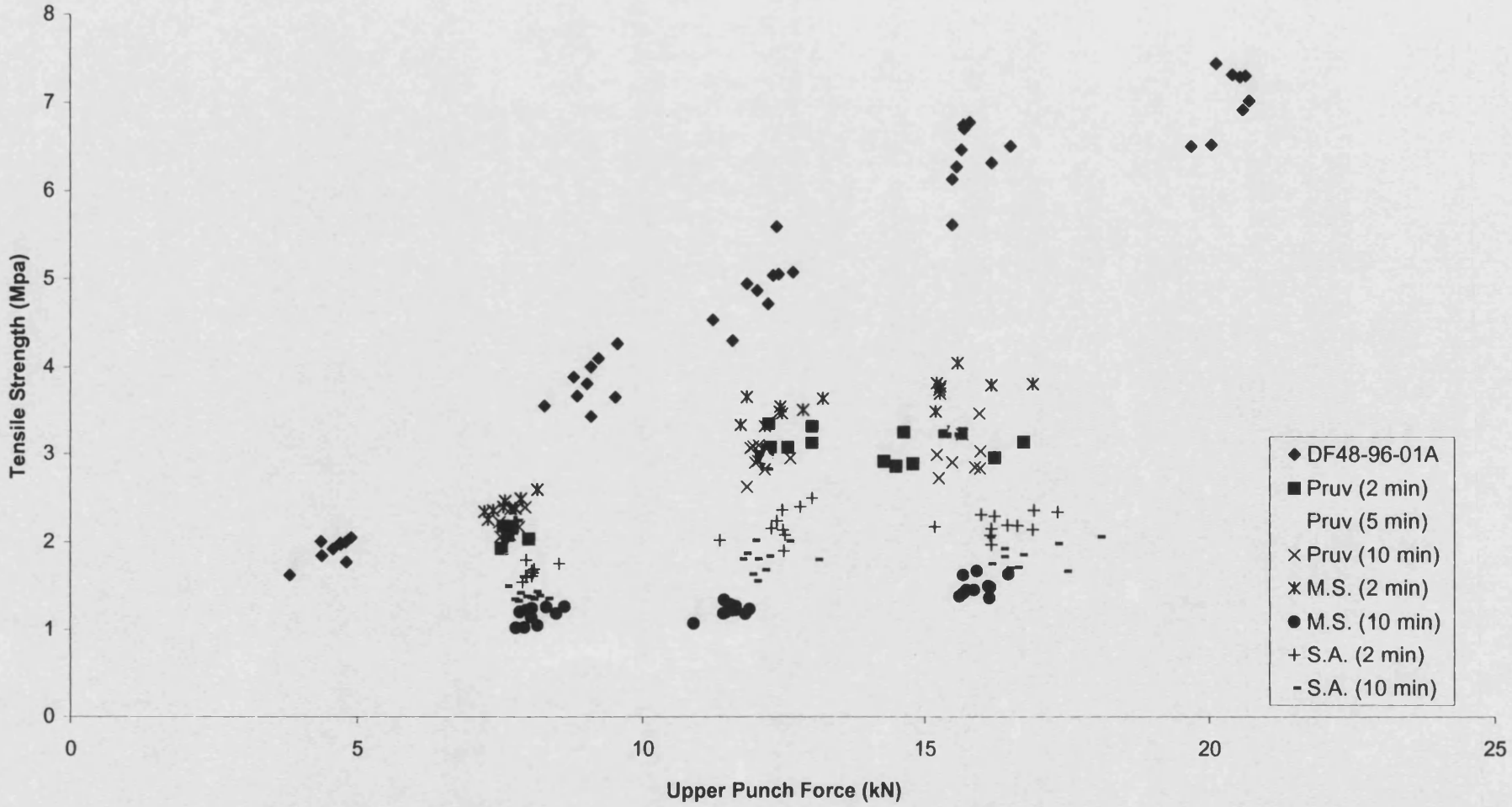

Figure 2.13: Effect of blend time and lubricant choice on the tensile strength of DF48-Pr-01A compacts

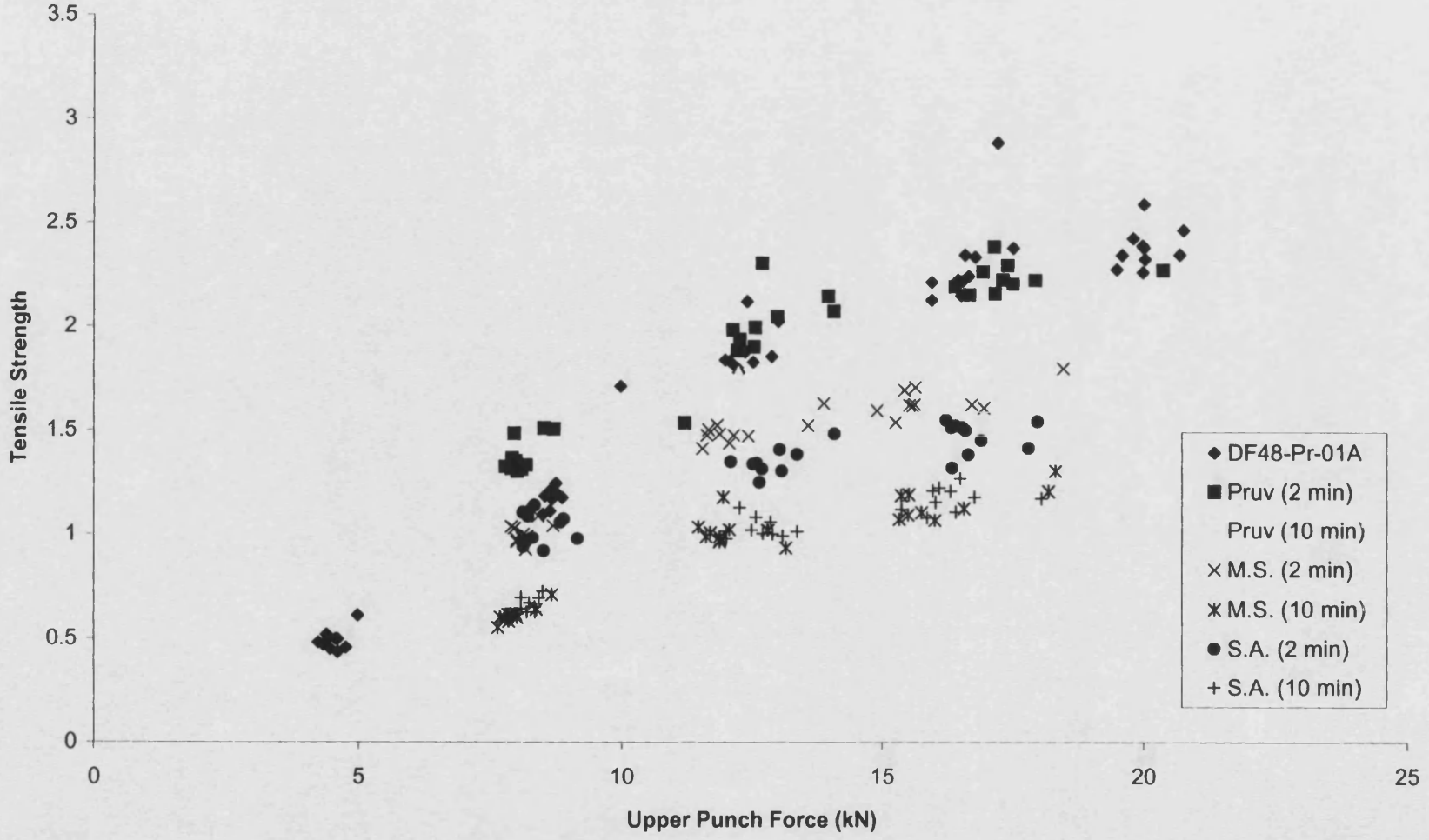

Figure 2.14: Effect of blend time and lubricant choice on the tensile strength of DF48-He-01A Compacts

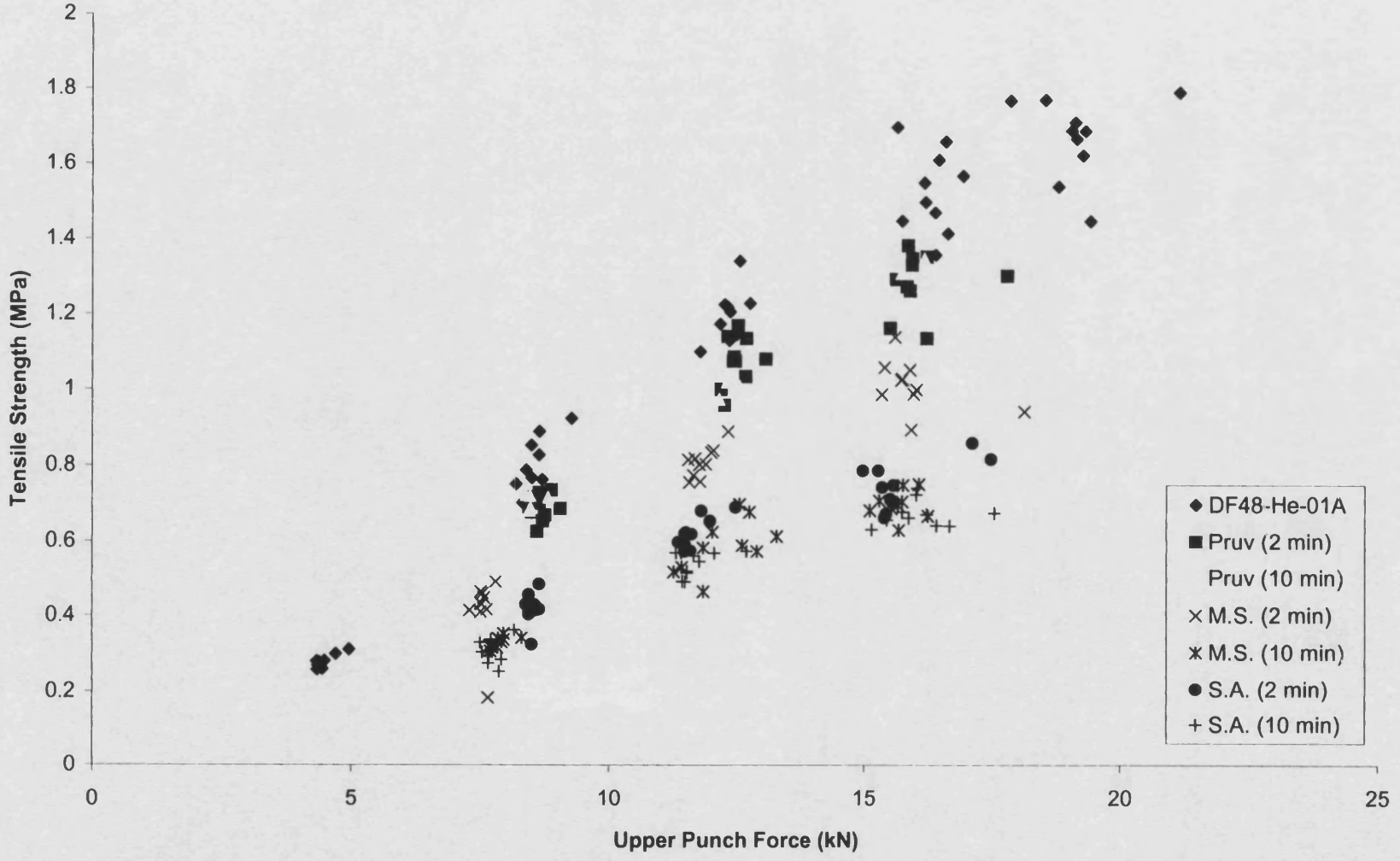

Figure 2.15: Tensile strength of Starch 1500 compacts prepared using a rotary tablet press and a compaction simulator

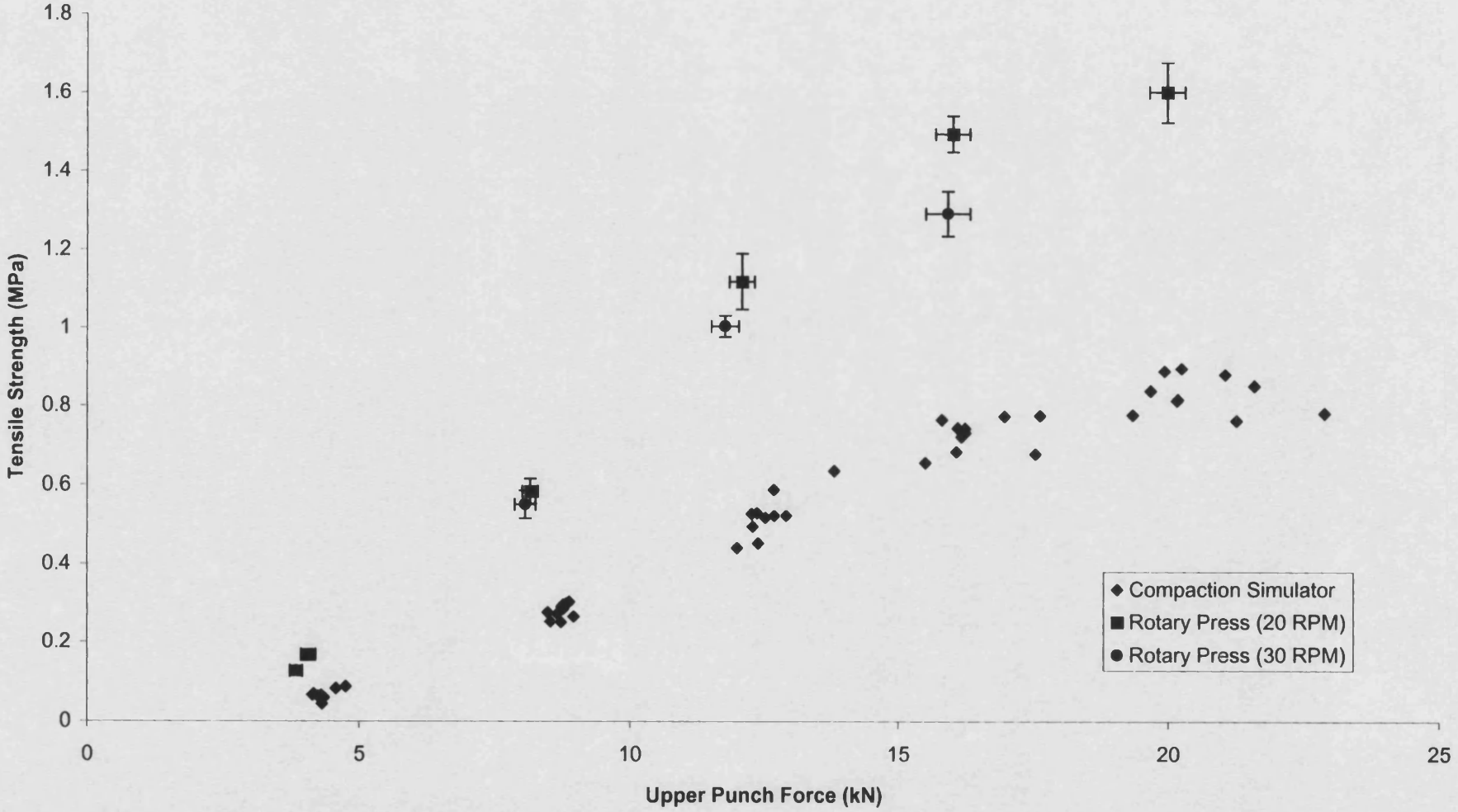

Figure 2. 16: Comparison of the tensile strength of DF48-96-03A compacts prepared on a compaction simulator and a rotary tablet press

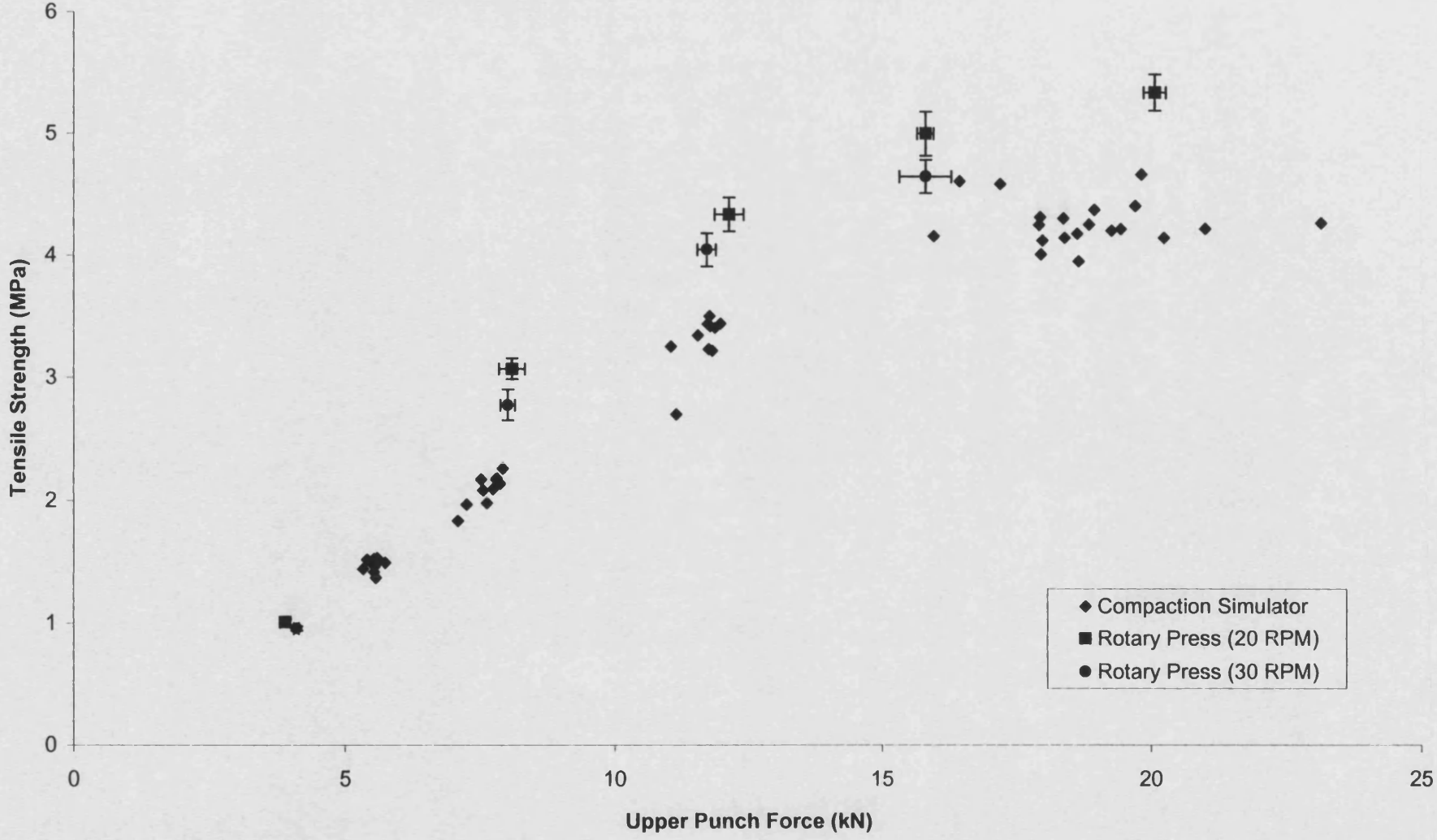

Figure 2.17: Ejection forces of Starch 1500 and DF48-96-03A compacts prepared using the Piccola Rotary Tablet Press at 20RPM

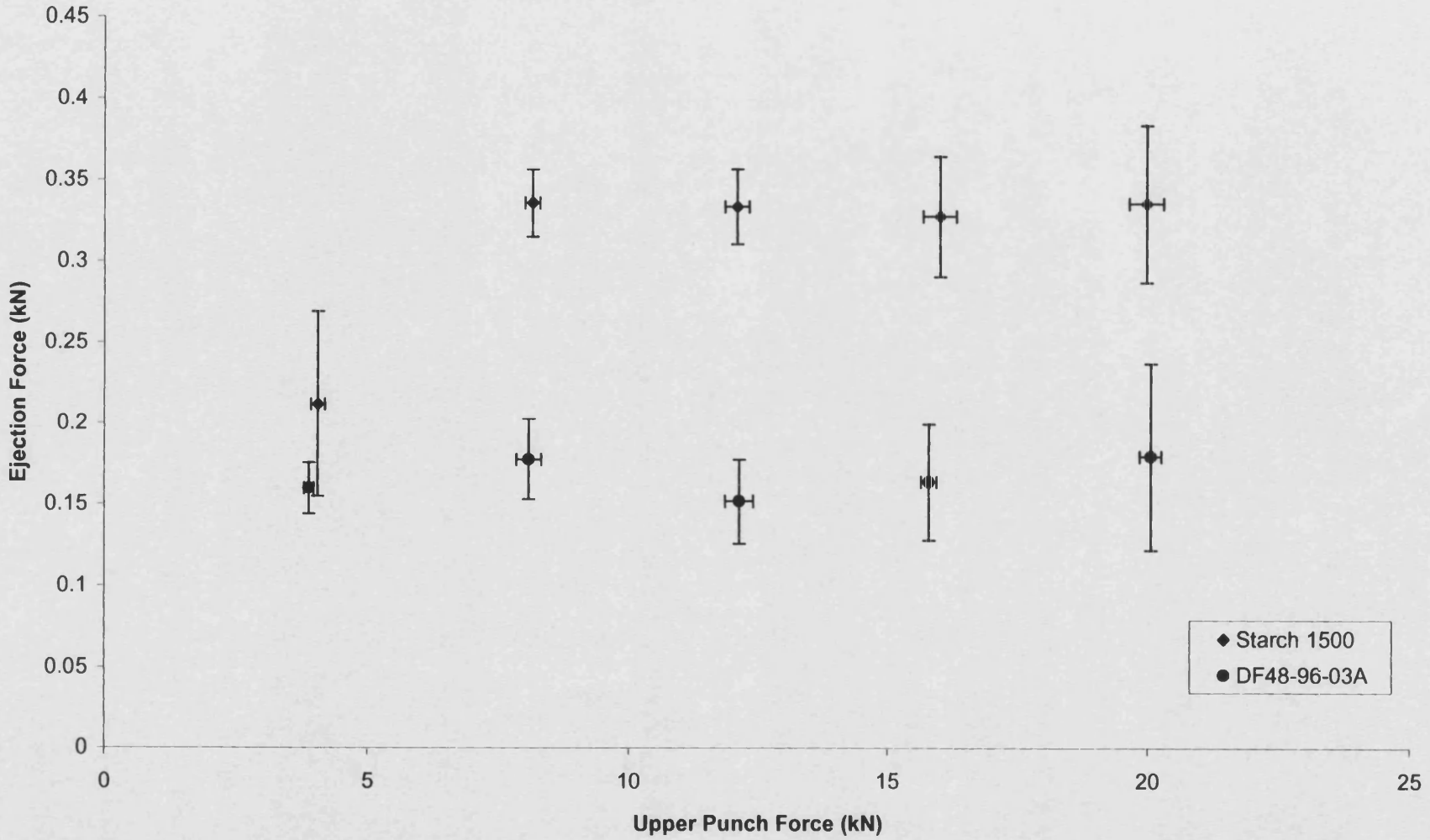

Figure 2.18: Ejection forces of Starch 1500 and DF48-96-03A compacts prepared using the Piccola Rotary Tablet Press at 30RPM

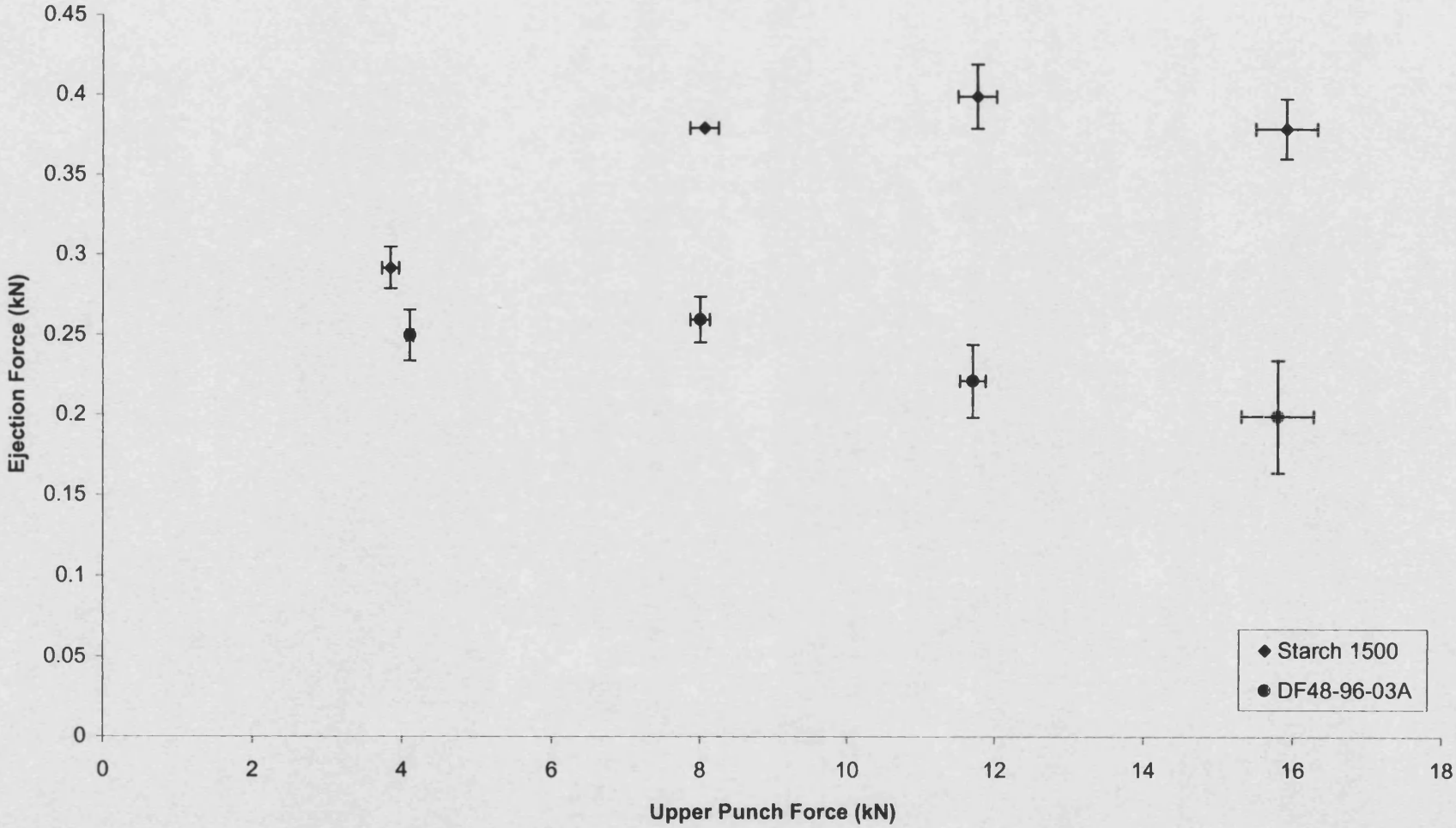

Figure 2.19: comparison of the relative densities of Starch 1500 and DF48-96-03A compacts prepared at 20 and 30 RPM using a Rotary Tablet Press

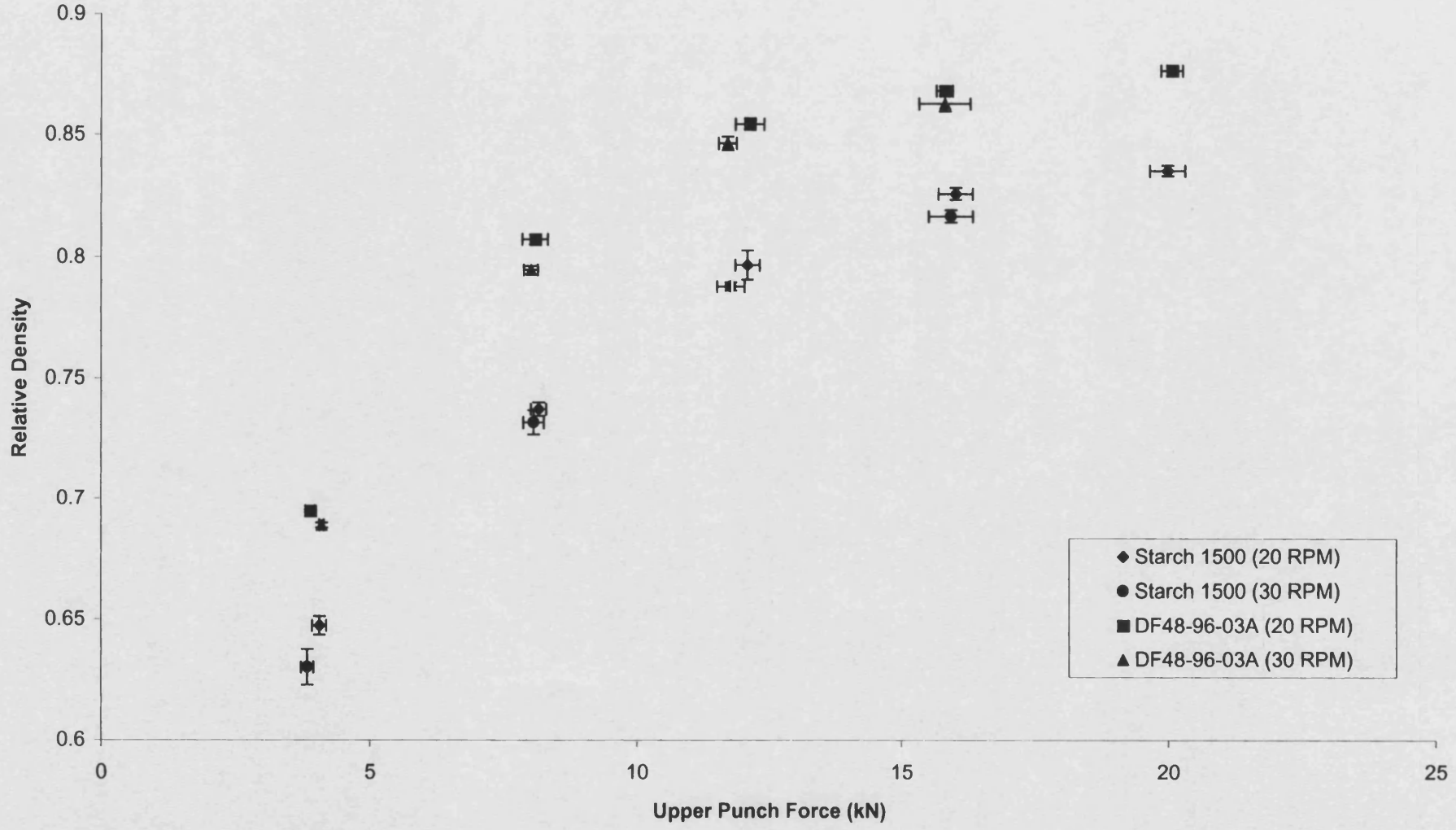

CHAPTER 3

LIPID EXTRACTION AND ANALYSIS FROM STARCH 1500 AND NATIVE MAIZE STARCH

3.1 GENERAL INTRODUCTION

The study undertaken in Chapter 2 demonstrated that on exposure of Starch 1500 to various hot solvent systems, by means of Soxhlet extraction, a material with improved tableting properties was formed. This material produced compacts that displayed increased tensile strength and were also less sensitive to the addition of hydrophobic lubricants. It was proposed that these effects resulted from the extraction of plant lipids present in Starch 1500. The source and distribution of lipids associated with starch granules has been discussed in Chapter 1.

This study was performed to establish the nature and composition of the extracted materials and to determine whether these factors varied with the solvent systems which were used. The analytical techniques that are used to characterize the extracts are well established in the field of lipid analysis (Gunstone et al, 1994). These techniques have been applied to the analysis of the lipid composition of starches from various botanical sources (Goshima, 1985; Vasanthan and Hoover 1992).

3.1.1 Soxhlet Extraction Apparatus

The Soxhlet apparatus is a well established means extracting compounds from solid-state materials and is one of the most commonly used methods by which lipids are extracted from starches (Whistler et al, 1965). Granular structure is known to limit the removal of larger molecules from the central regions of native starches (Whistler and Hilbert, 1944). Soxhlet extraction has been shown to be a time-dependent process (Whistler and Hilbert, 1944; Lehrman, 1942) in which greater yields of extract result if granular integrity is reduced. Such an effect has been achieved by mechanical (Whistler and Hilbert, 1944) and chemical (Evans and Briggs, 1941; Taylor and Nelson, 1920; Taylor and Sherman, 1933; Lehrman, 1929, 1930 and 1932) means.

3.1.2 Supercritical Fluid Extraction (SFE)

Supercritical fluid extraction is a technique that has received considerable attention as an alternative to conventional solid-phase methods such as Soxhlet extraction. SFE has found a wide range of applications within the food industry (Rizvi, 1986) and is routinely used in the decaffeination of coffee (Zosel, 1981). Supercritical carbon dioxide (SC-CO_2) is the most commonly used solvent in this process. It allows virtually solvent-free extraction and its low critical temperature allows the extraction of thermolabile compounds which may suffer degredation on exposure to

extraction of thermolabile compounds which may suffer degredation on exposure to hot solvents (Cheung et al, 1998). SC-CO_2 has been successfully used for the extraction of lipids from various foods (Myer et al, 1992; Hopper et al, 1995; Doane-Weiderman et al, 1998) and cereal products (Taylor et al, 1993; Zou et al, 1999). In general the amount of fat extracted is equivalent to that obtained by Soxhlet extraction. It has been proposed that SFE may supercede Soxhlet extraction in systems where the lipid is easily accessible and does not interact strongly with the solid phase of the matrix (Dionisi et al, 1999).

3.2 METHODS

3.2.1 Extraction Procedures

3.2.1.1 Soxhlet Extraction

Two sets or apparatus were used in this study; a standard Soxhlet extractor for use with 43 x 123mm cotton cellulose thimbles and a giant Soxhlet extraction apparatus (Ace Glass Incorporated, Vineland, NJ, U.S.A.) for use with 74 x 220mm cotton cellulose thimbles (as pictured in Figure 3.1). The larger soxhlet simply allowed the production of 500g batches of defatted material for testing as opposed to 80g yield possible with the standard apparatus. The quantity of solvent to be used for extraction was calculated as twice the volume of the extraction thimble for use in that Soxhlet. Anti-bumping granules were added with the solvent to prevent damaging the apparatus. Maize starch was weighed directly into the extraction thimble and its mass recorded. Based on initial studies and earlier published data (Evans and Briggs, 1941; Vasanathan and Hoover, 1991) an extraction time of 48 hours was selected.

3.2.1.2 Supercritical Fluid (SCF) Extraction

This work was performed by Phasex Corporation, 360 Merrimack Street, Lawrence, MA, USA. Requests for details of the method and conditions of extraction were not fulfilled. However it can be assumed that the method was based around the technology described at the company's website (*www.phasex4scf.com*).

Figure 3.1 Photograph of the giant Soxhlet apparatus

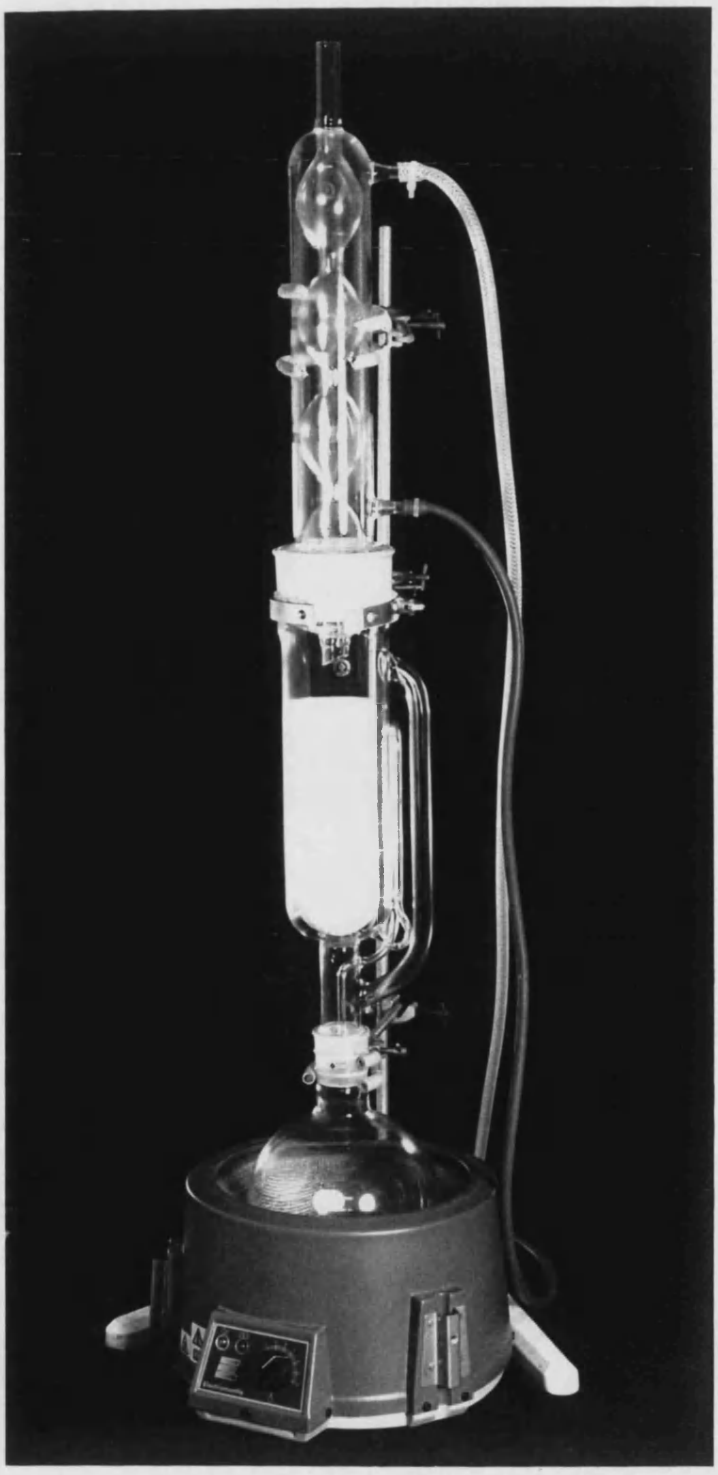

3.2.2 Analytical Procedures

3.2.2.1 Mass of Extract

Starch 1500 was defatted continuously for 48 hours, using the Soxhlet apparatus with various solvents. After defatting the flask containing solvent and extract was removed. Its contents were filtered into a clean flask to remove the anti-bumping granules and any Starch 1500 particles, which may have entered the flask during refluxing. The original flask was repeatedly washed into the second flask with methanol to ensure complete removal of the extract. Methanol was used for all washings regardless of the solvent system used for extraction as its high polarity allowed solubulisation of lipid traces on the glassware. Residual solvent removed in vacuo using a rotary evaporator (Buchi Rotavapor R-114, Buchi, Switzerland) at water aspirator pressure. To ensure that the material was completely dry the flask was transferred to a high vacuum pump for 24 hours. The flask was weighed and the mass of extract calculated simply by subtracting the weight of the empty flask from it. It should be noted that the decision to defat the starches for a period of 48 hours was primarily determined by the observed improvement in tabletting properties and not as a means to optimize lipid extraction from the starch.

3.2.2.2 Gas Chromatography/Mass Spectrometry (GC/MS)

Solutions were prepared containing 4 – 5 $mg.ml^{-1}$ of the extract in methanol. Initial studies were performed by firstly methylating the samples. This was achieved by combining the 5mg of extract with 150ml of N,N-dimethylformamide dimethyl acetal (Methyl-8 Concentrate supplied by Aldrich, Milwaukee, WA, U.S.A) in a 1ml vial and equilibrating at 60°C for 10 to 15 minutes prior to the addition of methanol. Analysis of underivatised lipids were performed using the same concentration of extract. Analysis of the extract was performed in a 30m x 0.25mm DB5 column (J&W Scientific, CA., U.S.A.) using a HP 5890A Gas Chromatograph coupled to a 5970 Series Mass Selective Detector (both Hewlett Packard) which uses 70 eV electron-impact ionization (EI) to fragment the samples. The initial oven temperature was 180°C. This was ramped to 250°C at a rate of 7.5°C min^{-1} at which it was held for a further 10 minutes. The flow rate of the helium carrier gas was 1ml min^{-1}.

3.2.2.3 Thin Layer Chromatography (TLC)

Analytical TLC was performed with aluminium-backed coated with Kieselgel 60 F_{254} (Merck, KgaA, Darmstadt, Germany). The chromatograms were visualized using either anisaldehyde or bromocresol green stains. TLC was employed in the initial

studies as a technique to identify the number of compounds in samples of DF48-99-01 and DF48-Pr-01.

3.2.2.4 Nuclear Magnetic Resonance Studies

Samples were prepared by dissolving 10 – 20mg of extract into approximately 500µl of $CDCl_3$. The solution was filtered through cotton wool to remove any insoluble material prior to analysis. ^1H NMR and ^{31}P NMR spectra were recorded using either the JEOL GX 270 (operating at 270.2MHz for ^1H) or the JEOL EX 400 (operating at 399.8 MHz for ^1H and 161.8 MHz for ^{31}P) spectrometers. Chemical shifts were recorded in parts per million on the δ scale. The ^1H NMR and ^{31}P NMR spectra were referenced internally using TMS for ^1H and ^{31}P.

3.2.2.5 Mass Spectrometry

The mass spectra were recorded using a VG AutoSpec Q instrument. Electron impact (EI) ionization was performed at 70 eV and <70 eV, while high- and low-resolution fast-atom bombardment (FAB) used *m*-nitrobenzyl alcohol (mNBA) as the securing matrix within which the sample is held.

3.3 RESULTS & DISCUSSION

3.3.1 Mass of Extract

Comparison of the values reported in the literature for the lipid content of starches shows that the results vary widely (Taylor and Nelson, 1920; Lindeman 1951; Morrison and Coventry, 1985; Vasanthan and Hoover 1992). This may be attributed to factors that were not quantified in previous studies such as starch granule damage and the age of the granules, which are known to influence lipid content (Morrison and Gadan, 1987; Mc Donald et al, 1991). For this reason such a comparison with literature values shall not be attempted.

As can be seen from figure 3.2 polar solvents, such as methanol, remove more lipid than non polar solvents such as hexane. This result is in agreement with trend identified in earlier work (Schoch, 1942). The same effect was observed on defatting with a binary solvent system of ethanol and distilled water. Figure 3.3 shows that quantity of extract recovered increases as the proportion of ethanol in the solvent system is reduced. The polarity of such solvent systems is described in section 2.3.3.

In one series of experiments, Starch 1500 was defatted with two different solvent systems. The rationale for this is described in section 2.3.6. As can be seen in figure 3.4, more lipid is removed during extraction with absolute ethanol in DF48-99(He) than in DF48-(He)99. At first this may seem surprising as some lipid has already been extracted with hexane. However it is possible that this initial treatment with hexane resulted in a reduction in the structural integrity of the material (section 5.3.2.3). Such a modification may allow lipid to be extracted more efficiently by a second solvent such as absolute ethanol. Furthermore it is suggested that in the case of hexane its non-polar nature acts as the rate-limiting step to extraction, rather than granule integrity. This is exemplified by a negligible difference in the quantity of lipid extracted by hexane in both solvent systems.

A similar approach was taken to explaining the results shown in figures 3.5 and 3.6. Figure 3.5 illustrates that more lipid is removed with 96% ethanol in the standard Soxhlet extractor than in the giant apparatus. This effect may be caused by the difference in extraction thimble dimensions. A smaller surface area for extraction is available with the larger thimbles and as such lipid removal may be retarded. This difference is observed when using a polar solvent such as ethanol, yet less polar solvents such as propan-1-ol and hexane may act as the rate-limiting step to lipid extraction rather than the effective surface area.

As can be seen from figure 3.6 more extract is removed from native maize starch than from Starch 1500, using the ethanolic solvent systems. There is a negligible difference in the quantity of lipid extracted when using hexane in native maize starch and Starch 1500. It is possible that some lipid is lost during the production of Starch 1500 from native maize starch, as a result lower extract yields would be expected from the modified material. Furthermore the difference in particle morphology of the two materials may influence the rate of lipid extraction. Native maize starch has a higher surface area and lower bulk density than Starch 1500 allowing the solvent to penetrate the powder bed more easily. These properties may increase the rate of extraction, leading to greater yields than those obtained from Starch 1500.

The difference in lipid yields is most apparent on defatting with absolute (99.7 – 100%) ethanol, where native maize starch yields more than twice the mass of extract than is removed from Starch 1500. Here, the surface area and the packing of the powder bed may act as the rate-limiting step to lipid removal. Upon defatting

with 70% ethanol, the quantity of lipid removed from both native maize starch and Starch 1500 increases, however the difference between the yields is reduced. This may be attributed to the use of a more polar solvent system, which can remove lipid more effectively. As a result the influences of particle morphology become less significant as the solvent's polarity once more becomes the rate-limiting step to extraction.

Treatment of Starch 1500 using SCF techniques yielded only 0.013g of extract per 100g of Starch 1500. Further treatment with absolute ethanol yielded 0.2479g of extract per 100g of Starch 1500. This indicated that the conditions used for SCF extraction were not optimized for the removal of lipid.

Figure 3.2: Effect of Solvent Polarity on Extraction Efficiency

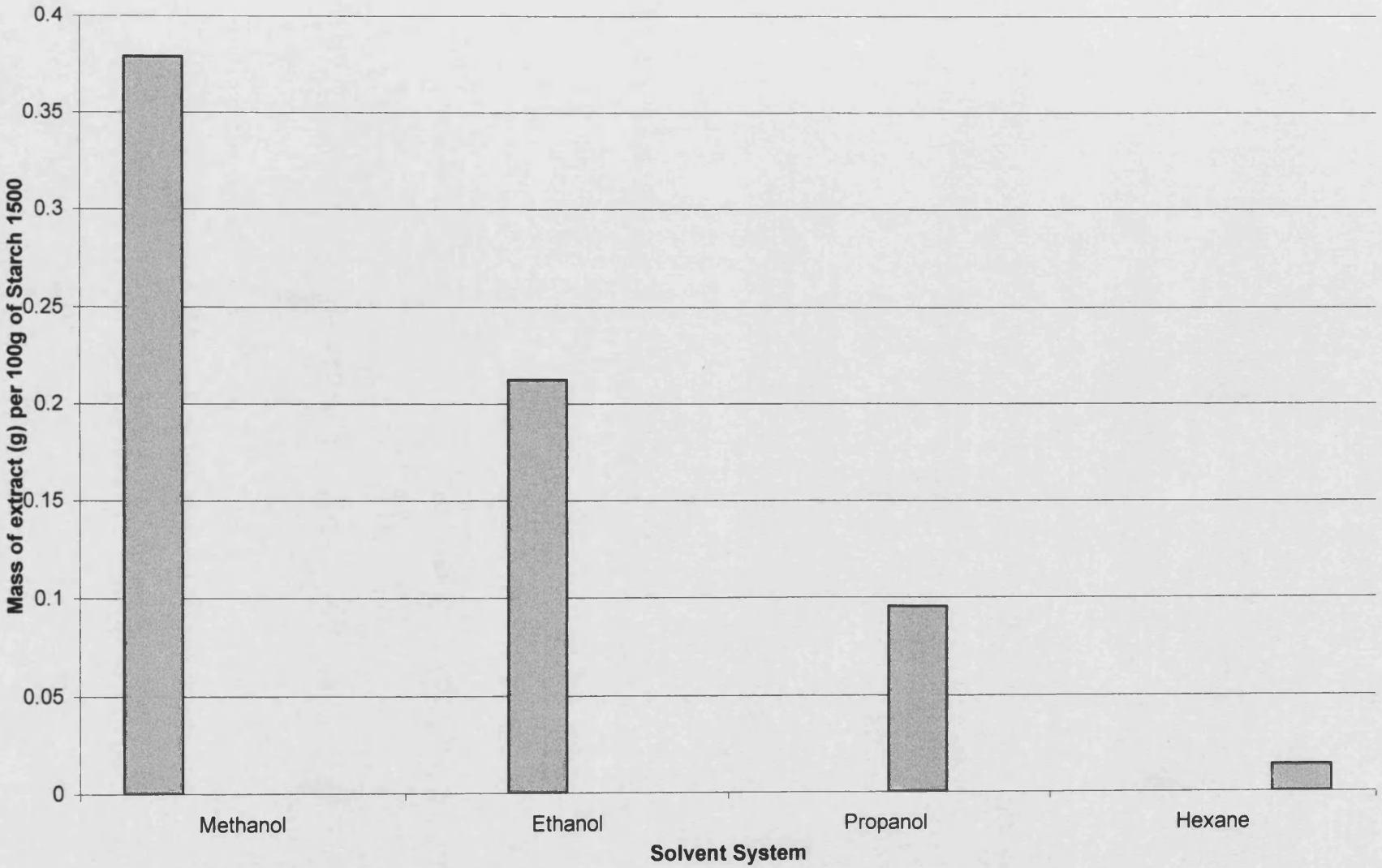

Figure 3.3: Effect of Ethanol Concentration on Extraction Efficiency

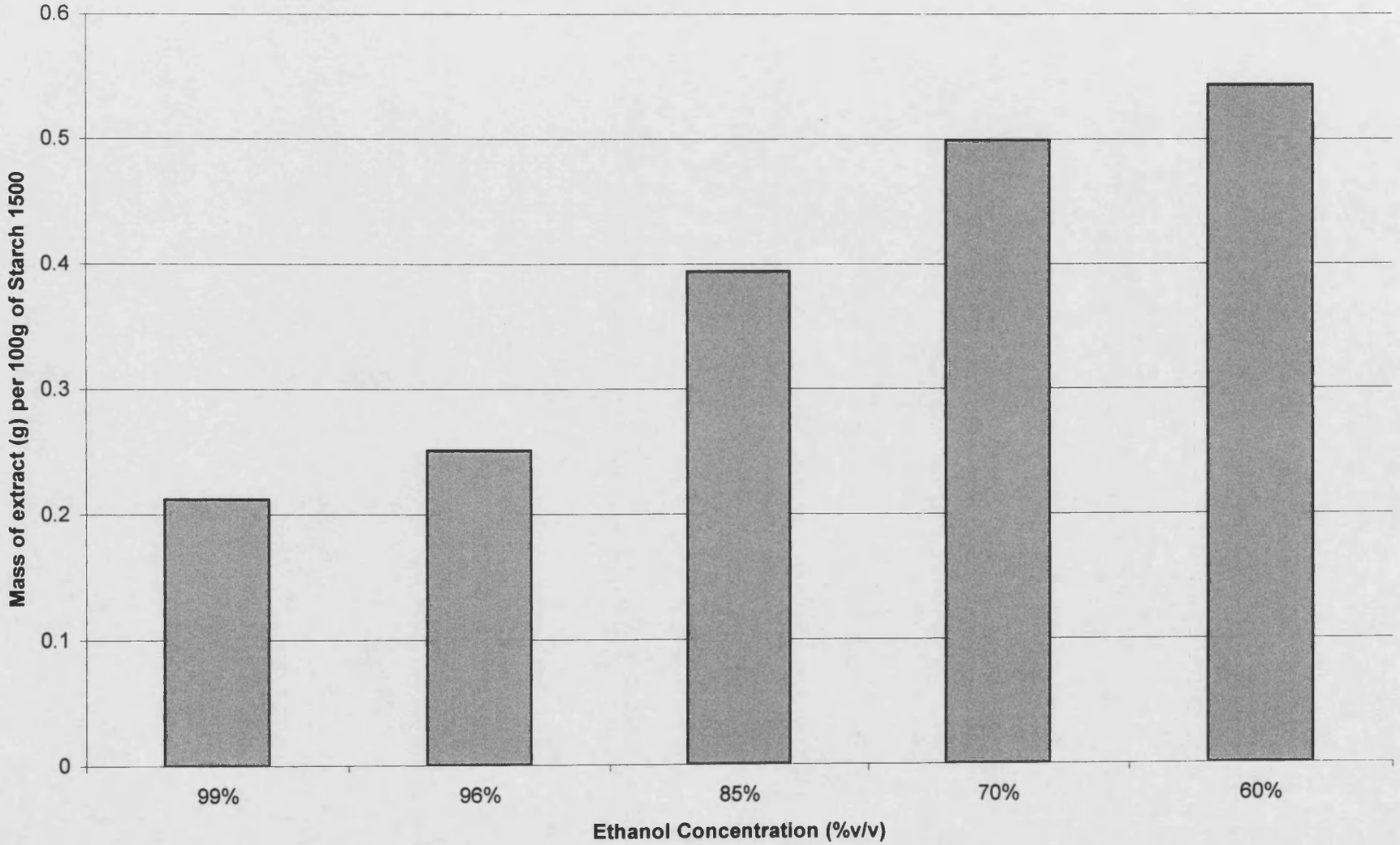

Figure 3.4: Comparison of the Mass of Extract for DF48-99(He) and DF48-He(99)

Figure 3.5: Comparison of extraction efficiency of Giant and Standard Soxhlet Extractors

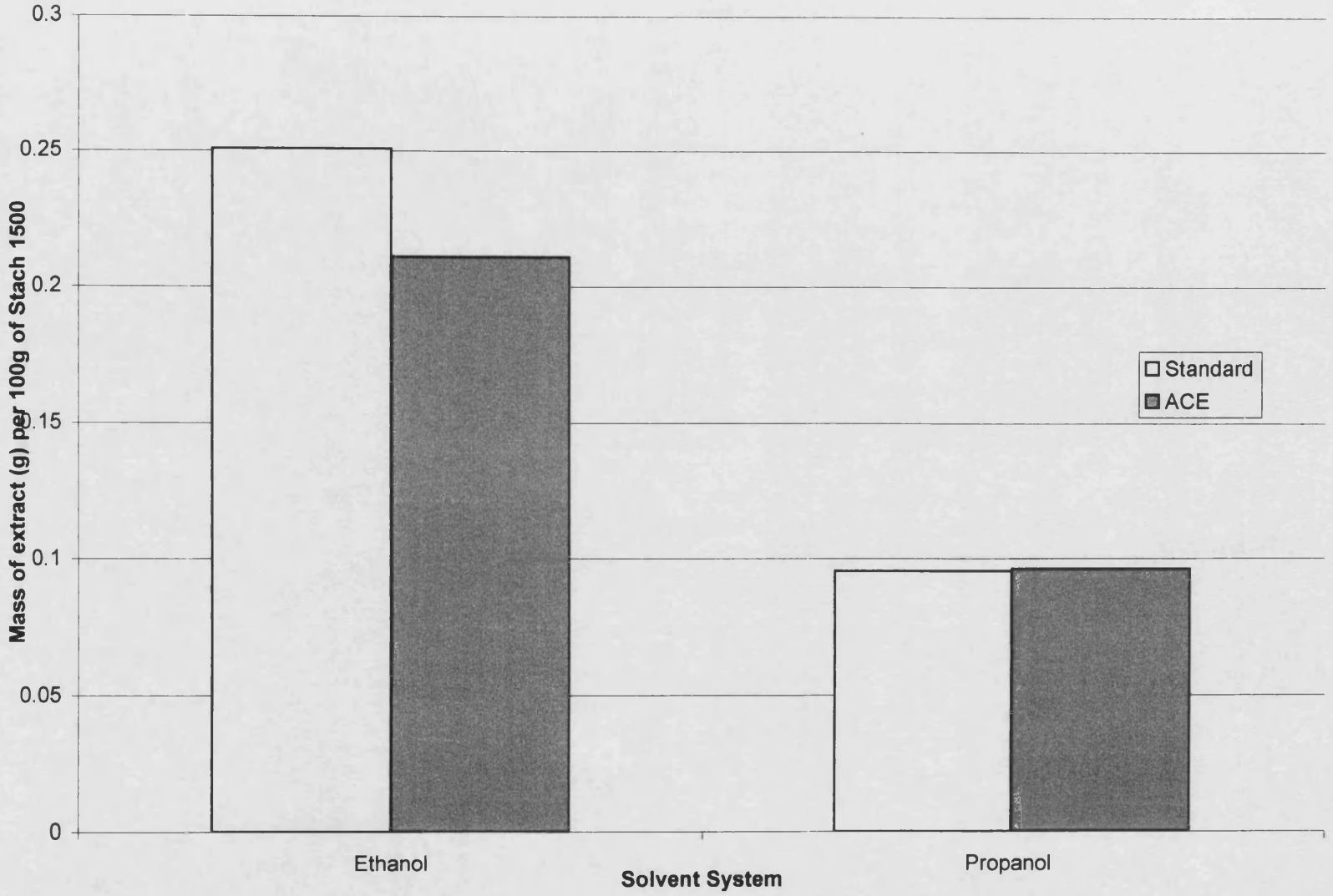

Figure 3.6: Mass of extract from Starch 1500 and Native maize Starch using several solvent systems

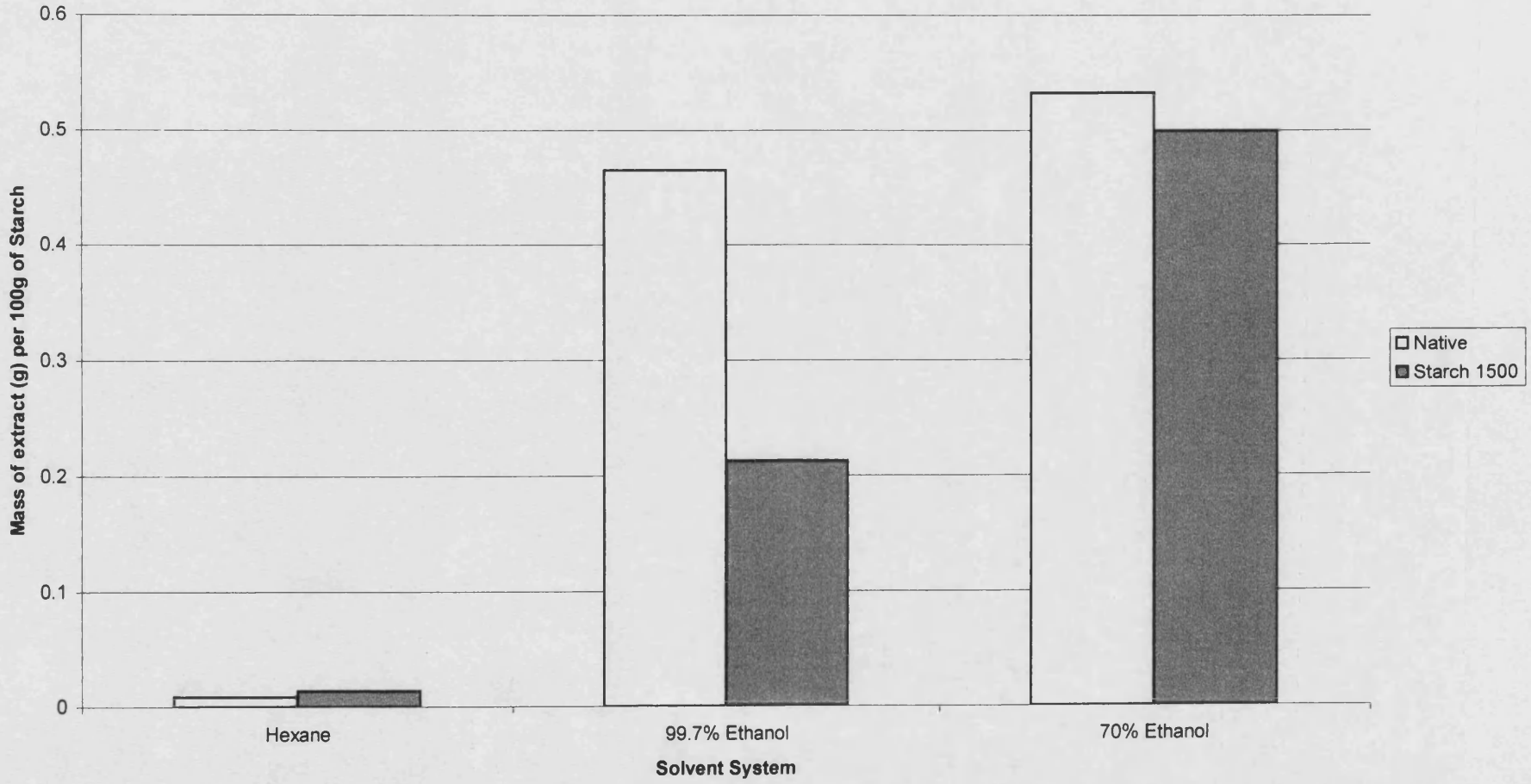

3.3.2 Thin Layer Chromatography (TLC)

A solvent system composed of hexane and ethyl acetate 60:40$^{v}/_{v}$ allowed the separation of the constituents of DF48-99-01 and DF48-Pr-01. The Rf values for the extracts are given in Table 3.1. Anisaldehyde allows the identification of oxygen containing group, whereas bromocresol green stains for acidic groups. Two major (Rf: 0.68 and 0.38) and two minor components (0.52 and 0.15) were identified in DF48-99-01 using the anisaldehyde stain. The Rf values of 0.43 and 0.38 in DF48-99-01 are possibly representative of the same constituent. It is therefore proposed that DF48-99-01 is composed of 4 oxygen-containing species, one of which is an acid. Equally if the Rf values of 0.44 and 0.46 in DF48-Pr-01 are indicative of the same constituent, this extract is comprised of 2 oxygen-containing species, one of which is an acid. The lipids present in cereal starches contain high proportions of monoacyl lipids (Morrison et al, 1981), thus it is possible that the TLC results indicate the presence of a free fatty acid and several related fatty acid esters.

Table 3.1: Rf values for DF48-99-01 and DF48-Pr-01

DF48-99-01		**DF48-Pr-01**	
Bromocresol Green	**Anisaldehyde**	**Bromocresol Green**	**Anisaldehyde**
0.43	0.68	0.46	0.73
	0.52		0.44
	0.38		
	0.15		

3.3.3 Gas Chromatography/Mass Spectrometry (GC/MS)

The results for the analysis of the extracts by GC/MS are summarised in appendix 2. The quality of the matches between the extracted compounds and the library of mass spectra used by the GC/MS software is stated in percent. In general, the quality of the match was reduced by the presence of additional peaks in the mass spectra of the extracted materials. These may result from solvent impurities.

As can be seen from appendix 2, the major constituents of the extracts are esters of hexadecanoic acid and octadecadienoic acids. This is in agreement with the results obtained by TLC and the previous findings of Vasanthan and Hoover (1992). Although monoacyl lipids are inherent in cereal starches (Morrison, 1981) it is possible that some degree of esterification occurs during extraction with ethanolic solvents. This is exemplified by the presence of ethyl esters in DF48-99-01 and

DF48-99-02 and propyl esters in DF48-Pr-01, DF48-Pr-02, DF48-Pr-03 and DF48-Pr-01A. In general, a greater proportion of constituent compounds were seen in the extracts, which were derivatised prior to analysis. This is demonstrated in illustrated in DF48-99-01. However is it noteworthy that methylation did not ensure the reproducibility of results. This can be seen on comparison of the derivatised samples DF48-99-01 and DF48-99-02.

The composition of the derivatised extract of NS48-99-01 is similar to that of DF48-99-01 and DF48-99-02 indicating that Starch 1500 production has little effect on lipid content of the material. There was no evidence of lipid detected by GC/MS for the supercritical fluid extracted Starch 1500 sample (SFE-01). However treatment of this material with absolute ethanol by Soxhlet extraction (SFE-99) resulted in the extraction of methyl esters of hexadecanoic acid, 9,12-octadecadienoic acid and 9-octadecenoic acid. This result suggests that SFE failed to remove any detectable quantity of lipid from Starch 1500 and as such may explain why the tensile strengths of compacts prepared from this material were comparable to those of unmodified Starch 1500 (Table 2.3).

3.3.4 Nuclear Magnetic Resonance Studies

Figures 3.7 to 3.11 show the 1H NMR spectra of the lipid extracts from DF48-Me-01, DF48-99-01, DF48-96-01, DF48-Pr-01 and NS48-99-01. Table 3.2 details the 1H NMR chemical shifts, which were common to all 5 spectra. This evidence supports the results obtained by GC/MS in that the signals displayed in the NMR spectra can be attributed to functionalities of the 2 major compounds identified in the extracts, namely the esters of hexadecanoic acid and 9,12-octadecadienoic acid.

Table 3.2: ^{1}H chemical shifts common to the spectra shown in figures 3.7 to 3.11

Functional Group	Literature Value (δ_H)
CH_3-R	0.9
R-**CH_2**-R	1.4
R-**CH_2**-CH_2-CO-O-R	1.6
R-**CH_2**-C=C	2.0
R-**CH_2**-CO-O-R	2.2
R-CH=CH-**CH_2**-CH=CH-R	2.7
R-**CH=CH**-R	5.4

Figure 3.7: Nuclear magnetic resonance spectra for DF48-Me-01 extract

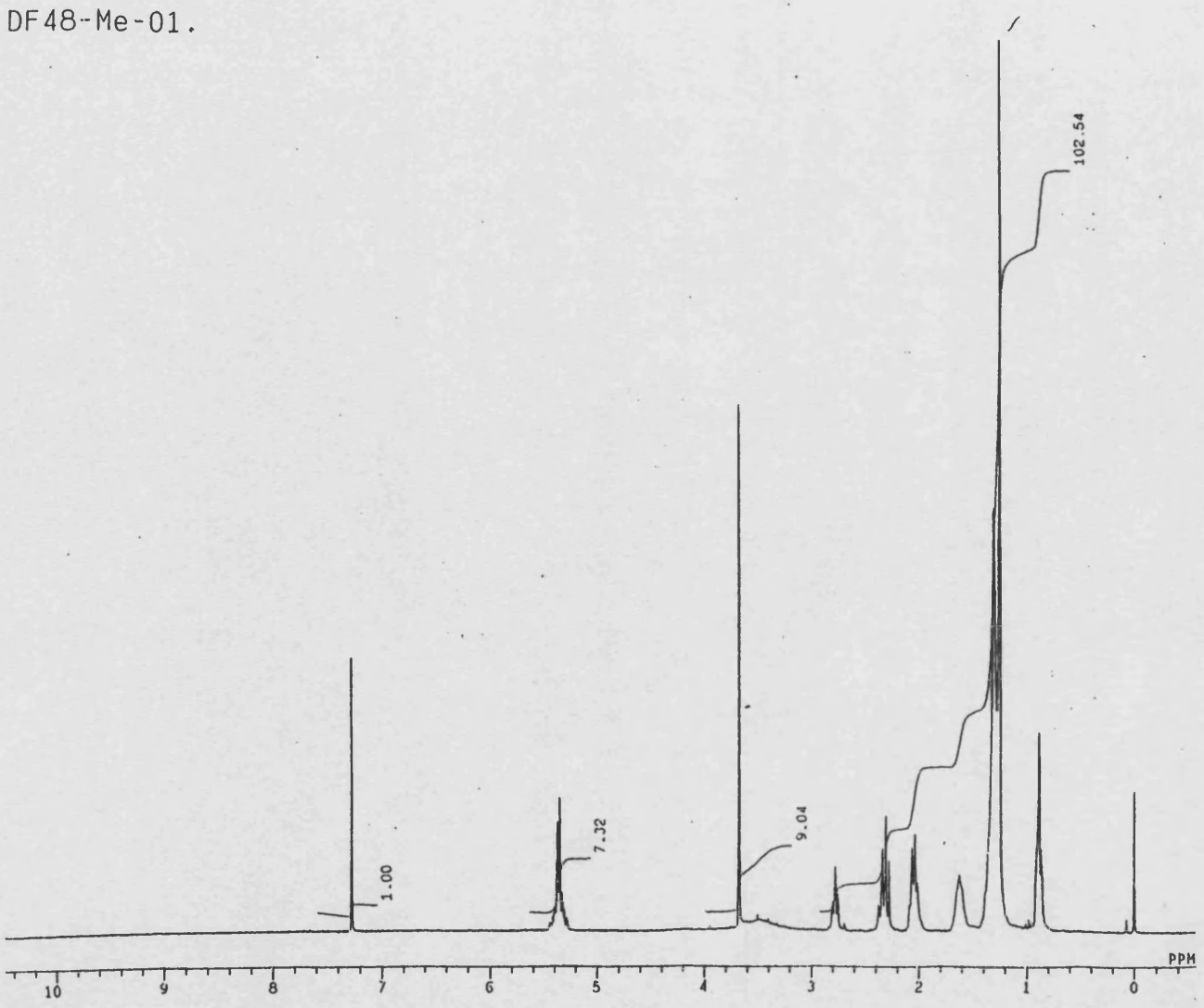

Figure 3.8: Nuclear magnetic resonance spectra for DF48-99-01 extract

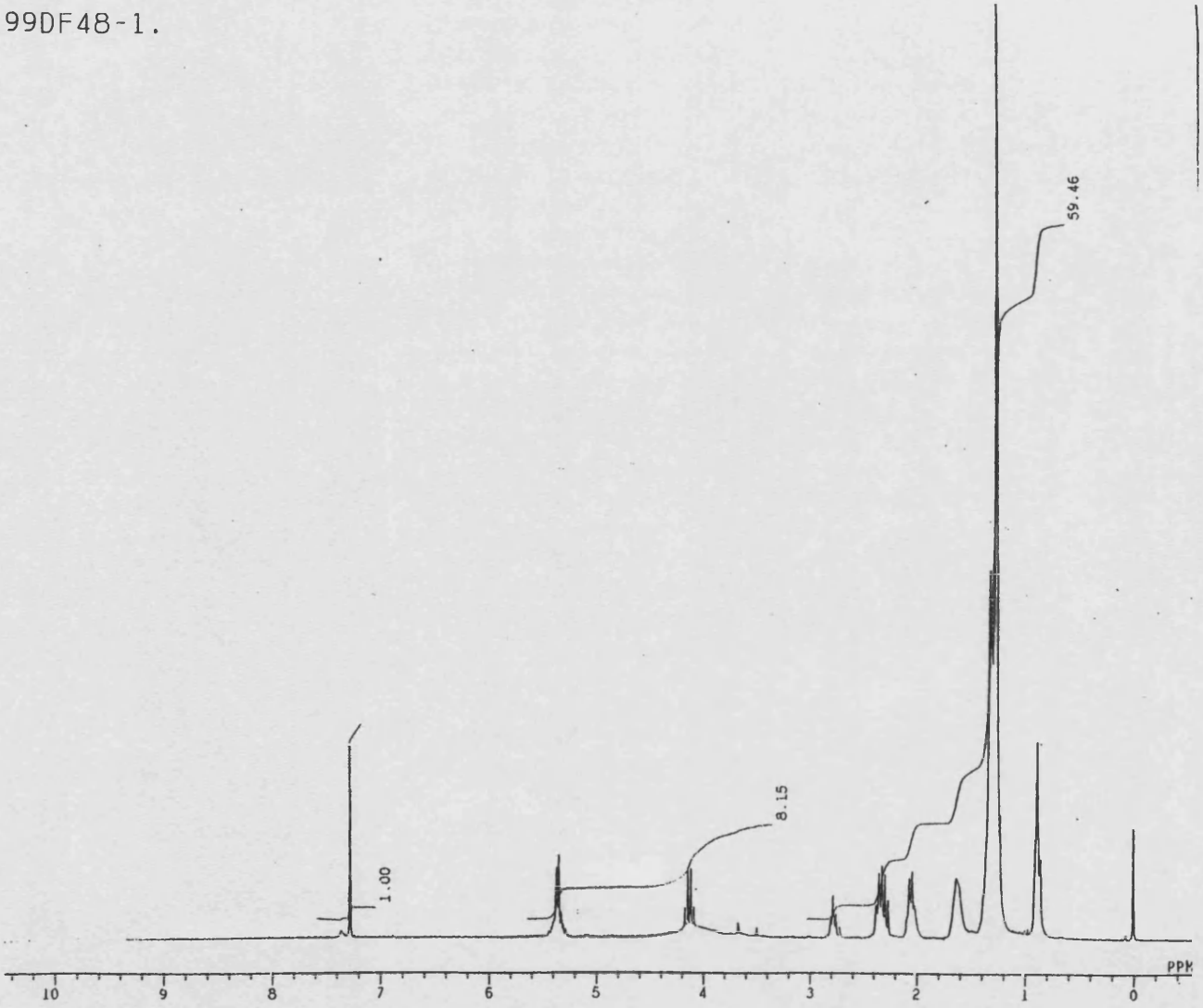

Figure 3.9: Nuclear magnetic resonance spectra for DF48-96-01 extract

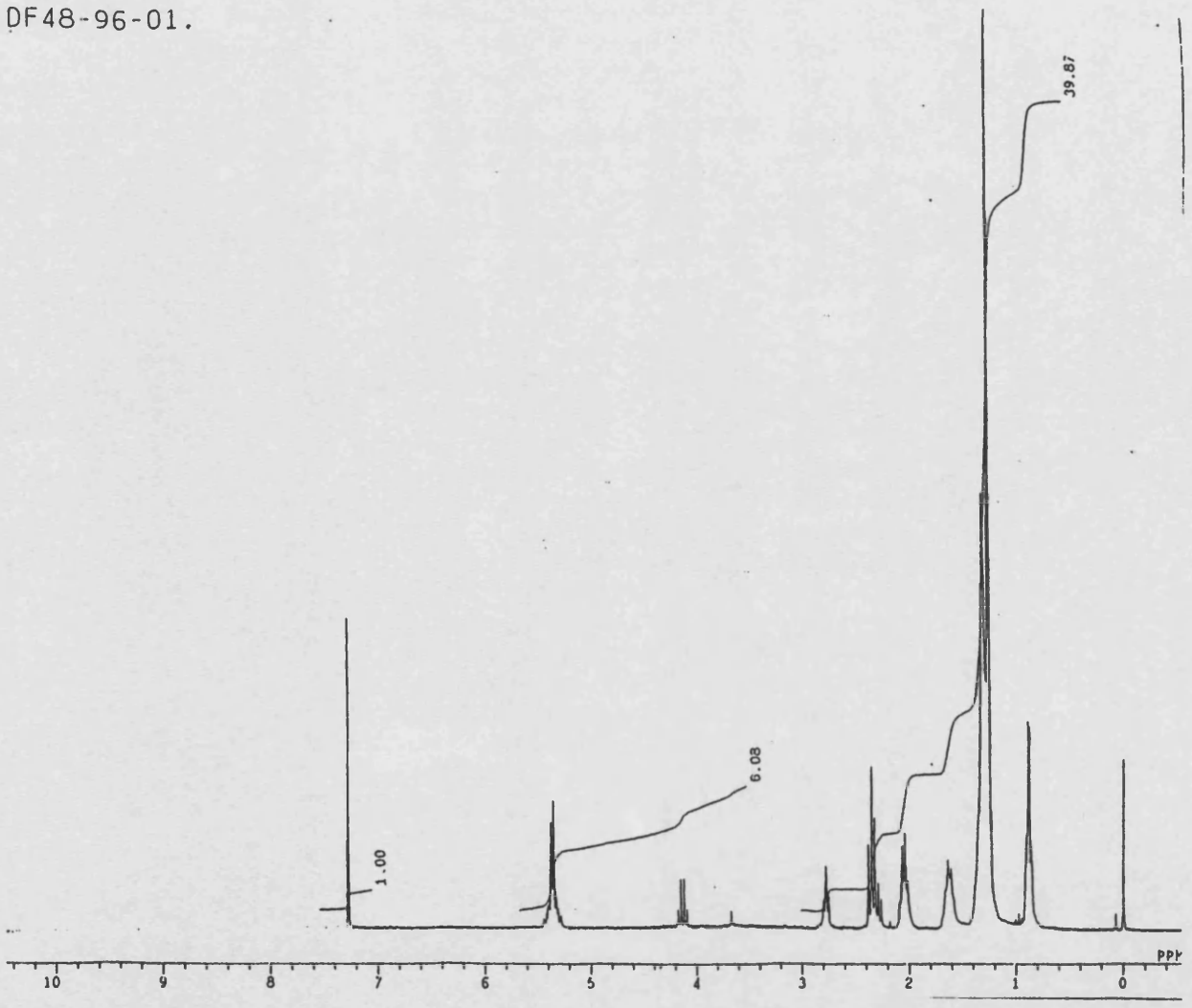

Figure 3.10: Nuclear magnetic resonance spectra for DF48-Pr-01 extract

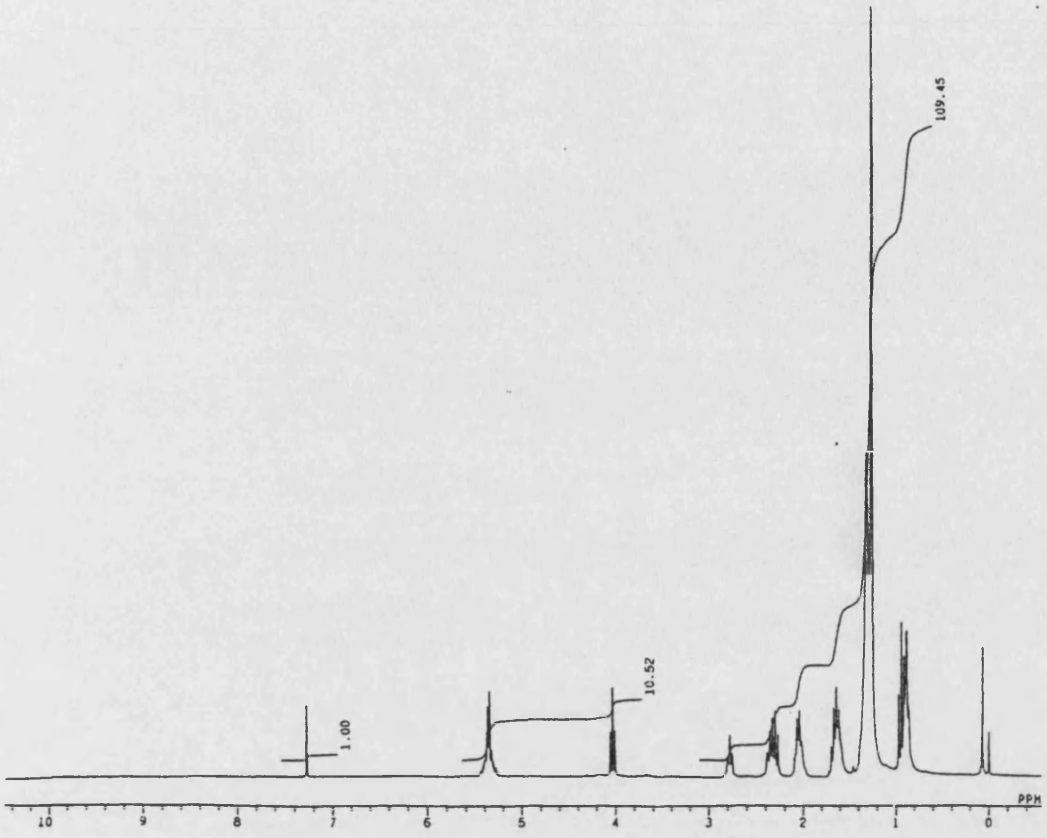

Figure 3.11: Nuclear magnetic resonance spectra for DF48-99-01 extract

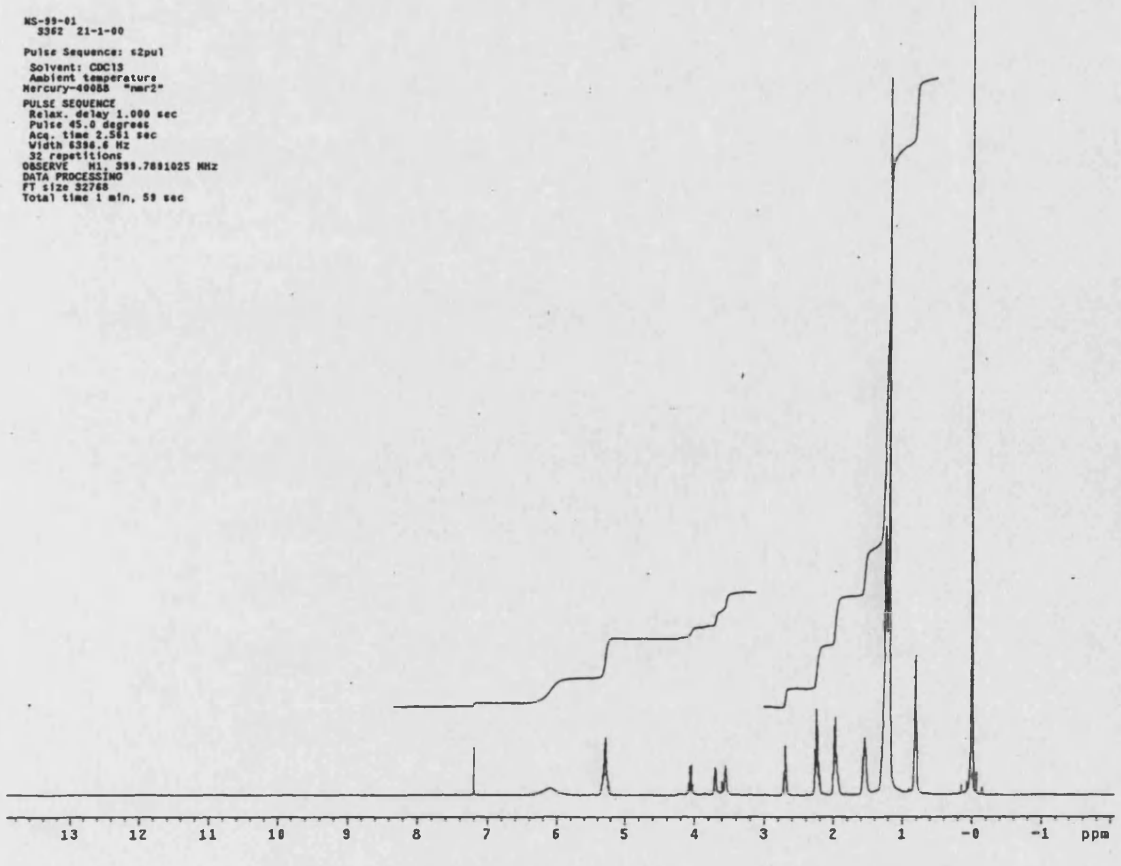

The signal at δ 7.25 results from residual chloroform in the deuterated solvent, $CDCl_3$ .The signal at δ 3.7 in the ^1H NMR spectra for DF48-Me-01 may be attributed to the protons of a methyl ester group. This signal is missing from the other four spectra but is replaced by a quartet at δ 4.1, which is indicative of a methylene group on an ester. It has been suggested that partial esterification occurs during Soxhlet extraction of fatty acids with various alcohols. Thus the signal at δ 4.1 be attributed to the methylene groups of ethyl and propyl esters.

The ^{31}P NMR spectra for DF48-99-01 and NS48-99-01 were absent of any signals, thus qualifying the GC/MS and mass spectrometry results, which did not identify the presence of phosopholipids in the extracts. This is contrary to the finding of previous groups that also isolated glycolipids as a major constituent of cereal starch lipids (Morrison, 1981; Galliard and Bowler 1987; Vasanthan and Hoover, 1992). The absence of phosphorus-containing compounds from both native maize starch and Starch 1500 suggests that this material is not lost during the production of the commercial material. Alternatively it is possible that the phospholipids may be lost during the processing of native starch from maize.

3.3.5 Mass Spectrometry

The EI mass spectra for DF48-Me-01, DF48-99-01 and DF48-96-01 are given in figures 3.12 to 3.14. By comparing these spectra with those obtained using GC/MS it was possible to identify the compounds present in each extract. The results are summarized in table 3.3. The constituents of DF48-96-01 were identified from the GC/MS result of other compounds extracted with 96% ethanol.

Table 3.3 Composition of lipid extracts as identified by EI Mass Spectrometry

Extract	m/z	Compound
DF48-Me-01	294	9,12 Octadecadienoic acid, methyl ester
	270	Hexadecanoic acid, methyl ester
DF48-99-01	284	Hexadecanoic acid, ethyl ester
	312	Octadecanoic acid, ethyl ester
DF48-96-01	256	Hexadecanoic acid,
	284	Hexadecanoic acid, ethyl ester
	308	9, 12 Octadecadienoic acid, ethyl ester

Figure 3.13: Mass spectrometry trace for DF48-99-01 extract

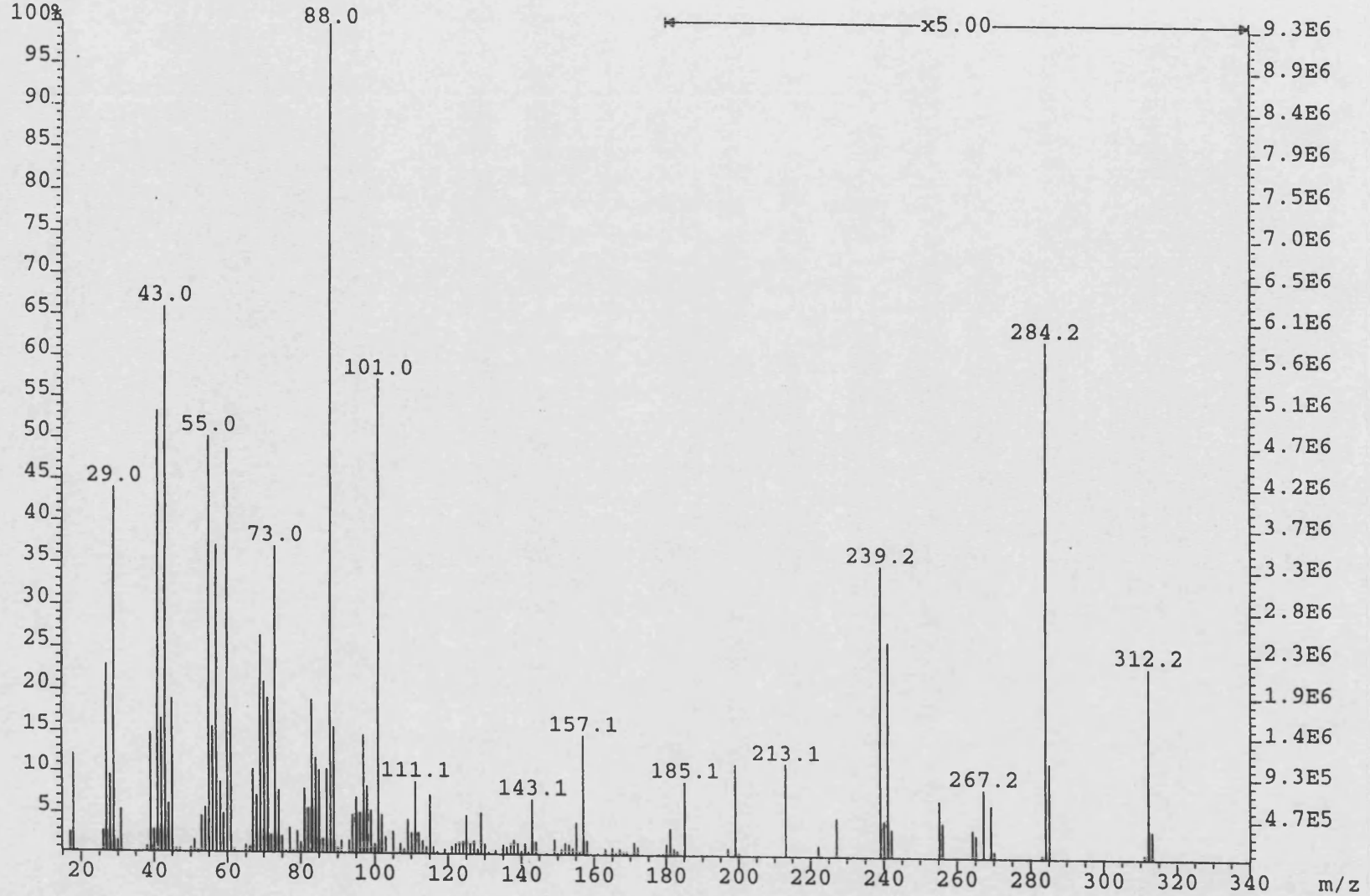

Figure 3.12: Mass spectrometry trace for DF48-Me-01 extract

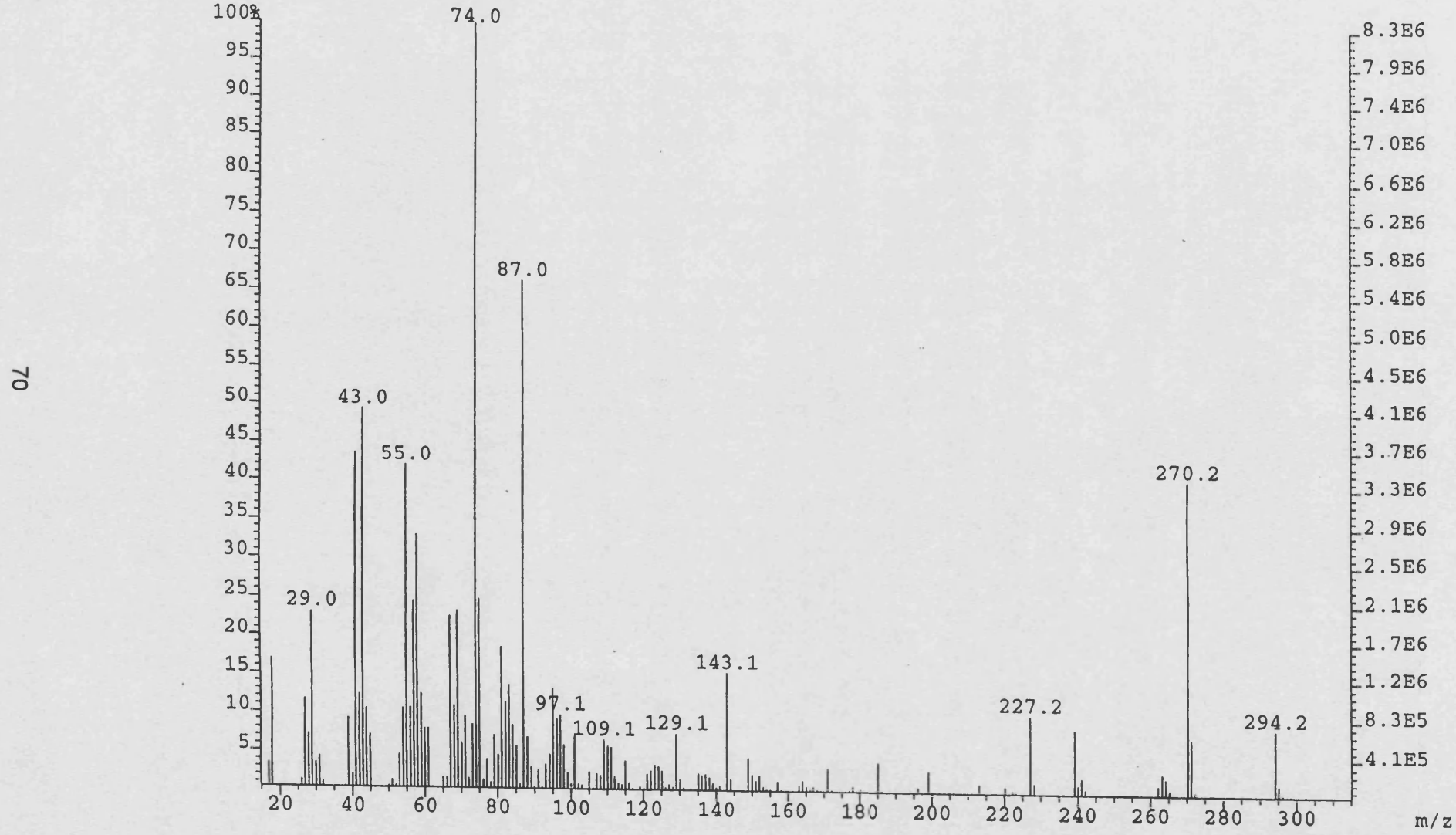

Figure 3.14: Mass spectrometry trace for DF48-96-01 extract

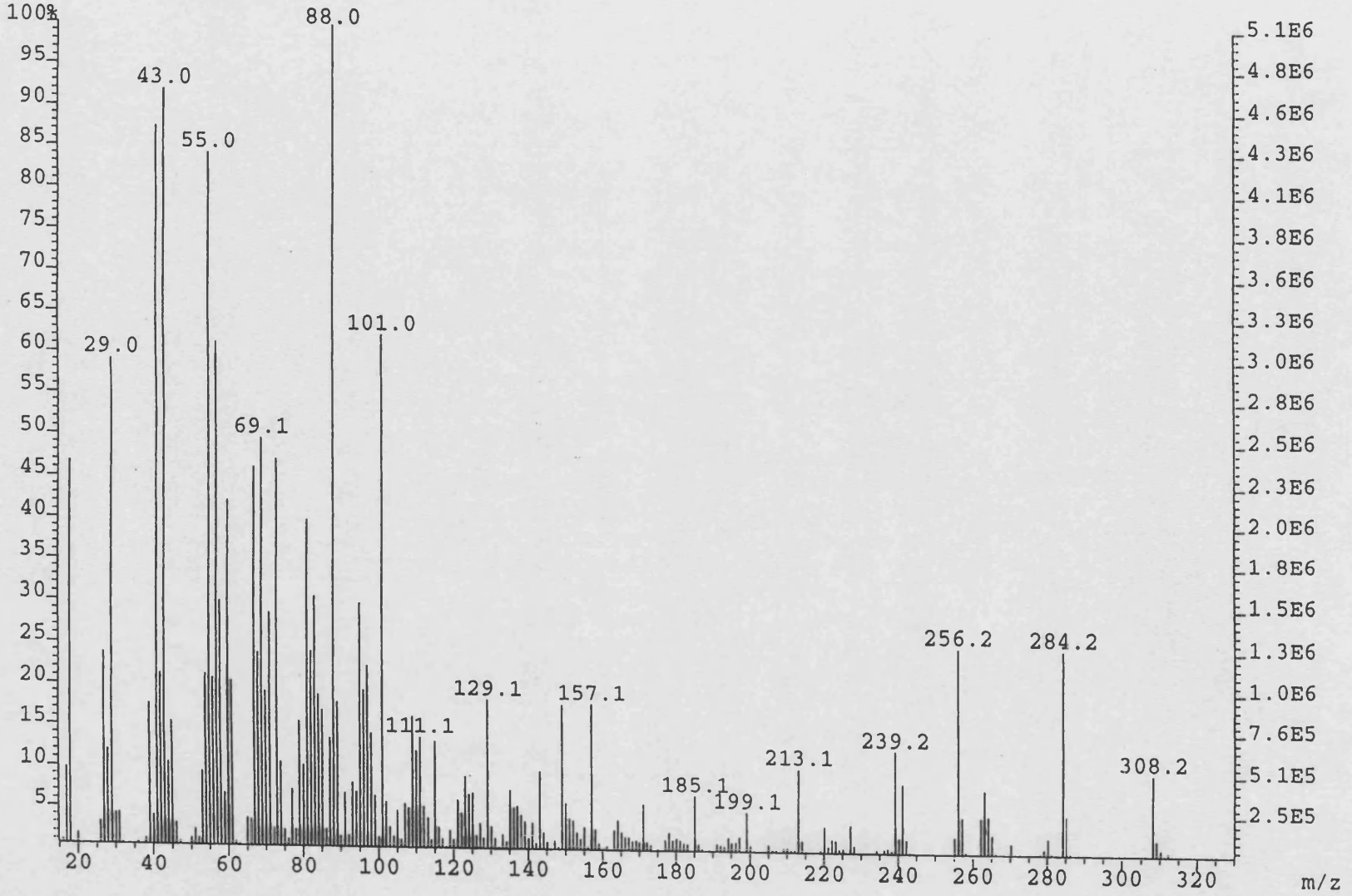

Mass spectrometry allowed the identification of several constituents of the lipid extracts, the most common of which were esters of hexadecanoic acid. The GC/MS results indicated that more compounds were present than were identified by this technique.

3.4 GENERAL DISCUSSION

GC/MS analysis allowed the identification of the constituents of the extracted from defatted native maize starch and Starch 1500. Techniques such as thin-layer chromatography, ^{1}H NMR and mass spectrometry provided further evidence to support these findings. The two major constituents of the extracts were esters of hexadecanoic acid and 9,12-octadecanoic acid. The choice of solvent seemed to determine the quantity of lipid removed rather than the composition of the extract. The quantity of lipid removed correlated well with both solvent polarity and the tensile strength of the compacts formed from the defatted material.

CHAPTER 4

MATERIALS AND GENERAL CHARACTERISATION METHODS

4.1 General Introduction

This chapter deals with the physical characterisation of Starch 1500 both as received from the supplier and that, which has been subjected to various defatting techniques which were outlined in chapter 3. This chapter will concentrate on the analysis of the bulk powder properties using both well-established techniques such as particle size and surface area analysis. Furthermore, the use of novel techniques such as thermogravimetry coupled with mass spectrometry will be used to assess the effect of solvent treatment on Starch 1500.

4.2 Materials

Starch 1500, lot number 710057 as supplied by Colorcon Ltd. Indianapolis, Illinois, U.S.A. was the subject of the initial characterisation studies. Colorcon Ltd. also supplied a sample of the native maize starch (lot number 135) that was used for the production of Starch 1500.

4.3 Methods

4.3.1 Particle size analysis

Initial studies of the particle size distribution of Starch 1500 were performed using the techniques of low angle laser light scattering (LALLS) and time-of-flight aerosol beam spectroscopy (TOFABS).

4.3.1.1 Low Angle Laser Light Scattering

Instruments, which operate using the principle of LALLS, calculate particle size distribution (by volume) from the pattern and intensity of scattered light from a dispersed powder system passing through a laser beam. The Mastersizer X (Malvern Instruments Ltd., Malvern, U.K.) employs a helium-neon laser beam (λ = 633 nm) that is shone through a cell in which the particles are suspended (Diffraction Training, 1993). The scattering of particles is predicted by the Mie theory (Zhang and Xu, 1992) and such information may be used to calculate particle size (Diffraction Training, 1993). The theoretical particle size, which most closely fits the experimental pattern, is presented by the instrument (Diffraction Training, 1993).

LALLS investigations were performed using the Mastersizer X equipped with a dry powder feeder and attached to a vacuum cleaner (Electrolux Power System 1500W), with cyclone attachment. This set-up creates an airstream, which transports the fluidised particles across the path of the detecting laser beam.

Approximately 2-3mg of Starch 1500 was drawn through the dry powder feeder at a flow rate of approximately 100 litres min^{-1}. Particle size analysis in air was chosen rather than analysis in liquid media as alterations in particle size distribution may occur through dissolution and/or swelling of the material (Hindle and Byron, 1995). The average of 5 repeat, particle size analyses of Starch 1500 using the Mastersizer X is summarised in table 4.1.

Table 4.1: Particle size distribution of Starch 1500 determined by LALLS

Size Range (μm)	% In-size
0.5 - 25.46	32.495
25.46 - 56.09	26.322
56.06 - 101.44	25.263
101.44 - 150.57	11.083
150.57 - 272.31	4.152
272.31 - 492.47	0.665

Deaggregation occurs during the fluidisation of the particles within the airstream and is dependent on the amount of shear that is generated by a vacuum cleaner. This variable may not be directly controlled and as such the reproducibility of test conditions is questionable.

4.1.1.1 Time of Flight Aerosol Beam Spectroscopy (TOFABS)

The particle size distribution of Starch 1500 was also assessed by the technique of TOFABS (Niven, 1993) using an Aerosizer® equipped with an Aerodisperser® (API, Hadley, MA. U.S.A.). The Aerodisperser® is a computer controlled variable shear particle deaggregator which disperses the powder into an airstream which then channels the particles, carrying them to the Aerosizer® where they are detected. In the Aerosizer®, particles are accelerated to their terminal velocities and their aerodynamic diameter is determined by measuring the transit time between two laser beams (Mitchell and Nagel, 1996).

The Aerodisperser® allows direct control of the shear forces applied to the dispered powder. This may be achieved by varying the pressure drop across the annular gap between the disperser pin and the pin bowl (Hindle and Byron, 1995). Based on the initial data gained using the Mastersizer X and on the evidence of previous work (Hindle and Byron, 1995), the optimum operating parameters were determined

as those, which gave the least variability between results. The operating parameters chosen for Starch 1500 and native maize starch particle size analysis are summarised in table 4.2. A low shear rate was chosen for Starch 1500 based on it`s large particle size and distribution. Samples of Starch 1500 were analysed under normal deagglomeration conditions and with pin vibration disabled to reduce potential damage to large Starch 1500 agglomerates which were identified by low temperature scanning electron microscopy (section 5.3.2.2). The run conditions for native maize starch were selected on the basis of its low particle size and and cohesive nature. A high shear rate, high deagglomeration and activation of pin vibration were all employed to elicit maximal dispersion of the individual starch granules. The different run times selected for the two materials were chosed based on their particle size distributions. A run time of 600 seconds is recommended for materials such as excipients which show polydisperse particle size distributions (Hindle and Byron, 1995). For materials such as native maize starch which exhibit a much narrower particle size distribution a run time of 180 seconds is sufficient for particle size analysis.

Particle size analysis using the Aerosizer® was deemed to be the more appropriate method owing to the greater control of such operating variables. Using a sample thief, Starch 1500 was extracted from different depths of the powder bed and analysed for the uniformity of the distribution. The particle size analysis data given in appendix 3 details the aerodynamic diameter based on volume frequency distribution of Starch 1500. The true densities of the powders (which are required be the instrument to calculate particle size) were determined by helium pycnometry (section 4.3.4).

Table 4.2: Aerodisperser® Operating parameters for Starch 1500 and native maize starch particle size analysis by TOFABS

	Starch 1500	Native Maize Starch
Shear Rate	1.0	4.0
Run Time (sec)	600	180
Deagglomeration	Normal	High
Pin Vibration	Off	Normal
Feed Rate (particles sec^{-1})	5,000	5,000

One-way analysis of variance was performed in conjunction with Fisher's pairwise comparisons on the data given for Starch 1500 in appendix 3. As may be seen from table 4.3, analysis revealed that there was no significant difference between samples taken from different depths of the powder bed for each particle size range

Table 4.3: One-way analysis of variance performed in conjunction with Fisher's pairwise comparisons on Starch 1500 particle size distribution data (appendix 3)

Aerodynamic Diameter (μm)	F	P
0.5 – 20.0	1.14	0.37
20.0 – 50.1	0.53	0.72
50.1 – 70.2	1.32	0.30
70.2 – 90.2	1.00	0.43
90.2 – 145.0	0.44	0.78
145.0 – 200.0	0.96	0.46

Particle size analysis data obtained for a range of defatted Starch 1500 samples is also given in appendix 4. The particle size distributions of these materials were analysed using the sample parameters as for unmodified Starch 1500. Table 4.4 details the results of the one-way analysis of variance data performed in conjunction with Fisher's pairwise comparisons of the particle size distributions for unmodified and defatted starch 1500 samples. Statistical analysis revealed significant ($P < 0.05$) differences between the particle size distributions of Starch 1500 and DF48-Me-02, DF48-96-01, DF48-Pr-02 and DF48-Bu-01 in the range of 50.1 to 70.2μm.

Figure 4.1 shows a typical particle size distribution for Starch 1500 and native maize starch obtained by TOFABS. The native maize starch powder sample fitted a normal distribution, the mean particle diameter was 17.12μm (standard deviation 1.33 μm) and the observed values agree with published results (Swinkels, 1985). Starch 1500 shows a bimodal distribution It has been reported that an average particle size cannot be given for Starch 1500 due to a wide range of particle sizes and highly variable particle morphology (Wurster et al, 1982). The peak between 10 and 20 μm correlates well with that for the particle size distribution of native maize starch and is likely to result from native granules present in Starch 1500.

Figure 4.1: Particle size distribution for Starch 1500 and native maize starch

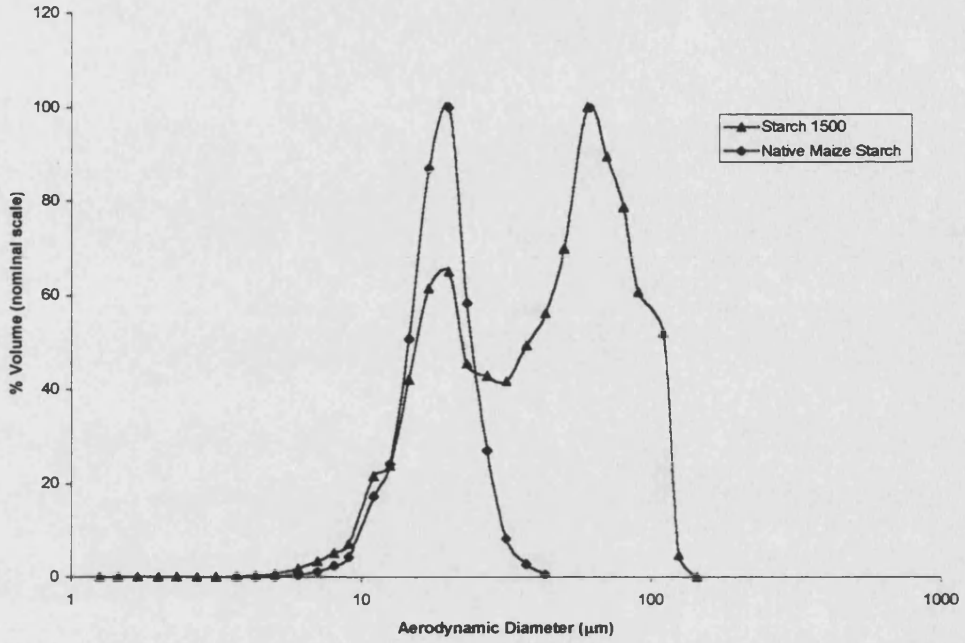

4.3.2 Surface area analysis

The surface area of Starch 1500 was determined using a Gemini 2360 Analyser (Micromeritics Instrument Corporation, Norcross, GA, U.S.A.). The surface area is determined by measuring the pressure differential of the adsorbate (nitrogen) gas between the sample tube and an empty (blank) tube of identical dimensions. Filler rods were placed in both sample tubes to minimise the headspace volume, thus reducing the error of the measurements (Webb and Orr, 1997). Isothermal conditions were achieved by performing the analysis in liquid nitrogen.

Accurately weighed samples were loaded into the large volume sample tubes (volume: 12 cm^3) and degassed at 70°C for a period 16 hours using a FlowPrep 060 Degasser (Micromeritics Instrument Corporation, Norcross, GA, U.S.A.). After degassing, the samples were reweighed at the dry mass was used for subsequent surface area determinations. The observed weight losses on degassing were in the order of 10-12$^{w}/_{w}$, which correlated well with loss on drying studies (section 4.3.3) and thus were deemed to be capable of removing pre-adsorbed gases and vapors from the surface of the solids.

Table 4.5 summarises the results for the specific surface area of Starch 1500 and the defatted materials. The correlation coefficient is deemed acceptable if it is in the range of 0.999 to 1.000 (Webb and Orr, 1997). The C constant is a measurement of the affinity of the adsorbate for the material. Its values usually range from 5 to well above 100. Values of less than 5 are indicative of gas-to-gas affinity competing with gas-to-solid affinity and as such compromising the assumptions of BET theory.

Table 4.5: Specific surface area measurements for Starch 1500 and defatted materials

Run	Adsorption Parameters			Specific Surface Area ($m^2 g^{-1}$)
	C	Intercept	Correlation Coefficient	
Starch 1500	44	0.38	0.9999	0.26
	40	0.40	0.9999	0.27
	38	0.40	0.9998	0.29
	39	0.40	0.9999	0.28
	44	0.38	1.0000	0.26
DF48-Me-02	53	0.18	0.9999	0.45
	48	0.20	0.9997	0.45
	51	0.20	0.9998	0.44
	50	0.19	0.9998	0.46
DF48-96-01	74	0.19	1.0000	0.30
	76	0.18	1.0000	0.31
	70	0.20	1.0000	0.32
	62	0.22	1.0000	0.32
	73	0.20	0.9999	0.31
DF48-96-01A	82	0.16	0.9999	0.32
	77	0.17	1.0000	0.33
	81	0.17	0.9999	0.32
	73	0.18	1.0000	0.33
	68	0.19	1.0000	0.34
DF48-60-01	77	0.20	0.9999	0.28
	67	0.22	1.0000	0.29
	72	0.20	1.0000	0.30
	65	0.22	0.9999	0.30
	69	0.21	1.0000	0.29
DF48-Pr-04	94	0.15	1.0000	0.31
	83	0.17	1.0000	0.31
	80	0.18	0.9999	0.30
	87	0.16	0.9999	0.31
	85	0.16	1.0000	0.31
DF48-Bu-01	79	0.20	1.0000	0.28
	83	0.20	1.0000	0.27
	81	0.19	0.9999	0.29
	70	0.21	1.0000	0.30
	73	0.21	1.0000	0.29
DF48-He-01	63	0.24	1.0000	0.29
	64	0.24	1.0000	0.28
	61	0.25	1.0000	0.28
	60	0.25	0.9999	0.29
	70	0.23	1.0000	0.27

4.3.3 Loss on drying measurements

Materials were conditioned at a relative humidity of approximately 44%, which was maintained by storing the samples in an enclosed system with a saturated solution of potassium carbonate (BDH Laboratory Supplies, Poole, U.K.). Samples were conditioned for at least 48 hours prior to analysis using an infrared moisture balance

(Mettler LP16, Switzerland). The materials were heated at 105°C until no further weight loss occurred (approximately 20 minutes). Analyses were performed in triplicate. Table 4.6 details the loss on drying values for unmodified and defatted Starch 1500.

Table 4.6: Loss on drying (LOD) measurements for unmodified and defatted Starch 1500

Sample	Mean %LOD (n = 3)
Starch 1500	10.4
DF48-Me-02	11.2
DF48-96-01A	12.0
DF48-Pr-03	10.8
SEF-01	9.6
SEF-99	12.2

Table 4.6 shows that no correlation exists between the percent LOD and the polarity (section 2.3.3) of the solvent used for defatting or the mass of lipid removed from Starch 1500 (section 3.3.1). Studies to determine whether the solvent lost on the drying was water or residual solvent from the defatting process in the Soxhlet is discussed in section 4.3.12.

4.3.4 True density measurements

True density measurements were performed using a helium-air pycnometer (Type 1302, Micromeritics Instrument Corporation, Norcross, GA, U.S.A.). Samples were accurately weighed into the sample holder of the helium pycnometer. The powder samples were purged with helium gas prior to the collection of ten sequential density measurements, from which the mean density was determined. These experiments were performed in triplicate and the mean true density values are summarised in table 4.7.

Table 4.7: True density measurements for unmodified and defatted Starch 1500

Sample	Mean True Density (g/cm^3)
Starch 1500	1.496 ± 0.004
DF48-Me-01	1.520 ± 0.004
DF48-99-01	1.506 ± 0.004
DF48-96-01	1.502 ± 0.002
DF48-Pr-01	1.498 ± 0.001
DF48-He-01	1.505 ± 0.002

No significant difference was detected between the true densities of unmodified and defatted Starch 1500 except for DF48-Me-01, which was found to have a higher true density than any of the other samples. This difference was however considered to be of no practical significance with respect to the functionality of the material.

2.2.5 Bulk density measurements

Prior to testing materials were conditioned for a minimum of 48 hours in a controlled environment, maintained at approximately 44% relative humidity. The poured bulk volume of the materials was determined using a standardised method in which the material was poured into a pre-weighed $100cm^3$ glass, measuring cylinder. The bulk density, ρ_o, of the material was determined by dividing the sample mass by the poured bulk volume. Measurements were repeated 3 times with different powder samples thus allowing the mean value of ρ_o to be determined.

Following the determination of the bulk density of the materials, the cylinder and its contents were tapped 500 times using a jolting volumeter (STAV 2003, J. Engelsman, Germany) and the tapped volume of the sample noted. Further tapping was performed in sets of 500 taps until there was negligible change in the volume. The volume showed only minor variations after 1,500 taps. By dividing the tapped volume by the sample mass, the tapped density, ρ_t, was determined. Again this test was repeated 3 times with different powder samples to determine a mean value for ρ_t.

4.3.6 Packing geometry and flowability determination

Equations 4.1 and 4.2 detail the compressibility index (Carr, 1970) and the Hausner ratio (Wells and Aulton, 1988) respectively. These equations can be used to

quantify the flowabilty of a material and are determined from ρ_t and ρ_o as detailed below:

$$\text{Carr's compressibility index} = \frac{\rho_t - \rho_o}{\rho_t} \times 100 \qquad \text{Equation 4.1}$$

$$\text{Hausner ratio} = \frac{\rho_t}{\rho_o} \qquad \text{Equation 4.2}$$

The mean values for the Carrs compressibility index and the Hausner index for unmodified and defatted Starch 1500 are summarised in table 4.8. Previously reported literature gave values of 18 – 23% for the Carr's compressibility index and 1.33 ± 0.01 for the Hausner index of Starch 1500 (Lordi, 1994; Mondero Perales et at, 1996). These differences may be related to the tendency of the particle size distribution of Starch 1500 to alter during handling (Brittain et al, 1991a). As a consequence parameters such as surface area and bulk and tapped density may also be expected to alter. In all cases the defatted Starch 1500 samples displayed a lower compressibility index and Hausner ratio than unmodified Starch 1500. Based on the work of Carr (1970) the flow of these materials may be classified as either "poor" (compressibility index 23 – 35), "fair to passable" (compressibility index 18 –21) or "good" (compressibility index 12 – 16).

Table 2.8: Compressibility index and Hausner ratio for unmodified and defatted Starch 1500 materials.

Sample	Compressibilty index (%)	Hausner ratio
Starch 1500	27.80 ± 0.86	1.39 ± 0.02
DF48-Me-02	20.38 ± 1.82	1.26 ± 0.03
DF48-Me-03	20.88 ± 2.35	1.26 ± 0.04
DF48-96-01	23.91 ± 2.28	1.31 ± 0.04
DF48-96-01A	19.14 ± 2.99	1.24 ± 0.05
DF48-85-01	21.55 ± 1.07	1.27 ± 0.02
DF48-70-01	18.25 ± 2.26	1.22 ± 0.03
DF48-Pr-03	16.90 ± 2.50	1.20 ± 0.04
DF48-He(99)-01	22.62 ± 1.79	1.29 ± 0.03

4.3.7 Mercury Intrusion Porosimetry

Pore size distributions were determined by mercury intrusion porosimetry using an Autopore II 9220 instrument (Micromeritics Instrument Corporation, Norcross, GA, U.S.A.). The principle by pore diameter and area may be determined is based on the capillary rise phenomenon, in which applied pressure forces a non-wetting liquid (mercury) into narrow voids (Brittain et al, 1991b). If the pores of a material are assumed to be cylindrical then the relationship between applied pressure (P) and pore size opening (D) may be determined using equation 4.3, (Washburn, 1921).

$$D = \frac{-4\gamma \cos \theta}{P} \qquad \text{Equation 4.3}$$

Where θ is the contact angle and γ is the surface tension. The instrument used, was equipped with a low-pressure chamber that operated from atmospheric pressure (0.172 MPa) down to 0.0034 MPa and a high-pressure chamber that operated from 0.172 up to 414 MPa. If it is assumed that the contact angle of mercury is 130° and the surface tension is 485 $gcms^{-2}$, it would be possible to analyse pores having median diameters in the range of 360 to 0.003μm (Webb and Orr, 1997). Pressure was generated within the instrument by means of a hydraulic pump. A conductance detector monitored the movement of mercury in the penetrometer stem. Pore size distributions were determined for Starch 1500 bulk powder. Between 1.5 and 1.6g of Starch 1500 was accurately weighed into a 15ml powder penetrometer that had a stem volume of 1.1310 ml. The penetrometer volume was calibrated in triplicate prior to use. The penetrometer was evacuated to remove adsorbed gases and moisture from the material prior to filling with mercury. Due to the high water content of Starch 1500 this low-pressure step took up to 10 hours to complete.

Figure 4.2 illustrates the incremental intrusion plots for DF48-96-01 and Starch 1500 bulk powder. Incremental intrusion (ml/g) is presented on a linear scale and pore diameter (μm) is on a logarithmic scale. Analysis of Starch 1500 powder was performed at pressures equating to pore sizes between 0.0034 and 18.1μm. Within this range voids due to both inter- and intra-particulate voids will occur. Determination of the porosity of a material relies on there being a distinct difference between these two types of void (Dees and Polderman, 1981). Examination of unmodified and defatted Starch 1500 by low temperature scanning electron microscopy revealed the presence of intra-particulate voids of 30 μm and less, thus

a point at which the filling of intra-particulate voids begins cannot be identified. In figure 4.2, between 2 and 4 μm, there is a sharp drop in intrusion volume, which may indicate the end point for inter-particulate void filling for both materials.

The median pore diameter as estimated from the cumulative intrusion volume is the most commonly used measurement of the pore size distribution of a material (Dees and Polderman, 1981). Table 4.9 details the porosity, total pore volume and the median pore diameter for Starch 1500 and DF48-96-01 bulk powder. No differences in pore parameters were detectable between these two materials. To determine if any porosity differences between Starch 1500 and DF48-96-01 were being masked by the packing properties of the materials, the pore size distributions were studied from 2μm down to 3.1nm. Table 4.10 details the porosity of Starch 1500 and DF48-96-01 between 3.1nm and 2μm, were all pores are assumed to result from intraparticulate voids. Analysis of this data failed to reveal any difference between Starch 1500 and DF48-96-01, therefore either defatting does not significantly alter the porosity of Starch 1500 or such differences cannot be detected as they occur in the region of inter and intraparticulate voids are simultaneously filled.

Table 4.9: Pore parameters of Starch 1500 and DF48-96-01 bulk powder

Porosity (%)		Median Pore Diameter (μm)		Total Pore Volume (ml g^{-1})	
DF48-96-01	Starch 1500	DF48-96-01	Starch 1500	DF48-96-01	Starch 1500
48.75	45.68	11.5	9.7	0.575	0.502
45.38	39.54	11.3	10.4	0.502	0.441
46.87	44.70	11.1	9.8	0.528	0.496
49.71	44.87	10.4	9.9	0.540	0.500
47.43	46.28	11.0	9.8	0.545	0.520

Figure 4.2: Incremental intrusion plots for Starch 1500 and DF48-96-01 bulk powder

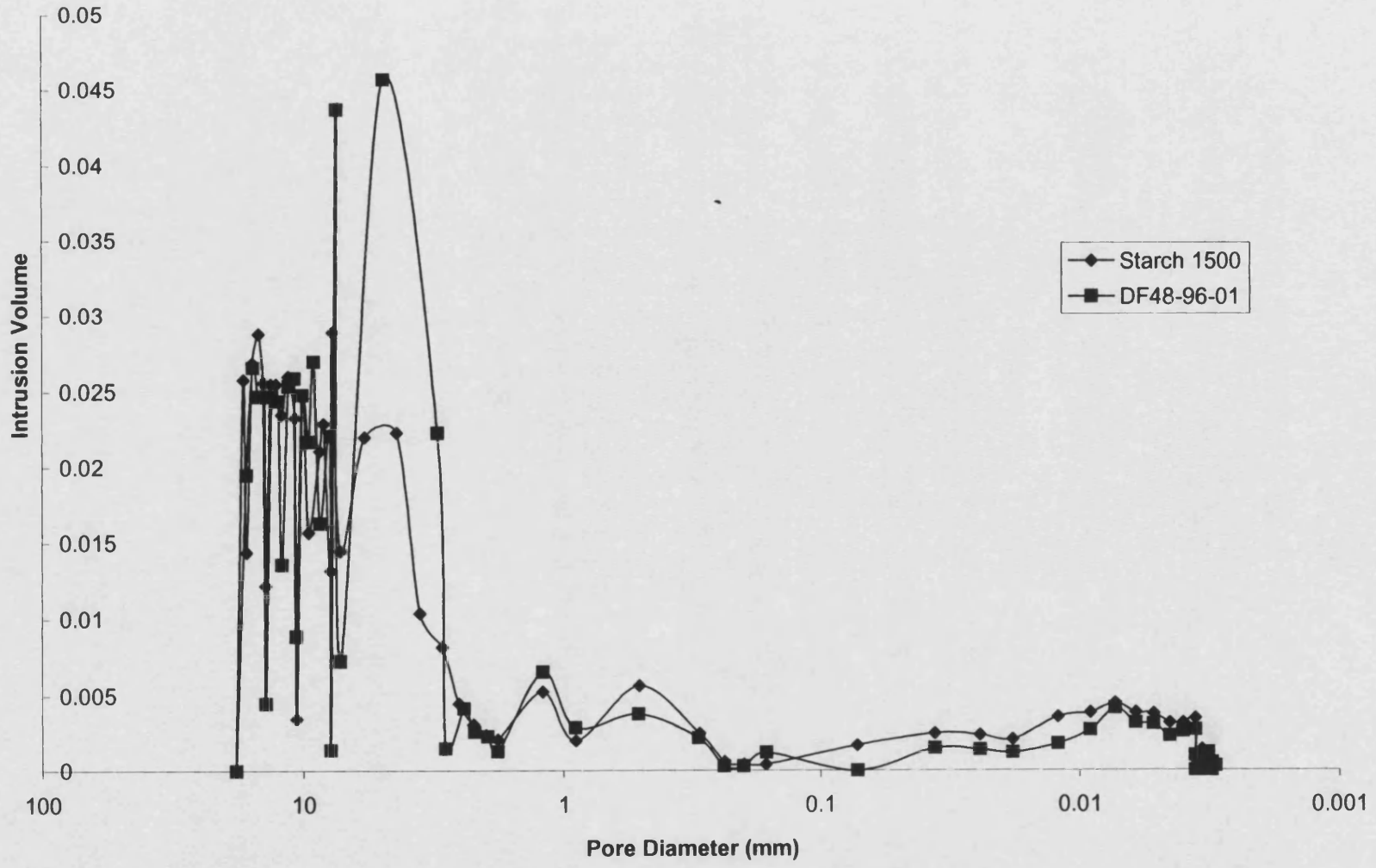

Table 4.10: Porosity of Starch 1500 and DF48-96-01 between pore diameters of 3.1nm and 2μm

Porosity (%)	
Starch 1500	DF48-96-01
4.84	5.41
5.58	5.70
4.90	5.53
4.63	6.08
4.81	5.98

4.3.8 Differential Scanning Calorimetry (DSC)

On gelatinisation, starch granules undergo an irreversible order-disorder transition, which may be measured by DSC. The molecular events, which are responsible for the DSC traces during starch gelatinisation, are uncertain but several mechanisms have been proposed (Biliaderis, 1990). There is a linear relationship between the enthalpy of gelatinisation and the amount of gelatinized material in a starch sample (Lund, 1983). This approach has been used successfully to determine the degree of gelatinized material in a number of partially pregelatinised spray-dried potato starches (Herman et al, 1989) and microwave treated wheat, corn and rice starches (Ndife et al, 1998). In chapter one it was stated that Starch 1500 was thought to be composed of 20% pregelatinised maize starch and 80% native material, thus according to the proposed model the gelatinisation endotherm for Starch 1500 should be approximately 20% smaller than for native maize starch. The following study was performed to determine degree of pregelatinisation of Starch 1500.

Approximately 3mg of starch was accurately weighted into an aluminium sample pan. Distilled water was added from a microsyringe to produce a 20%$^{w}/_{w}$ suspension. The sample pan was hermetically sealed and equilibrated for one hour prior to analysis. An indium standard was used to calibrate the melting temperature and ΔH and an empty pan was used as a reference. The calorimeter furnace was continually purged with nitrogen at a flow rate of approximately 25ml min^{-1}. Tests were performed in triplicate between 30°C and 120°C using a Thermal Analysis DSC 2910 (TA Instruments Ltd., Leatherhead, U.K.).

Figures 4.3 and 4.4 show typical DSC traces for native maize starch and Starch 1500 respectively. Based on the results of previous workers (Lund, 1983; Herman et al, 1989; Ndife et al, 1998) the absence of a gelatinisation endotherm in the DSC trace of Starch 1500 would infer that this material is completely pregelatinised. Evidence of ungelatinised material is presented in Chapter 5 in the form of intact starch granules as visualised by SEM and in Chapter 6 as birefringent structures, which may be viewed by polarised light microscopy.

The presence of ionic and non-ionic solvents, such as sodium chloride and sucrose cause an increase in gelatinisation temperature and decrease in the enthalpy of this endothermic process (Wootton and Bamunuarachchi, 1980). During extrusion starch is subjected to high shear forces that physically cleave glycosidic linkages, in turn forming lower molecular weight fragments that exhibit cold-water solubility. Analysis of the cold-water soluble fraction of mechanically damaged maize starch revealed it to be composed primarily of amylopectin fragments. Further damage resulted in the release of amylose and amylopectin (Glennie et al, 1987). Investigations were made to determine whether the cold-water soluble fraction of Starch 1500 was masking the gelatinisation endotherm associated with native starch. This was performed by blending 80%w/w native maize starch with 20% Starch 1500 or fully gelatinized maize starch. The DSC traces for these blends yielded the characteristic endotherm associated with gelatinisation, which a 20% reduction in the enthalpy of this transition compared to 100% native maize starch. The DSC trace for one such blend is given in figure 4.5 and the enthalpy values for the blends and native maize starch are shown in table 4.11.

Table 4.11: Details of observed enthalpy reduction on blending native maize starch with fully or partially pregelatinised maize starch

Material	Peak Gelatinisation Temperature (°C)	Gelatinisation Enthalpy (J g^{-1})	Relative Enthalpy (%)
100% Native Starch	69.66	8.73	100
80% Native Starch 20% Starch 1500	69.32	6.44	74
80% Native Starch 20% Starch 1500	69.46	6.67	76
80% Native Starch 20% Gelled Starch	70.98	6.80	78

Figure 4.3: DSC trace of native maize starch in excess water

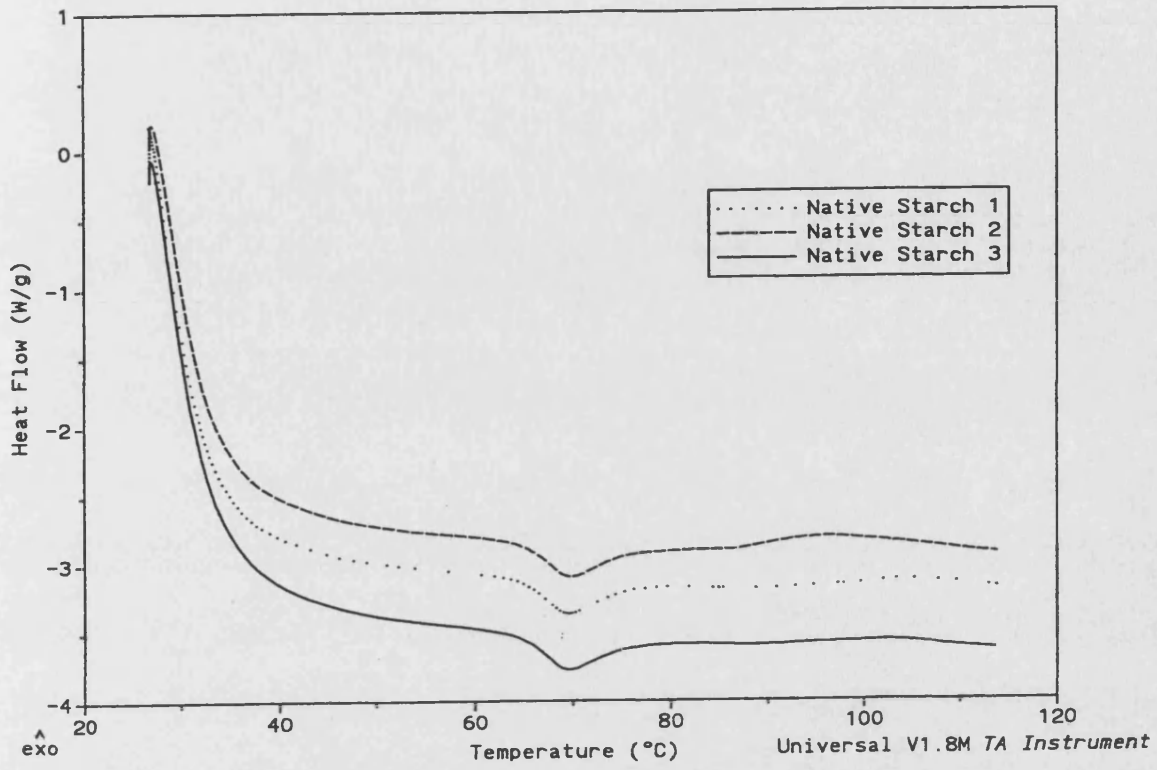

Figure 4.4: DSC trace of Starch 1500 in limited water

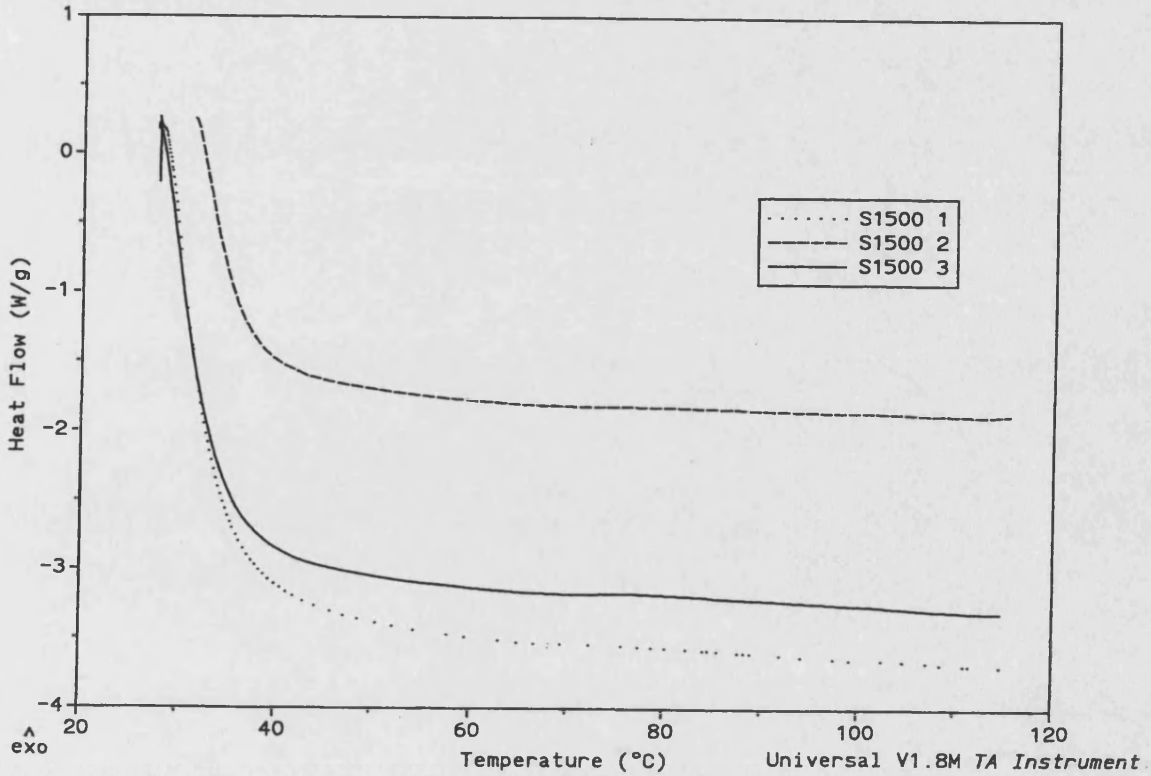

Figure 4.5: DSC trace of 80% native maize starch and 20% Starch 1500 blend in excess water

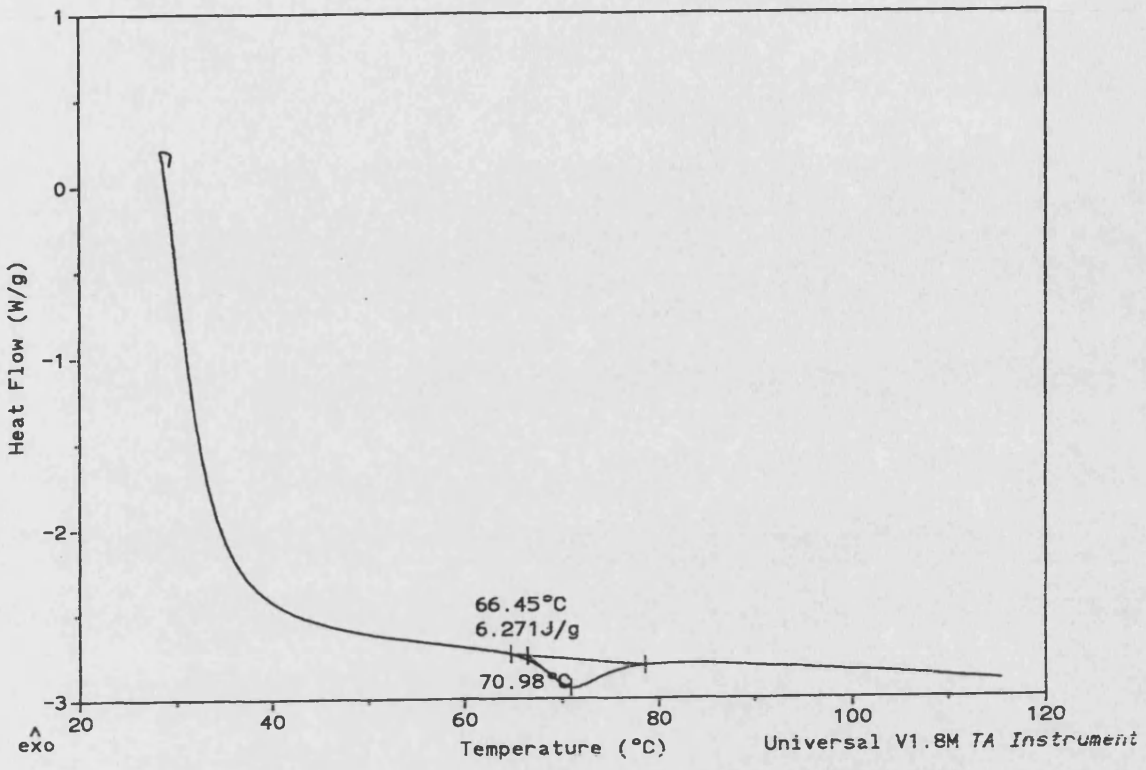

Figure 4.6: DSC traces of Starch 1500 and DF48-96-01 in limited water

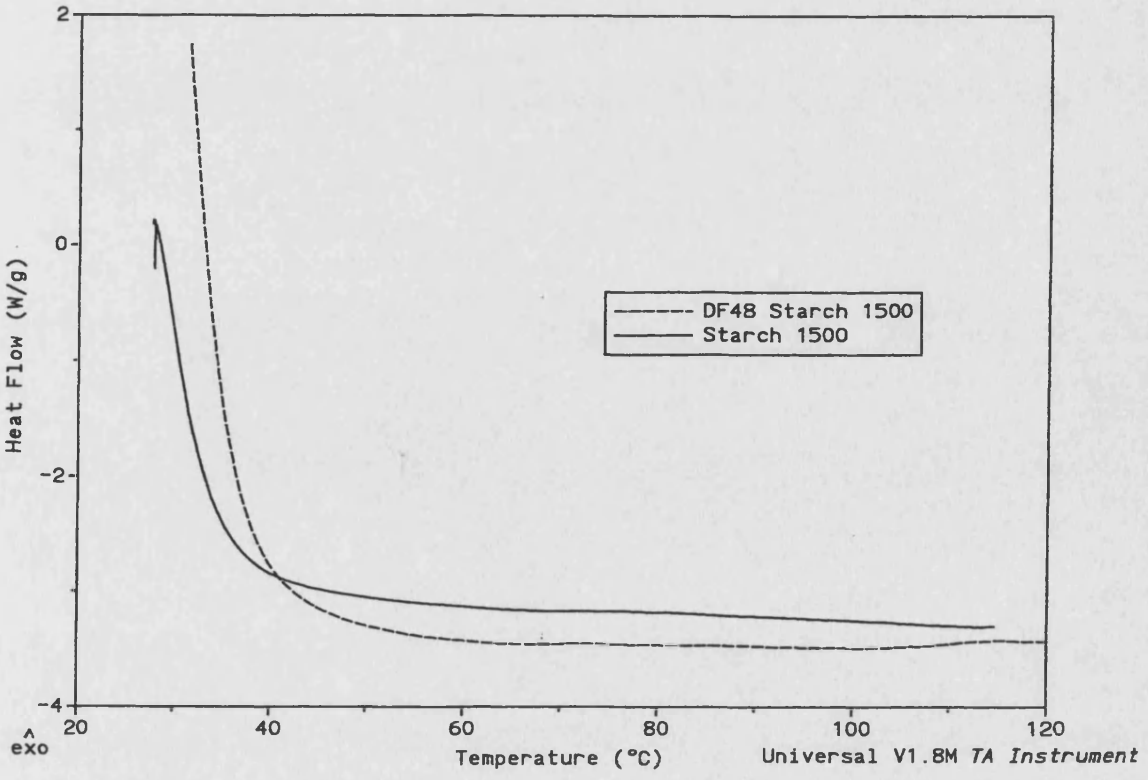

The data shown in table 4.11 indicates that pregelatinised starch does not mask the endotherm associated with the gelatinisation of native starch or greatly alter the peak gelatinisation temperature. Such a result indicates that the order-disorder transition, which is usually observed during gelatinisation, may have already occurred during Starch 1500 production from native maize starch.

When native starch is heated in excess water only one transition is observed, this is referred to as the gelatinisation endotherm. If the proportion of water is reduced a second transition may observed, which is referred to as the melting endotherm. The melting endotherm becomes proportionally larger as the ratio of water to starch decreases. At very low moisture contents, a point is reached where the gelatinisation endotherm is lost and starch transitions occur solely by melting (Donovan, 1979).

As was alluded to in chapter one, Starch 1500 production involves the extrusion of maize starch at low water contents in which the melting transition will dominate. Analysis of Starch 1500 by DSC failed to reveal either a gelatinisation or melting endotherm. The melting endotherm may not be detectable because of a shifting to higher temperatures and broadening which occurs as a consequence of starch extrusion at very low moisture contents (Barron et al, 2000). The absence of a gelatinisation endotherm indicates that thermal modification has occurred to the whole population maize starch granules during Starch 1500 production in the form of melting. Evidence of this can be seen by both SEM and TEM in chapters 5 and 6 respectively, as a disruption of the material in the hilum of the granule. Such an effect has been identified to occur during the industrial extrusion of starch granules (Stute, 1990).

Analysis of defatted Starch 1500 using the same method resulted in DSC traces identical to those of Starch 1500 (figure 4.6). This was expected in that no endotherms were apparent for unmodified Starch 1500. It is noteworthy that defatted Starch 1500 did not yield any peaks for the liberation of residual solvent. The possibility that such a solvent loss was being masked by the evaporation of water was tested by heating Starch 1500 and DF48-96-01 in hermetically sealed pans without additional distilled water (figure 4.7). Again this study failed to highlight any difference between Starch 1500 and DF48-96-01.

Figure 4.7: DSC traces of Starch 1500 and DF48-96-01 in limited water

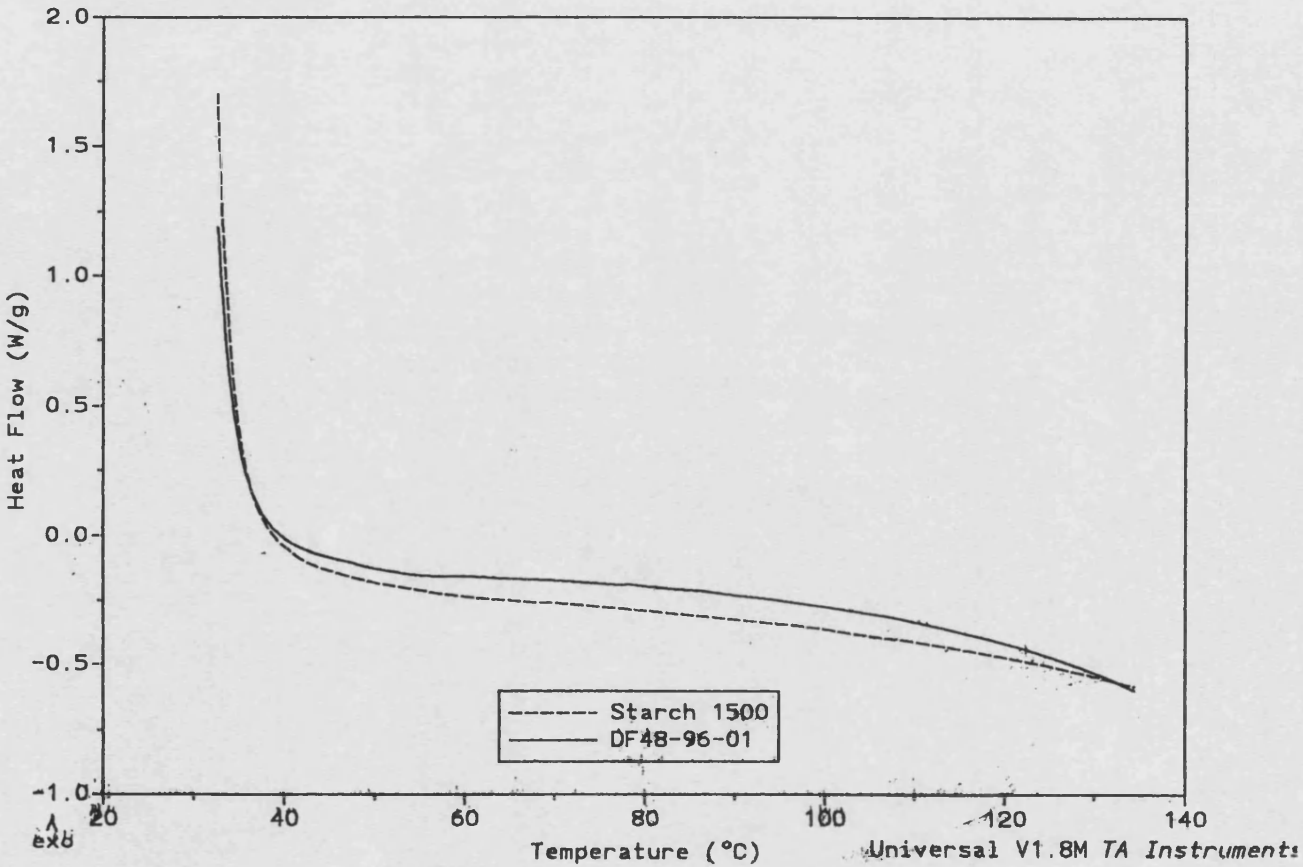

4.3.9 Modulated temperature differential scanning calorimetry (MTDSC)

When an amorphous polymer system is exposed to low temperatures, the polymer chains become immobilised in a "glassy" state. Upon the application of sufficient thermal energy to the polymer system a point is reached whereupon molecular movement within the backbone of polymer chains is initiated. The temperature at which this occurs is known as the glass transition point (Tg). It is firmly established that the Tg of polymers may influence properties such as the mechanical strength of a material (Shen and Eisenberg, 1966). Below their Tg, polymers behave like a brittle glassy solid whereas above this critical temperature their behavior may be likened to a rubber liquid. Many factors are known to influence the Tg of polymers, including the incorporation of low molecular weight solvents, which have been shown to depress the glass transition point (Fuzek, 1980). By reducing the Tg, a polymer becomes more plastic at a given temperature and moisture content (Campbell, 1994).

Analysis of the Tg of starch is commonly performed on cooled aqueous systems that have been heated to gelatinise and destroy the thermal history of the polymer. Such a treatment increases the amorphous component of the starch and in turn generates a larger glass transition. Furthermore it has been reported that the Tg of native starch is masked by the endothermic transition associated with starch gelatinisation.

The technique of modulated temperature differential scanning calorimetry (MTDSC) varies from conventional DSC by the application of a sinusoidal, as opposed to linear, heating or cooling signal to a sample material. MTDSC allows the resolution of complex thermal events though their separation of total heat flow into reversible and non-reversible transitions. Glass transitions are observed in the reversible response, whereas endothermic relaxations such as that associated with starch gelatinisation are seen in the non-reversible response.

Samples of unmodified and defatted Starch 1500 were prepared for analysis by the method described in section 4.3.8 for conventional DSC. MTDSC studies were performed using a DSC 2920 Modulated DSC (TA Instruments, Leatherhead, U.K.) equipped with a Refrigerated Cooling System unit. The calorimeter furnace was continuously purged with nitrogen at a flow rate of 40ml min^{-1}. Calibration of the instrument was performed using the melting of indium, cyclohexane, n-octadecane, and n-decane standards. Heat capacity calibration was performed using an

aluminium oxide standard. Analyses were performed in aluminium hermetic pans (Perkin Elmer) at a scan rate of 2°C min^{-1} from 0 to 150°C. Modulation amplitudes of 0.2 to 0.5°C were used for a modulation period of 30 seconds. Five replicates were performed for each sample in both excess water (approximately 20%$^{w}/_{w}$ starch) and at equilibrium moisture contents (section 4.3.3).

Studies of Starch 1500 in excess water, using conventional DSC failed to resolve any transitions (section 4.3.8). MTDSC was used to determine whether the glass transition point of Starch 1500 could be resolved using this technique. Furthermore samples of defatted Starch 1500 were analysed to ascertain if exposure to the solvents used in soxhlet extraction altered the glass transition point.

Figures 4.8 and 4.9 illustrate the total heat flow data and the reversing and non-reversing signals for native maize starch at equilibrium moisture content and in excess distilled water respectively. A moisture content of approximately 27%$^{w}/_{w}$ has been suggested to elicit the maximal plasticising effect on a retrograded starch system (Silvero et al, 1996). Previous studies would suggest that the glass transition point of native starch in excess water would be present between 20 and 30°C (Zeleznak and Hoseney, 1987). The reversing heat flow signal for native maize starch in excess water shows no such transition (figure 4.9). At equilibrium moisture contents of 10 to 12% the Tg of native starch was expected to occur between 100 and 130°C (Zeleznak and Hoseney, 1987) however figure 4.8 illustrates that no such transition may be observed in the reversing heat flow signal in the range of temperatures tested.

Three explanations have been proposed to describe the absence of a Tg from native maize starch (Biliaderis et al 1986 and 1991): (1) the amorphous domains are surrounded by crystalline domains; (2) physical crosslinks inhibit the movement of amorphous chain segments; and (3) the presence of alternating amorphous and crystalline regions distort normal thermal behaviour of the amorphous material. These factors may indeed explain the absence of a Tg for native maize starch.

As previously stated, Tg studies of starch usually involve firstly heating to remove the thermal history of the material (Zeleznak and Hoseney, 1987; Thiewes and Steeneken, 1996). In doing so the endotherm associated with gelatinisation is eliminated and in turn the amorphous content of the starch is increased. As the studies of Starch 1500 in section 4.3.8 show, the endotherm associated with

gelatinisation is absent from this material. Therefore it is suggested that Starch 1500 production mimics the thermal conditioning applied to starch prior to the determination of its glass transition point. Previous studies, using conventional DSC methods, have identified Tg`s of approximately 80°C (approx 16% moisture content) and 90°C (approx. 13% moisture content) for thermally conditioned native potato and wheat starches respectively (Thiewes and Steeneken, 1996; Zeleznak and Hoseney, 1987).

Figures 4.10 and 4.11 detail the total heat flow data and the reversing and non-reversing signals for Starch 1500 at equilibrium moisture content (approx. 10.4%) and in excess distilled water respectively. Starch 1500, in both limited and excess water, displays a transition beginning at approximately 70°C that can be observed in the total and non-reversing heat flow signals. Figure 4.10 illustrates that this transition is displayed more clearly in limited water and correlates well with the transition observed by previous workers (Thiewes and Steeneken, 1996; Zeleznak and Hoseney, 1987). However these previous studies have used the total heat flow data provided by conventional DSC to attribute this signal to the presence of a glass transition. The deconvolution of total heat flow into reversing and non-reversing heat flow possible by MTDSC shows that this transition is not present in the reversing heat flow data and therefore is not due to a glass transition.

Figures 4.12 and 4.13 illustrate the total heat flow data and the reversing and non-reversing signals for DF48-96-03 at equilibrium moisture content (approx. 12%) and in excess distilled water respectively. It can be seen from these data that the transition observed for Starch 1500 is absent from DF48-96-03. On the basis of the available data it is not possible to draw conclusions about the effect of defatting on Starch 1500 without further investigation.

Figure 4.8: MTDSC trace of Native Maize Starch in limited water

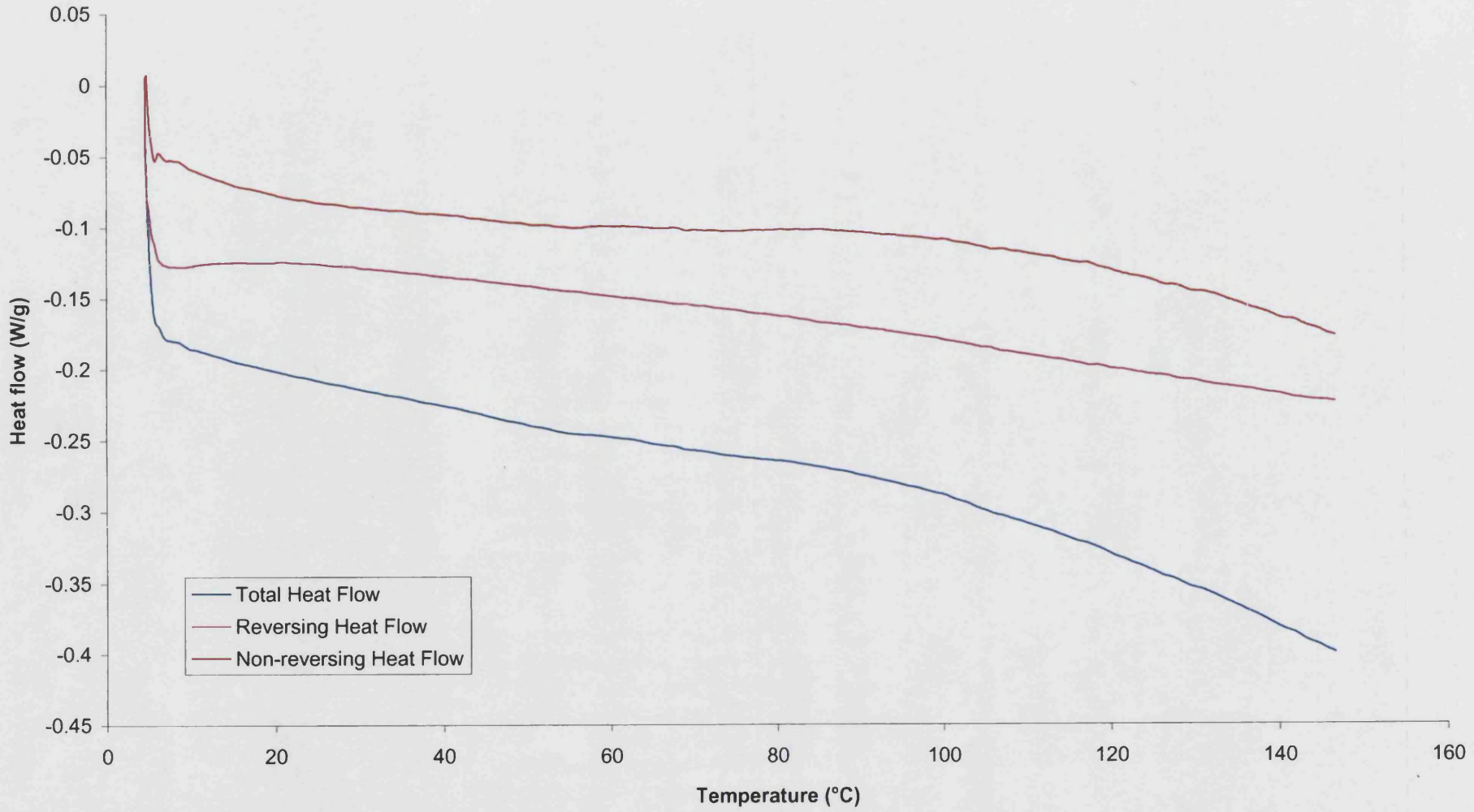

Figure 4.9: MTDSC trace of native maize starch in excess water

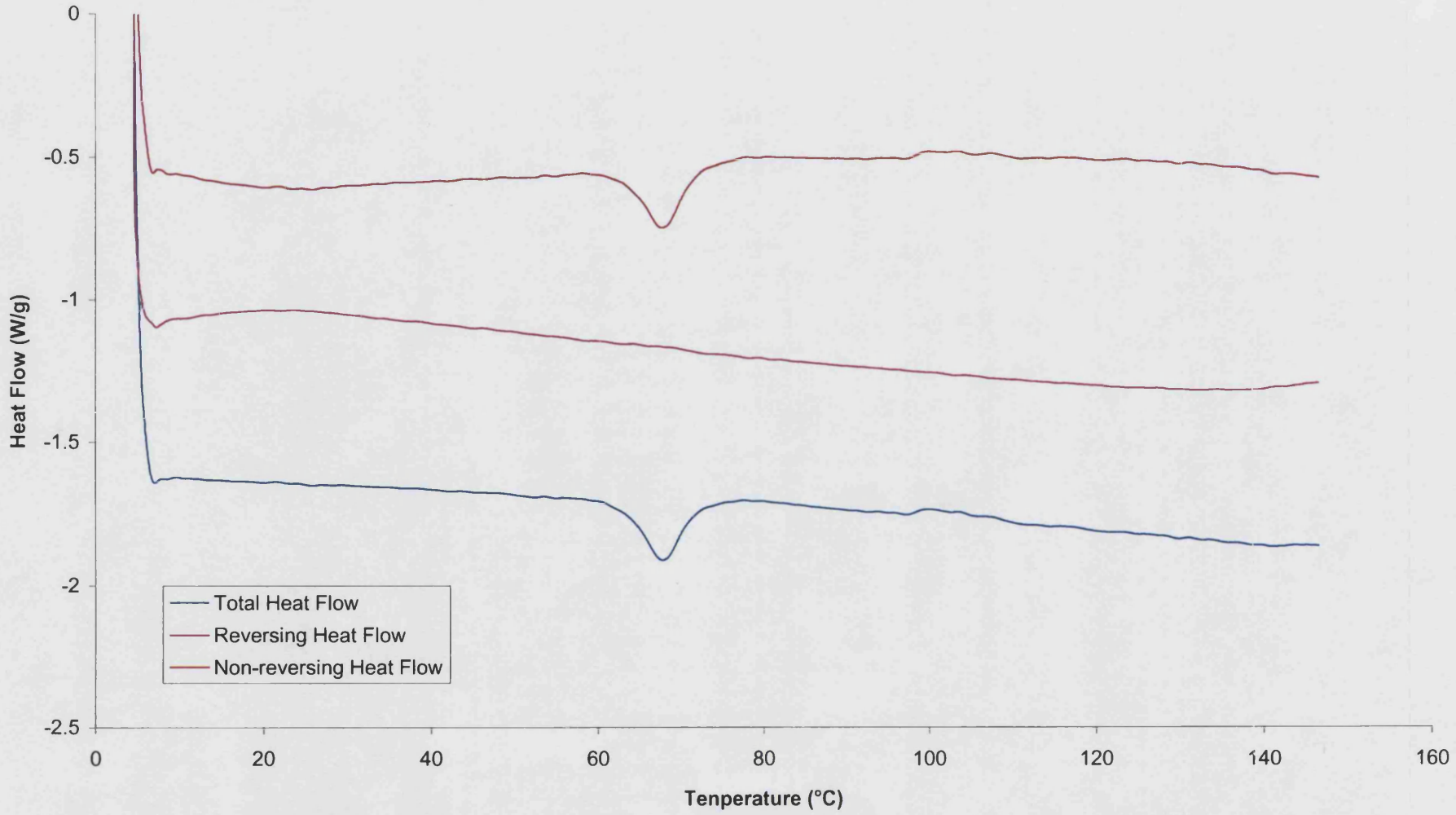

Figure 4.10: MTDSC trace of Starch 1500 in limited water

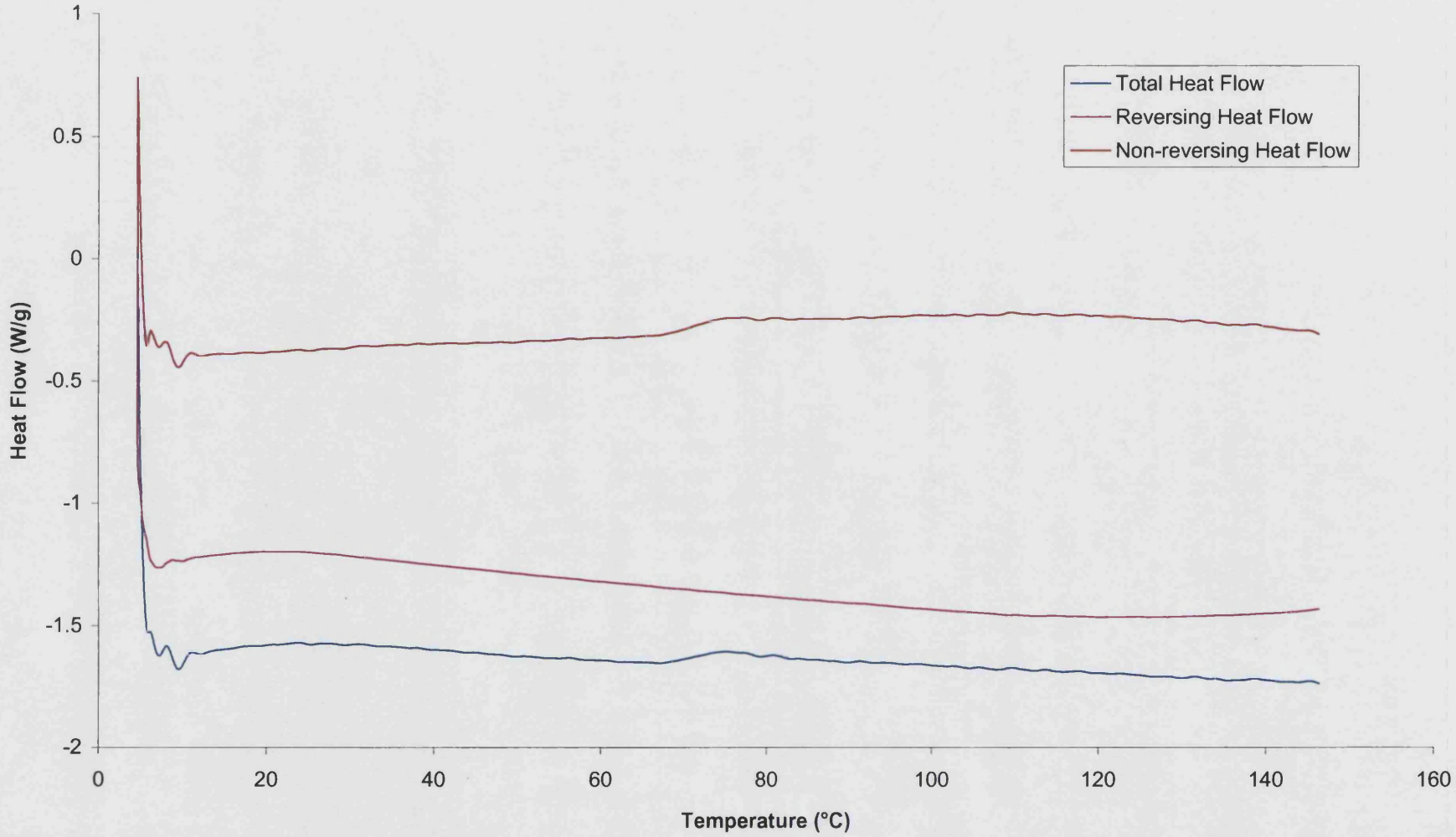

Figure 4.11: MTDSC trace of Starch 1500 in excess water

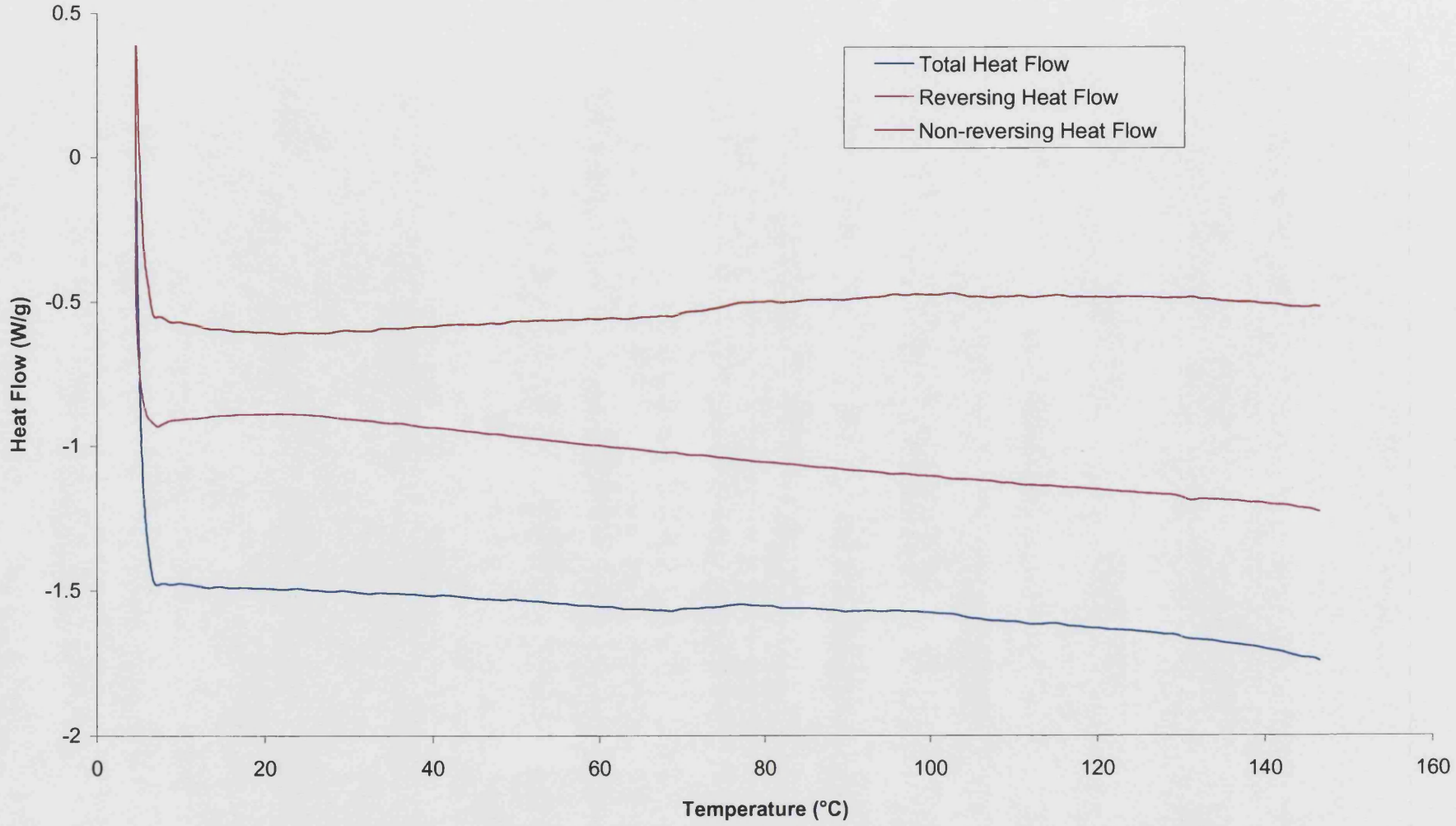

Figure 4.12: MTDSC trace of DF48-96-01 in limited water

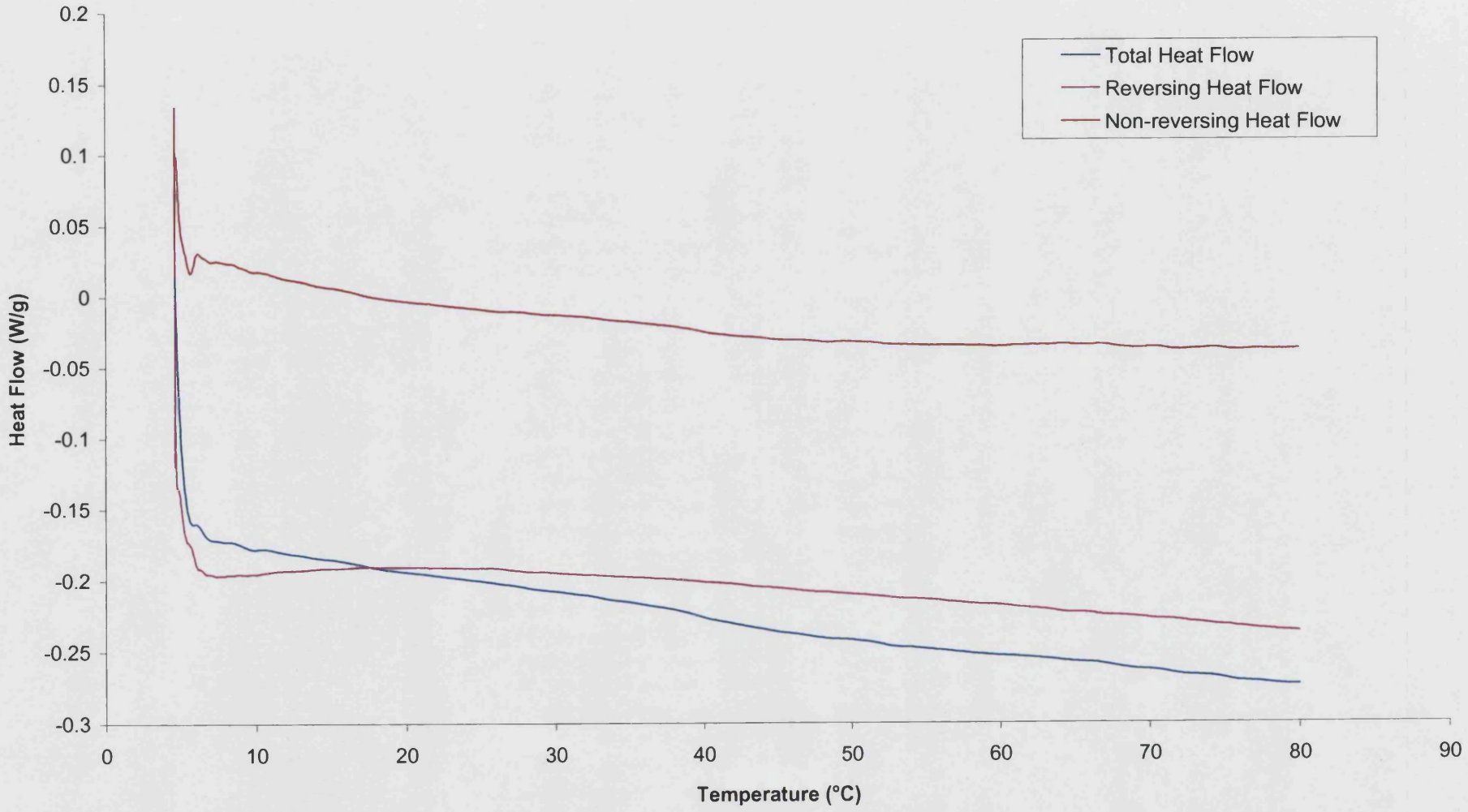

Figure 4.13: MTDSC trace of DF48-96-01 in excess water

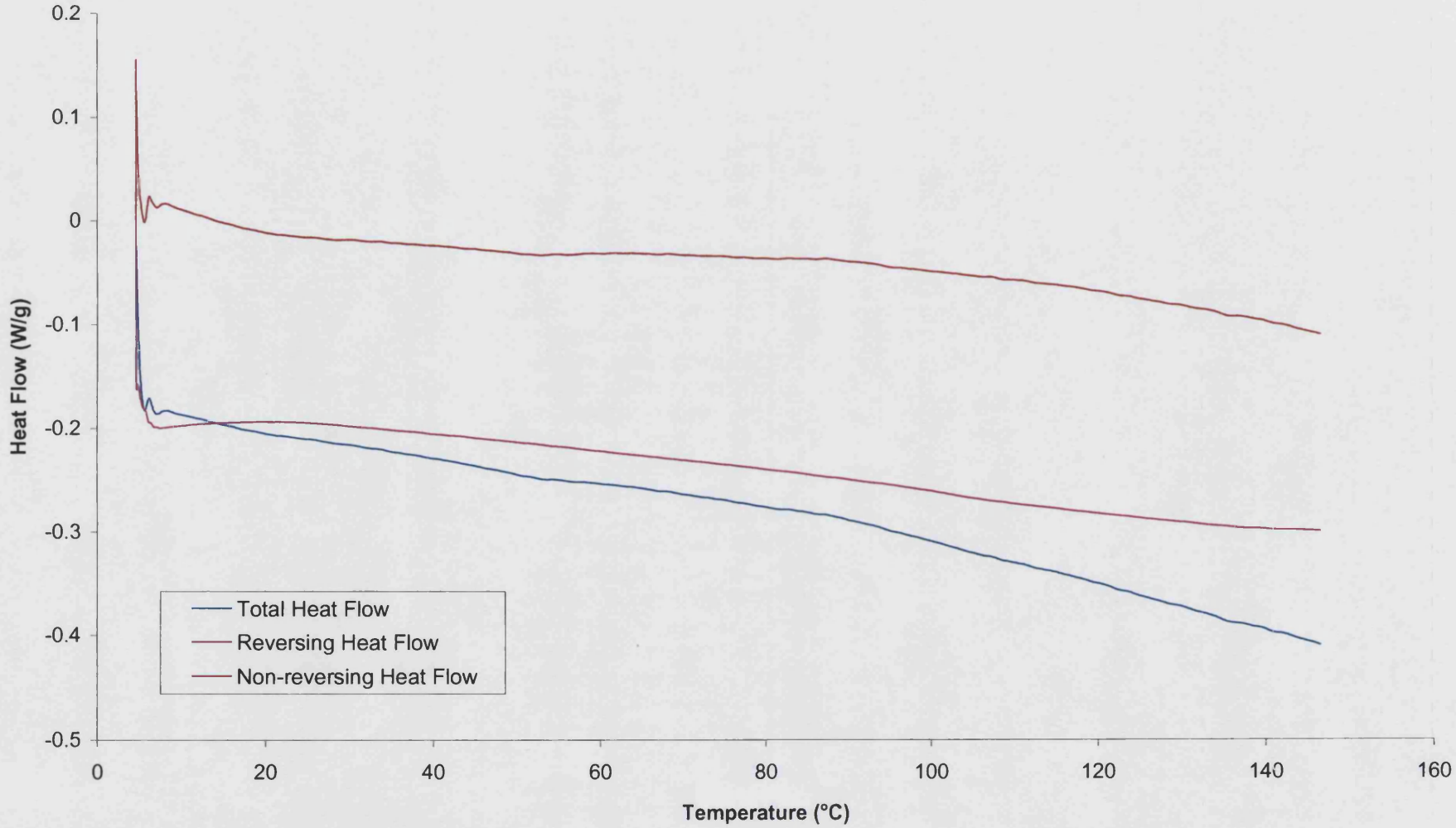

4.3.10 X-ray powder diffraction

The crystallinity of starch has been attributed to the long range molecular ordering of amylopectin double helices (French, 1984). It has previously been shown that defatting maize starch results in a small increase in the relative crystallinity of the material (Vasanthan and Hoover, 1992). It has been suggested that the increased temperatures to which starch is exposed on defatting allows the reorganisation of amylose chains present between the amylopectin double helices. As a result of the reorganisation of the trapped amylose chains a higher degree of long-range molecular order is observed as an increase in starch crystalinity. Analysis of unmodified and defatted Starch 1500 using an X-ray diffraction instrument (Phillips X-ray analytical, Cambridge, U.K.) equipped with a 4kW X-ray generator (type PW 1730/00); a long fine-focus 2kW copper target X-ray tube (type PW 2273/20), which was operated at 40 kV and 25 mA; a computer controlled vertical diffractometer goniometer (type PW 1820/00); a xenon proportional counter (type PW 1711/10) with graphite monochromater (type PW 1752/00) and automatic divergence slit assembly (type PW 1368/55); a microprocessor diffractometer control (type PW 1710/00) and diffraction software (Type PW 1877 PC-APD, version 3.5b). Samples were scanned through the 2θ range of 5 to 90° with a step width of 0.02° with a 13 second dwell time. Analyses for each sample were performed in duplicate.

Figure 4.14 illustrates X-ray diffraction traces for Starch 1500 and DF48-99-01. This result is in agreement with earlier work where differences in crystallinity may be observed at 2θ values of 13.14, 15.82 and 18.26° (Vasanthan and Hoover, 1992). The difference in crystallinity of Starch 1500 before and after defatting is considered however to be insignificant with reference to the improved tabletting properties of the material.

Figure 4.14: XRD trace for unmodified and defatted Starch 1500

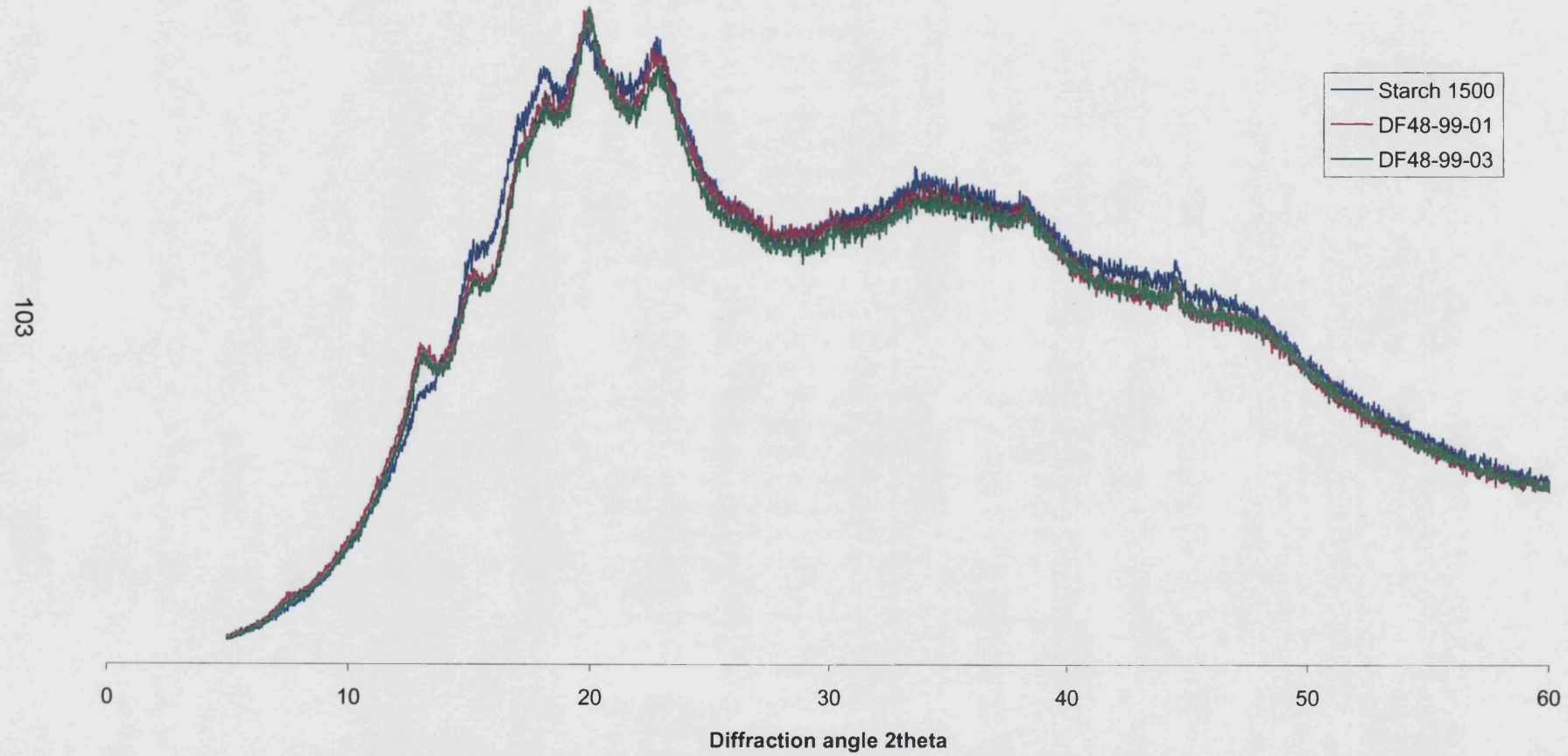

4.3.11 Solid-State Nuclear Magnetic Resonance (SS-NMR) studies

Solid-state NMR was performed on unmodified and defatted Starch 1500 primarily to determine whether any residual solvent was present in the material after the material had been dried under ambient laboratory conditions. Furthermore comparison of the spectra for defatted and unmodified Starch 1500 was performed to determine whether any changes could be attributed to lipid removal.

Analyses were performed using a Bruker DMX-400 instrument (Bruker Instruments, Coventry, U.K.) which was equipped with a 9.4-T magnet and a 4mm variable temperature probe. The samples were individually packed into zirconia rotors with Kel-F end caps. Samples were analysed by both ^{13}C Cross- and Direct-Polarization Magic Angle Spinning (CPMAS and DPMAS respectively). These two experiments vary only in the number of repetitions performed during the analysis. There are a larger number of repetitions in performed in a DPMAS experiment and so there is greater likelihood of detecting fast relaxing species such as solvent residues. A contact time of 0.6 – 0.8 ms was used for the CPMAS experiments. A relaxation delay of 2.0 s was employed, thus favoring the detection of fast relaxing species such as solvents. It is noteworthy that under these acquisition conditions quantitative analysis of solvent residues is not possible due to the difference in relaxation times of the solid and liquid components. The carbon chemical shift reference compound used was $(CH_3)_4Si$.

Figure 4.15 illustrates CPMAS traces for Starch 1500, DF48-Me-01, and DF48-He-01. It is evident from figure 4.15 that defatting Starch 1500 using either polar (methanol) or non-polar (hexane) solvents causes no detectable chemical change to the material when analysed by this technique. These spectra correlate well with previously published results for native corn starch (Aggarwal and Dollimore, 1998; Bugay and Findlay, 1999). Cross-polarisation spectra were obtained for a range of defatted Starch 1500 samples and in all cases this technique failed to highlight any difference between their spectra. Cross-polarisation studies also failed to identify the presence of solvent residues across the range of samples. DPMAS NMR spectra for traces for Starch 1500, DF48-Me-01 and DF48-He-01 are detailed in figures 4.16, 4.17 and 4.18 respectively. Comparison for the direct- and cross-polarisation spectra for Starch 1500 (figures 4.15 and 4.16 respectively) show that there is a much greater level of background noise observed in the former due to the greater number of repetitions in the analysis. In all samples tested there were no additional peaks present in the direct-polarisation NMR spectra.

Figure 4.15: 13C CPMAS NMR Spectra for unmodified and defatted Starch 1500 samples

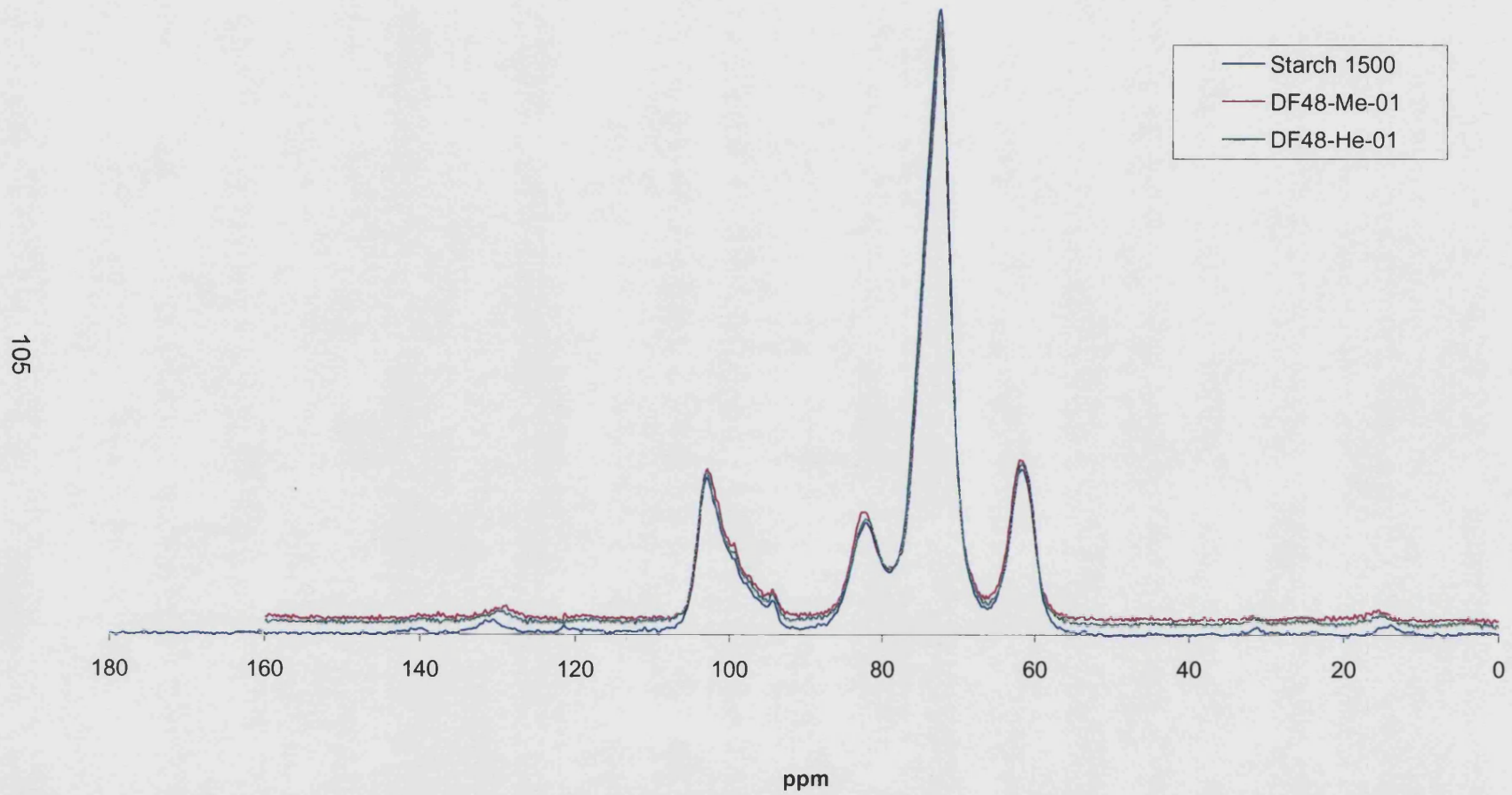

Figure 4.16: 13C DPMAS NMR Trace for Starch 1500

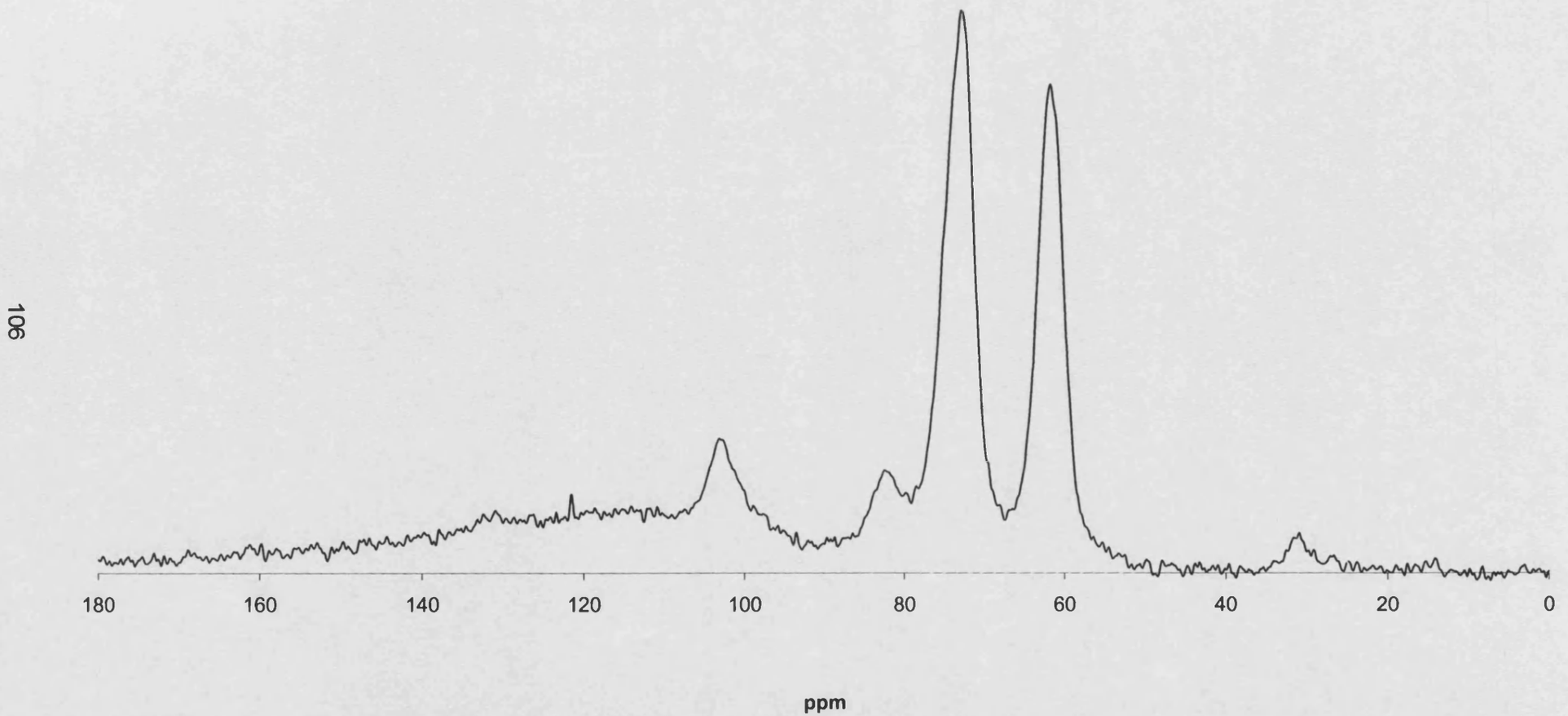

Figure 4.17: 13C DPMAS NMR Spectra for DF48-Me-01

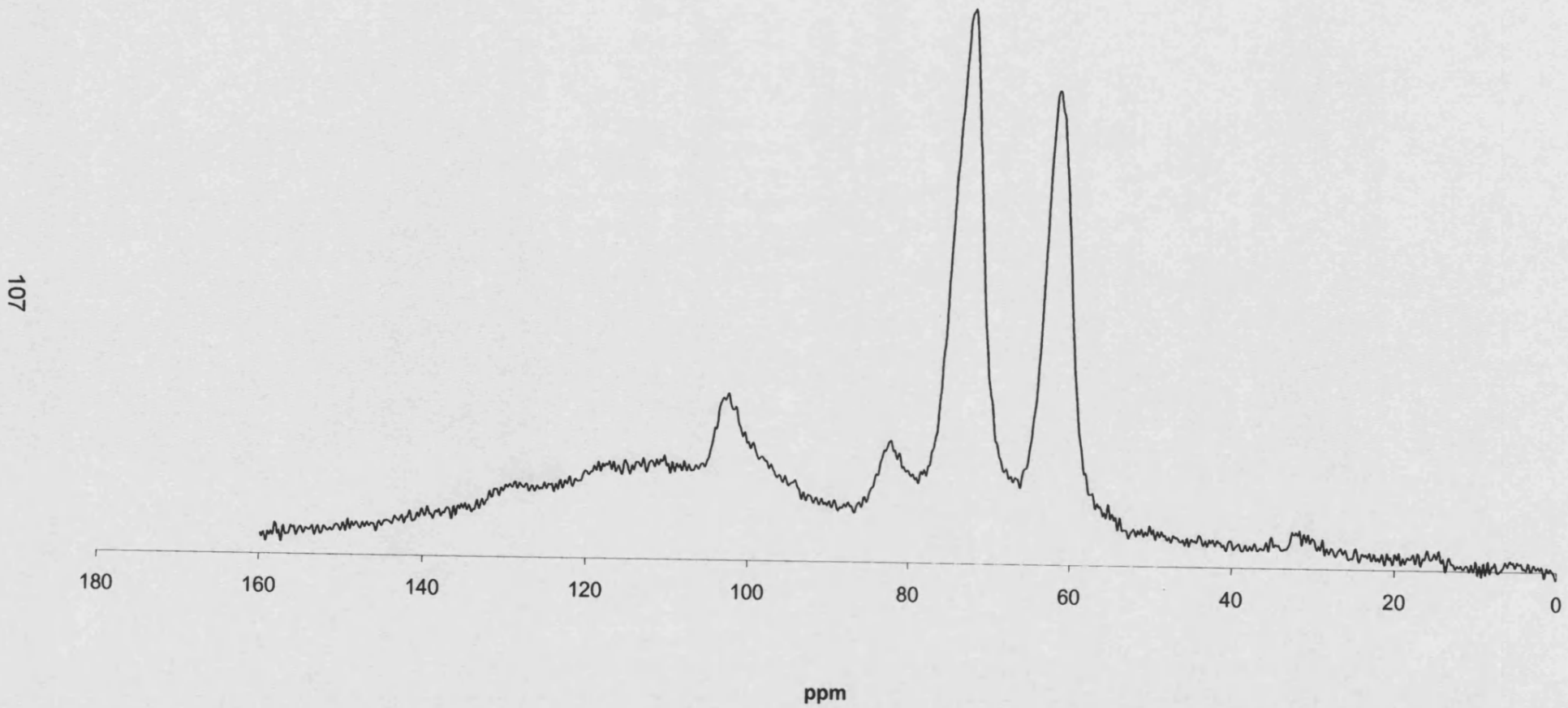

Figure 4.18: 13C DPMAS NMR Spectra for DF48-He-01

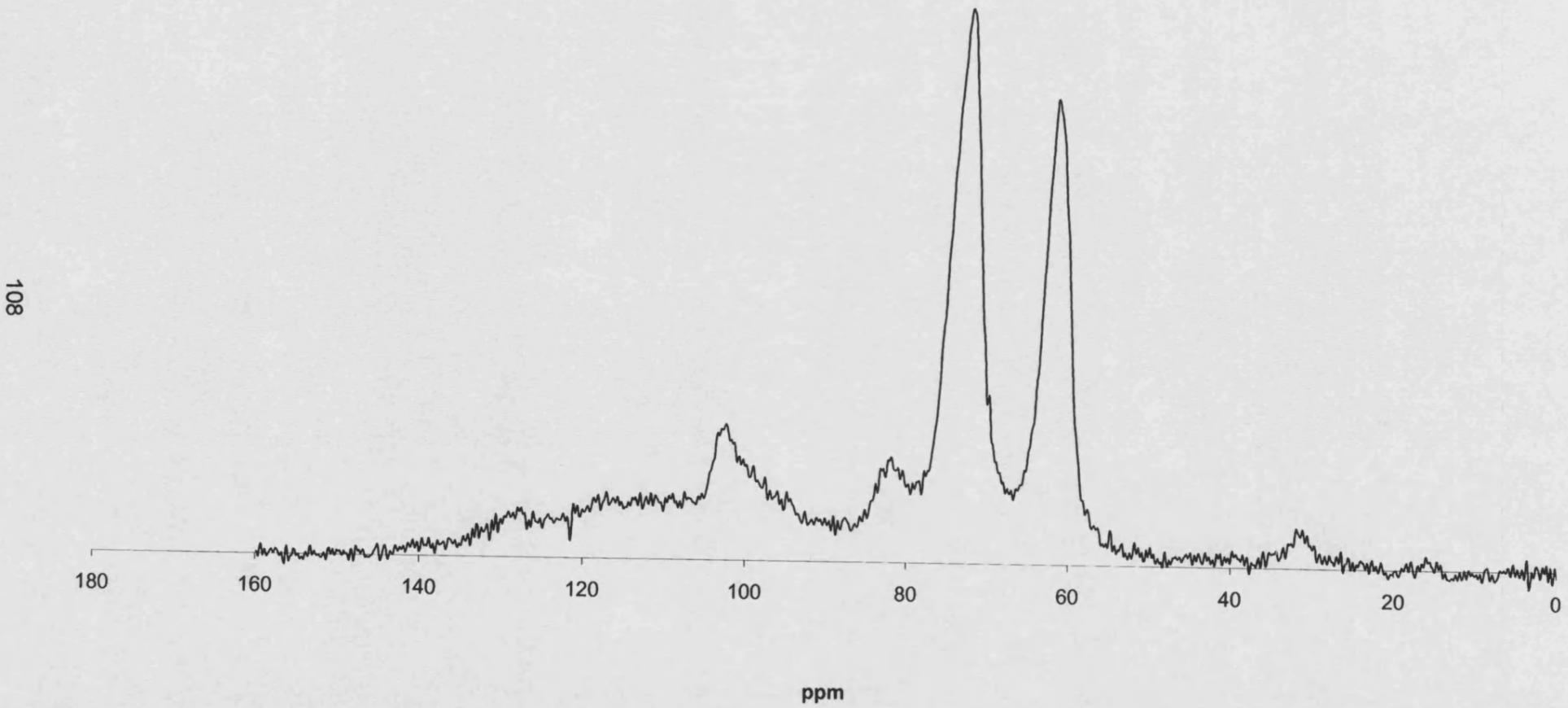

Such a result indicates that either residual defatting solvents are absent from the materials that were tested or are present in quantities which are undetectable by this technique. The low signal to noise ratio generated in the direct-polarisation study may prevent the differentiation of small signals, indicative of residual solvent, from the backgound noise of the trace.

4.3.12 Thermogravimetry/Mass Spectrometry (TG/MS) studies

TG/MS studies were performed on unmodified and defatted Starch 1500 samples as a means of further investigation into the analysis of solvent residues. Unlike solid-state NMR, this technique has the advantage of providing quantitative analysis of solvent residues. A detailed description of the technique of thermogravimetry (TG) can be found elsewhere (Charsely and Warrington, 1992). However the basic principle involves the quantitative measurement of thermally induced weight variations with respect to either temperature or time (for isothermal studies). During thermogravimetric analysis sample weight variations are continuously monitored over a specified temperature range by a null point electromagnetic balance. The balance consists of a sample holder, which is attached to a horizontal quartz beam maintained at the null point by the current flowing through the transducer of the balance. Weight fluctuations are detectable by a pair of photodiodes that monitor the deflection of the quartz beam. A current, which is proportional to sample weight change, is applied to the transducers of the balance to return the beam to the null point. Computer software may be used to generate plots of change in sample weight with temperature or time.

By coupling the technique of thermogravimetric analysis with mass spectrometry it is possible to determine the identity of thermally evolved compounds released from the sample. Evolved gas analysis involves the determination of the absolute composition of the purge gas exiting the thermogravimetric furnace, whereas evolved gas detection involves the identification of pre-selected components in the liberated gas.

TG profiles were obtained using a Polymer Laboratories TGA 1500 instrument which was run from 0 to 400°C (300°C in the case of Starch 1500) at atmospheric pressure using a nitrogen stream (25 ml min^{-1}). Simultaneous analysis of the evolved gases was performed via mass spectrometry using a Leda Mass Mini-Lab mass spectrometer (Leda Mass, Chorley, U.K.) operating at a minimum detection limit of 100ppm. This was connected to the TGA 1500 by a quartz transfer line.

Figure 4.19: Thermogravimetric analysis trace of Starch 1500

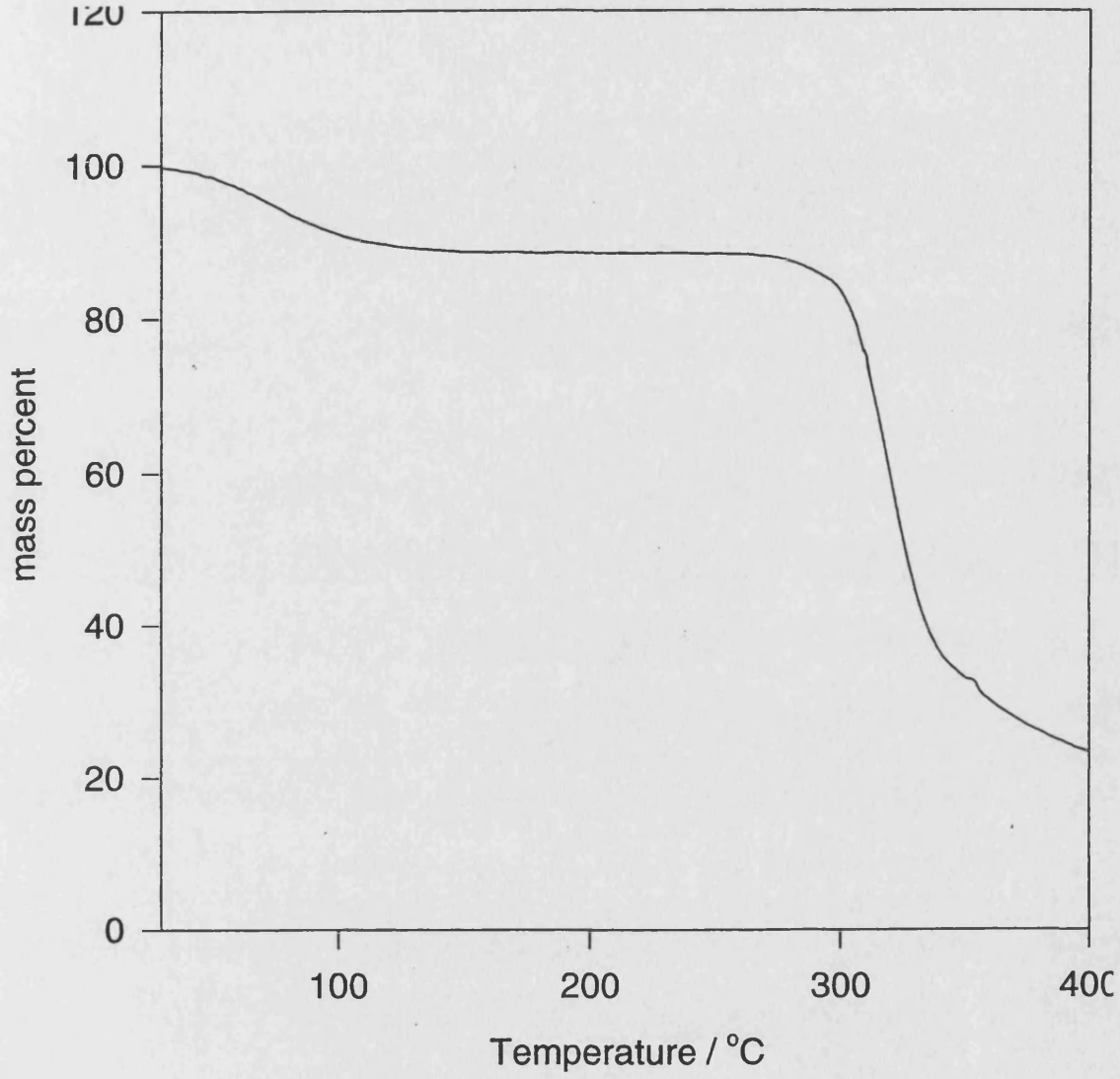

Figure 4.20: Thermogravimetric analysis trace of DF48-Me-01

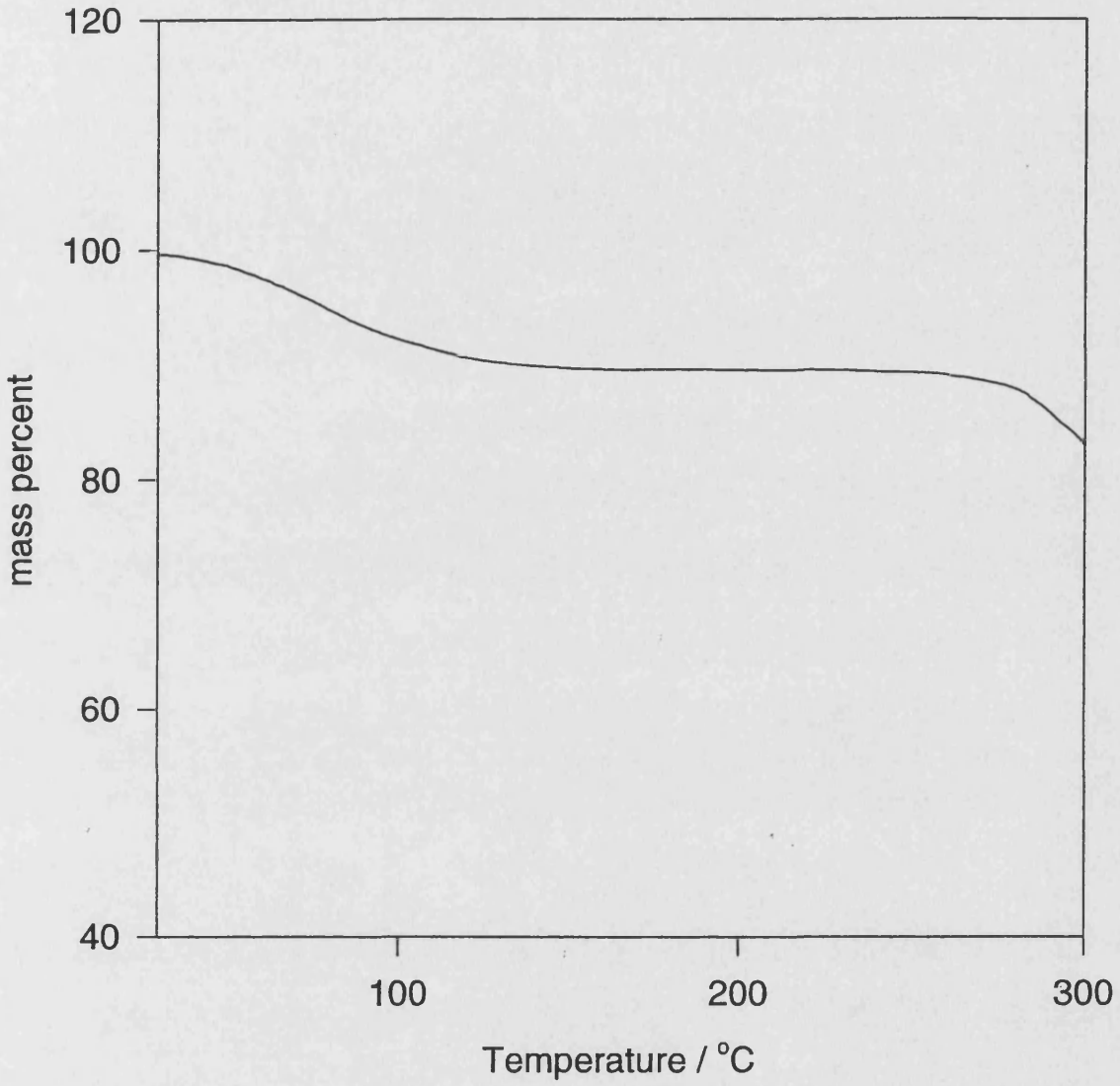

Figure 4.21: Mass spectrometry trace for Starch 1500

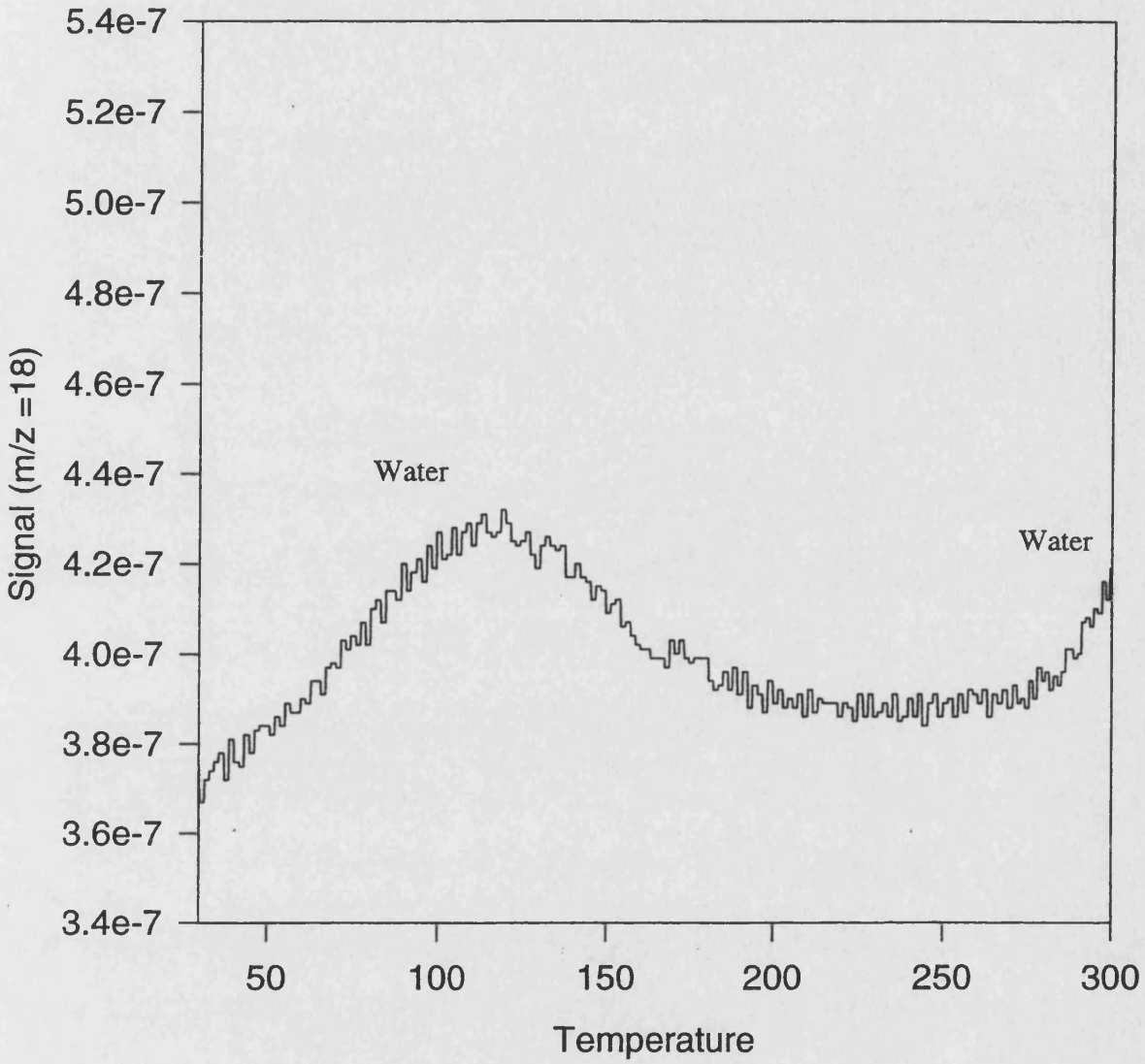

Figure 4.22: Mass spectrometry trace for DF48-Me-01

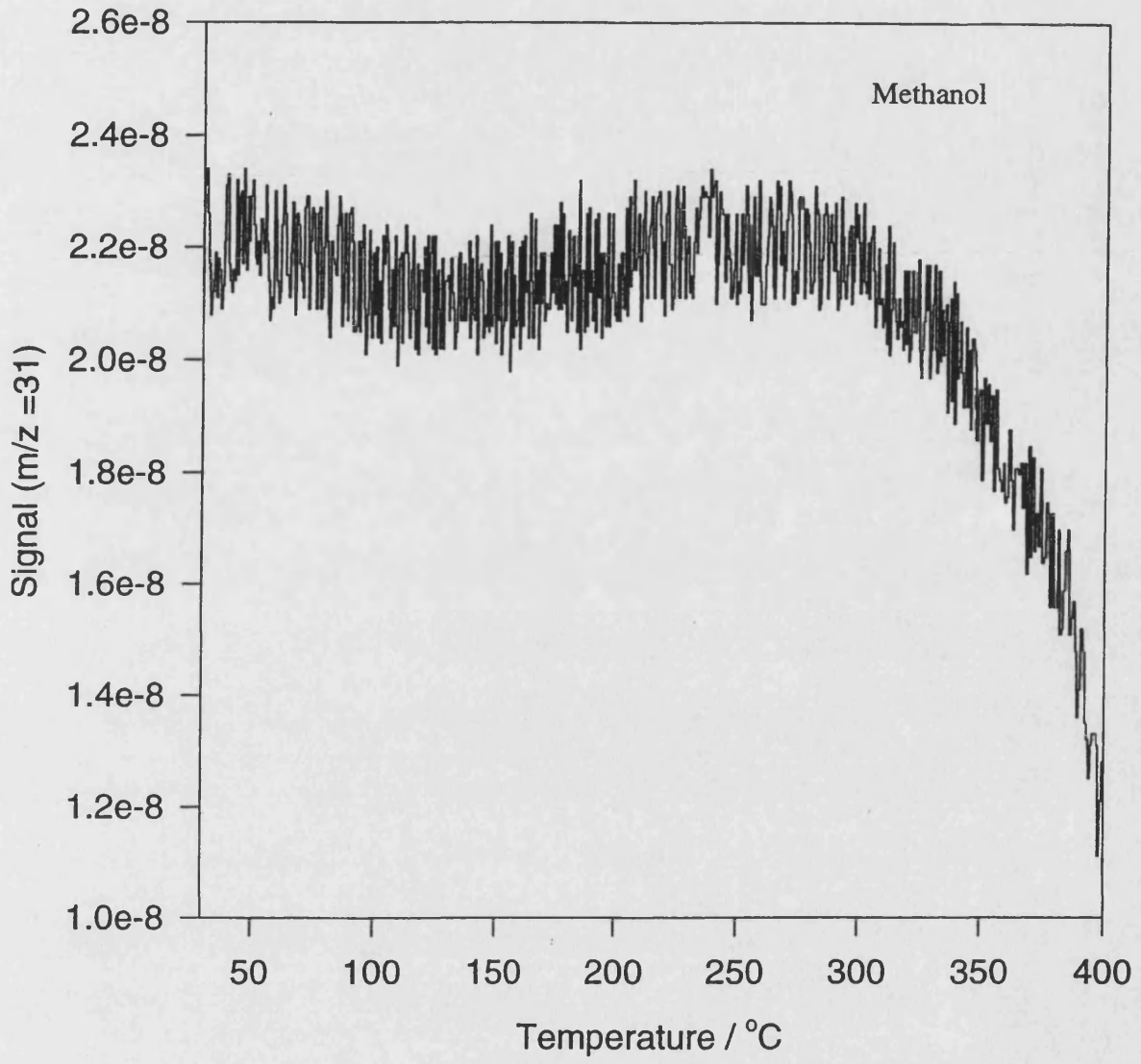

4.4 Other characterisation techniques

The other methods employed to characterise starches are described in separate chapters. Microscopy and associated preparatory techniques are described in chapters 5 and 6.

4.5 General Discussion

A wide range of techniques was employed to characterise the bulk powder properties of unmodified and defatted Starch 1500. Minimal differences were identified between the samples using techniques such as particle size analysis by TOFABS and surface area analysis. The techniques of SSNMR and TG/MS failed to detect the presence of residual solvent on the defatted materials or reveal that any physical changes to the material had occurred on defatting.

CHAPTER 5

SCANNING ELECTRON MICROSCOPY AND ENERGY DISPERSIVE X-RAY ANALYSIS

5.1 General Introduction

The morphology of native starches has been comprehensively characterised using conventional electron microscopy techniques (Evers, 1969; Gallant et al, 1973; Gallant and Guilbot 1973). However there has been little attention to the area of starches used as pharmaceutical tabletting excipients (Shangraw et al, 1981). The basis of this work was to investigate Starch 1500 in relation to its composition of native and pregelatinised starch.

5.1.1 Scanning Electron Microscopy (SEM)

Conventional SEM involves the bombardment of a sample surface with a fine beam of electrons. Upon impact, secondary electrons are liberated from the surface of the sample and are subsequently detected, resulting in the generation of an image. Scanning Electron Microscopy is classically performed under ambient temperature conditions and ideally requires a sample which is electrically conducting, mechanically stable, non volatile and dry.

During the irradiation of pharmaceutical powders, such as Starch 1500, there is some net absorption of the beam electrons. To avoid the accumulation of a negative charge at the specimen surface, it is essential that these absorbed electrons are earthed. This may be achieved by increasing the specimen surface conductivity through coating with a layer of gold. This coating also acts as the main source of secondary electrons.

Starch 1500 has a nominal moisture content of 10-12%, thus making it difficult to image using conventional SEM. The low pressures generated within the SEM chamber result in evaporation of water from the surface of the starch particles. As a consequence there is distortion on the surface of the particles and damage to the conducting layer of gold. This, in turn, leads to extensive sample charging. This water loss may also result in dimensional changes within the sample (Beckett and Read, 1986).

5.1.2 Low Temperature Scanning Electron Microscopy (LTSEM)

The use of LTSEM allows materials with high moisture contents to be analysed in their fully hydrated state. Through freezing and therefore stabilising surface water, fewer artefacts relating to dehydration of the sample are observed. It is now well established that LTSEM provides improved preservation of the samples fine structure (Jeffree and Read, 1991b). However, for high-resolution studies, attention

must be made to avoid generating artefacts, e.g. ice crystal formation, water vapour contamination and electron beam damage (Jeffree and Read, 1988).

5.1.3 Energy Dispersive X-ray Analysis (EDAX)

When imaging a sample by SEM, characteristic X-rays are generated when the high-energy electron beam interacts with the sample. The energy of the x-ray emitted by the exited atom is unique to that element. EDAX allows chemical analysis to be performed on a well defined ($1\mu m^2$) region of the material (Goldstein et al. 1992).

5.2 MATERIALS & METHODS

5.2.1 Conventional SEM

Conventional SEM was performed using a JEOL 6310 computer-controlled scanning electron microscope (JEOL, U.K.). Samples of Starch 1500 were mounted on aluminium specimen-stubs using double sided carbon coated adhesive tabs. Prior to examination the samples were gold coated for five minutes (Sputter Coater, Model S150B, Edwards High Vacuum, Sussex, U.K.).

5.2.2 LTSEM

The preparation of a frozen hydrated sample for LTSEM involves three main operational stages:

Cryofixation

The powder samples were mounted on double sided carbon coated adhesive tabs which were then attached to aluminium specimen stubs, using a mixture of cryo-adhesive (Tissue-Tek O.C.T. Compound, Miles Laboratories Inc., U.S.A) and a conducting compound, colloidal carbon (Leit-C, Gerhard Neubauer, Munster, Germany). Cryofixation was achieved by plunging the samples into sub-cooled nitrogen (nitrogen slush) at -210°C. This process results in instant freezing of the sample and should therefore stabilise the material's physical structure. The samples were transferred to the cryogenic unit (CT1300 Cryo-Trans system, Oxford Inst., U.K.) using an evacuated transfer device to reduce atmospheric water condensation onto the specimen surfaces. Contaminating frost was removed by increasing the sample stage temperature to approximately -85°C in the SEM chamber. Sublimation of this superficial ice from the powder surface was achieved in approximately 5 minutes. This process, termed partial freeze-drying (Jeffree and Read, 1991a) can be directly visualised in the SEM.

Coating

The samples were sputter coated with gold for three minutes within the cryo-preparation chamber at 180°C. During coating a vacuum of 20 Pa was drawn and a current of 2mA at 4V applied across the sample.

Examination

Examination of the samples was conducted at approximately -175°C using a computer-controlled scanning electron microscope with low temperature facility (SEM 6310, JEOL, U.K.). The chamber was maintained at this temperature using liquid nitrogen. Powder samples were imaged at magnifications at a range of x 220 to 5,5000 at an accelerating voltage of 5 - 10kV. This technique allowed visual characterisation of Starch 1500 and also comparison with native and defatted starches.

5.2.3 Energy Dispersive X-ray Analysis (EDAX)

Native maize starch was studied using EDAX whilst being examined by LTSEM (the sample stage temperature was approximately –170°C). The X-ray signals were analysed with an X-ray analyser (AN1000, Oxford Instruments, U.K.). The sample was irradiated for 100 to 200 seconds at an accelerating voltage of 10kV.

5.3 Results and Discussion

5.3.1 Conventional SEM

The images of Starch 1500 obtained using conventional SEM (figures 5.1 and 5.2) show the heterogeneity of the material. A wide distribution of particle size and morphology is exhibited. Intact native starch granules can be observed both as discrete particles and incorporated in larger agglomerates of pregelatinised starch. This agrees with the particle size analysis data, which shows a bimodal distribution.

Higher magnification studies of Starch 1500 resulted in an accumulation of negative charge at the sample surface. It is likely that this results from damage to the conductive gold coating, due to evaporation of water from the sample when under vacuum.

It is possible to reduce such sample charging by drying or storing the material at low humidities. However, since starches have a high moisture content it was considered important to image the sample in its fully hydrated state using LTSEM.

5.3.2 Low Temperature SEM

Samples of native maize starch were imaged alongside unmodified and defatted Starch 1500 as a control to demonstrate that the images obtained were not artefacts of the technique, i.e. that the physical processes of freezing, coating and imaging the samples did not result in the disruption of starch granule structure and that the displayed morphology of Starch 1500 was a consequence of partial pregelatinisation.

Native starch

The particle size distribution and morphology imaged (figures 5.3 and 5.4), agreed with the published results for native maize starch (Farhadieh, 1994; Zobel, 1988). Some of the particles exhibited a pitted surface. This has been previously reported to result from the impression of zein bodies on the granules surface (Christianson et al, 1969).

Starch 1500

As was observed with conventional SEM, Starch 1500 contains large agglomerates of native and pregelatinised maize starch. However, on viewing using LTSEM (figures 5.5 to 5.13), bridges of gelatinised material are seen to cover native granules. It is suggested that the gelatinised fraction serves to bind together the native granules. Further evidence of this is given in chapter 6 (section 6.3.1). These gelatinised bridges were not observed by conventional SEM. This is likely to be because they are destroyed during water loss when the sample is placed under vacuum.

Defatted Starch 1500

Due to the great variety of structures observed in the Starch 1500 particle distribution it is impossible to state confidently than any differences in morphology, which may arise, are directly due to the defatting process (figures 5.14 to 5.47). In general the defatted starch seems to show a higher degree of particle agglomeration. This is apparent to some degree with each solvent, as can clearly be seen in DF48-69-01A and DF48-He-01. Images taken of DF24-96-01 at higher accelerating voltages (15kV) show the surface of the pregelatinised starch fraction to be rougher and flakier after the defatting process.

5.3.3 Energy Dispersive X-ray Analysis (EDAX)

Initial studies of the images of native maize starch revealed small fragments of an unknown material on its surface (figures 5.3 and 5.4). EDAX revealed small sodium and iron signals which were absent from native starch (5.48 and 5.49). It is suggested that these particles are residual plant material remaining from the extraction of the native granules from the maize endosperm. It is noteworthy that these fragments are possibly too small to study by EDAX and that the generated signal may arise mainly from the native starch granules on which the target material is located. As such the elemental analysis results were deemed inconclusive.

5.4 General Discussion

LTSEM proved to be an invaluable technique in the imaging of Starch 1500. By freezing and thus stabilising the powder system, the integrity of the delicate bridges of pregelatinised starch was maintained. This technique allows visualisation of hygroscopic hydrated pharmaceutical materials without the charging experienced with conventional SEM. A positive correlation was observed between the amount of lipid removed from Starch 1500 and the level of agglomeration of the imaged particles.

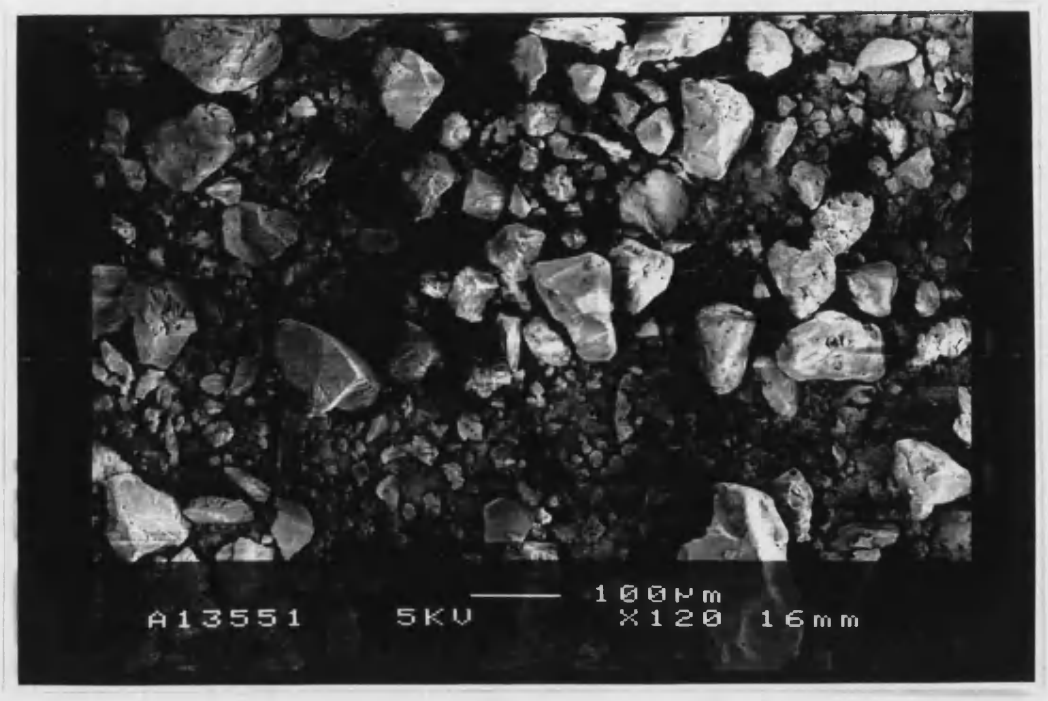

Figure 5.1: Conventional SEM of Starch 1500 particle distribution.

Figure 5.2: Starch 1500 agglomerate. The image shows characteristic charging as seen on viewing the material by conventional SEM

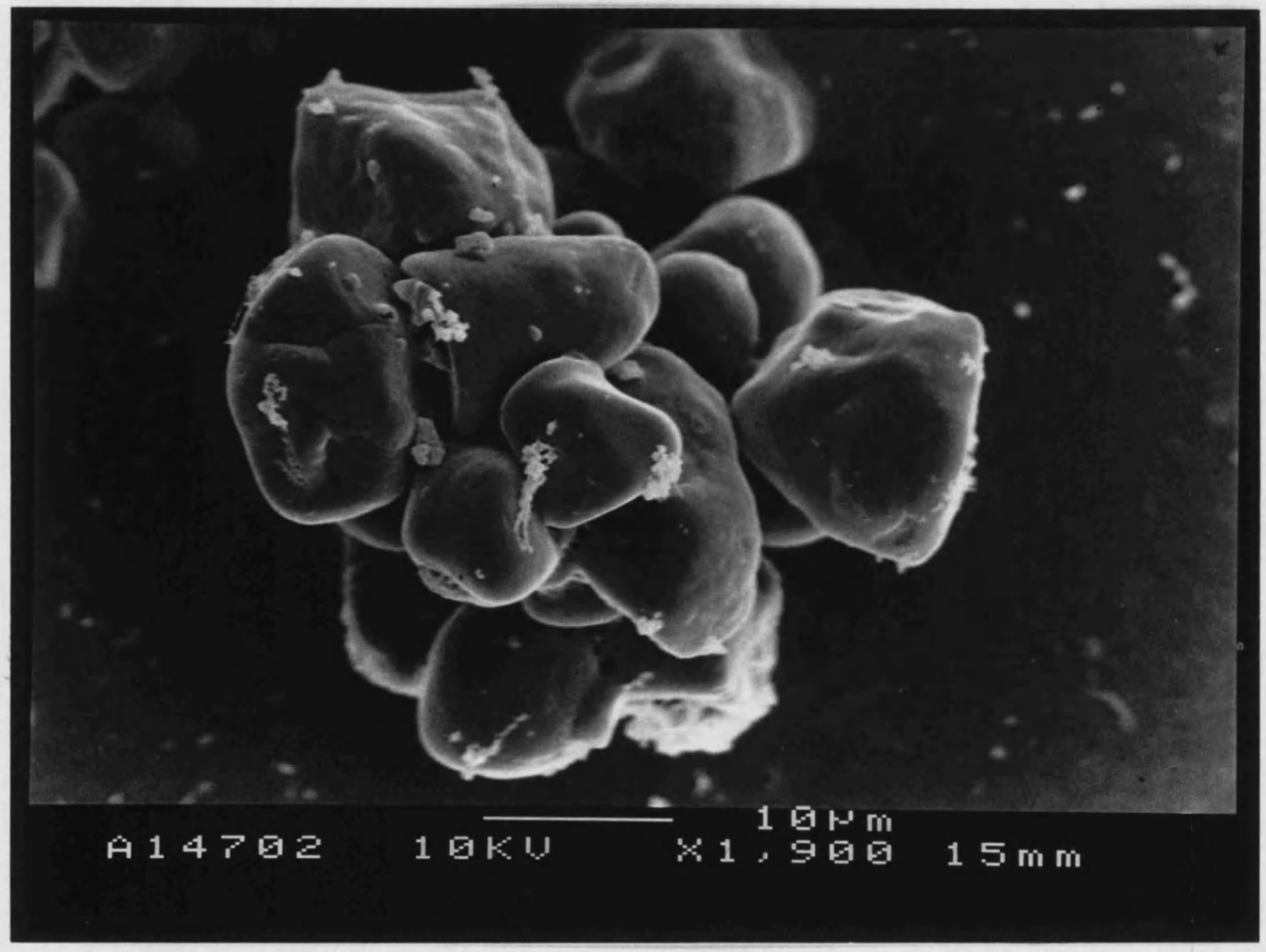

Figure 5.3: Native maize starch agglomerate and evidence of small particles (possibly residual plant material).

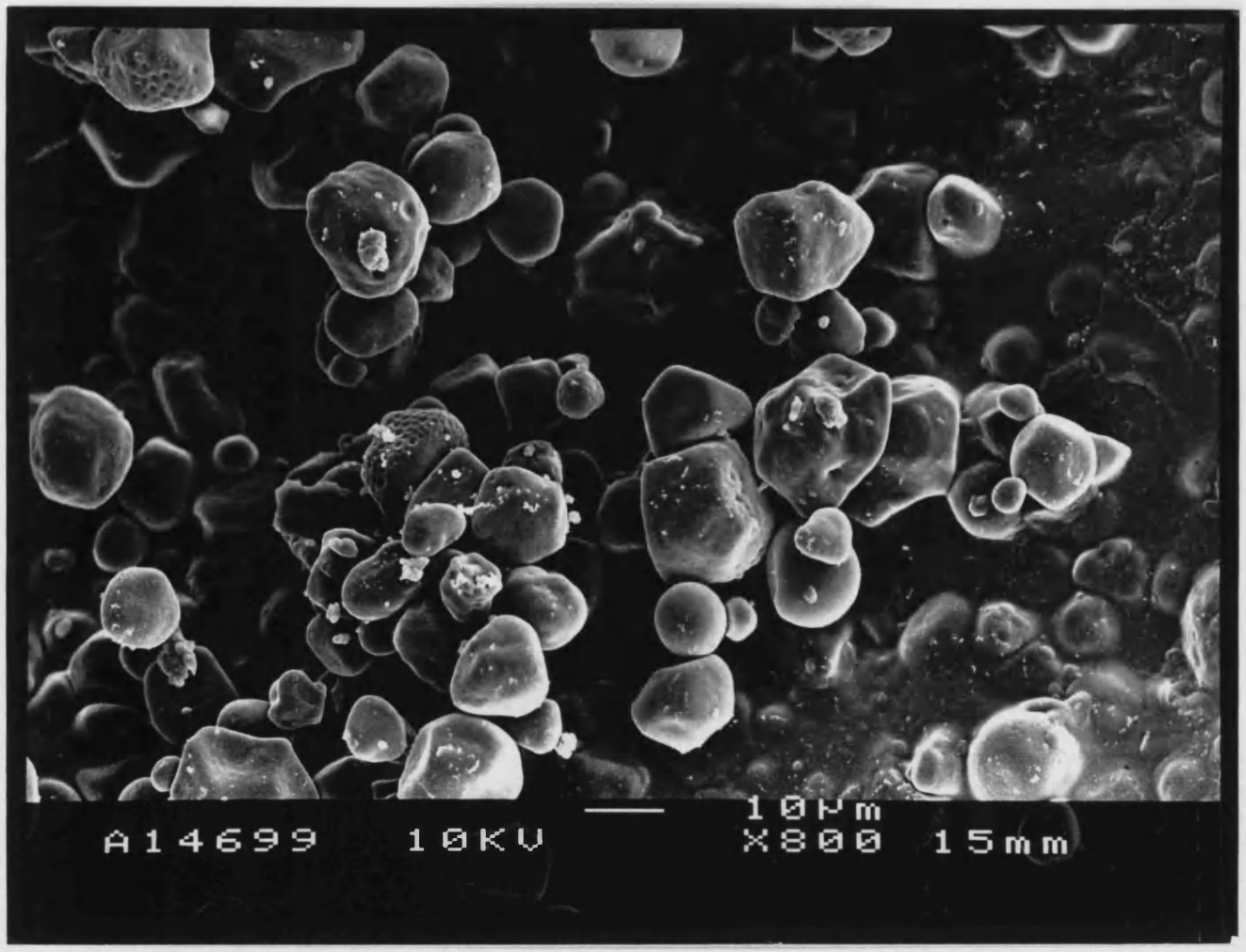

Figure 5.4: Distribution of native maize starch particle size and morphology.

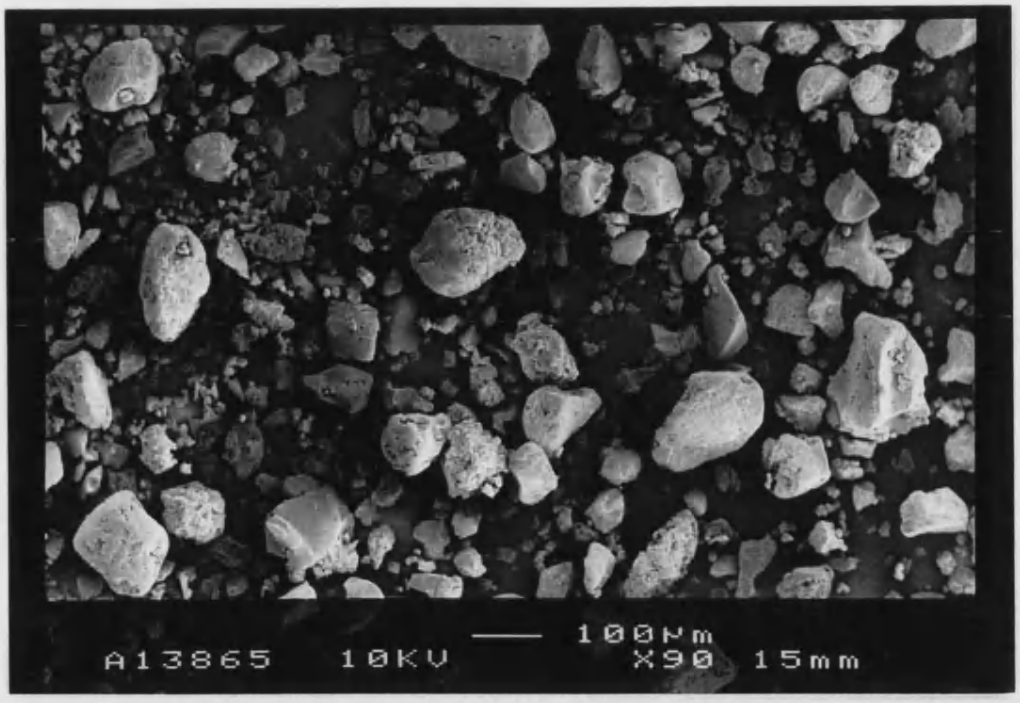

Figure 5.5: LTSEM of Starch 1500 particle distribution

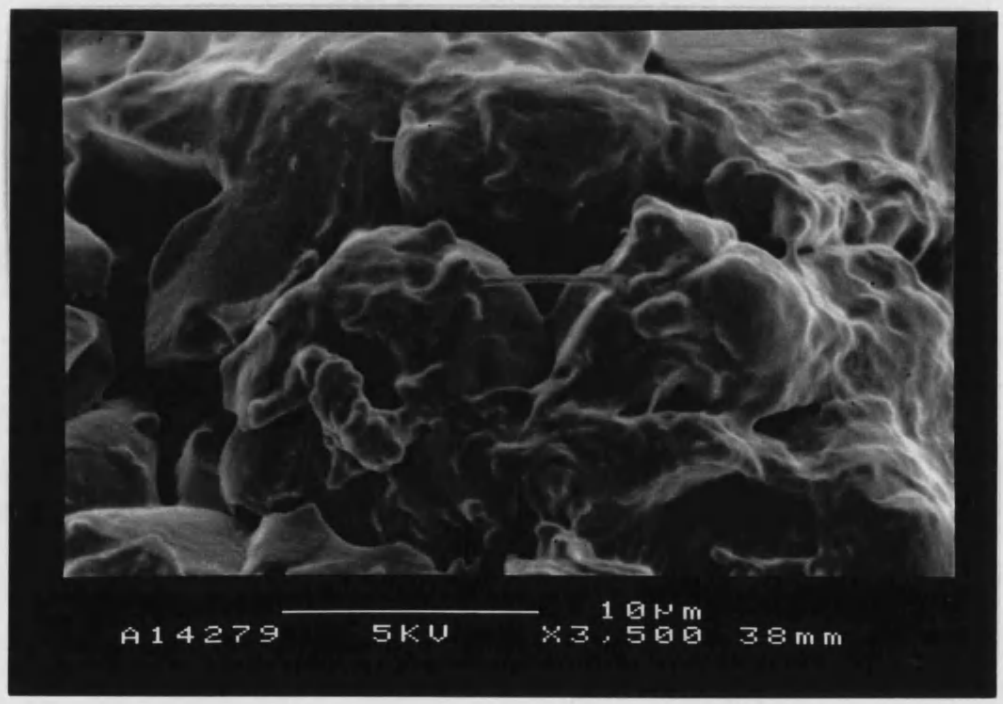

Figure 5.6: LTSEM image of Starch 1500. The micrograph shows detail of "pregelatinised bridges" coating native granules of starch.

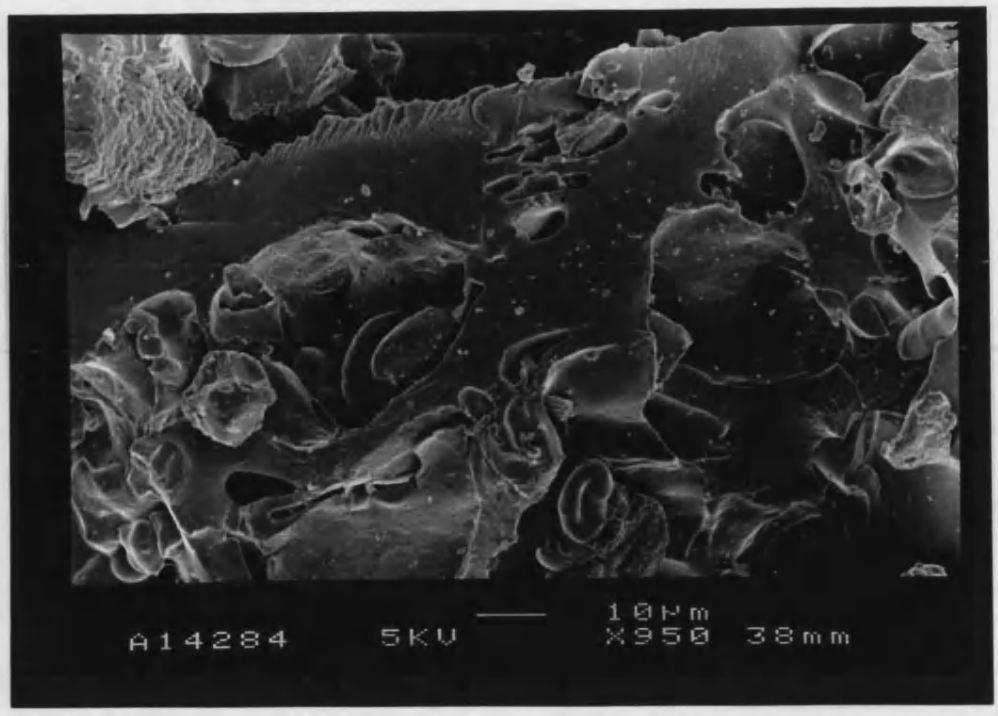

Figure 5.7: A particle of Starch 1500 consisting primarily of pregelatinised starch. The particle contains open pores, which may arise from native granules being dislodged from its surface.

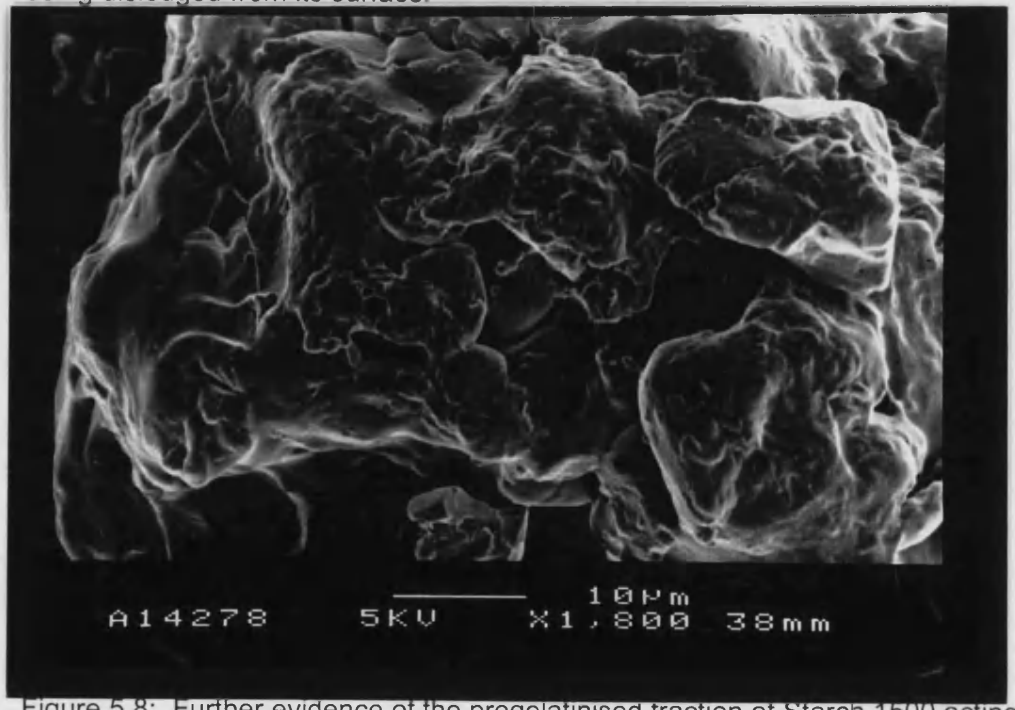

Figure 5.8: Further evidence of the pregelatinised fraction of Starch 1500 acting as binder to incorporate the native granules into larger agglomerates.

Figure 5.9: Large particle of Starch 1500, with evidence of pores similar in diameter to native maize starch granules.

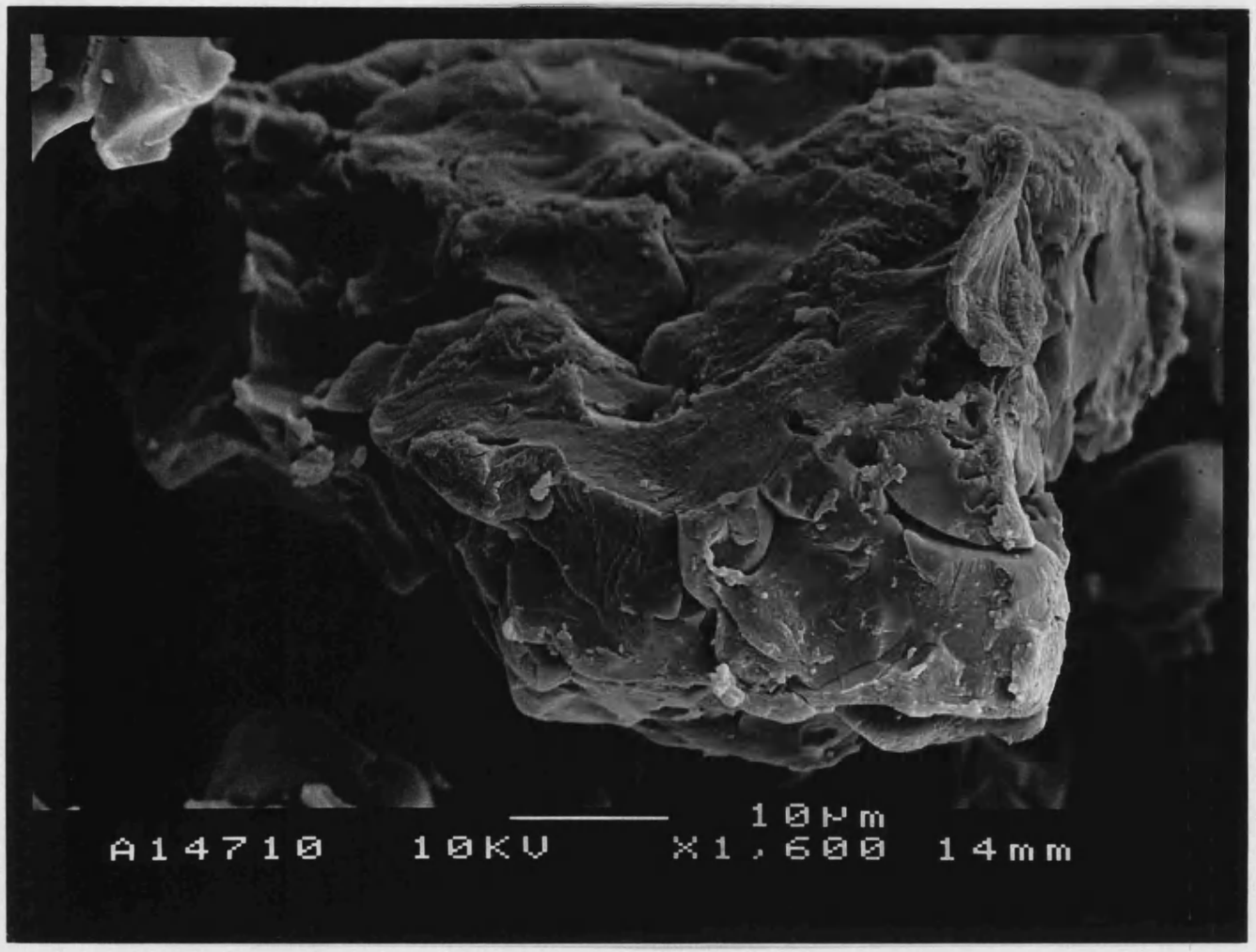

Figure 5.10: Detail of a pregelatinised particle of Starch 1500.

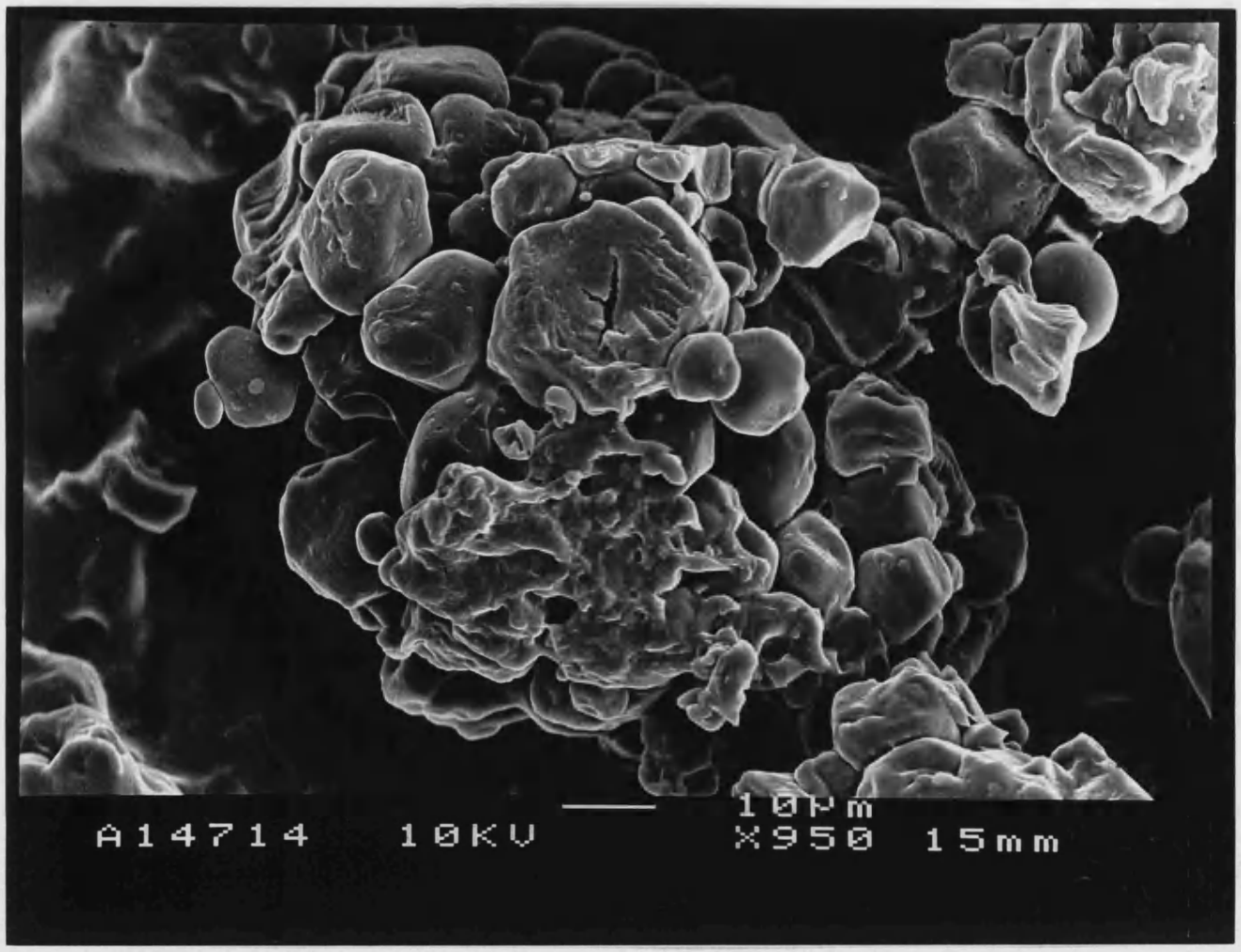

Figure 5.11: Loose agglomerate of native and pregelatinised starch. Evidence of a ruptured granule in the centre of the micrograph.

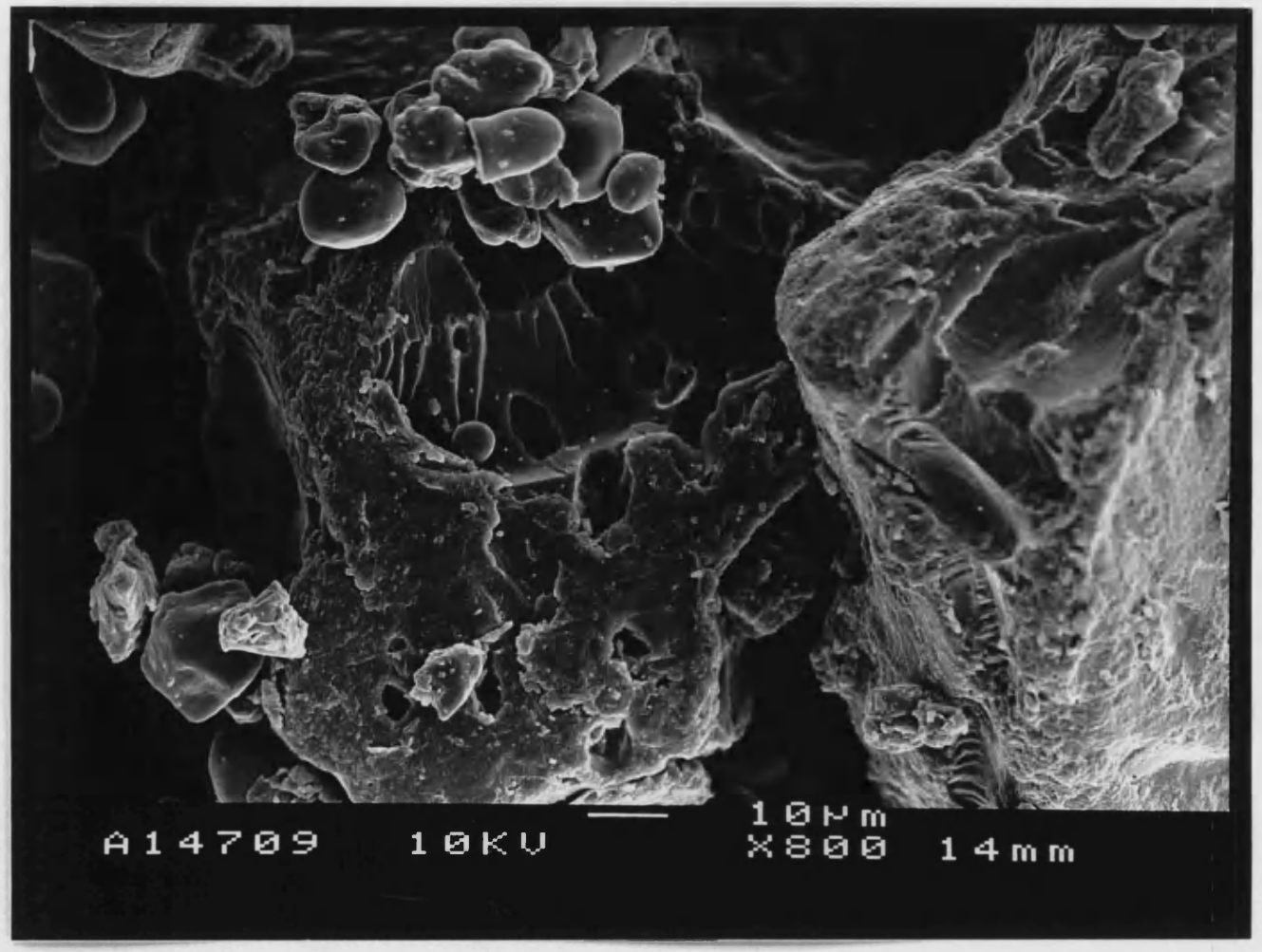

Figure 5.12: Further evidence of the morphology of Starch 1500 particles.

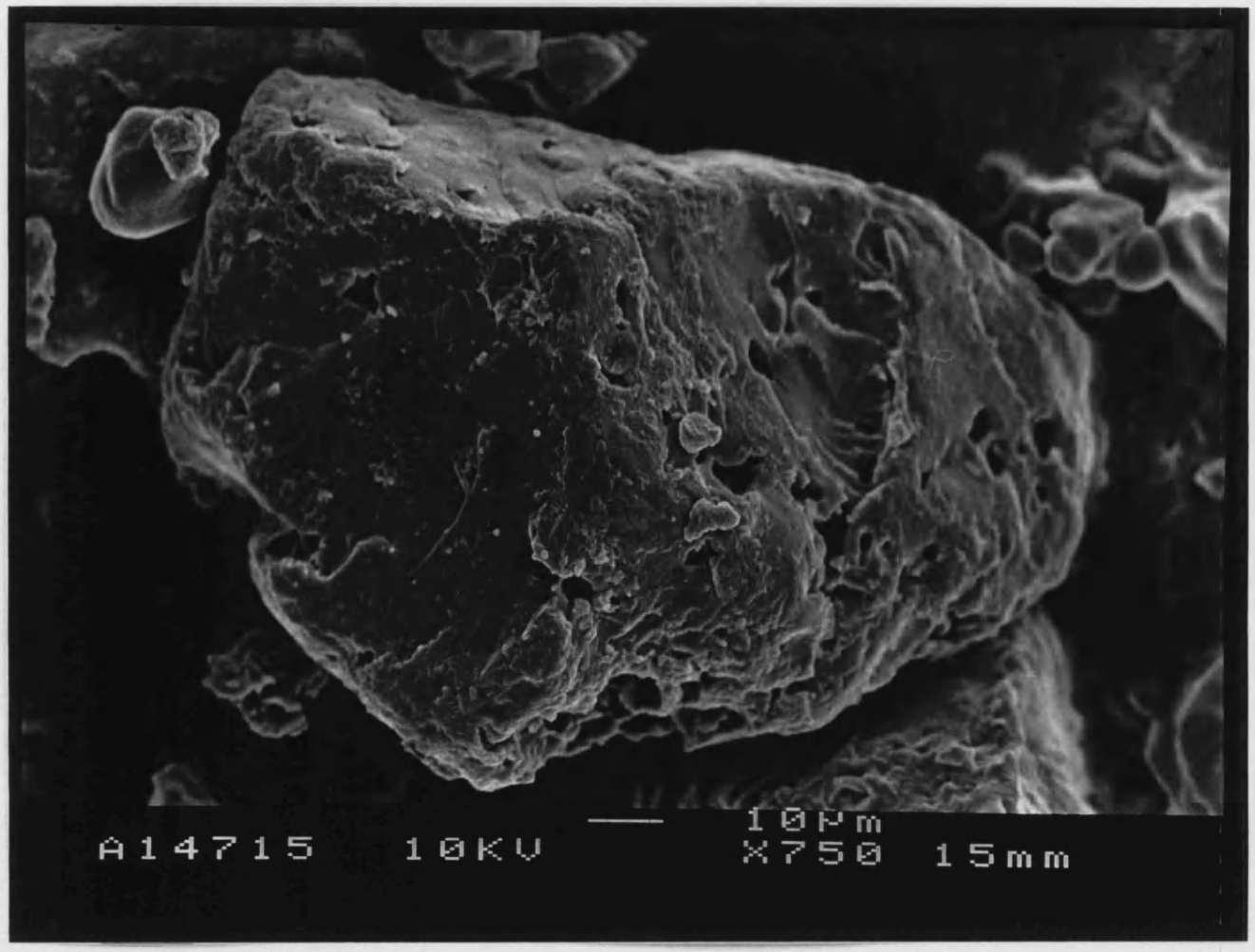

Figure 5.13: Large pregelatinised Starch 1500 particle. No evidence of incorporated native granules.

Figure 5.14: Porous particle of DF24-96-01.

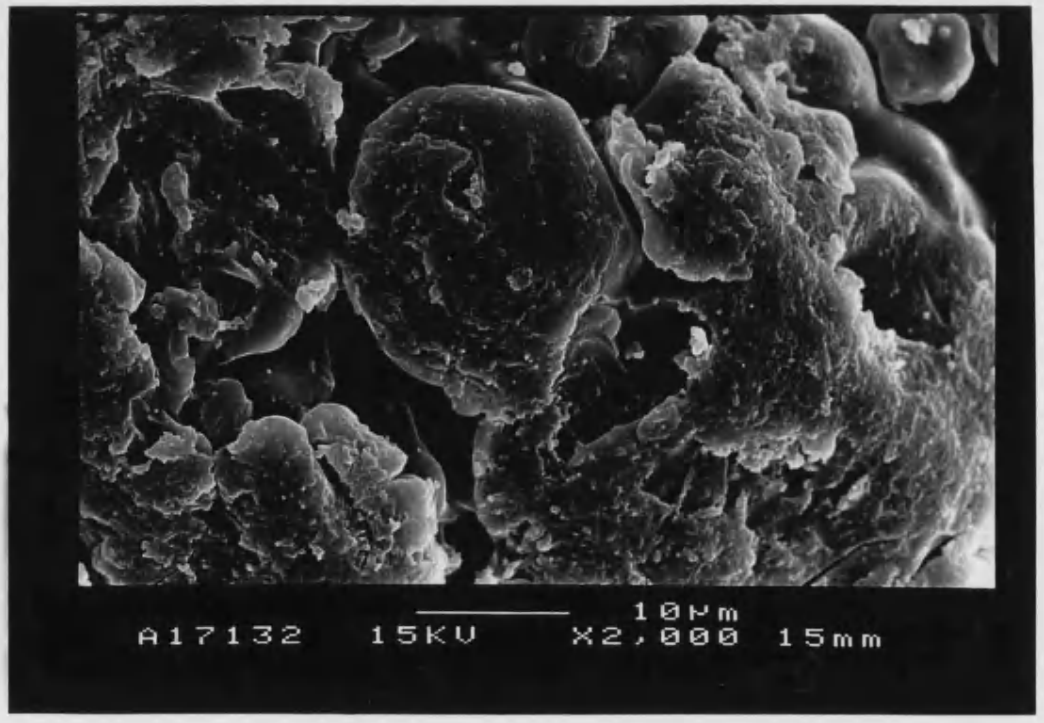

Figure 5.15: Detail of pregelatinised fraction of DF24-96-01.

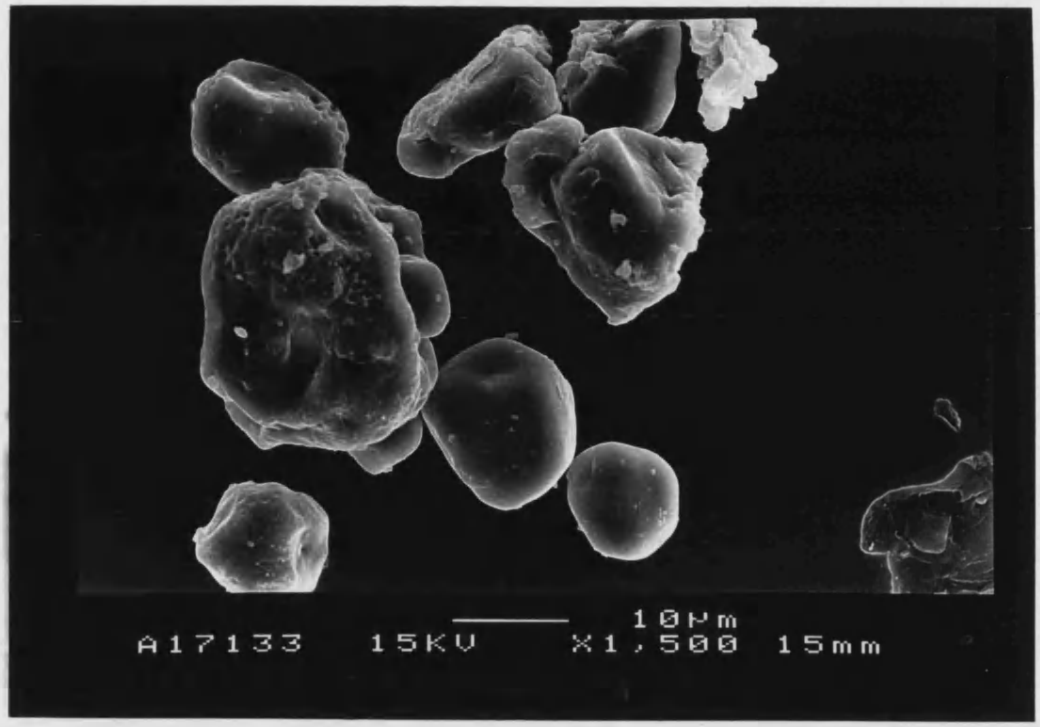

Figure 5.16: Native granules from DF24-96-01.

Figure 5.17: Agglomerate of DF24-96-01.

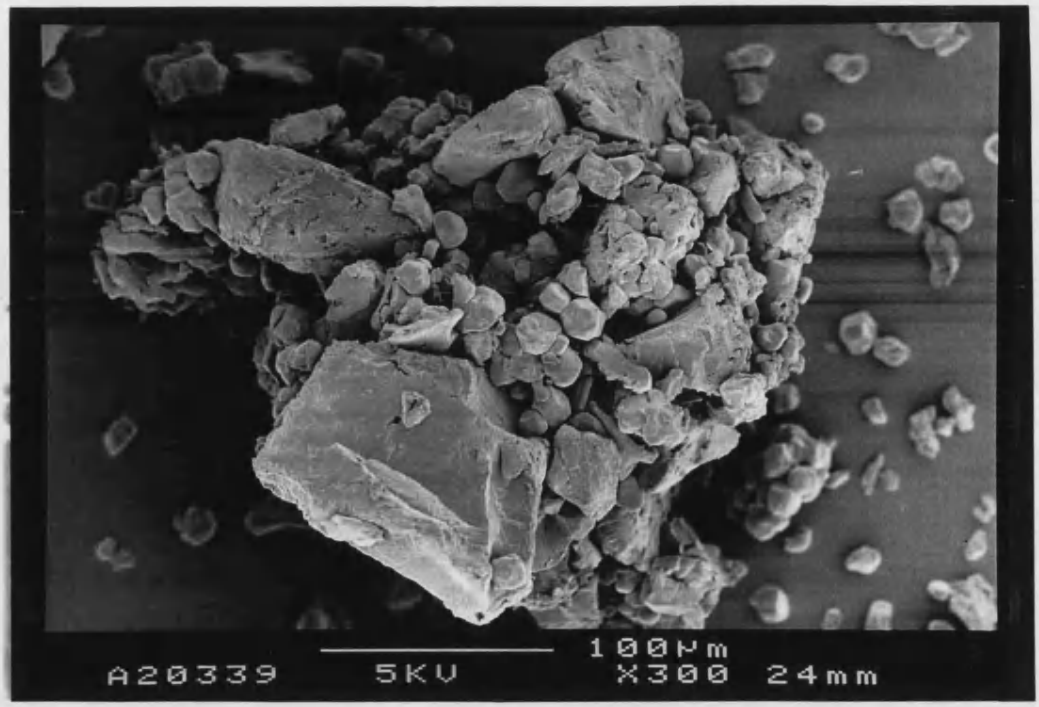

Figure 5.18: Agglomerate of DF48-Me-01

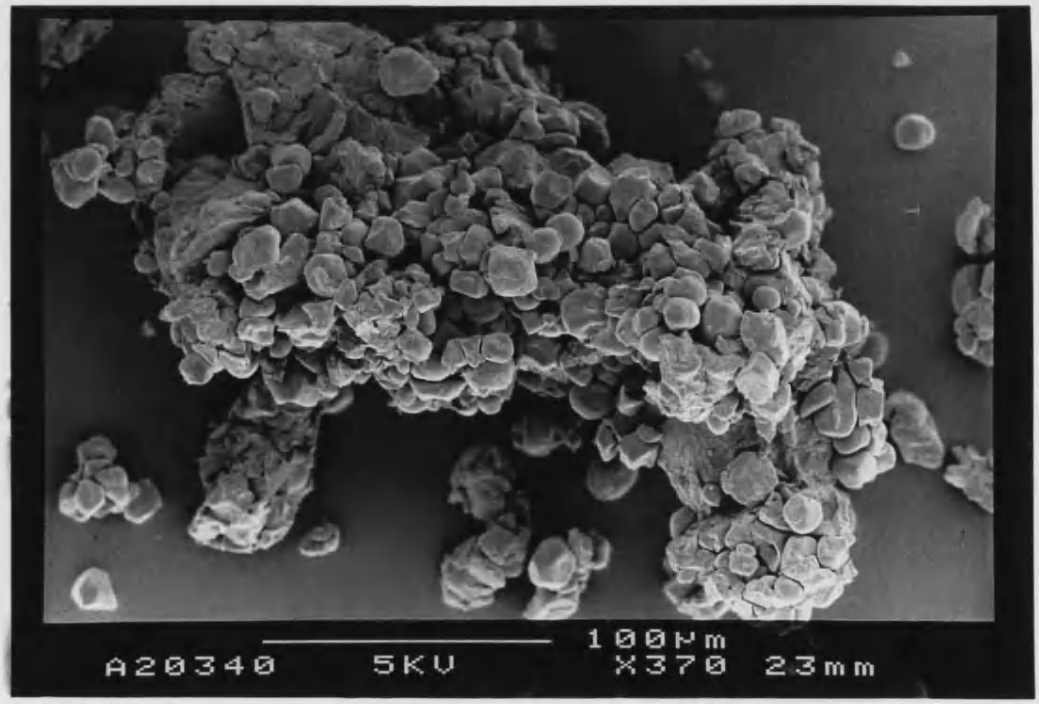

Figure 5.19: Large agglomerate of native maize starch in DF48-Me-01

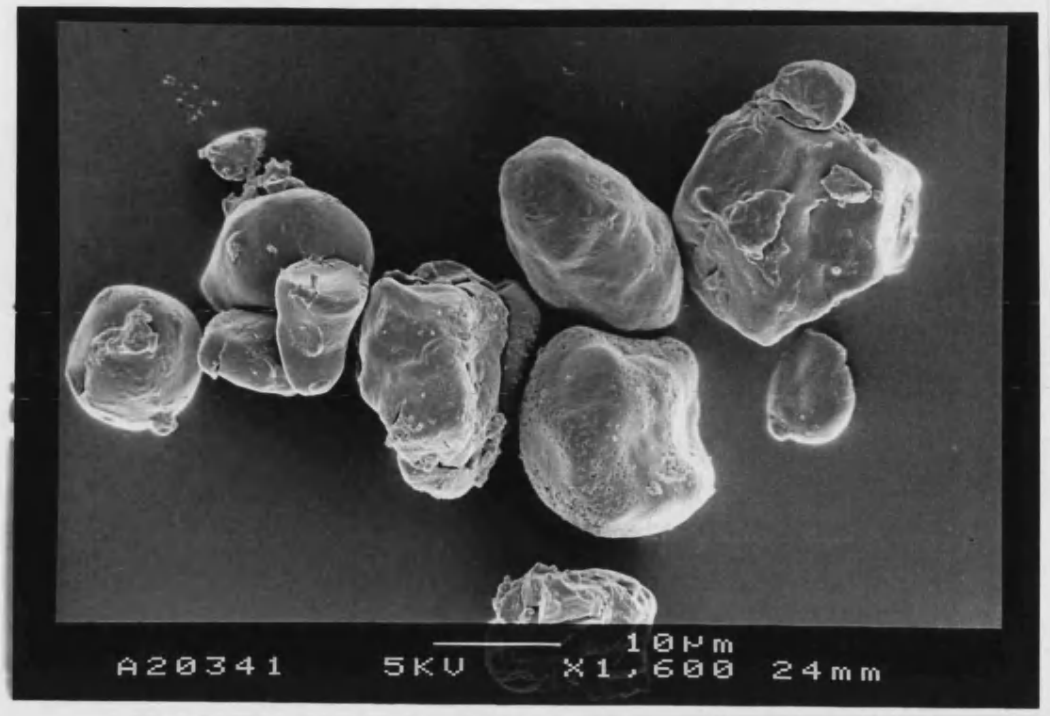

Figure 5.20: Native granules from DF48-Me-01 with some evidence of gelatinised material on their surface.

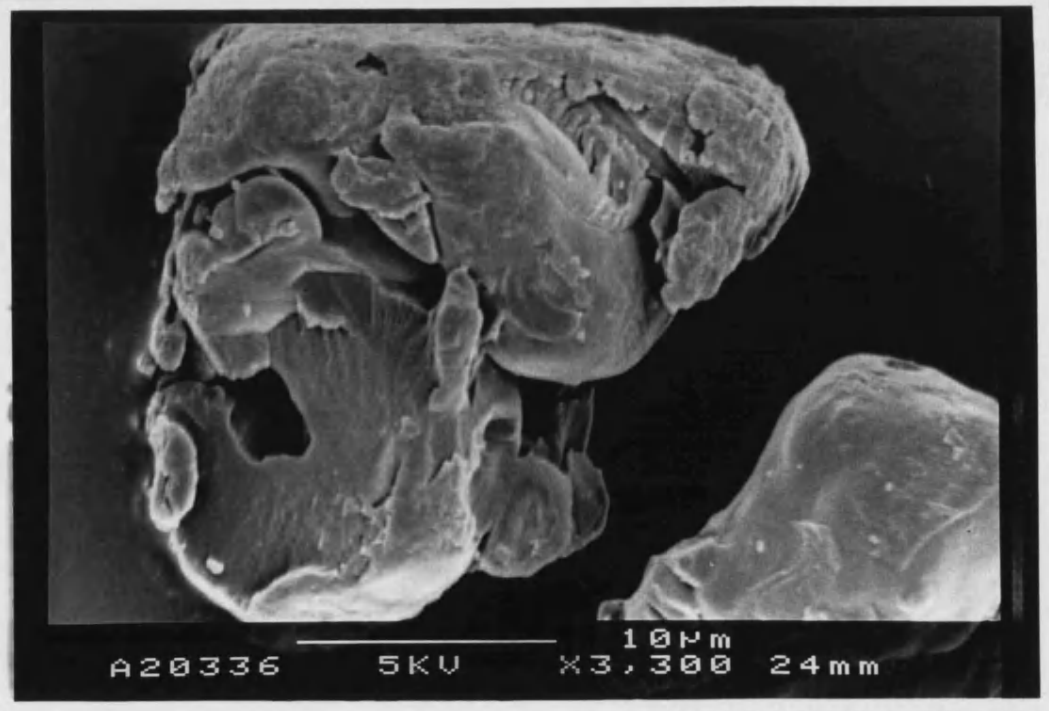

Figure 5.21: Image of a sheared granule of native starch from DF48-Pr-04.

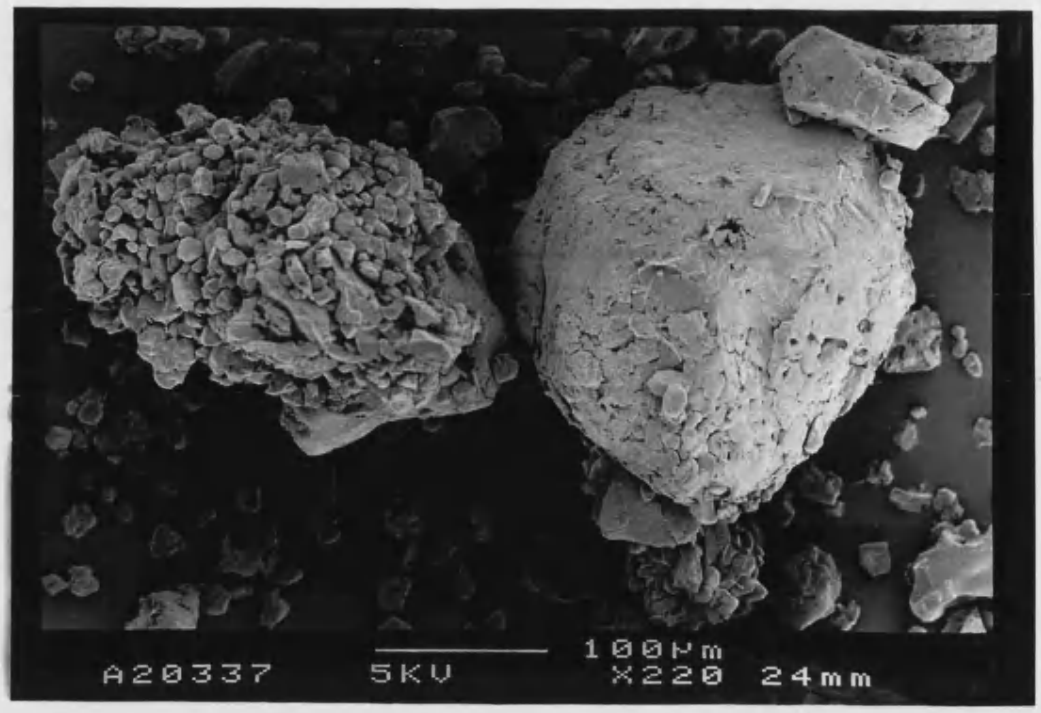

Figure 5.22: An agglomerate and pregelatinised particle from DF48-Pr-04.

Figure 5.23: An agglomerate of native granules with a coating of gelatinised starch.

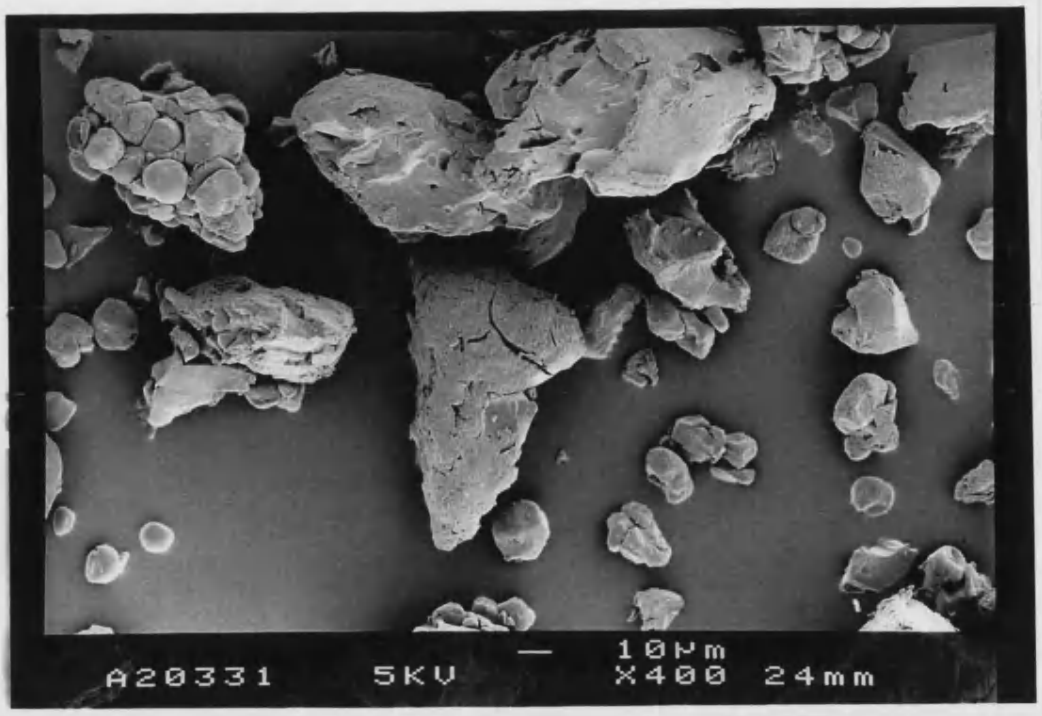

Figure 5.24: DF48-99-03 particle distribution.

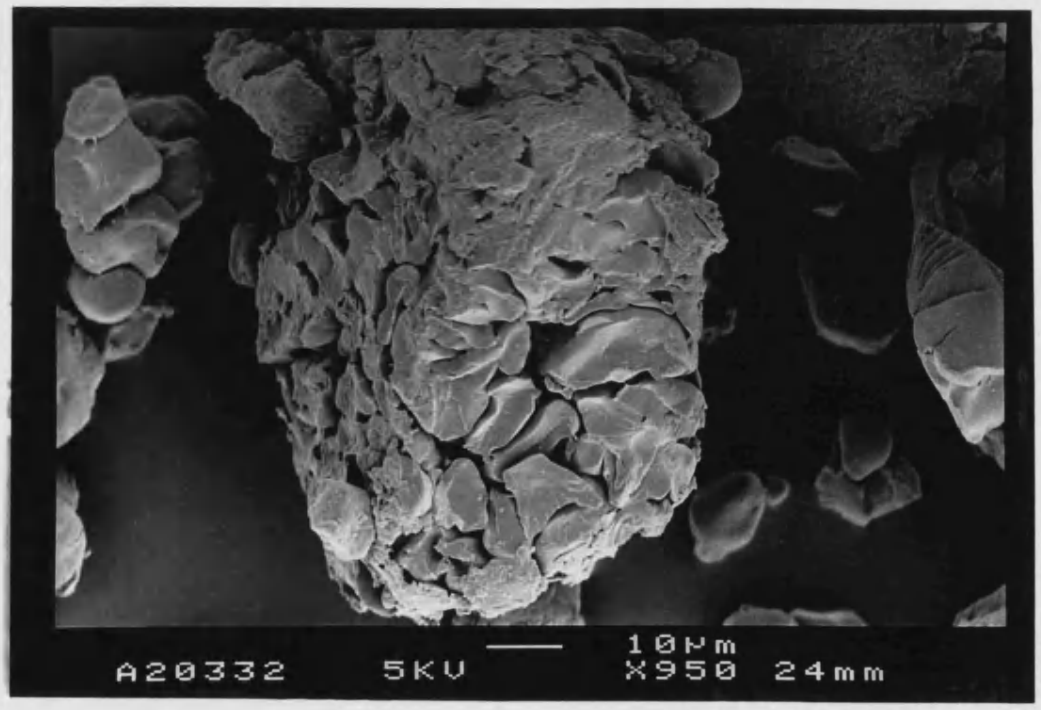

Figure 5.25: DF48-99-01 agglomerate. The constituent particles do not resemble native starch granules.

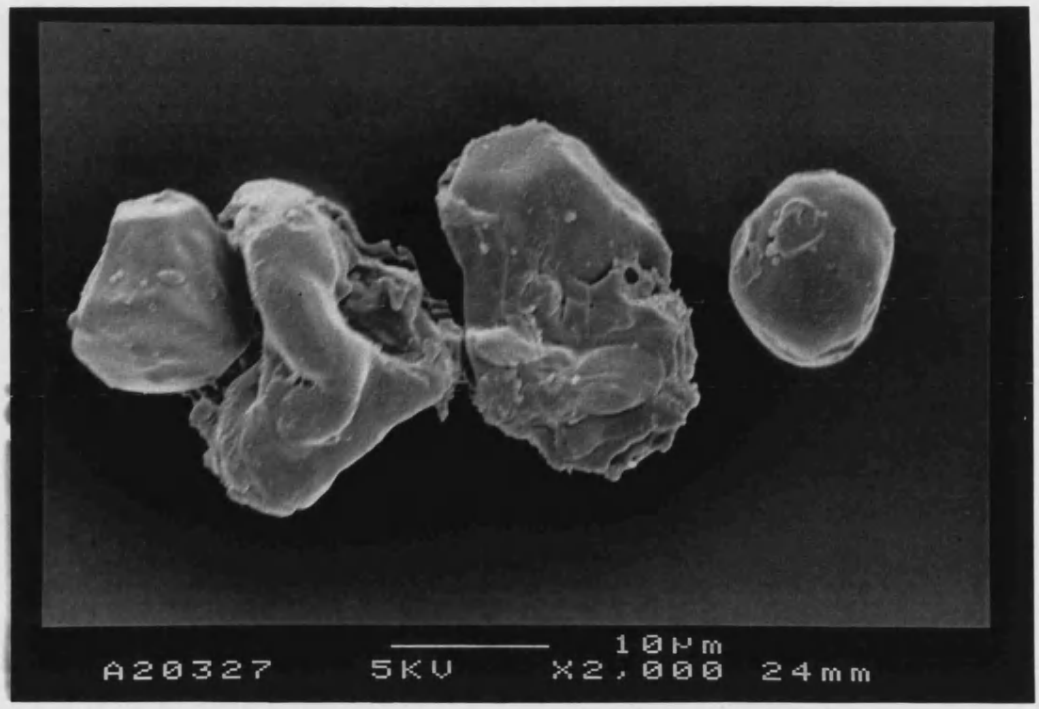

Figure 5.26: Native and pregelatinised particles from DF48-96-03.

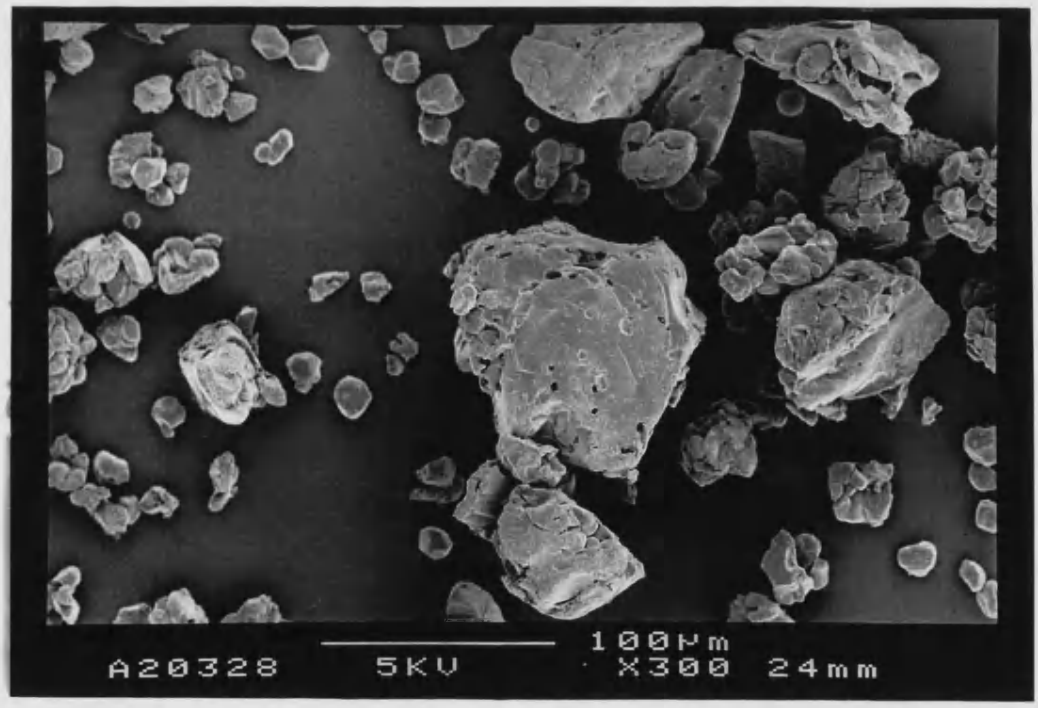

Figure 5.27: Particle distribution in DF48-96-03.

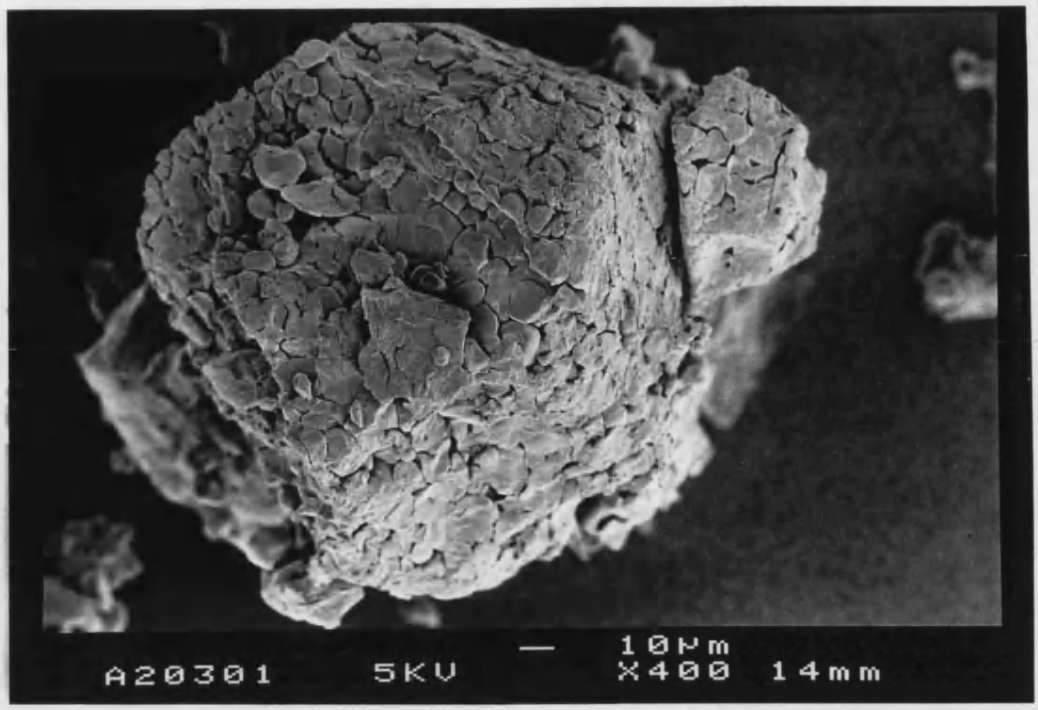

Figure 5.28: Tightly packed agglomerate of DF48-96-01A

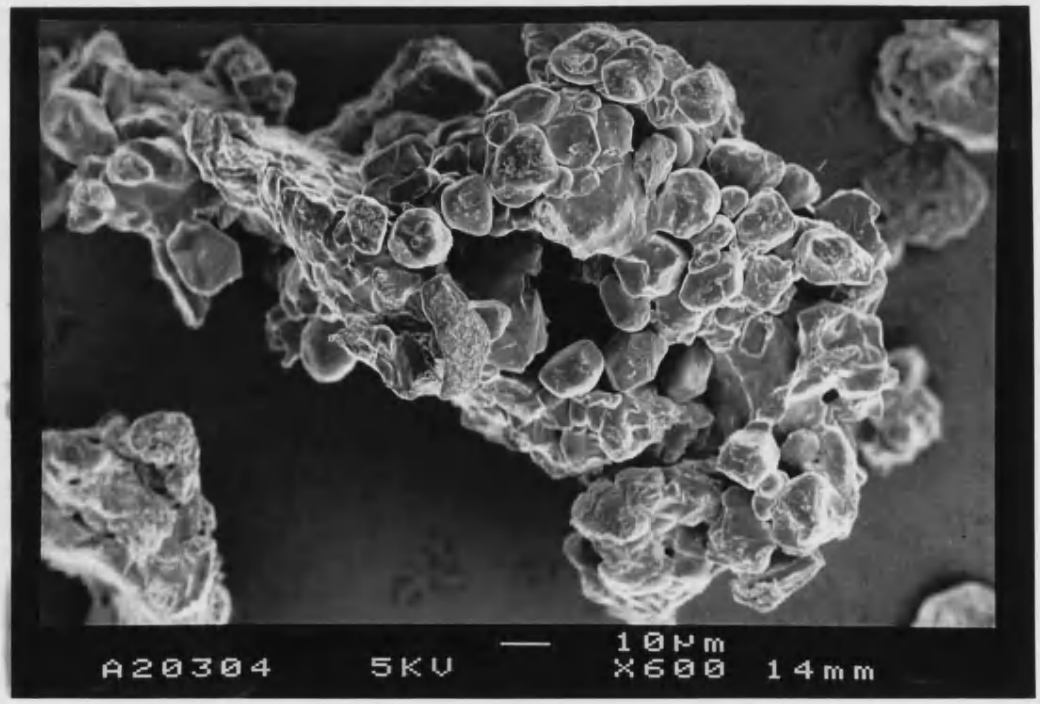

Figure 5.29: Loosely packed agglomerate of DF48-96-01A.

Figure 5.30: Particle of DF48-85-01containing gelatinised and native material.

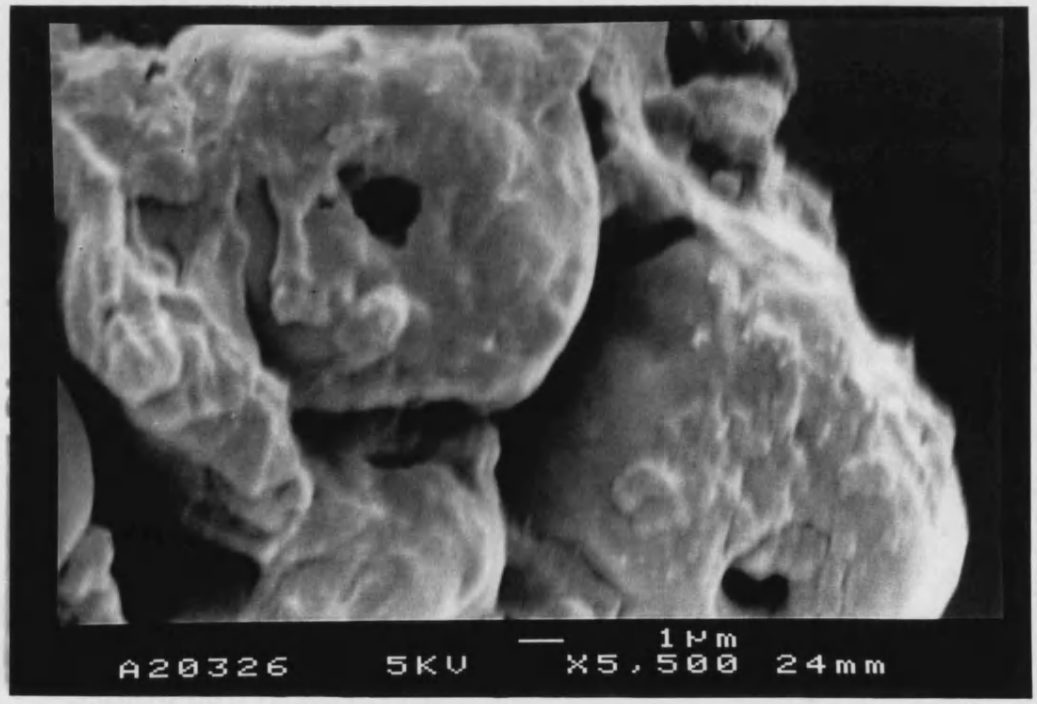

Figure 5.31: Detail of figure 5.30 showing the hilums of cleaved native granules, seemingly covered in gelatinised starch

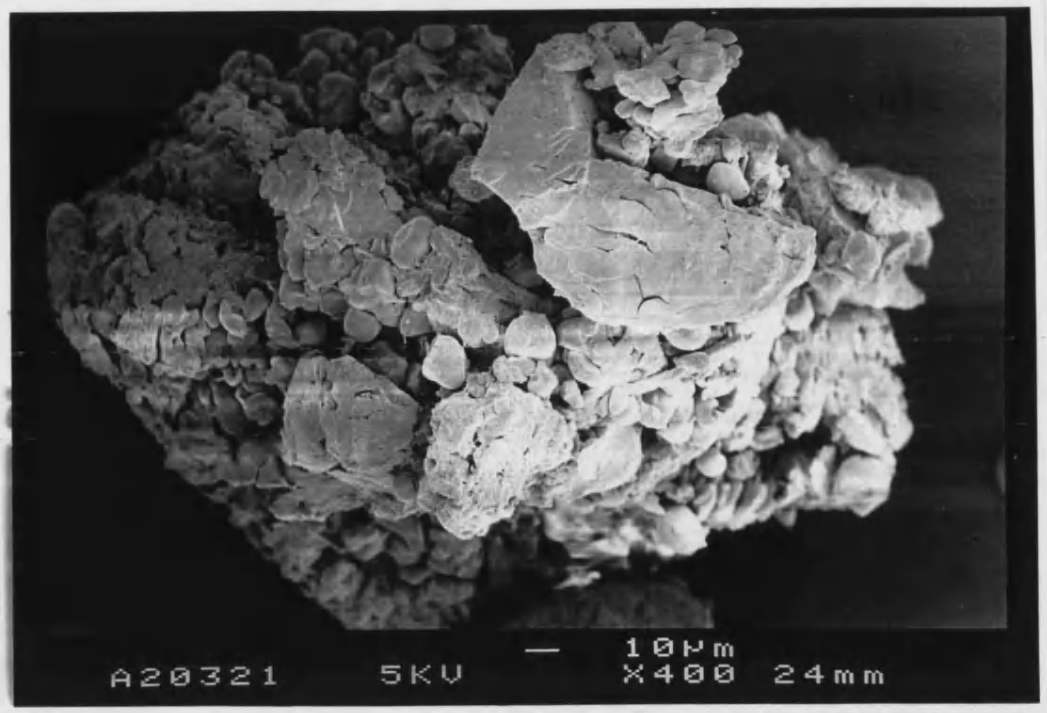

Figure 5.32: Large tightly packed agglomerate of native and pregelatinised material from DF48-70-01

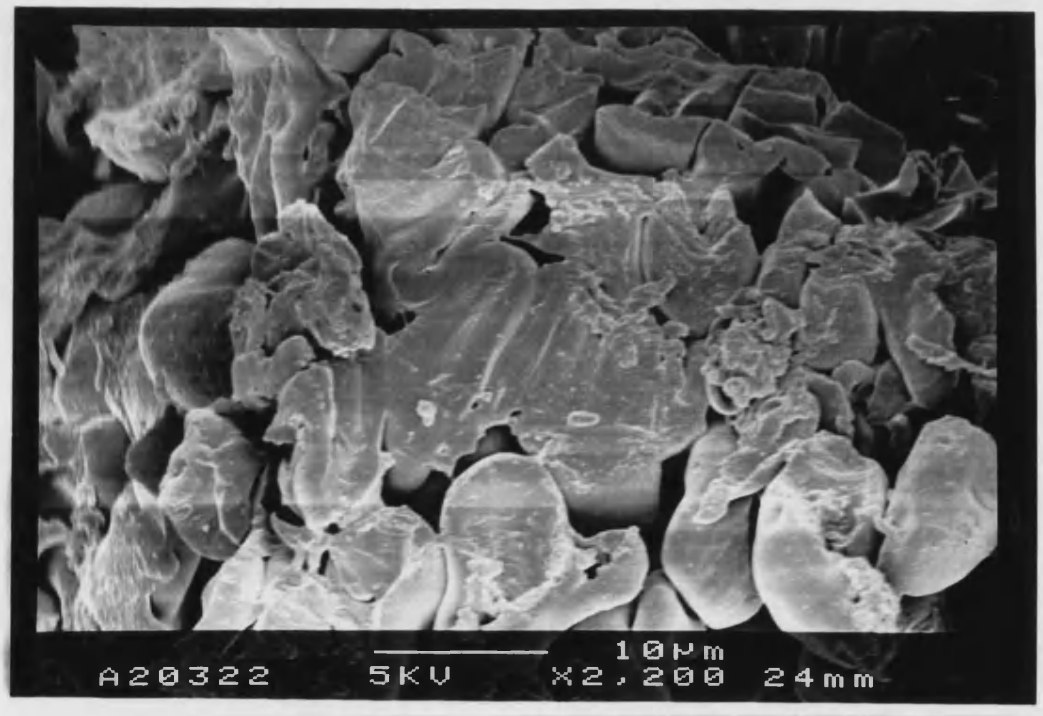

Figure 5.33: Surface of pregelatinised particle of DF48-70-01

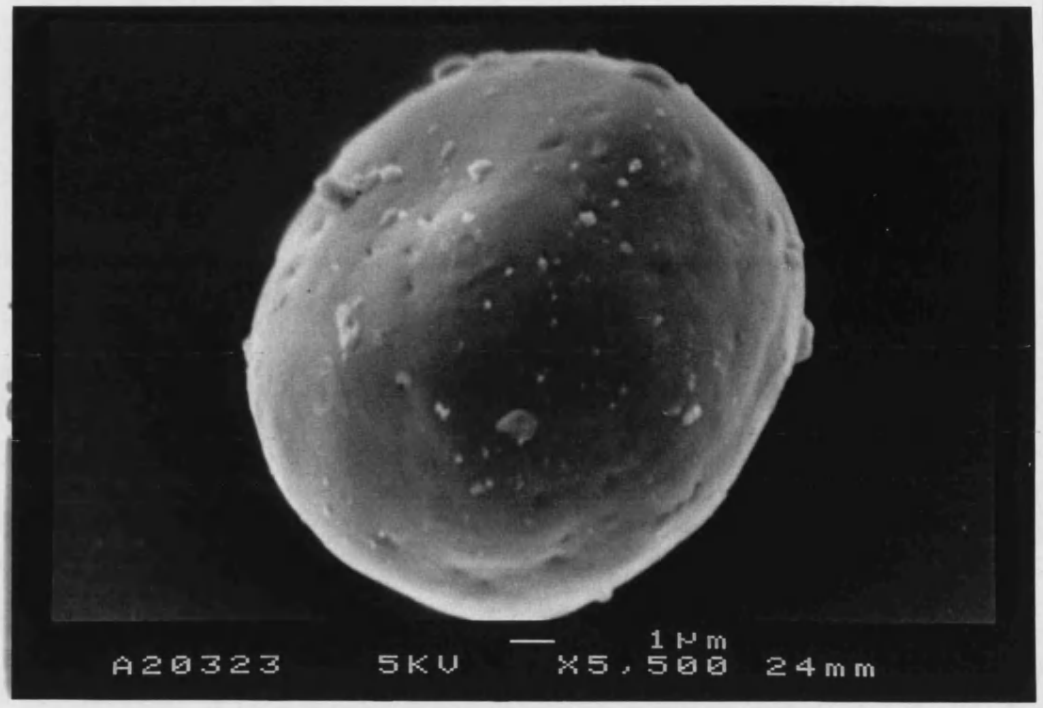

Figure 5.34: Native granule from Df48-70-01

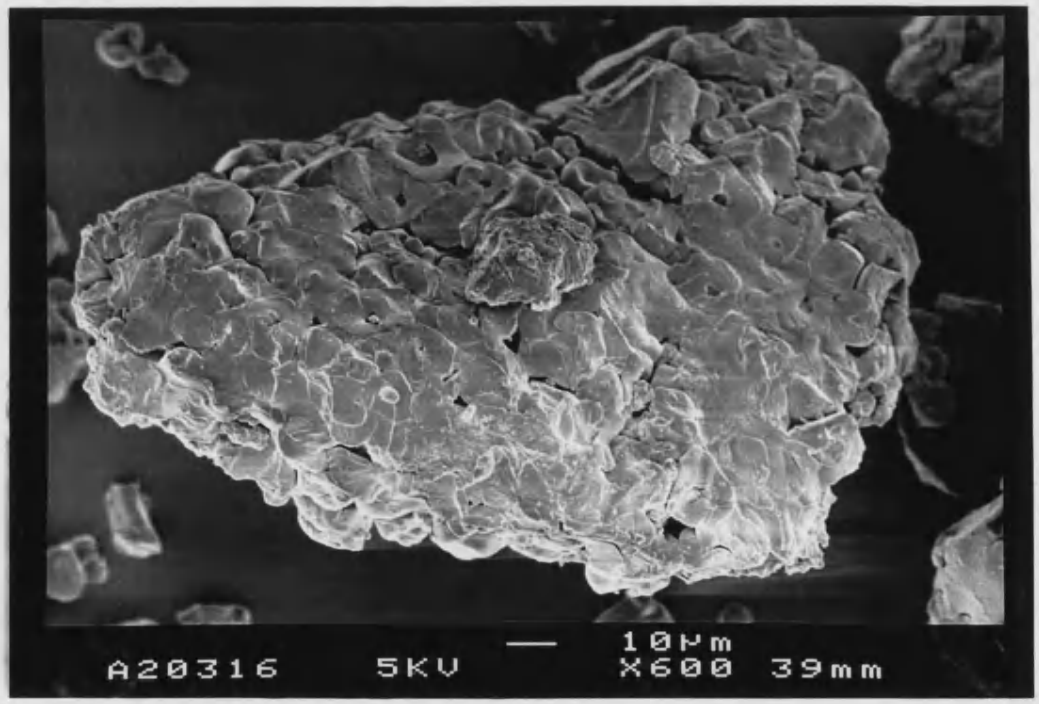

Figure 5.35: tightly packed DF48-60-01 agglomerate of starch particles coated in pregelatinised material. The hilums of some granules can be seen on the surface of the particle.

Figure 5.36: Evidence of native granules in DF48-60-01

Figure 5.37: Evidence of intact and ruptured starch granules in DF48-60-01

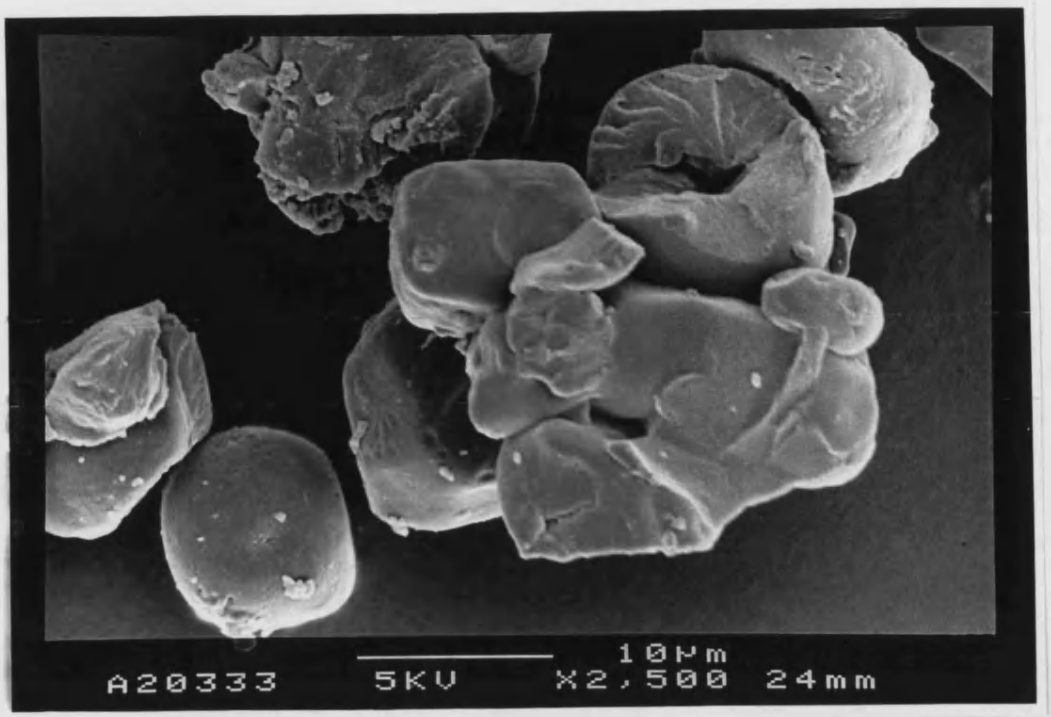

Figure 5.38: Ruptured native starch granules in DF48-He-01

Figure 5.39: Particle distribution of DF48-He-01

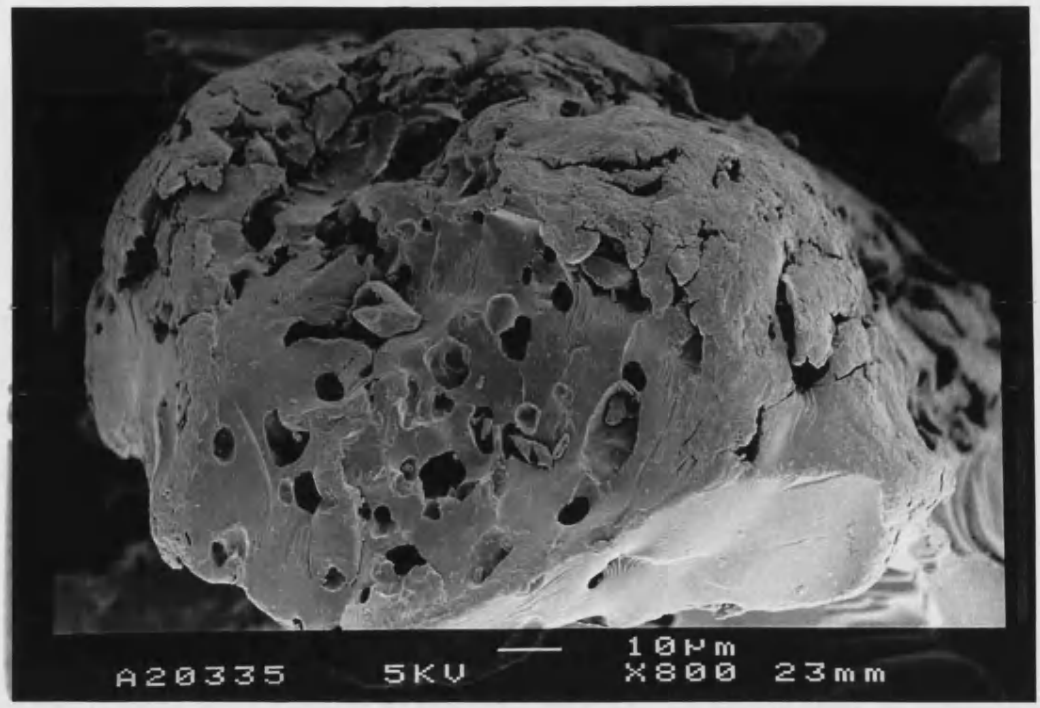

Figure 5.40: Porous particle of DF48-He-01. The porous regions to the left of the micrograph resemble hilums in the native starch granules

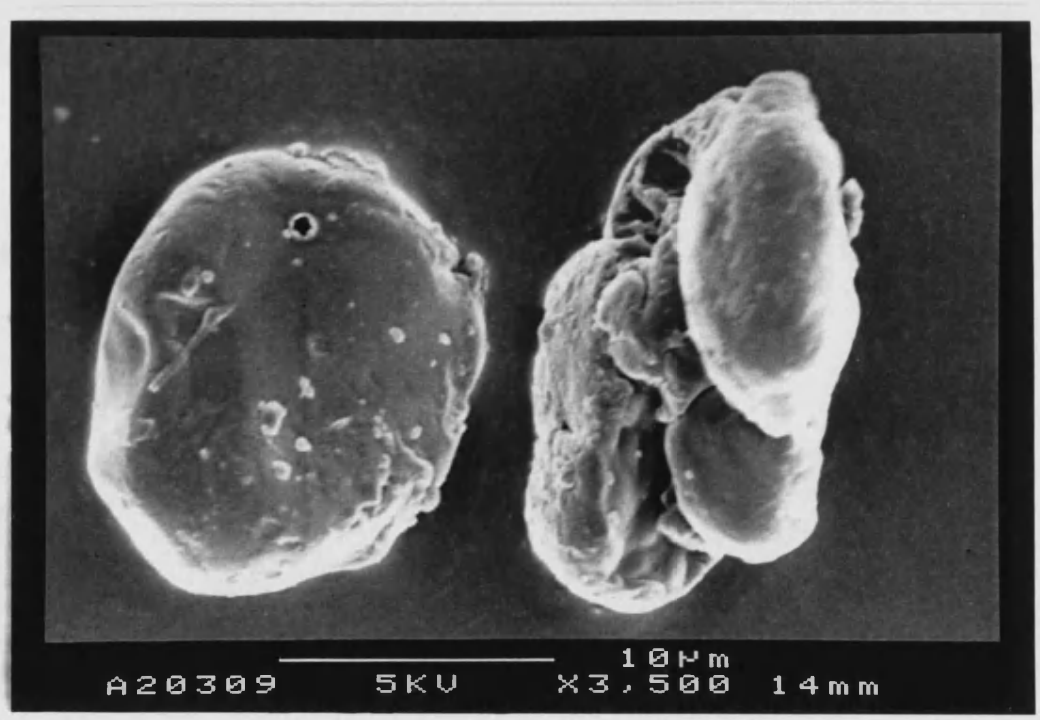

Figure 5.41: Evidence of native and pregelatinised starch in DF48-He(99)-01

Figure 5.42: Tightly packed agglomerate of DF48-He(99)-01

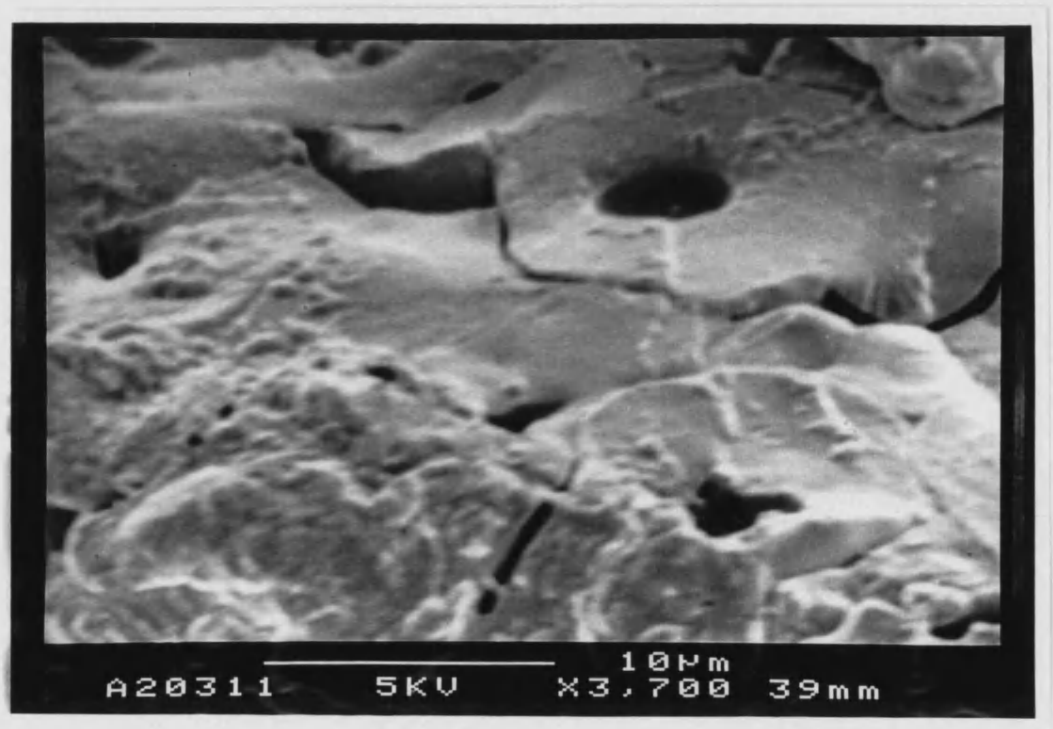

Figure 5.43: detail of figure 5.42, showing sheared native granules on the surface of the agglomerate

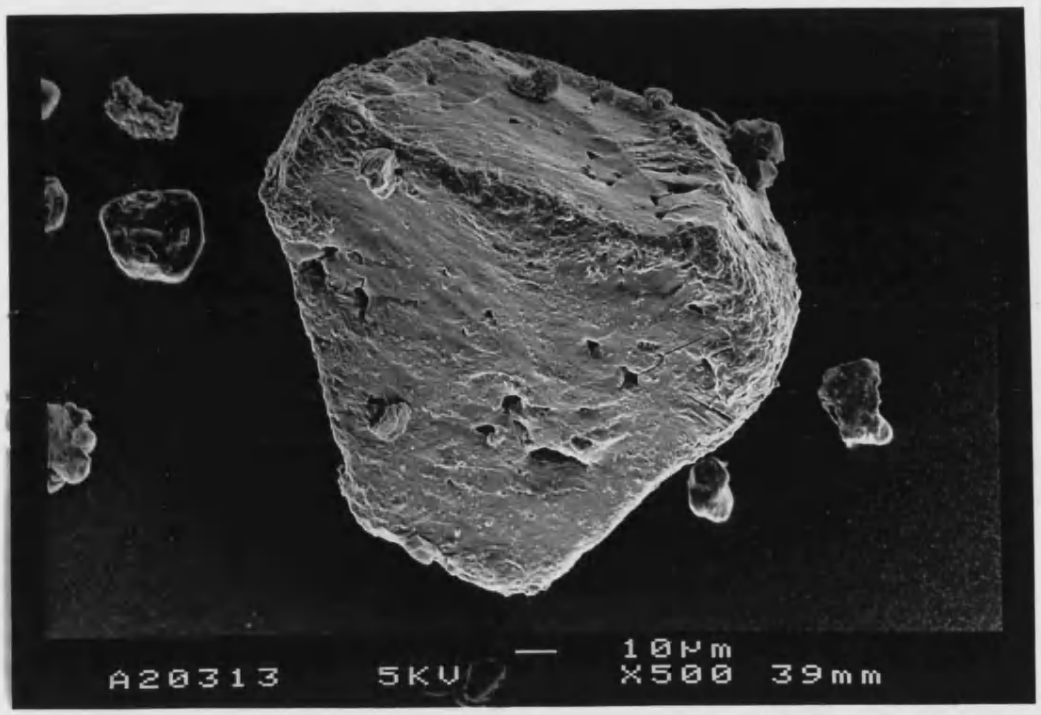

Figure 5.44: Pregelatinised starch particle from DF48-99(He)-01

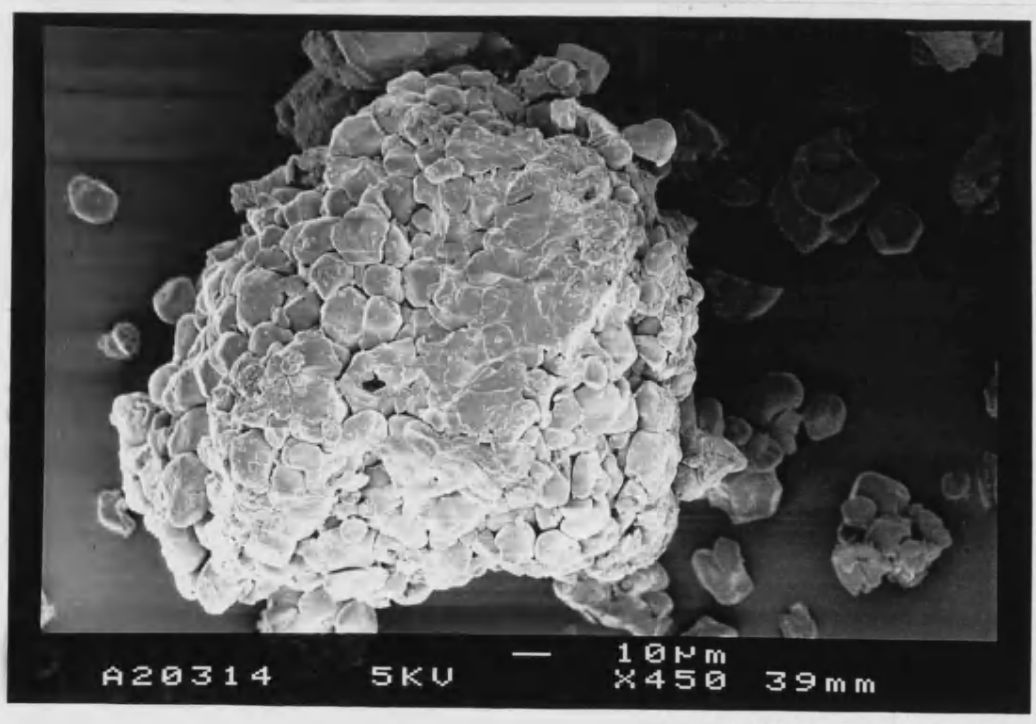

Figure 5.45: Tightly packed agglomerate from DF48-99(He)-01

Figure 5.46: Agglomerate from DF48-Bu-01 with some evidence of "pregelatinised bridges" as seen in unmodified Starch 1500.

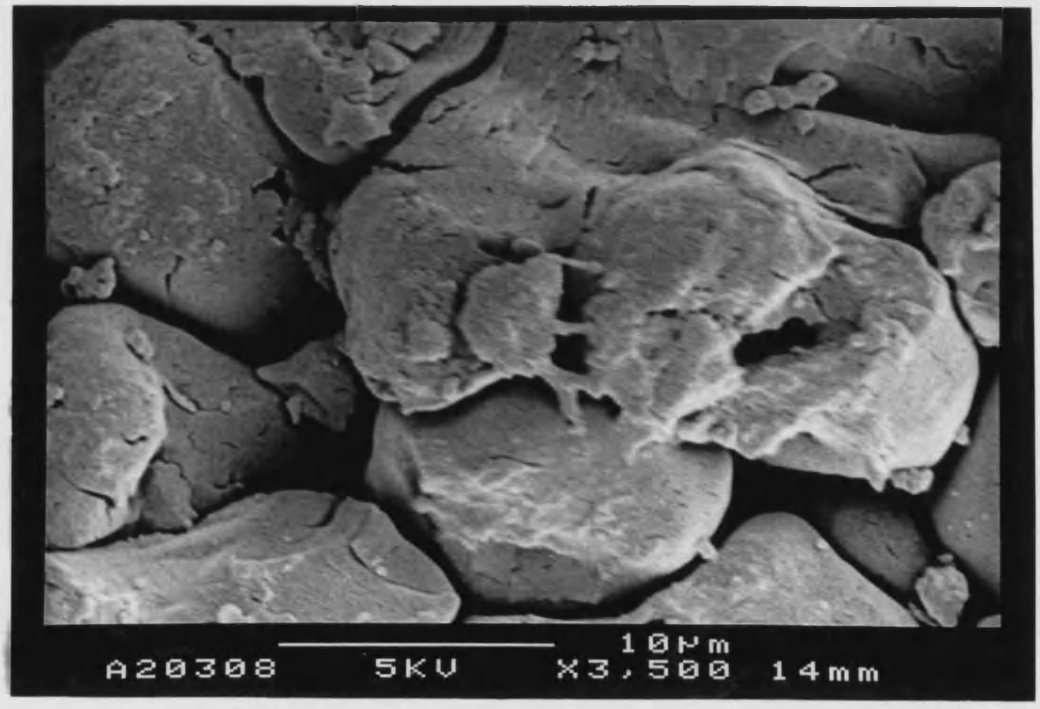

Figure 5.47: Detail of figure 5.46. The defatted pregelatinised material appears dry and damaged on comparison to unmodified Starch 1500.

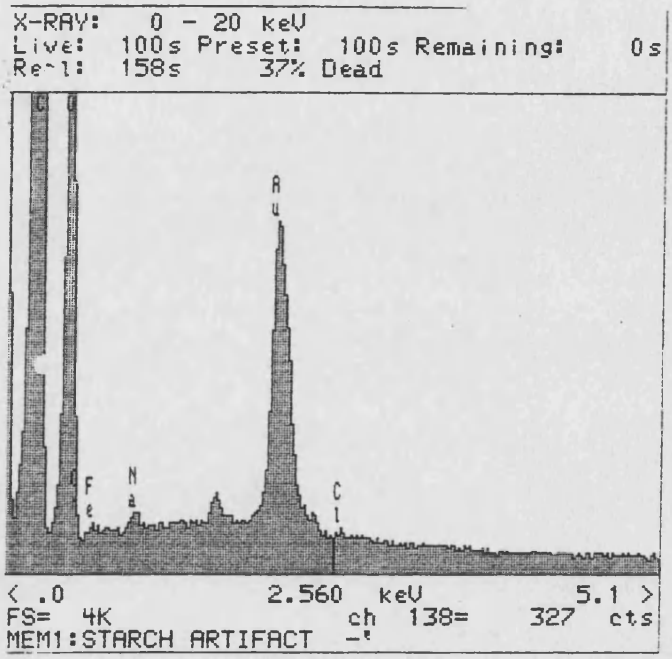

Figure 5.48: EDAX spectra of fragments on the surface of native starch granules.

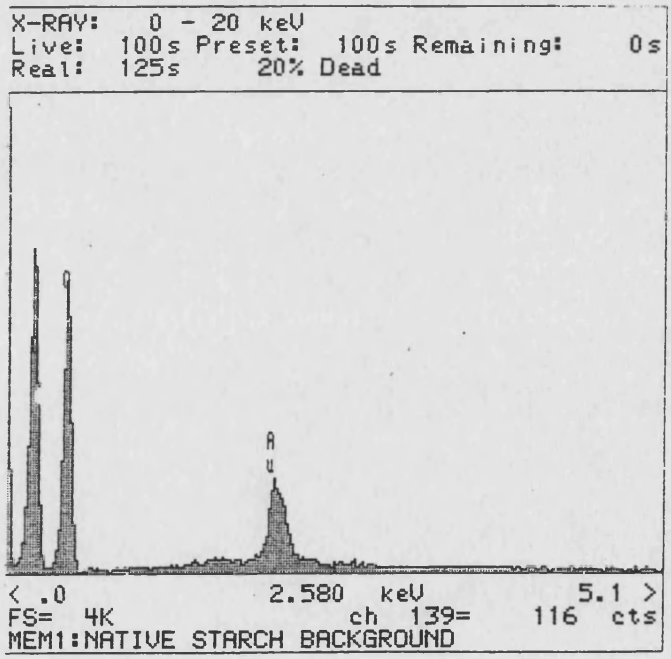

Figure 5.49: EDAX spectra of the surface of a native starch granule.

CHAPTER 6

A MICROSCOPIC STUDY OF THE INTERNAL STRUCTURE OF PARTICLES OF STARCH 1500 AND NATIVE MAIZE STARCH

6.1 General Introduction

In chapter 5, the technique of scanning electron microscopy was effectively used to elucidate the structure of the surface of defatted and unmodified Starch 1500, as well as native maize starch. As previously mentioned Starch 1500 can be regarded as a binary mixture of native and pregelatinised maize starch. It has been proposed that the pregelatinised fraction acts to bind the native granules into larger agglomerates. For this study the techniques of scanning and transmission electron microscopy were employed alongside conventional polarised light microscopy. The aims of this study were to gather evidence on the internal structure of Starch 1500 and investigate the effect of defatting on these maize starch materials.

6.1.1 Conventional SEM

To visualise the internal structure of a material using conventional SEM, it is necessary to secure the material, by embedding it in a resin matrix prior to sectioning. Epoxy and acrylic resins are widely used when embedding biological materials (Glauert, 1991) for visualisation by TEM. Conventional SEM has been used to image the internal structure of microcrystalline cellulose particles embedded in a chlorinated epoxy resin (Edge et al, 1998). This current study was undertaken to determine whether a similar technique could be employed to elucidate the internal structure of Starch 1500.

6.1.2 Transmission Electron Microscopy (TEM)

As its name implies the transmission electron microscope is used to obtain information from samples that are thin enough to transmit electrons. Due to its high resolving power, this technique provides information on the morphological and crystallographic microstructure of the materials being studied. The transmitted electrons that pass through the sample are focussed (by means of several electromagnetic lenses) onto a fluorescent screen, on which the resultant image is formed. The contrast of these generated images results from the scattering of electrons as they pass through the specimen. The brightness of each region in a sample is proportional to the amount of unscattered electrons detected on the fluorescent plate.

Initial studies into the ultrastructure of starches by TEM were performed on unstained sections of the material (Whistler and Turner, 1955; Whistler and Thornburg, 1957; Buttrose, 1960; Mussulman and Wagoner, 1968). To improve the quality and accuracy of the results, staining procedures were developed to exploit

the chemical reactivity of groups found on starch polysaccharides and with electron dense heavy metals. The PATAg technique (Thiéry, 1967) involves two main stages, an oxidative pre-treatment with periodic acid and the formation of a complex with an electron opaque metal such as silver. The PATAg method has been applied to the visualisation of starches (Gallant and Guilbot, 1969; Gallant, 1974). It was found in these studies that due to their greater accessibility the amorphous regions of the starch were more readily oxidised and thus stained darker than the corresponding crystalline regions. It is noteworthy that in unstained starch the opposite is observed, i.e. the crystalline regions appear darker as they are more electron dense (Mussulman and Wagoner, 1968).

6.1.3 Polarised Light Microscopy

As a consequence of the inherent crystallinity of native starches (Zobel, 1988), most starch granules exhibit a "Maltese Cross" when observed by polarised light microscopy. This positive birefringency (Gallant, 1974) theoretically indicates a radial orientation of the principle axis of the crystallites. On gelatinisation, birefringence is lost from starch granules (Olkku and Rha, 1978). The percent loss of birefringence has been used as a means to determine the degree of gelatinisation on heating native starches (Watson, 1974).

6.2 MATERIALS & METHODS

6.2.1 Conventional SEM

Sample Preparation

Prior to embedding the material in resin, a sample of Starch 1500 was air jet sieved specifically to remove any loosely adhered native starch granules from the surface of the larger Starch 1500 particles. An alpine air jet sieve (Augsburg, Germany) and a brass test sieve of 212μm (Endecotts, London, U.K.) were used to remove the undersize fraction. The sieved sample was placed in an Eppendorff tube and dehydrated by washing four times, for 15 minutes in acetone. This stage is necessary as any residual moisture can intactivate the resin accelerator (Glauert, 1991), which in turn adversely affects the strength of the resin block. The sample was then transferred to a mixture of 50:50 epoxy resin (Taab Premix Resin, Taab, Reading, U.K.) and acetone for a further 60 minutes. It was then embedded in 100% resin for 1 hour, which was replaced 3 times to allow complete removal of the acetone and ensure maximal penetration of the resin into intra-particle voids. Again complete removal of the acetone is essential to maintain the integrity of the resin block for sectioning (Mollenhauer, 1988). The resin embedded sample was then

transferred to a beam capsule and cured in an oven at 60°C for 24 hours. This has been identified as the maximum temperature for curing epoxy resins (Glauert, 1974). At higher temperatures additional cross-linking results in the formation of a resin block which it too hard to cut for thin sectioning. The cured resin blocks were trimmed to exposed the embedded Starch 1500 particles using an ultramicrotome (Reichert OMU3 - made by Leica) equipped with a glass knife. The resin block was mounted on an aluminium specimen stub using double sided carbon adhesive discs.

Coating

To ensure conductivity between the aluminium stub and the resin block, the sides of the block were painted with colloidal carbon (Leit-C, Gerhard Neubauer, Munster, Germany). The resin block was then sputter coated (Model S150B, Edwards High Vacuum, Sussex, U.K.) in gold for five minutes.

Examination

Studies were performed using a JEOL T330 scanning electron microscope, (Japanese Electron Optics Ltd., Tokyo, Japan) at an accelerating voltage of 10kV.

6.2.2 Transmission Electron Microscopy

Initial examination of the internal structure of Starch 1500 particles was performed on thin sections of the resin blocks produced for the conventional SEM. Sections of approximately 100nm thickness were produced using an ultramicrotome equipped with a glass knife. The thin sections were mounted on copper grids and examined using a JEOL JEM 1200EX transmission electron microscope (Japanese Electron Optics Ltd., Tokyo, Japan) at an accelerating voltage of 120kV.

Further studies were performed on samples of unmodified and defatted Starch 1500 and native maize starch, which had been treated according to the PATAg staining procedure. Prior to embedding in resin the samples were homogeneously dispersed and suspended in a 3% agar gel at 50°C. Once this had reached room temperature, it solidified and was cut into $1mm^3$ cubes. The cubes were then transferred to vials, placed on a specimen rotator, to assist the infiltration of the various reactants. Each sample was successively immersed in a 1% aqueous solution of periodic acid for 30 minutes, a saturated solution of thiosemicarbazide for 24 hours and a 1% aqueous solution of silver nitrate for 2 days. Following each step the samples were repeatedly washed with distilled water. The stained samples

were then gradually dehydrated using with a series of ethanol dilutions (50, 70, 80, 90, 95, 100 and 100% dried) with 3 changes of each dilution every 15 minutes. The ethanol was then exchanged for propylene oxide, which was in turn replaced by propylene oxide:epoxy resin mixtures (3:1, 1:1, 1:3), again with 3 changes of each solution every 15 minutes. Samples were then infiltrated with 100% resin for 24 hours. Several agar cubes from each sample were individually transferred to a separate beam capsule and topped up with more resin. These samples were cured at 60°C for 24 hours. Sections of 100nm thickness were prepared and imaged as previously described for the unstained material.

6.2.3 Polarised Light Microscopy

Studies were performed using a Standard Microscope 16 (Carl Zeiss, D-7082 Oberkochen, Germany), with a JVC TK-1270 Colour Video Camera attachment (Victor Company of Japan, Tokyo, Japan). A Polarising light filter and analyser (Carl Zeiss, D-7082 Oberkochen, Germany) were attached to the microscope for observation of the samples. The starch samples were prepared as 1% suspensions in distilled water. A cover-slip was gently lowered onto the slide taking care to removed any air bubbles. Images of the starch suspensions, were captured using the Optimas Image Analysis software V5.2 (Optimas Corporation). Samples were studied to determine whether of defatting and Starch 1500 production affected the birefringence of maize starch.

6.3 RESULTS & DISCUSSION

6.3.1 Conventional SEM

Figures 6.1 to 6.5 detail the internal structure of the resin embedded Starch 1500 particles as visualised by conventional SEM. The embedded particles seem to be composed of smaller particles, which resemble native starch granules. This result adds evidence to the concept that the gelatinised fraction of Starch 1500 serves to bind together the native granules. The smaller particles exhibited in some cases, irregular shapes and voids at their centres. Such structures may be a consequence of the rupturing or partial swelling of native granules during the production of Starch 1500. This is exemplified most clearly in figure 6.1 and will be described further in the general discussion at the end of this chapter.

6.3.2 Transmission Electron Microscopy

Figures 6.6 to 6.9 are images of unstained native maize starch as visualised by TEM. Faint, concentric rings of alternating light and dark material can be seen radiating from a point off-centre from the middle of the granule. The darker rings, which have previously been identified as the crystalline region of the granule (Mussulman and Wagoner, 1968), were most clearly distinguished in the mid region of the granule, as opposed near the hilum or the periphery.

The alternating amorphous and crystalline growth rings of native maize starch were more clearly visualised once stained by the PATAg method (figures 6.10 to 6.13). As was the case in the unstained granules, it can be seen (in figures 6.10 and 6.11) that the growth rings are most clearly defined in the mid region of the granule. In figures 6.12 and 6.13 darker lines of more amorphous material can be observed within the granule's crystalline regions. Such structures have previously been identified as radial "channels" or "canals" within the granule (Gallant, 1997).

Figures 6.14 to 6.18 detail the structure of thin sections of PATAg stained Starch 1500. Two types of structure were identified in this material, which were thought to be native and pregelatinised maize starch. It can be seen in figures 6.14 to 6.16 that the native granules were of a similar size and shape to the resin embedded particles of Starch 1500 which were imaged by conventional SEM. As was observed in figures 6.1 to 6.5, the granules were irregular in shape and exhibited a characteristic void at the centre. Further examination reveals little evidence of growth rings in the granule's microstructure. However a region of alternating light and dark material is shown in figure 6.15, close to the void at the centre of the granule, indicating the possibly some residual order.

Images of the pregelatinised material visualised by TEM are shown in figures 6.17 and 6.18. This material showed no defined shape or structure. The absence of an internal microstructure and homogeneity of the staining, suggest that the pregelatinised fraction of Starch 1500 is completely amorphous.

Figures 6.19 to 6.30 are TEM images of defatted native starch. As can be seen, granule shape remains unchanged. However in figures 6.19 and 6.21 there is some evidence of material loss from the centre of the granule. Such granular voids were also observed in resin embedded Starch 1500, as imaged by conventional SEM. However, it is also possible that these voids may result from a weakness in the resin blocks on thin sectioning. This must be considered as such voids were only

seen in a few particles of the NS48-He-01 sample. Furthermore, the lack of contrast within the void may indicate the absence of a supporting resin matrix.

Concentric rings were still apparent within the granule's microstructure after defatting. These could be clearly distinguished in the NS48-He-01 and NS48-99-01 samples and much less so in NS48-70-01 (figure 6.27). The lighter rings, which are crystalline regions of the granule, were approximately 200nm thick. This value agreed with the observed values for unmodified native starch, however the darker amorphous rings were much thinner in the defatted materials. One possible explanation for this could be loss of amorphous material from the granule during defatting. Amylose is known to leach from granules at temperatures below that at which gelatinisation occur (French, 1984), thus such a phenomenon may occur on exposure of starch to hot solvents. The faint growth rings observed in NS48-70-01 may be result from disorder introduced on defatting with a solvent of higher boiling point.

It has been reported that the radial "channels" (Gallant, 1997) of the granule's crystalline regions become "markedly fibrous" on defatting with ethanol (Nierle et al, 1998). No such evidence was found in this current study, however granular structures without growth rings could be observed within these specimens. This is exemplified in figures 6.22, 23, 25, 28 and 29, where such "channels", are seen to span the embedded particle.

Thin sections of defatted Starch 1500 samples DF48-He-01, DF48-99-01 and DF48-70-01 were imaged by TEM (figures 6.30 to 35). It was found that the samples looked very similar to unmodified Starch 1500, again suggesting an amorphous microstructure. There was no evidence of residual granular structure in the defatted starches studied. This is contrary to the evidence provided by SEM and polarised light microscopy studies and as such may be due to an absence of granules from the sections imaged.

6.3.3 Polarised Light Microscopy

Positive birefringency was observed in all of the powder samples analysed. In unmodified and defatted Starch 1500 some particles did not display the characteristic "Maltese Cross " pattern, these particles were deemed to constitute the pregelatinised fraction of the material. This technique provides a qualitative and

rapid means of assessing the effect of defatting on Starch 1500 and native maize starch.

6.1 General Discussion

Both TEM and conventional SEM provided evidence that the larger Starch 1500 particles are comprised of intact and ruptured native starch granules. Large voids, approximately 2 – 3μm in diameter were visible in the centre of some of these starch granules. These had previously been observed in heat/moisture treated potato and maize starches (Kawabata et al, 1994). It has been proposed that heat/moisture treatment causes rearrangement of the molecular structure at the centre of the granule, where it is considered that the tissue structure is weakest.

Use of the PATAg method allowed the internal microstructure of unmodified and defatted native starches to be successfully visualised by TEM. However, it is possible that artefacts may be generated as a consequence of the staining process. It is of note that the materials may have been exposed to some degree of lipid removal during the dehydration stages of this staining technique repeated washings in both acetone and ethanol. Furthermore, consideration should be made of how the pregelatinised fraction of Starch 1500 is affected by the highly aqueous environments of the agar embedding and periodic oxidation stages. Such effects may be overcome by fixing the specimens with osmium tetroxide prior to staining.

Comparison of the internal structure of native maize starch and the native granules in Starch 1500, by TEM and SEM, suggests that the latter undergoes ultrastructural modification during Starch 1500 production. Evidence of this is given by the voids in the centre of the granules and less well-defined growth rings. The defatting of native maize starch was seen to have a similar effect on granular architecture. Such modifications may arise as a consequence of the material being held at elevated temperatures during defatting by the exposure to hot solvents. In the context of the effect of defatting on Starch 1500 structure, no evidence of further modification could be found. This may be attributed to the fact that ultrastructural modifications have already occurred during the partial pregelatinisation of the material.

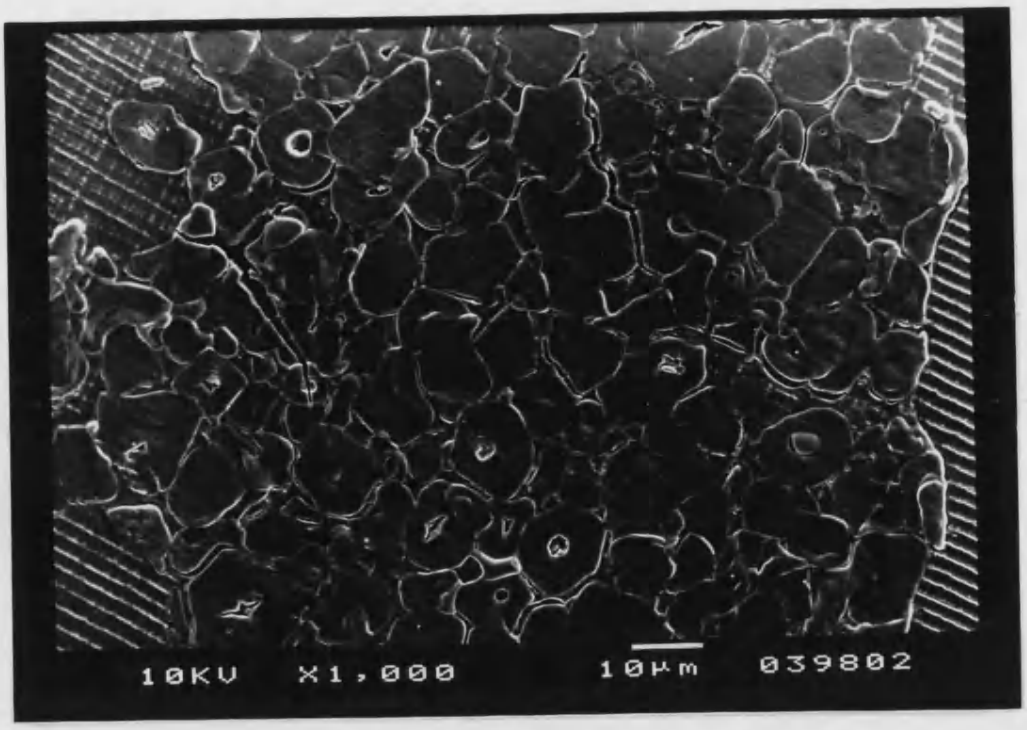

Figure 6.1: Cross section of resin embedded Starch 1500 particle as visualised by conventional SEM.

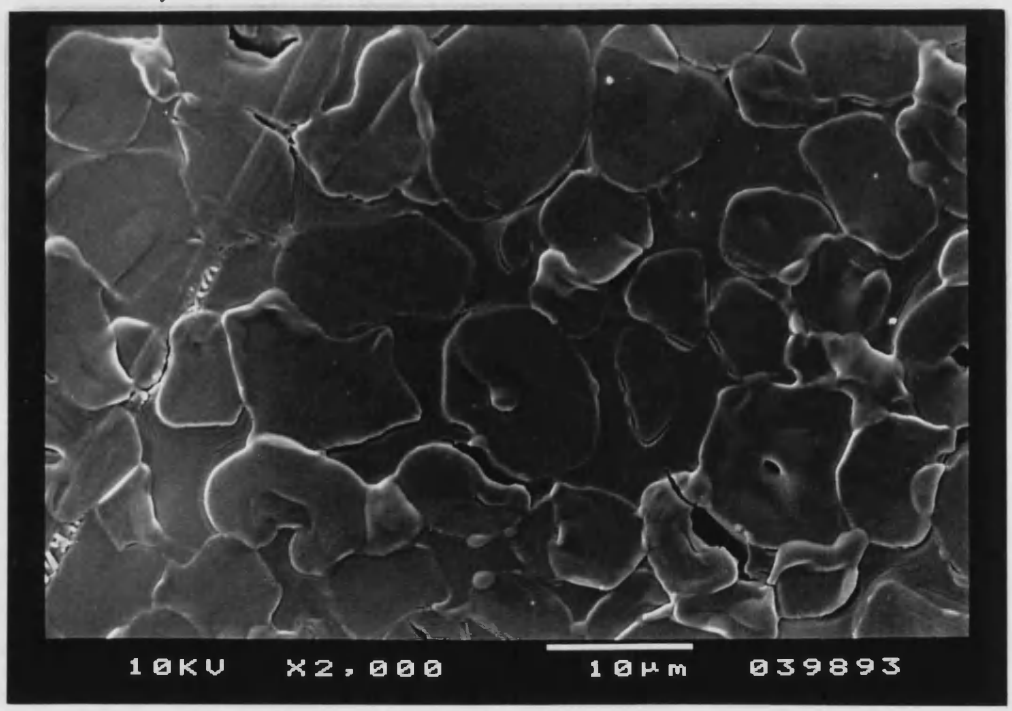

Figure 6.2: Detail of ruptured granules located within a sectioned Starch 1500 particle.

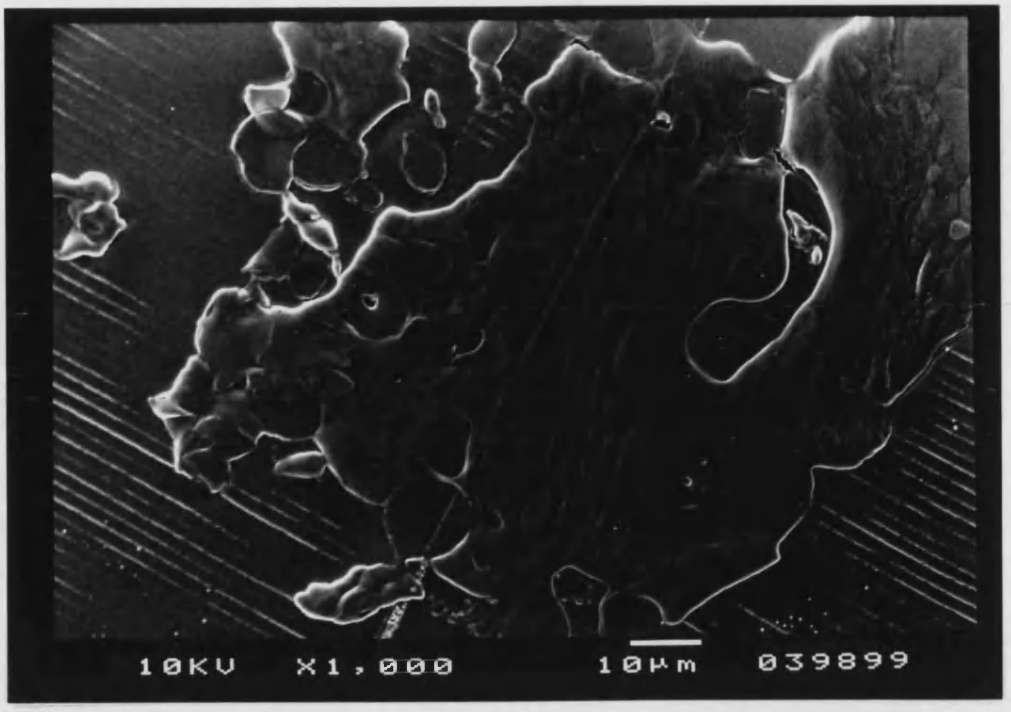

Figure 6..3: Cross section of Starch 1500 particle comprising native and pregelatinised material.

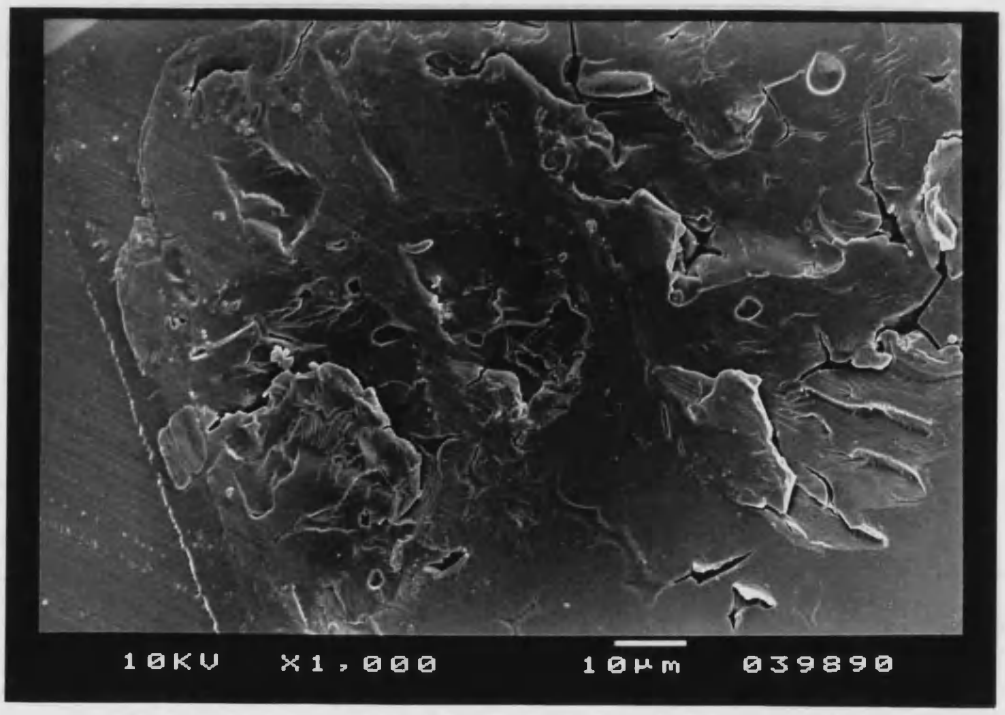

Figure 6.4: Internal structure of a cross-sectioned Starch 1500 particle, with some residual native granular structures.

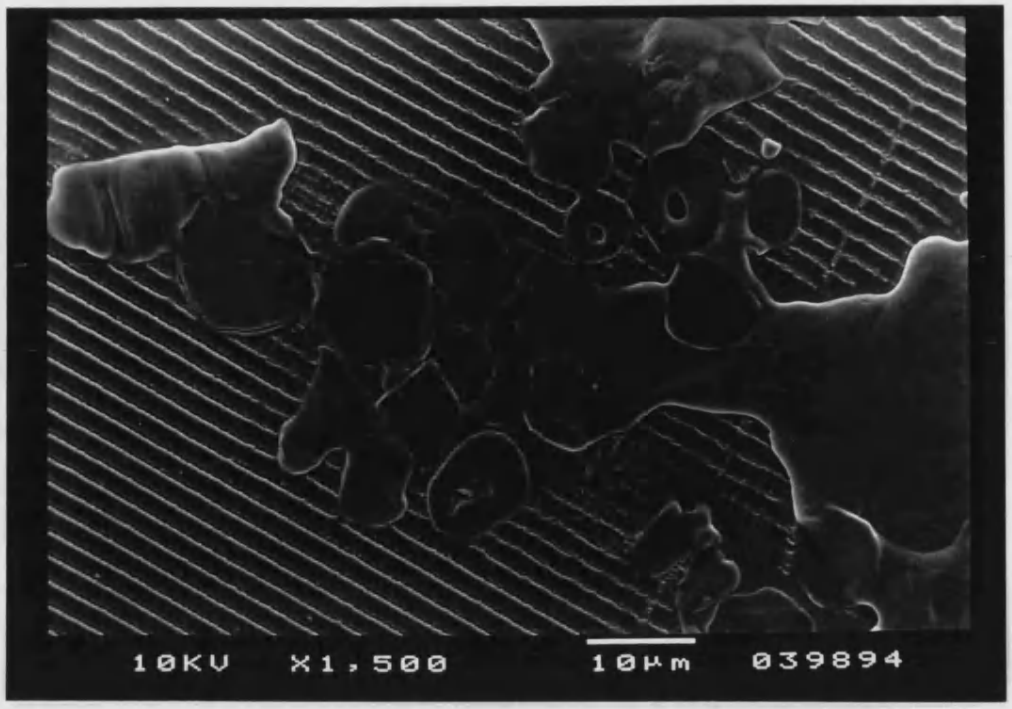

Figure 6.5: Cross section of a resin embedded Starch 1500 particle detailing pregelatinised material and native granules with hollow centres.

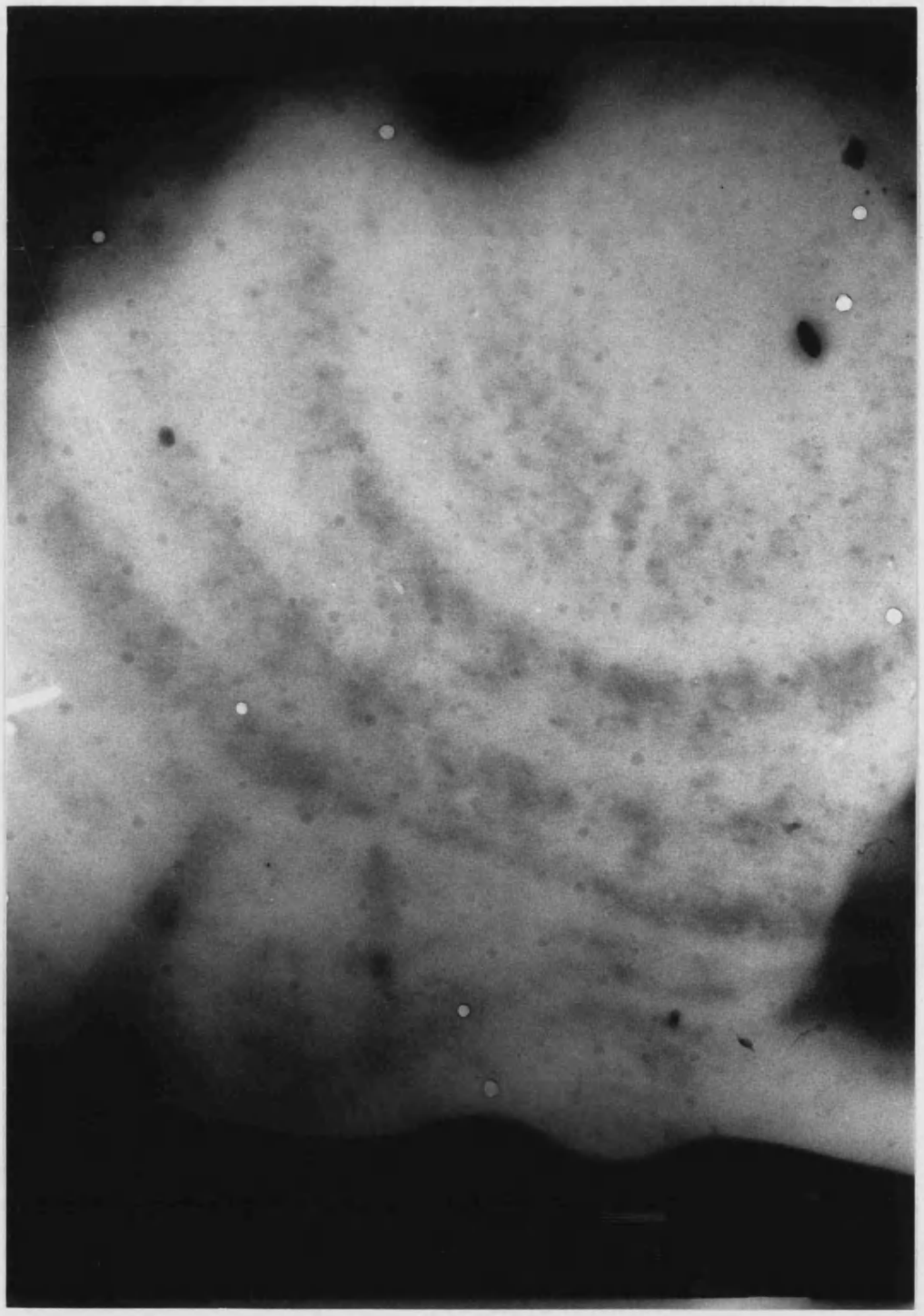

Figure 6.6: Thin section of unstained native maize starch, detailing amorphous and crystalline growth rings

Figure 6.7: Thin section of an unstained native starch granule.

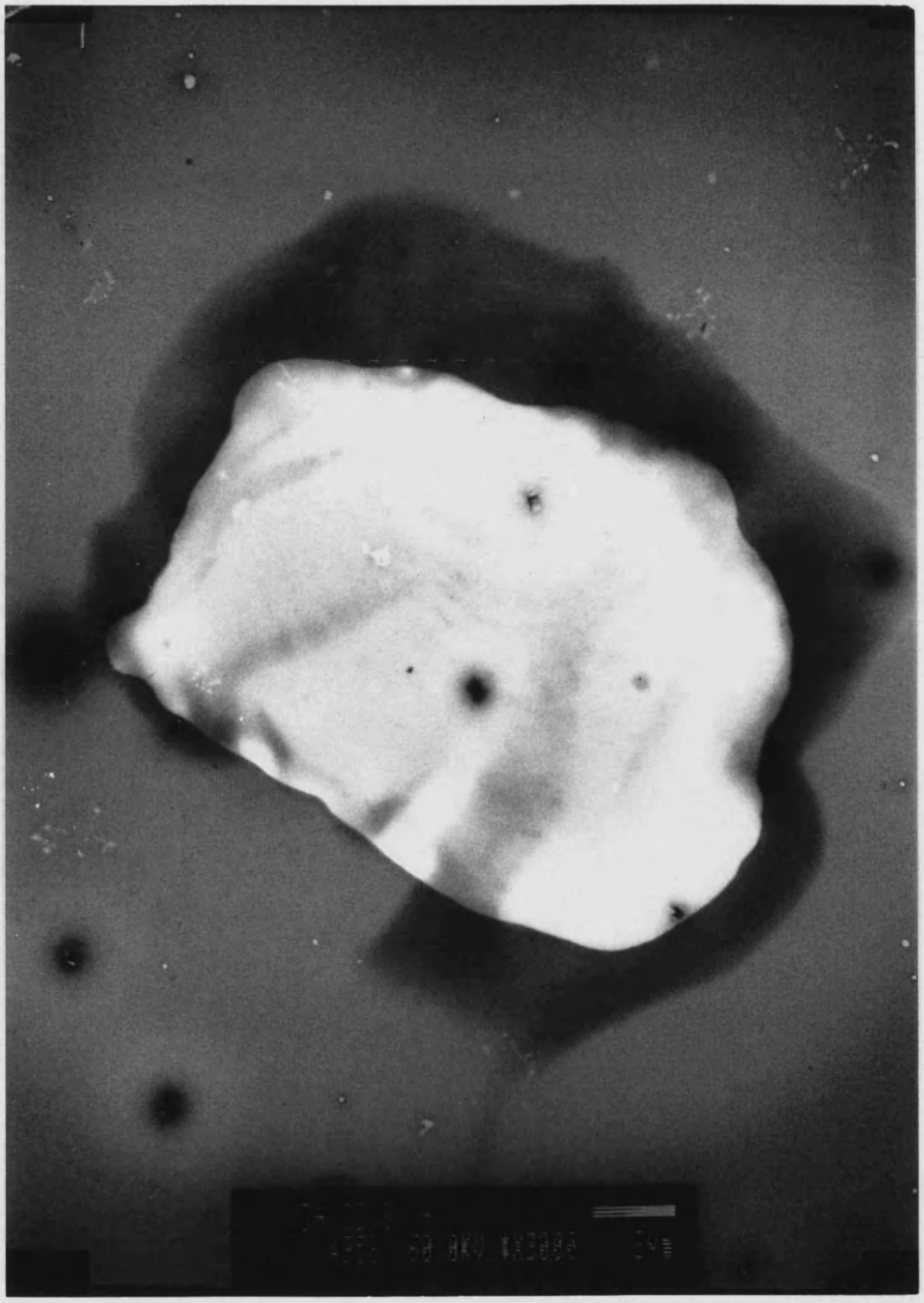

Figure 6.8: Thin section of a native maize starch granule imaged by TEM

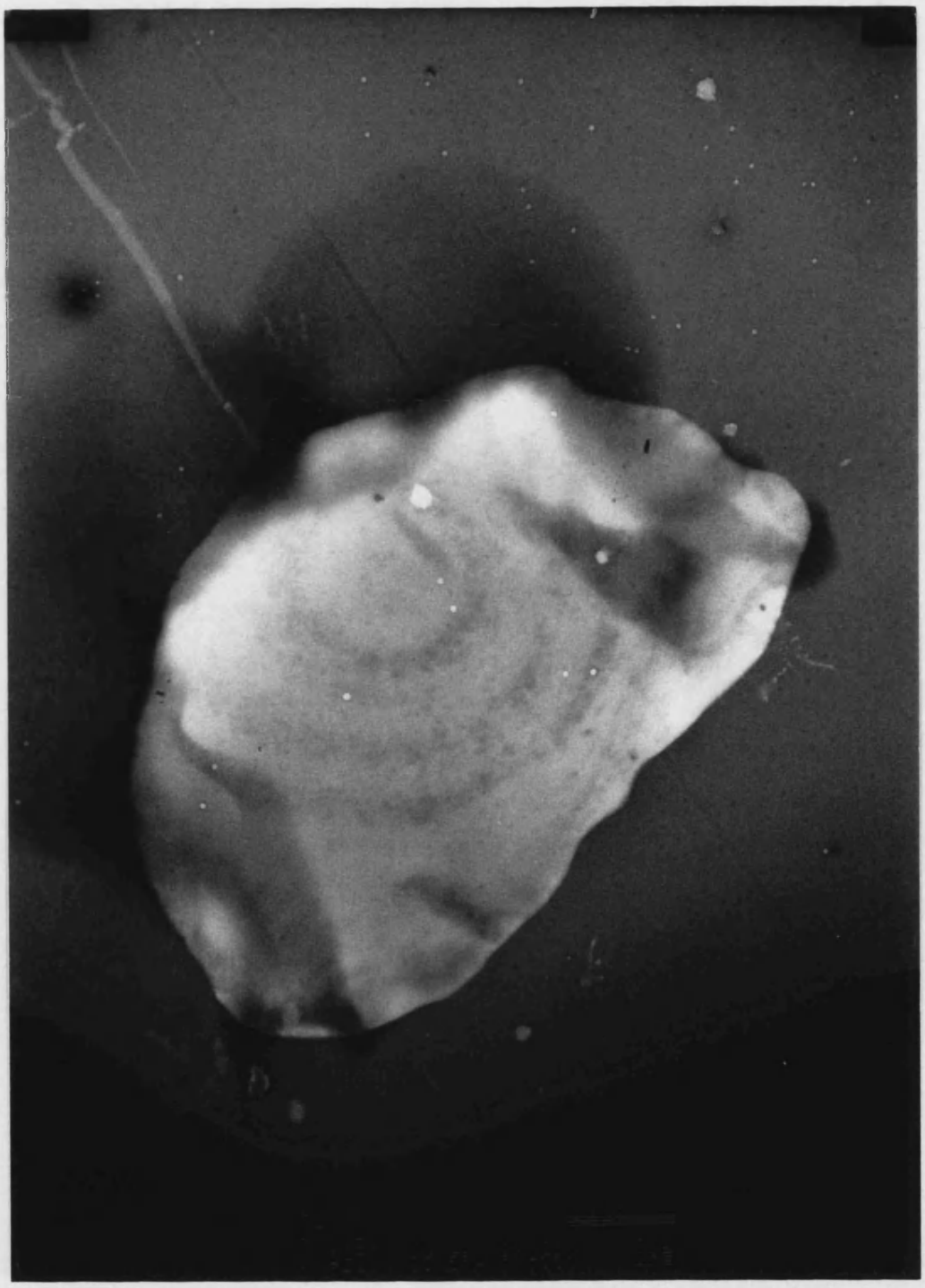

Figure 6.9: Cross section of a native maize starch granule detailing the amorphous and crystalline growth rings.

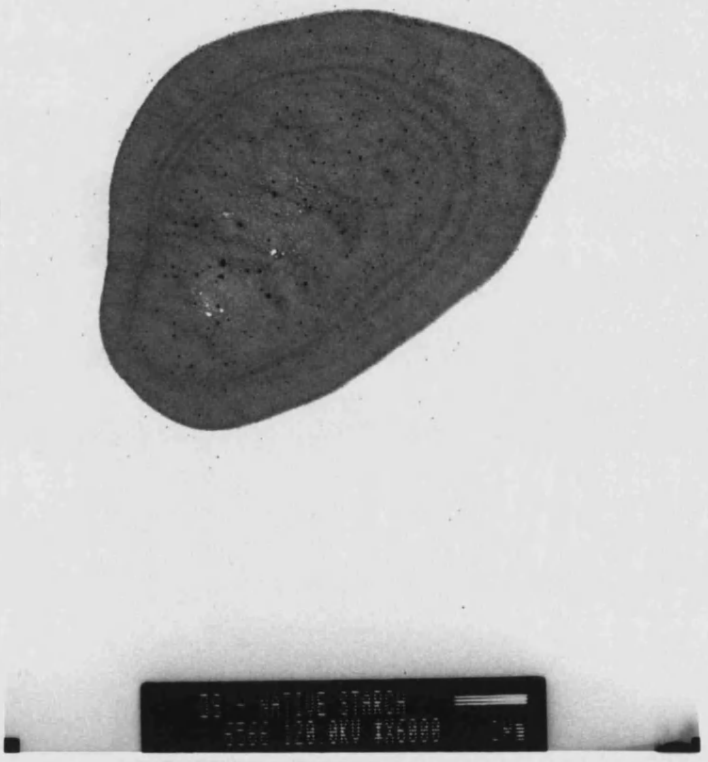

Figure 6.10: Thin section of PATAg stained native maize starch.

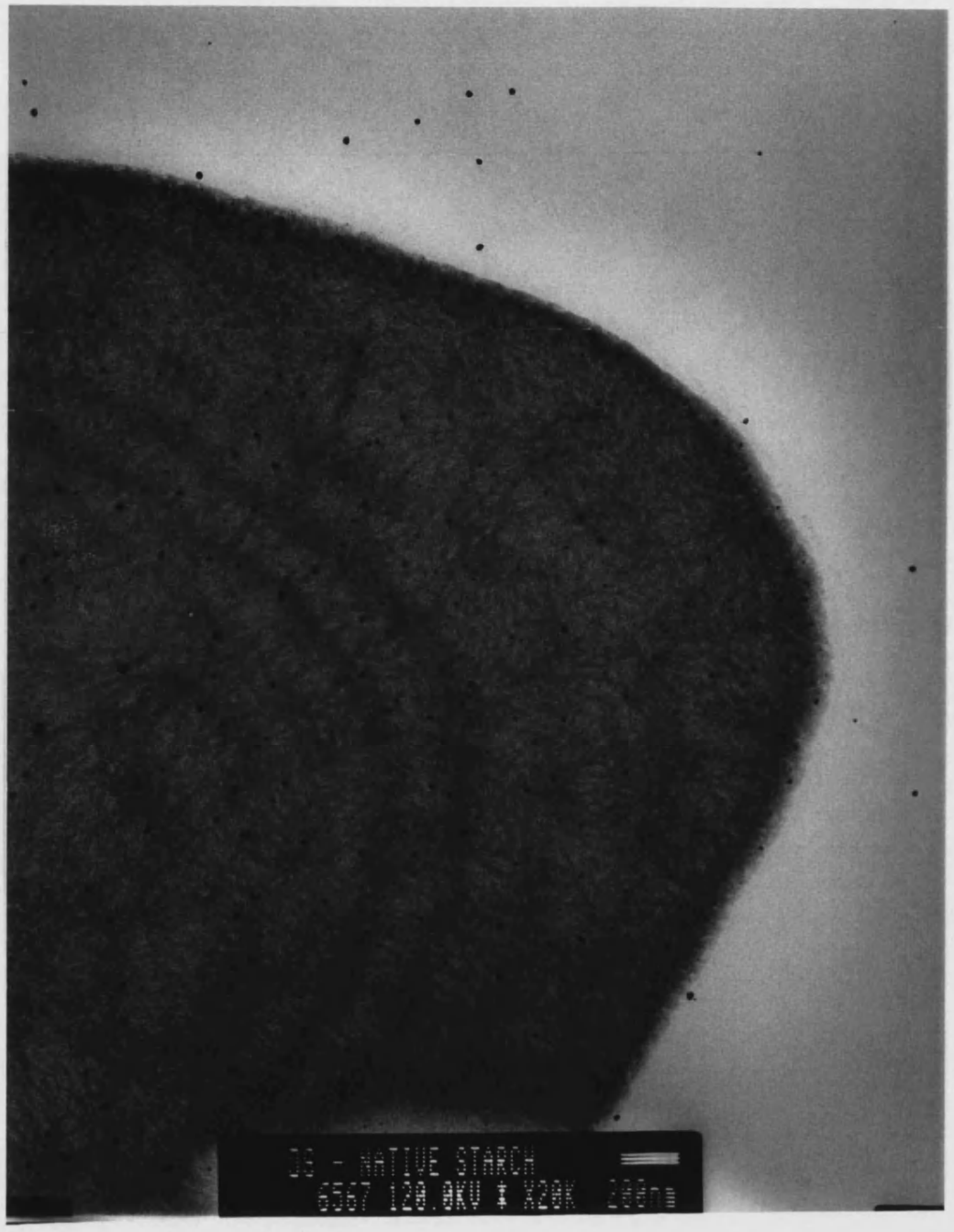

Figure 6.11: Detail of a thin section of PATAg stained native maize starch. The dark stained regions are amorphous growth rings.

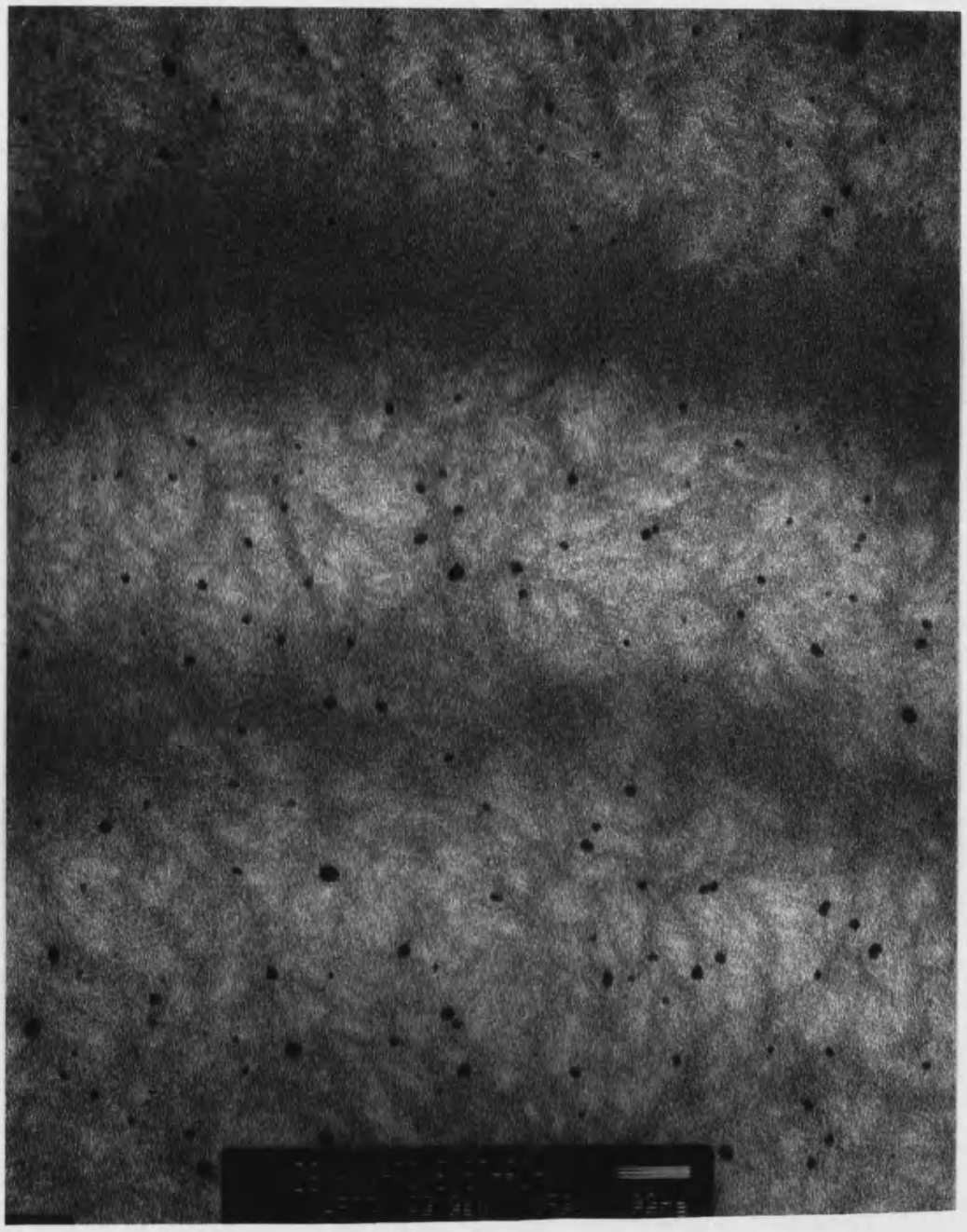

Figure 6.12: Image showing the amorphous radial channels within the crystalline growth rings observed in native maize starch.

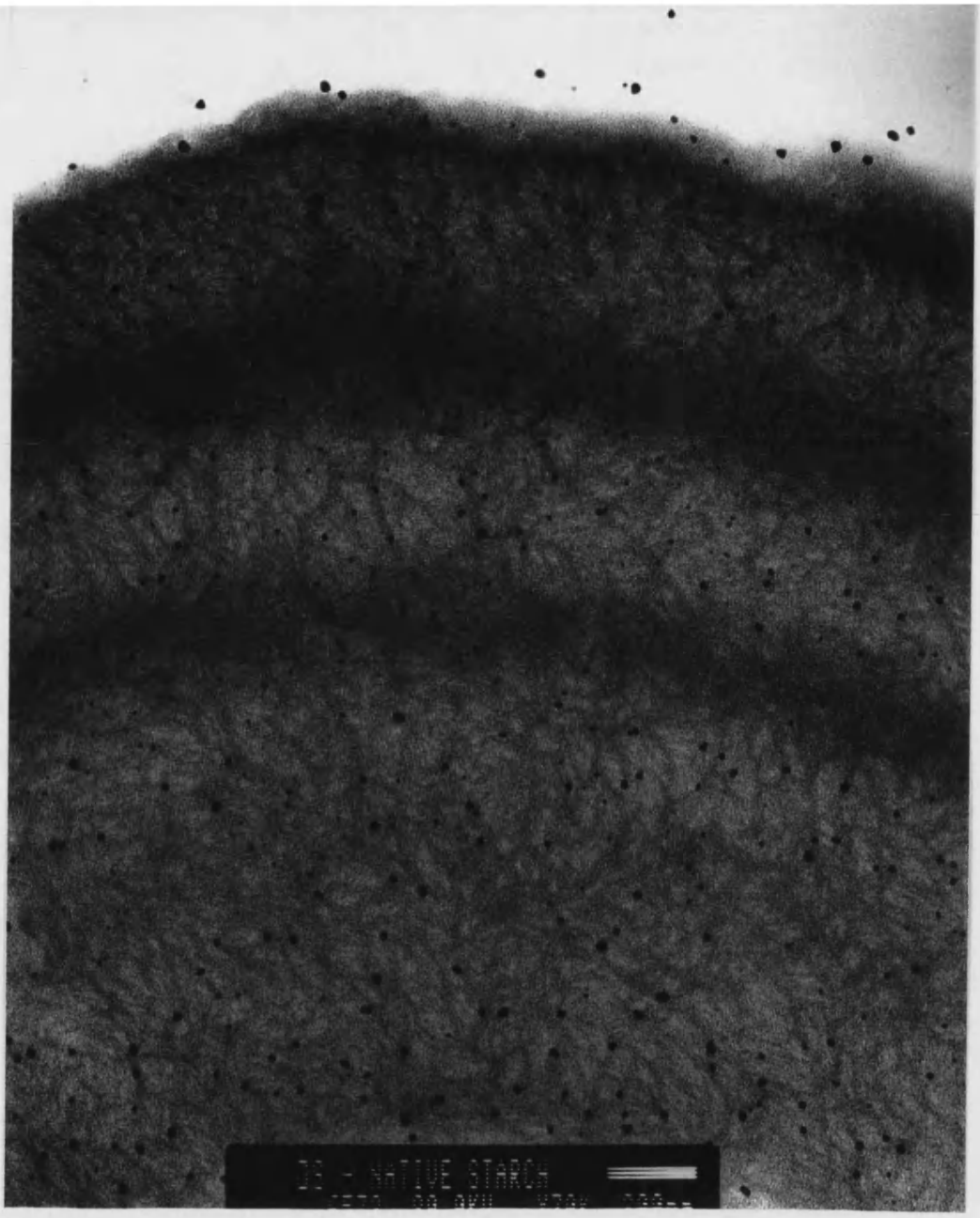

Figure 6.13: Detail of the amorphous and crystalline growth rings within native maize starch

Figure 6.14: Thin section of a native starch granule from PATAg stained Starch 1500, with detail of large hollow in the centre of the granule.

Figure 6.15: Detail of native granule from Starch 1500 showing evidence of residual growth rings.

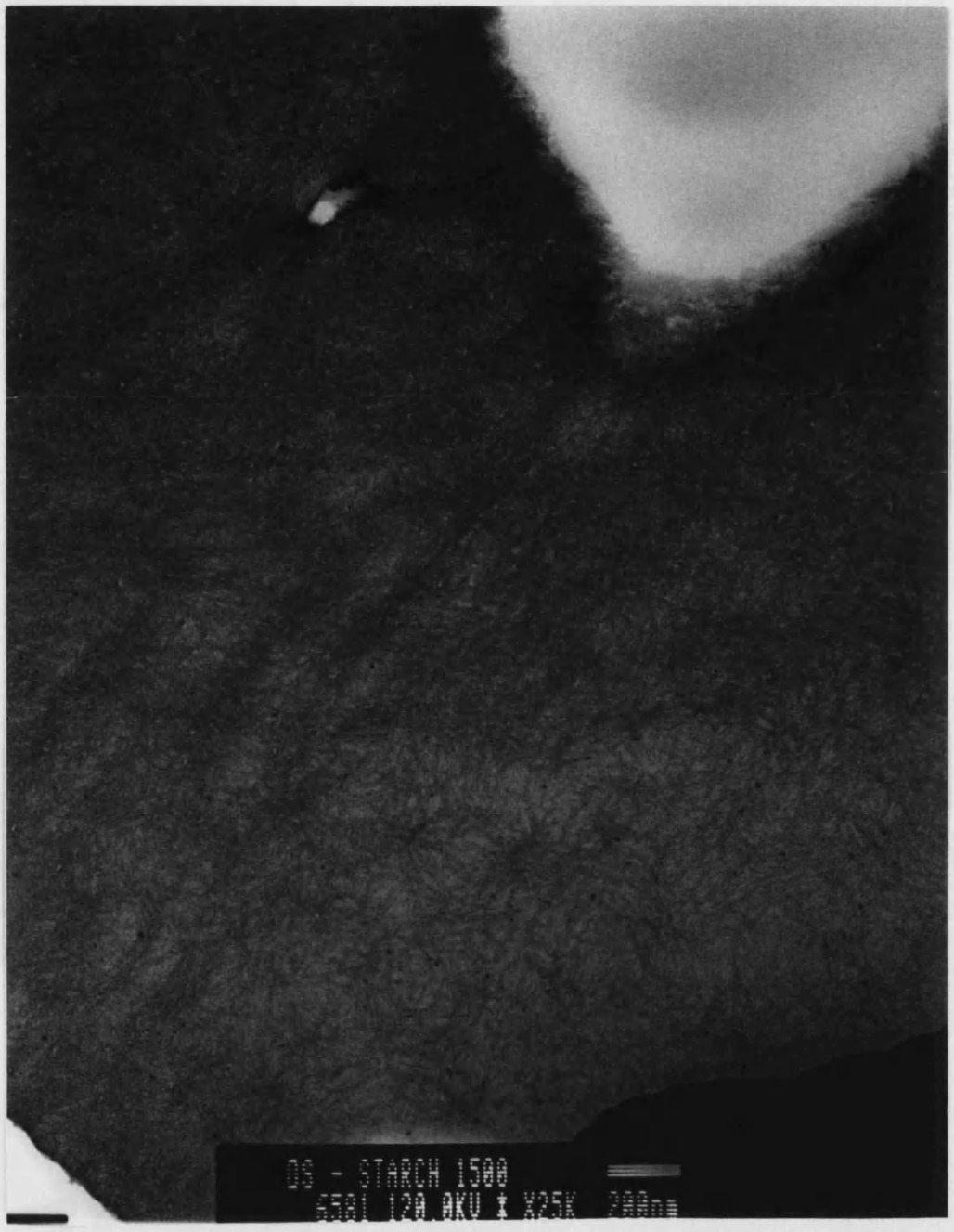

Figure 6.16: Detail of internal microstructure of native starch granule from PATAg stained Starch 1500.

Figure 6.17: Pregelatinised starch fragment from PATAg stained Starch 1500

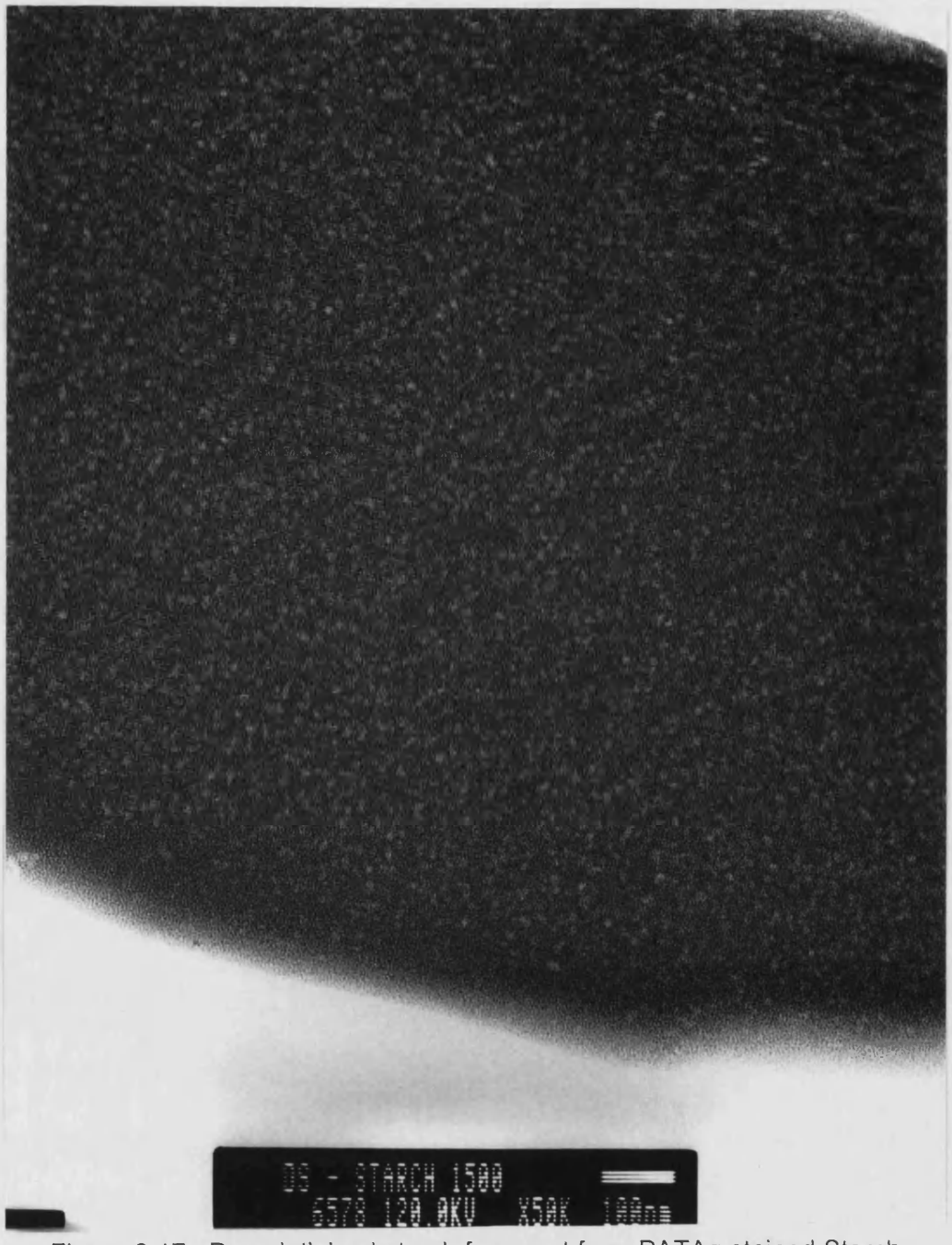

Figure 6.17: Pregelatinised starch fragment from PATAg stained Starch 1500

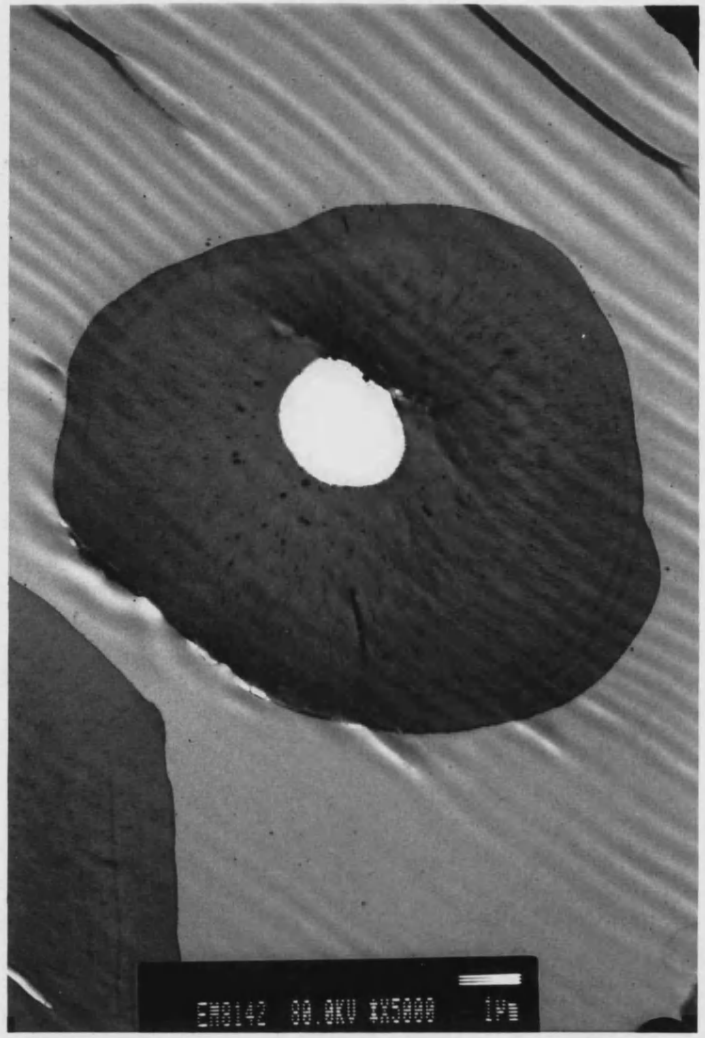

Figure 6.19: Cross section of a PATAg stained starch granule from NS48-He-01.

Figure 6.20: Detail of growth rings within a native starch granule from NS48-He-01

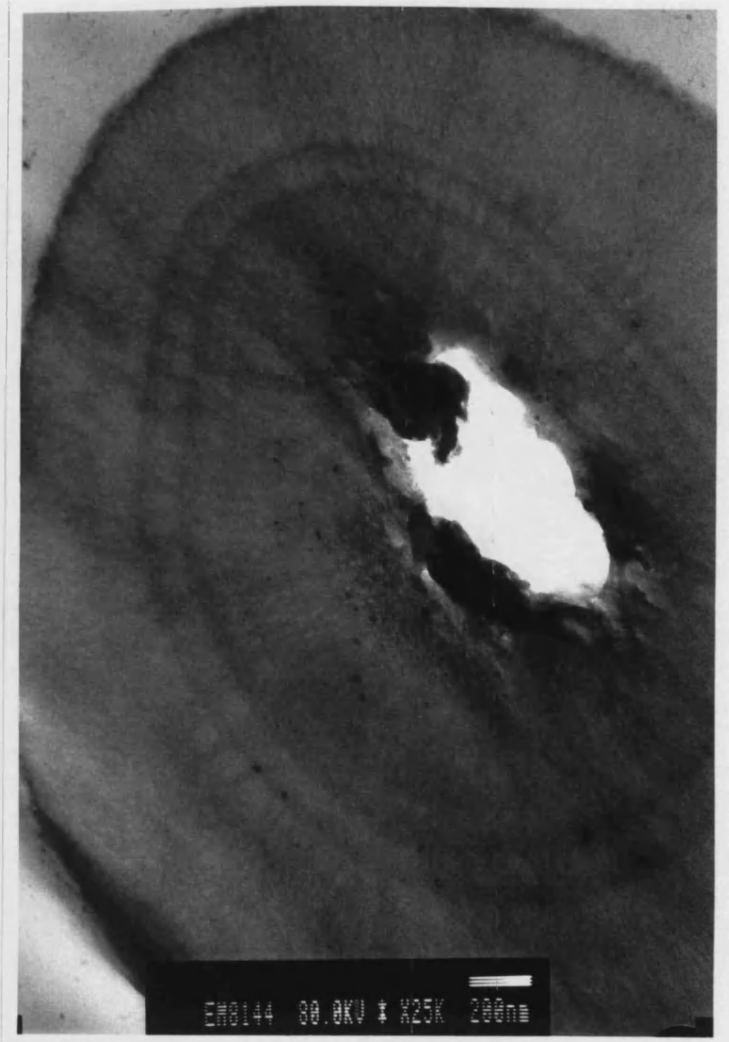

Figure 6.21: Detail of growth rings and internal hollow in a starch granule from NS48-He-01

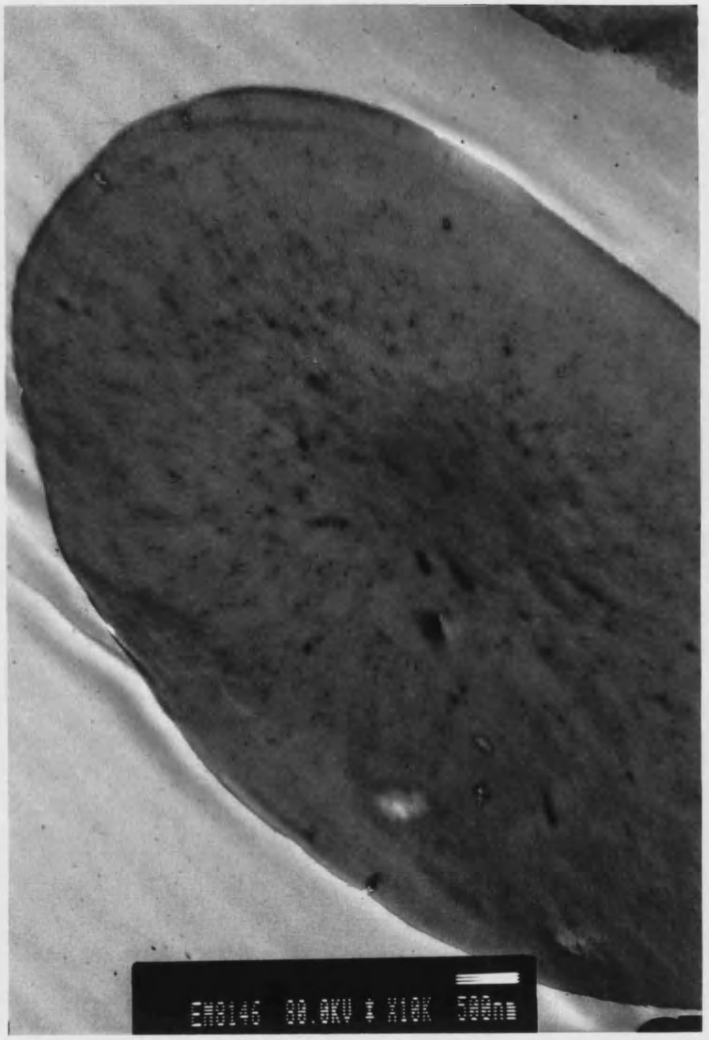

Figure 6.22: Cross section of particle from NS48-99-01 showing no evidence of amorphous and crystalline growth rings.

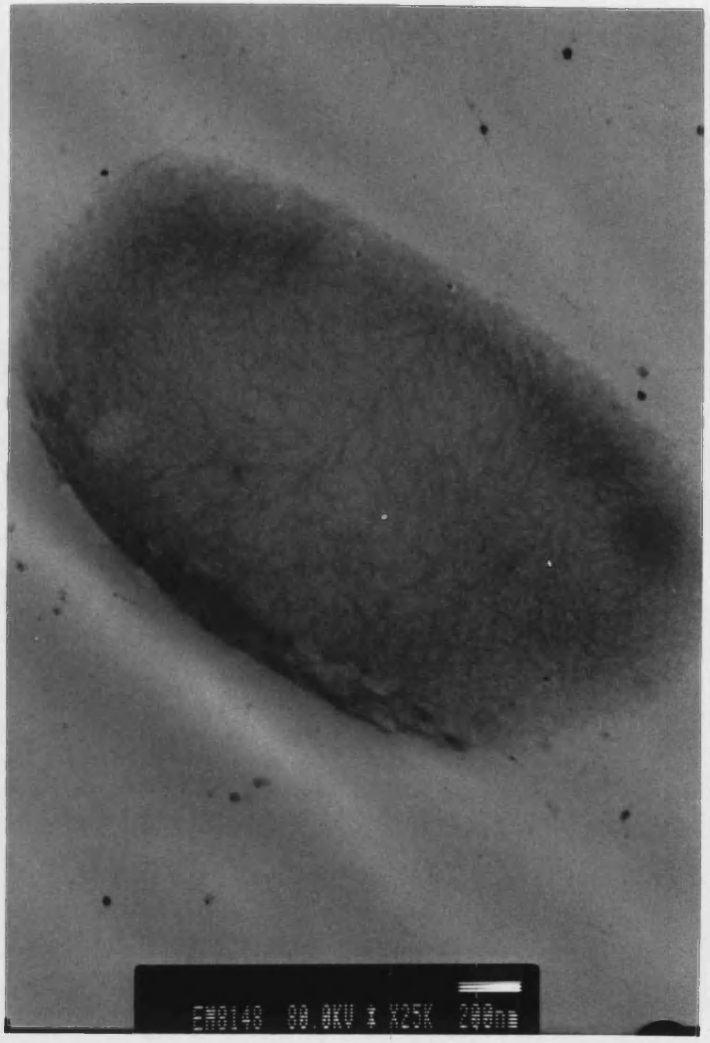

Figure 6.23: Detail of a particle from NS48-99-01 showing amorphous channels spanning the particle structure.

Figure 6.24: Thin section of a PATAg stained native starch granule from NS48-99-01 showing amorphous and crystalline growth rings

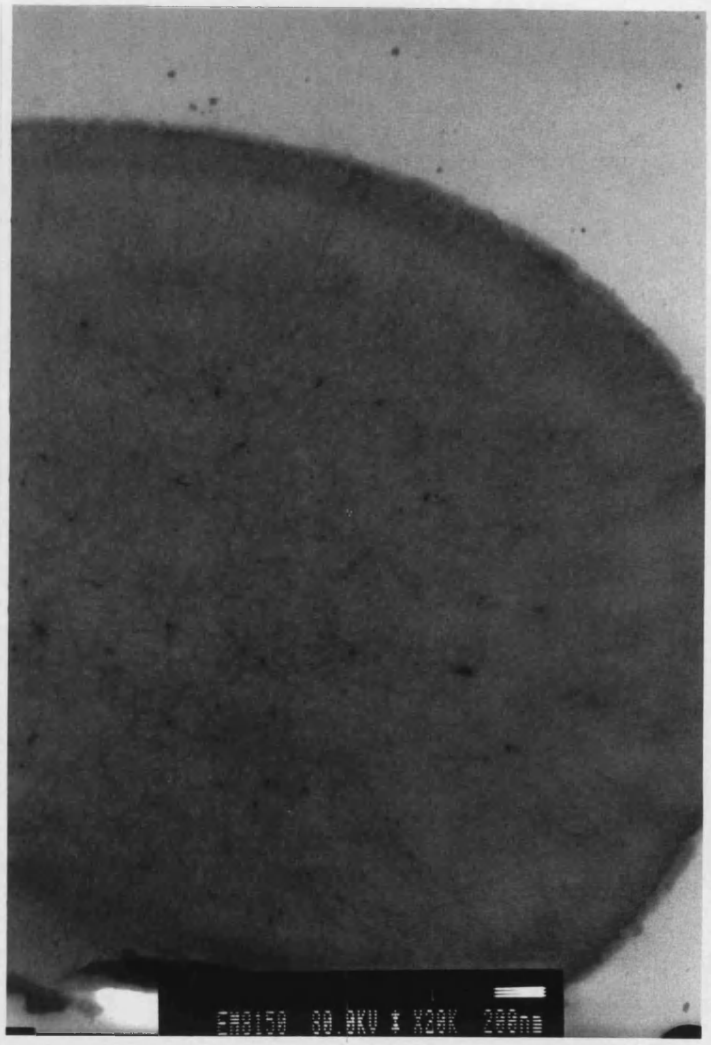

Figure 6.25: Cross section of native starch granule from NS48-99-01 detailing amorphous channels spanning its surface

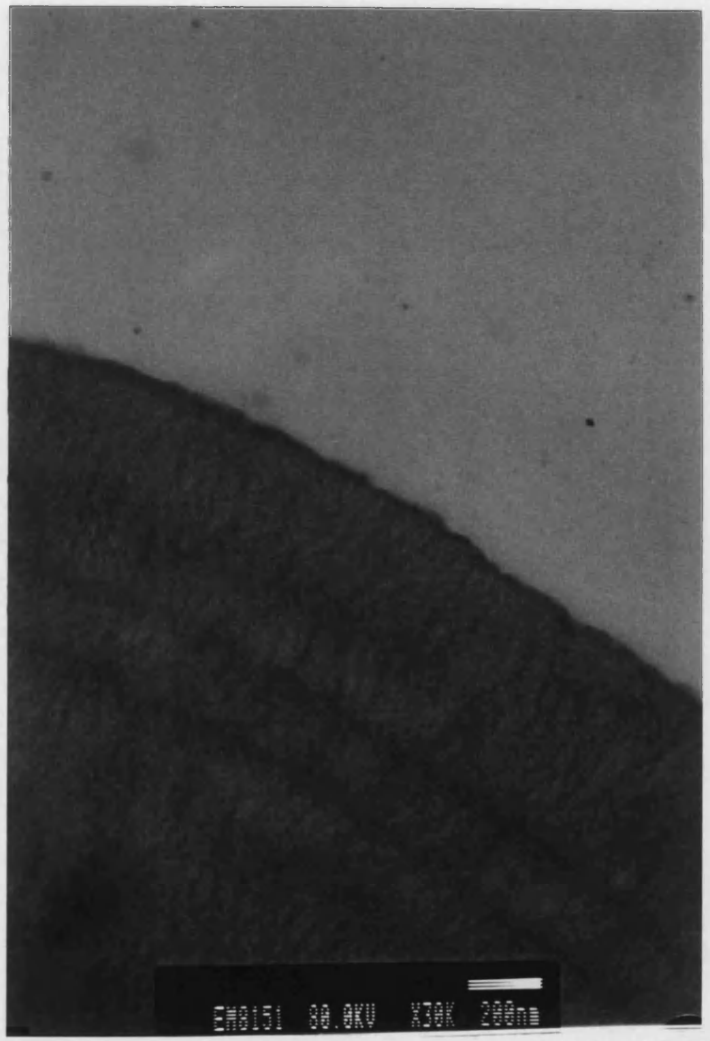

Figure 6.26: Detail of native starch granule from NS48-99-01showing the amorphous and crystalline growth rings.

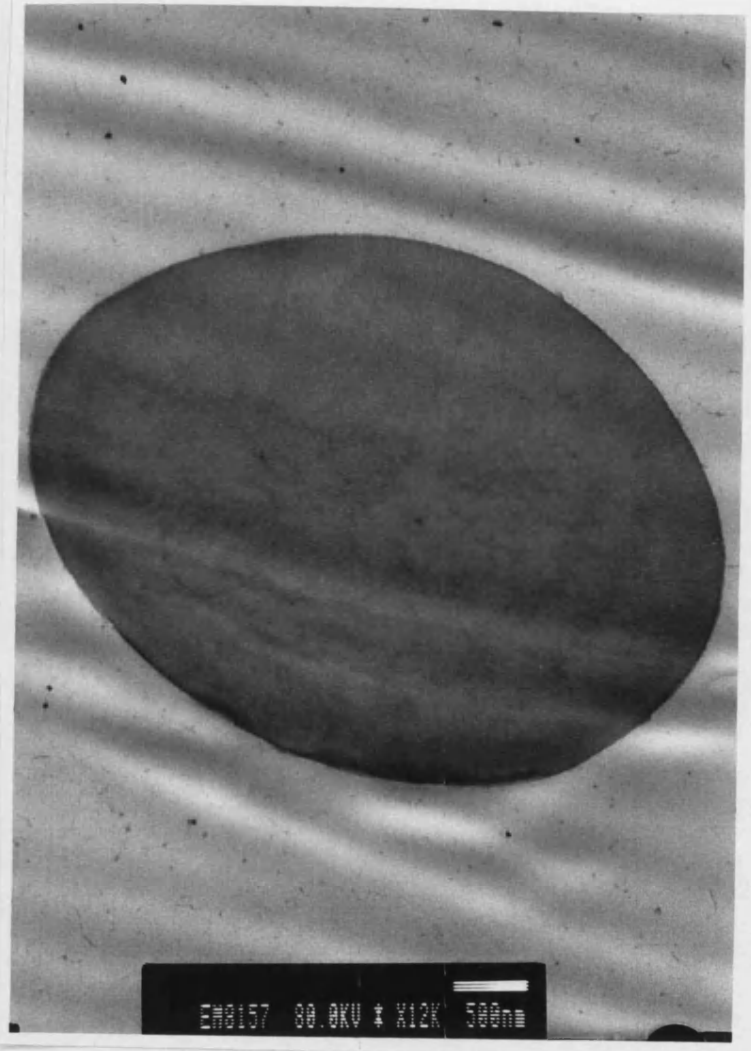

Figure 6.27: Native starch granule from NS48-70-01 with faint growth rings on the right hand side of the particle

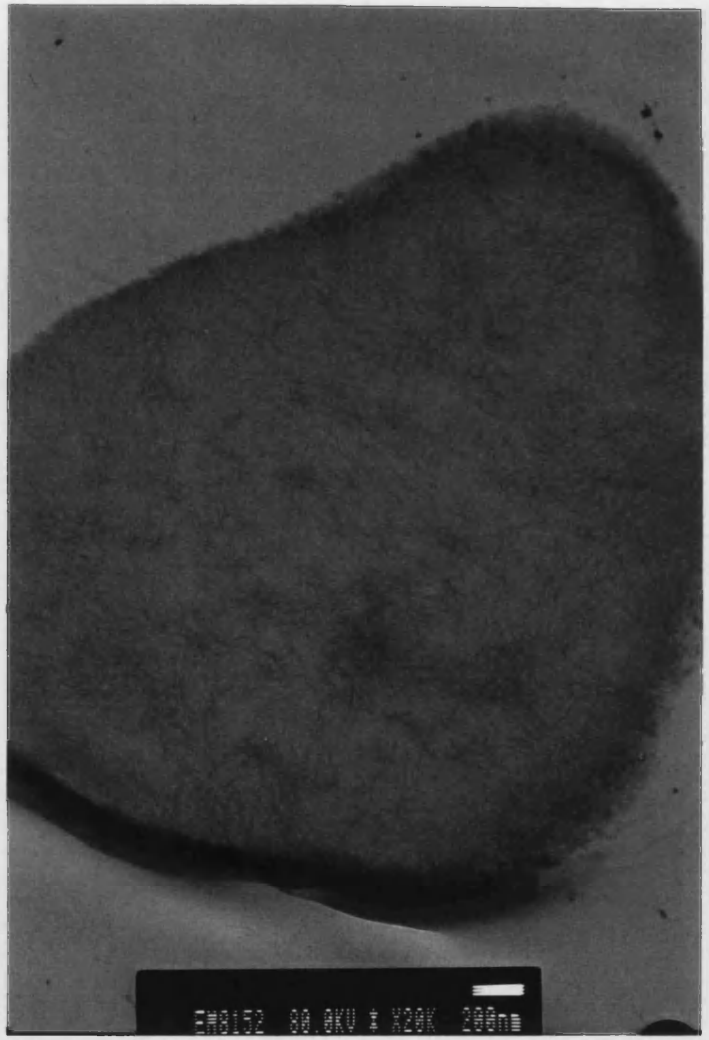

Figure 6.28: NS48-70-01 particle with no evidence of growth rings.

Figure 6.29: Detail of the amorphous channels within NS48-70-01

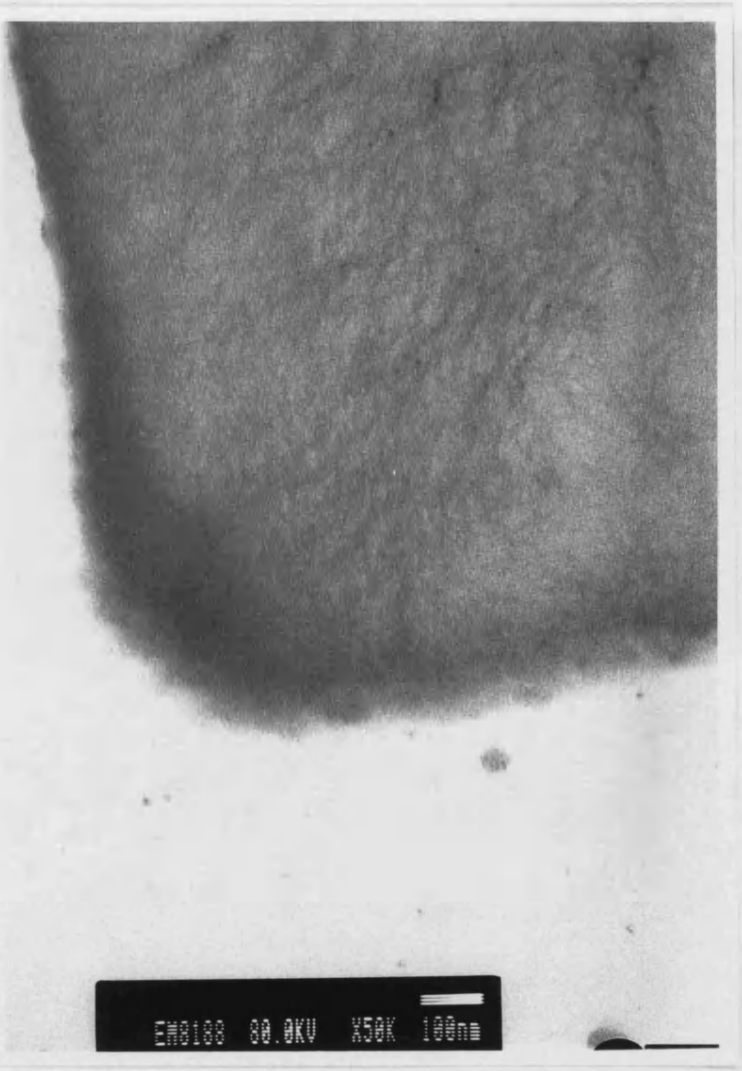

Figure 6.30: Detail of thin section of PATAg stained DF48-He-01

Figure 6.31: Thin section of an amorphous region of DF48-He-01

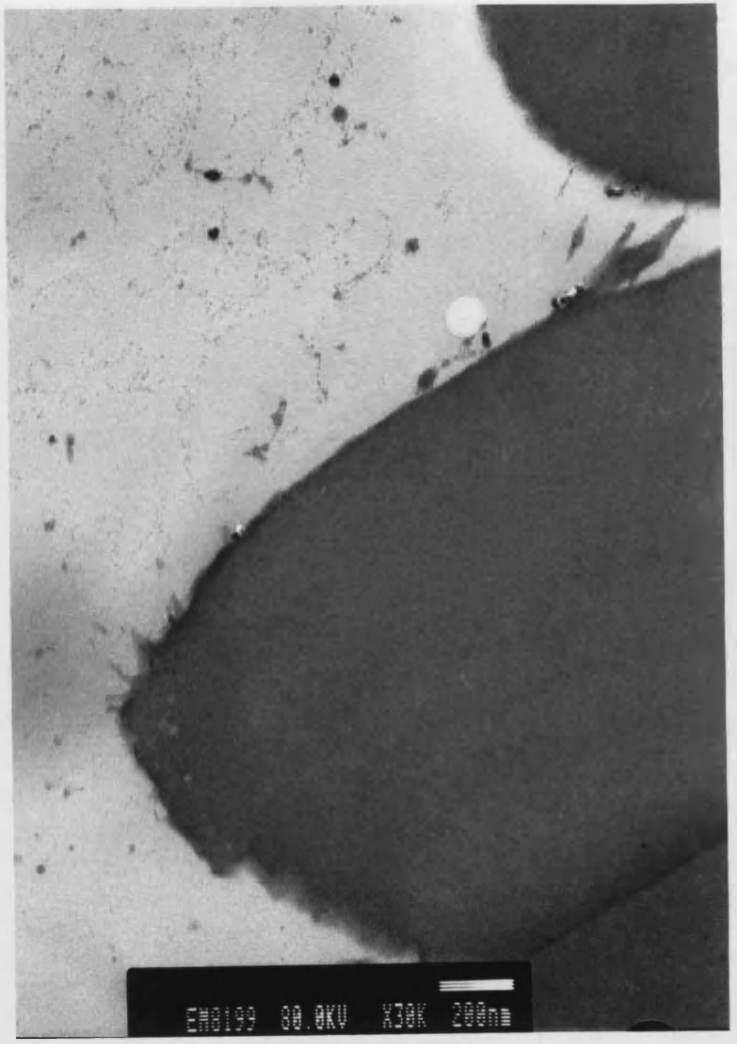

Figure 6.32: Thin section of PATAg stained DF48-99-01

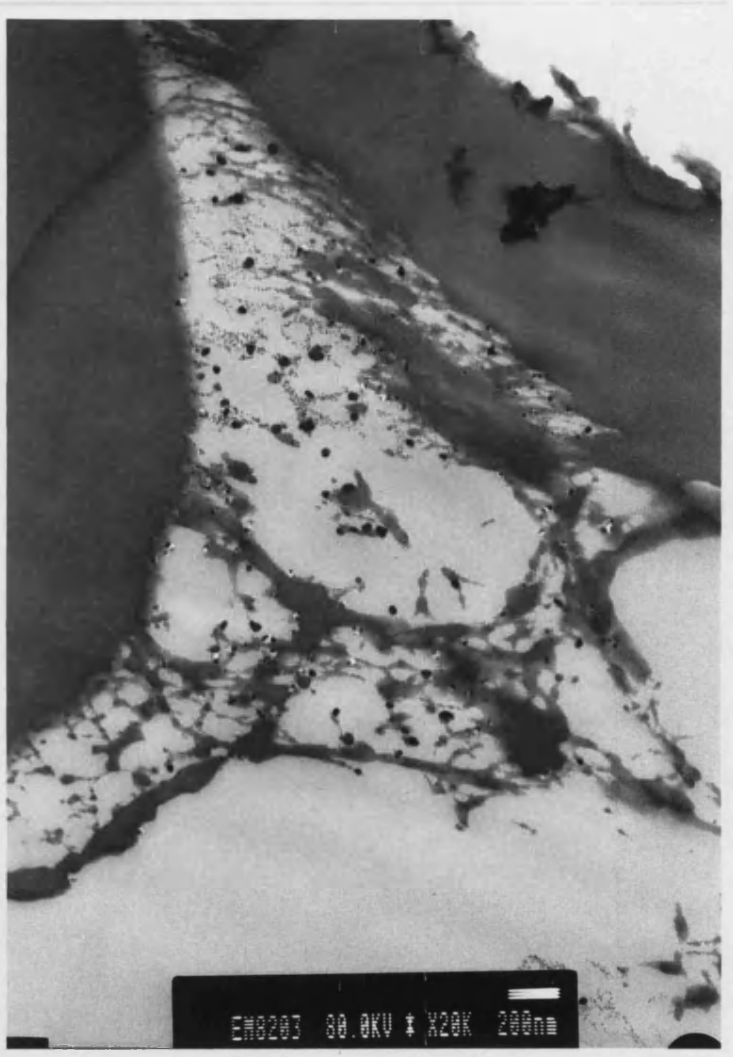

Figure 6.33: Thin section of material from DF48-99-01

Figure 6.34: Thin section of PATAg stained DF48-70-01

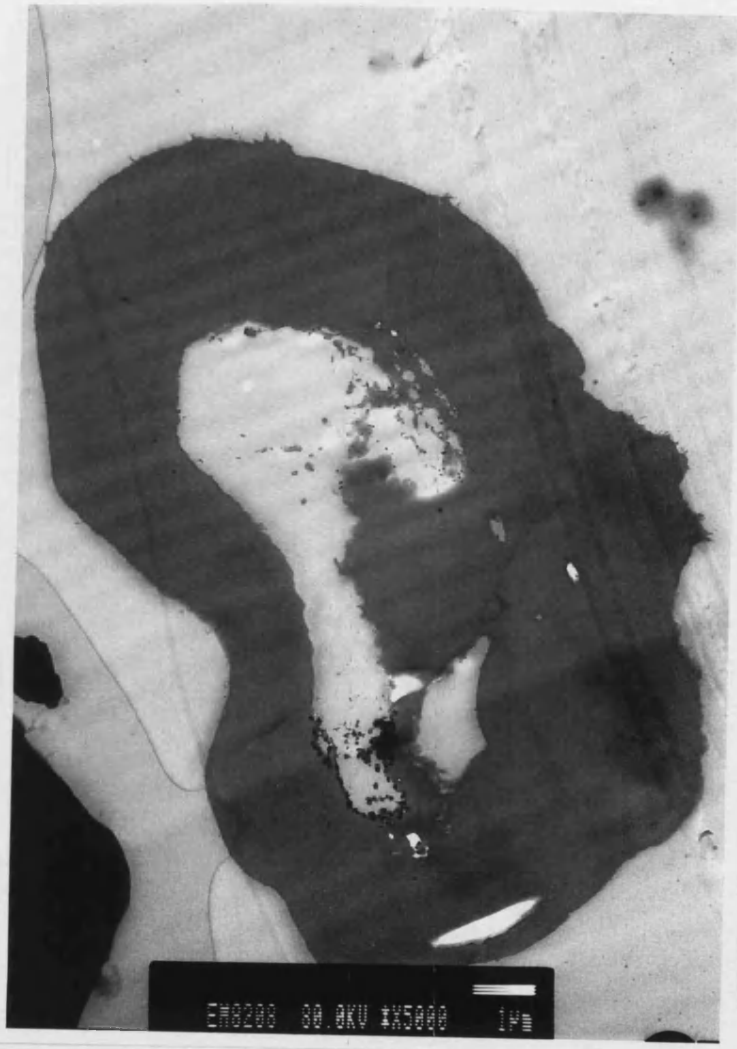

Figure 6.35: Section of material from DF48-70-01

Polarised light microscopy images of unmodified and defatted native maize starch and Starch 1500

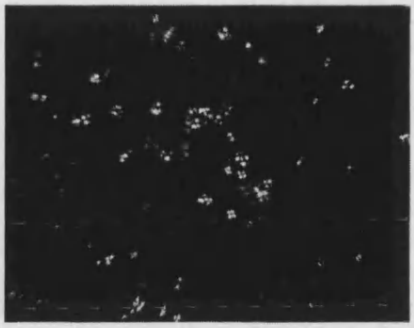

Figure 6.36: Starch 1500

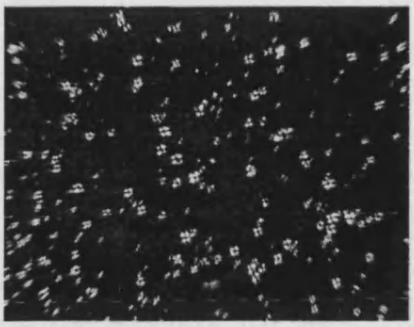

Figure 6.37: Native Maize Starch

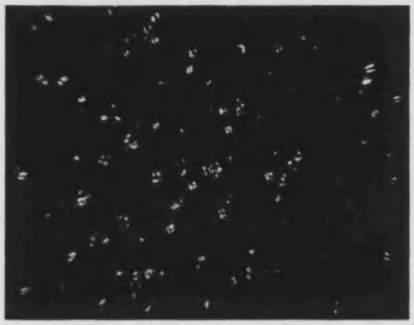

Figure 6.38: DF48-He-01

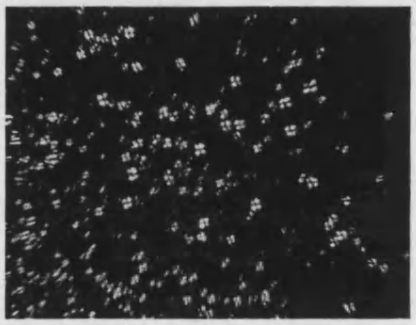

Figure 6.39: NS48-He-01

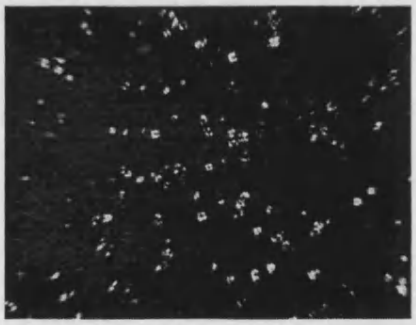

Figure 6.40: DF48-99-01

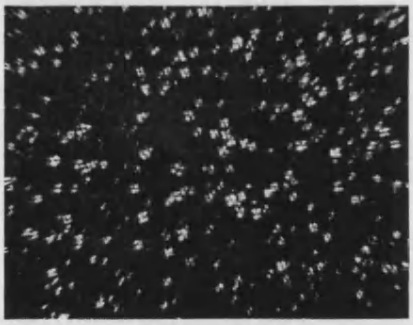

Figure 6.41: NS48-99-01

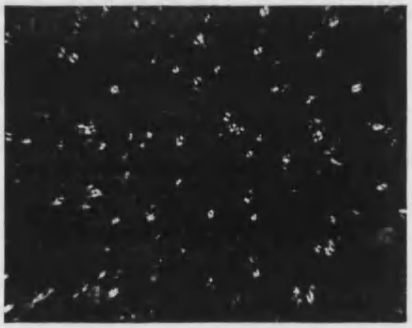

Figure 6.42: DF48-70-01

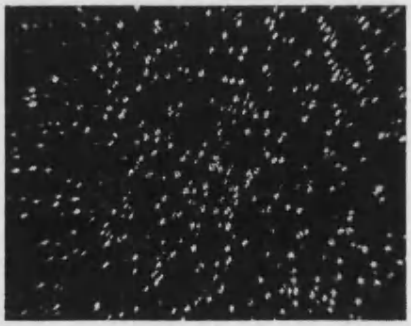

Figure 6.43: NS48-70-01

CHAPTER 7

DISCUSSION AND CONCLUSIONS

7.1 General Discussion

The aims of this study were to comprehensively characterise Starch 1500, identify the possible causes of its poor compactibility and flow and to improve the functionality of the material without chemical modification.

Starch 1500 is derived from maize starch and is regarded as being comprised of 20% pregelatinised starch and 80% native starch. Low temperature scanning electron microscopy (LTSEM) provided images of structures resembling native granules. These were present both as individual granules and as agglomerates incorporated in a matrix of pregelatinised starch. LTSEM studies confirmed the claim that the pregelatinised starch fraction acts to bind together native granules into larger agglomerates. Further weight was added to this theory by sectioning through resin embedded agglomerates from Starch 1500. Here structures resembling native granules were found within the agglomerates.

LTSEM allowed the material to be studied in its fully hydrated state allowing the fragile structure of pregelatinised starch bridges to be visualized for the first time in Starch 1500. The morphology of Starch 1500 particles could be subdivided into pregelatinised agglomerates and native starch granules. The native granules were uniform in shape and size, varying only by the presence or absence of indentations on the surface. These indentations may be caused by protein components called zein bodies. The size and morphology of the Starch 1500 agglomerates varied greatly, to such an extent that it was impossible to determine whether the various defatting processes employed were eliciting any effect on the material's structure.

The particle size distribution observed in the scanning electron micrographs supported the particle size analysis data obtained by time-of-flight aerosol beam spectroscopy (TOFABS). The study revealed a bimodal distribution with peaks at 17 and 90 μm relating to free native granules and agglomerates of native and pregelatinised starch respectively. With reference to the flow properties of Starch 1500 it is suggested that the free native granules retard powder flow and that their removal by further incorporation into the pregelatinised agglomerates may be desirable. However this may in turn adversely affect the disintegrant properties of the material by the removal of free native starch granules. Furthermore it is suggested that the poor compactibility of Starch 1500 may result from the presence

of native starch granules, which as was previously alluded to, resist applied compressive force.

Using the technique of differential scanning calorimetry (DSC), an endothermic transition may be observed accompanying the gelatinisation of native starch granules. This order-disorder transition was not observed in Starch 1500, which was attributed to the thermal modification of the whole population of starch granules during Starch 1500 production. Although structures may be observed by LTSEM, which resemble native maize starch granules, evidence of thermal modification is revealed by SEM and transmission electron microscopy (TEM) studies of the internal structure of Starch 1500. Thermal modification during Starch 1500 production results in the formation of a void at the hilum of the granule and a reduction in the definition of the growth rings that are readily identifiable in native maize starch samples. Although TEM reveals no evidence of growth rings in the native-like granules of Starch 1500, under polarized light microscopy positive birefringency is still clearly detectable. It is therefore suggested that some crystalline order is retained at the surface of the granule to elicit this effect.

Initial attempts to improve the compactibility of Starch 1500 focused on the ability of starches to form highly crystalline inclusion complexes with hydrophobic materials such as lipids and iodine. Starch 1500, as a plastic deforming material, demonstrates extreme lubricant sensitivity. It was suggested that complexation may result in the generation of a new, brittle material that did not display lubricant sensitivity. This approach proved wholly unsuccessful as the complexed materials exhibited even poorer compactibilty than Starch 1500. Therefore the second approach involved identification of possible causes of lubricant sensitivity in Starch 1500. A detailed study of the literature surrounding the lipids present in starches revealed a similarity to materials used as pharmaceutical lubricants in tablet production.

By treating Starch 1500 with various solvent systems it was possible to remove intrinsic lipids from the material. The composition of the extract was analysed by several techniques, which confirmed that the solvent system used influenced mainly the quantity rather than the composition of the extract. A degree of correlation was observed between the quantity of lipid removed from the material and the improvement in the tensile strength of compacts it forms.

Supercritical fluid extraction (SFE) failed to remove lipids from Starch 1500 and consequently there was no increase in the tensile strength of the material. The failure of this technique to remove lipids was attributed to the application of non-optimal extraction conditions. It is suggested that if further work resulted in the removal of the intrinsic lipid content of Starch 1500 a resultant increase in the tensile strength of the compacts would be observed.

A battery of tests were performed on the defatted material, which failed to highlight any difference form Starch 1500 in the particle size distribution (TOFABS and LTSEM) or morphology (LTSEM). TEM of defatted Starch 1500 again reveals a material showing large voids at the hilum of native-like granule structures and the absence of growth rings from the material. However, like unmodified Starch 1500, positive birefringency is detectable using polarised light microscopy indicating some residual crystallinity at the surface of the granules. Defatted native maize starch showed evidence of thermal modification such as voids at the centre of the granules and thinner amorphous growth rings than observed in untreated native granules. It was proposed that the latter phenomenon might be attributed to the leaching of amylose from the granule, at the elevated temperatures of defatting.

The results of the surface area analysis for unmodified and defatted Starch 1500 were anomalous. No correlation could be established between the quantity of lipid removed and the change in surface area that was observed for several of the samples.

The moisture content of unmodified and defatted Starch 1500 was comparable and modulated temperature DSC (MTDSC) failed to reveal any evidence of glass transition point modification. No evidence could be found to support the theory that the increased tensile strength of defatted Starch 1500 resulted from increased plasticisation of the material.

Studies performed using solid-state nuclear magnetic resonance (SS-NMR) failed to identify either a chemical modification by defatting Starch 1500 or the presence of residual defatting solvent. The former was supported by X-ray diffraction data, which failed to identify any significant changes in the crystallinity of the material. Evidence for the latter by was demonstrated using the technique of thermogravimetry coupled with mass spectrometry (TG/MS) confirmed that solvent

loss on heating the defatted materials could be attributed solely to the liberation of water.

Each solvent system that successfully defatted Starch 1500 yielded a material with greater compactibility and flow properties than unmodified Starch 1500. These materials were demonstrated to produce compacts of higher tensile strength using both a compaction simulator and a high-speed rotary tablet press.

The lubricant sensitivity of compacts of defatted and unmodified Starch 1500 was assessed. It was found that the defatted materials demonstrated a greater lubricant sensitivity than Starch 1500 although the compacts were still apparently stronger than those of the unmodified material. This was confirmed by the fact that the material extracted by defatting was very similar chemically to the hydrophobic lubricants used in this study. This finding added further weight to suggestion that the increased tensile strength of defatted Starch 1500 compacts resulted from the removal of surface lipids, which inhibit the formation of interparticulate bonds.

7.2 Further Work

The effect of defatting on the dissolution and disintegration properties of Starch 1500 needs to be assessed. This may be judged most effectively alongside the incorporation of the material into a formulation. Initial studies seemed to indicate that the defatted materials display a prolonged disintegration time, however studies were carried out on pure material (giving the disintegrant nothing to "push against") and at compaction forces where the access of water into the compact would be limited by the absence of mesopores. Further investigation should be performed on compacts of an equivalent hardness to those of unmodified Starch 1500.

Further work should concentrate on the surface characterization of unmodified and defatted Starch 1500. Using the technique of adhesion mapping, atomic force microscopy may provide an ideal tool with which to further these investigations.

As was alluded to in sections 6.3.1 and 6.3.2 voids exist at the centre of native starch granules after defatting. It was proposed that this phenomenon accompanied the leaching of amylose from the granules. With this in mind it would be desirable to analyse the extracts from defatted Starch 1500 for the presence of amylose. Equally analysis of the extract for proteins would be beneficial in relation to qualifying whether the improvement in the tensile strength of defatted Starch 1500 compacts was due purely to lipid removal.

Initial attempts to remove lipid from Starch 1500 using supercritical fluid extraction (SFE) techniques (section 3.3.1.1) proved unsuccessful. Therefore further work should concentrate on the potential of this technique to elicit lipid removal due to its advantages over conventional hot solvent extraction. Equally further work should concentrate on the scale-up of this process to produce larder quantities of defatted material for use on a commercial scale.

Starch 1500 has been demonstrated to show functional variability in relation to the season when the native starch is harvested (Cunningham, personal communication). Equally the lipid content of native starch may show seasonal variation, thus investigation of defatting as a means of reducing this variability should be performed. Furthermore the application of the defatting technique to other plastically deforming materials should be performed to determine whether an equivalent improvement in tensile strength is possible.

CHAPTER 8

REFERENCES

Acker, L. (1977). Die Lipide der Starken-ein forschungsgebiet zwischen kohlenhydraten und lipiden. *Fette, Seifen, Anstrichmittel,* **79,** 1 - 9.

Aggarwal, P. & Dollimore, D. (1998). A thermal analysis investigation of partially hydrolyzed starch. *Thermochimica Acta,* **319,** 17-25.

Alderborn, G. & Nystrom, C. (1982). Studies On Direct Compression of Tablets .3. the Effect On Tablet Strength of Changes in Particle-Shape and Texture Obtained By Milling. *Acta Pharmaceutica Suecica,* **19,** 147-156.

Alderborn, G. & Nystrom, C. (1982). Studies On Direct Compression of Tablets .4. the Effect of Particle-Size On the Mechanical Strength of Tablets. *Acta Pharmaceutica Suecica,* **19,** 381-390.

Armstrong, N.A. (1988). Tableting. In *Pharmaceutics: The science of dosage form design.* ed. Aulton, M. pp. 647 - 668. Edinborough: Churchill Livingstone.

Armstrong, N.A. & Palfrey, L.P. (1989). The Effect of Machine Speed On the Consolidation of 4 Directly Compressible Tablet Diluents. *Journal of Pharmacy and Pharmacology,* **41,** 149-151.

Banker, G. & Peck, G. (1980). Tablet formulation and design. In *Pharmaceutical Dosage Forms; Tablets.* ed. Lieberman, H. & Lachman, L. pp. 61 - 62. New York: Marcel Dekker, Inc.

Barron, C., Buleon, A., Colonna, P. & Della Valle, G. (2000). Structural modifcations of low hydrated pea starch subjected to high thermomechanical processing. *Carbohydrate Polymers,* **43,** 171 - 181.

Barton, A. (1983). *Handbook of solubility parameters and other cohesion parameters.* Baton Rouge,FL, U.S.A.: CRC.

Beckett, A. & Read, N. (1986). Low Temperature Scanning Electron Microscopy. In *Ultrastructural techniques for Micro-organisms.* ed. Aldrich, H. & Todd, W. pp. 45 - 86. New York: Plenum.

Bhatnagar, S. & Hanna, M.A. (1994). Amylose Lipid Complex-Formation During Single-Screw Extrusion of Various Corn Starches. *Cereal Chemistry,* **71,** 582-587.

Bhatnagar, S. & Hanna, M.A. (1997). Modification of microstructure of starch extruded with selected lipids. *Starch-Starke,* **49,** 12-20.

Biliaderis, C. (1990). *Thermal analysis of Food.* London: Elsevier Applied Science Publishers.

Biliaderis, C., Page, C., Maurice, T. & Juliano, B. (1986). Thermal characteristics of rice starches : A polymeric approach to phase transitions of granular starch. *J. Agric Food, Chem.,* **34,** 6.

Biliaderis, C. & Tonogai, J. (1991). Influence of lipids on thermal and mechanical properties of concentrated starch gels. *J. Agric. Food Chem.,* **39,** 833 - 840.

Bolhuis, G. & Chowan, Z. (1996). Materials for direct compaction. In *Pharmaceutical powder compaction technology.* ed. Alderborn, G. & Nystrom, C. pp. 419 - 500. New York, USA: Marcel Dekker, Inc.

Bolhuis, G., Lerk, C., Zijlstra, H. & De Boer, A. (1975). *Pharm. Weekblad,* **110,** 317.

Bolhuis, G.K., Reichman, G., Lerk, C.F., Vankamp, H.V. & Zuurman, K. (1985). Evaluation of Anhydrous Alpha-Lactose, a New Excipient in Direct Compression. *Drug Development and Industrial Pharmacy,* **11,** 1657-1681.

Bos, C., Bolhuis, G., Van Doorne, H. & Lerk, C. (1987). Native starch in tablet formulations: properties on compaction. *Pharm. Weekblad Sci. Ed.,* **9,** 274 - 283.

Bos, C., Vromans, H. & Lerk, C. (1991). Lubricant sensitivity in relation to bulk density for granulations based on starch or cellulose. *International Jornal of Pharmaceutics,* **67,** 39 - 49.

Brennan, K. (2000). Effects of supercritical fluid extraction on moisture content.

Brittain, H., Bogdanowich, S., Bugay, D., DeVincentis, J., Lewen, G. & Newman, A. (1991b). Physical characterization of pharmaceutical solids. *Pharmaceutical research,* **8,** 963 - 973.

Brittain, H., Sachs, C. & Fiorelli, K. (1991a). Physical characterization of pharmaceutical excipients: Practical examples. *Pharmaceutical Technology,* 38 - 52.

Bugay, D. & Findlay, W. (1999). *Pharmaceutical Excipients: Characterization by IR, Raman and NMR Spectroscopy.* New York: Marcel Dekker, Inc.

Buttrose, M. (1960). Submicroscopic development and structure of starch granules in cereal endosperms. *Journal of ultrastructural research,* **4,** 231 - 257.

Campbell, M., Pollak, L. & White, P. (1994). Effect of planting date on maize starch thermal properties. *Cereal chemistry,* **71,** 556 - 559.

Carr, R. (1970). Particle behaviour storage and flow. *British Chemical Engineering,* **15,** 1541 - 1549.

Cauvain, S., Gough, B. & Whitehouse, M. (1977). The role of starch in baked goods. Part 2, The influence of purification procedure on the surface properties of the granule. *Starch/Stärke,* **29,** 91 - 95.

Charsley, E.L., Hill, J.O., Nicholas, P. & Warrington, S.B. (1992). An Investigation of the Icta Certified Reference Materials For Dta As Potential Standards For the Temperature Calibration of Thermomechanical Analysis Equipment. *Thermochimica Acta,* **195,** 65-71.

Cheung, P., Leung, A. & Ang, P. (1998). Comparison of supercritical carbon dioxide and soxhlet extraction of lipids from a brown seaweed, Sargassum hemiphyllum (Turn) C. *Journal of Argicultural Food Chemistry,* **46,** 4228 - 4232.

Christianson, D., Nielson, H., Khoo, V., Wolff, M. & Wall, J. (1969). *Cereal Chemistry,* **45,** 372.

Collinson, R. (1968). Swelling and gelation of starch. In *Starch and its derivatives.* ed. Radley, J. Suffolk: The Chaucer Press.

Craig, S.A.S. & Stark, J.R. (1984). The Effect of Physical Damage On the Molecular-Structure of Wheat-Starch. *Carbohydrate Research,* **125,** 117-125.

De Boer, A., Bolhuis, G. & Lerk, C. (1978). Bonding characteristics by scanning electron microscopy of powder mixed with magnesium stearate. *Powder Technology,* **20,** 75 - 82.

Dees, P.J. & Polderman, J. (1981). Mercury Porosimetry in Pharmaceutical Technology. *Powder Technology,* **29,** 187-197.

Dionisi, F., Hug, B., Aeschlimann, J.M. & Houllemar, A. (1999). Supercritical CO_2 extraction for total fat analysis of food products. *Journal of Food Science,* **64,** 612-615.

Donovan, J. (1979). Phase transitions of the starch water system. *Biopolymers,* **18,** 263.

Duberg, M. & Nystrom, C. (1982). Studies On Direct Compression of Tablets .6. Evaluation of Methods For the Estimation of Particle Fragmentation During Compaction. *Acta Pharmaceutica Suecica,* **19,** 421-436.

Edge, S., Potter, U., Steele, D., Tobyn, M. & Staniforth, J. (1998). The use of a modified resin for studying the internal structure of microcrystalline cellulose particles. *Micron.*

Evans, J. & Briggs, D. (1941). *Cereal Chemistry,* **18,** 443.

Evers, A. (1969). Scanning Electron Microscopy of Wheat Starch I. Entire Granules. *Die Starke,* **21,** 96 - 99.

Fell, J. & Newton, J. (1970). Determination of tablet strength by diametral compression test. *Journal of Pharmaceutical Sciences,* **59,** 688 - 691.

French, D. (1972). Fine structure of starch and its relationship to the organisation of starch granules. *J. Jpn. Soc. Starch. Sci.*, **19**, 8 - 25.

French, D. (1984). Organisation of starch granules. In *Starch: Chemistry and Technology*. ed. Whistler, R., BeMiller, J. & Paschall, J. pp. 193 - 247. Orlando, USA: Academic Press.

Fuhrer, C. (1996). Interparticulate Attraction Mechanisms. In *Pharmaceutical powder compaction technology*. ed. Alderborn, G. & Nystrom, C. pp. 1 - 15. New York, USA: Marcel Dekker, Inc.

Fuzek, J. (1980). Glass transition temperature of wet fibers. In *Water in Polymers*. ed. Rowland, S. pp. 515. Washington DC: American Chemical Society.

Gallant, D. (1974). Contribution a l'etude de la structure et de l'ultrastructure du grain d'amidion. Paris: University of Paris.

Gallant, D., Bouchet, B. & Baldwin, P. (1987). Microscopy of starch: evidence fof a new level of granule organization. *Carbohydrate Polymers*, **32**, 177 - 191.

Gallant, D., Derrien, A., Aumaitre, A. & Guilbot, A. (1973). Degredation in vitro de l'amidion par le suc pancreatique. *Starch/Starke*, **25**, 56 - 64.

Gallant, D. & Guilbot, A. (1973). Development des connaissances sur l'ultrastructure du grain d'amidion. I. L'amidion de ble. *Starch/Starke*, 335 - 342.

Gallant, D. & Guilbot, A. (1969). Etude de l`ultrastructure du grain d`amidon a l'aide de nouvelles methodes de preparations en microscopie electronique. *Starch/Starke*, **21**, 156 - 163.

Galliard, T. & Bowler, P. (1987). Morphology and composition of starch. In *Starch: Properties and Potential.* ed. Galliard, T. pp. 55 - 78. New York: John Wiley & Sons.

Galliard, T. & Bowler, P. (1987). Morphology and composition of starch. In *Starch: Properties and Potential.* ed. Galliard, T. pp. 55 - 78. New York: John Wiley and Sons.

Glauert, A. (1991). Epoxy resins: An update on their selection and use. *Microscopy and Analysis,* 15 - 20.

Glennie, C.W., McDonald, A.M.L. & Stark, J.R. (1987). Some Observations On Damage in Commercial Starch Preparations. *Carbohydrate Research,* **170,** 263-268.

Goldstein, J., Newbury, D., Echlin, P., Joy, D., Fiori, C. & Lifshin, E. (1992). *Scanning Electron Microscopy and X-ray Microanalysis.* New York: Plenum Press.

Goshima, G., Abe, M., Sato, N., Ohashi, K. & Tsuge, H. (1985). Amylographic reproducibility of defatted potato starch by the re-introduction of lipid. *Starch/Starke,* **37,** 10 - 14.

Greenwell, P., Evers, A.D., Gough, B.M. & Russell, P.L. (1985). Amyloglucosidase-Catalyzed Erosion of Native, Surface-Modified and Chlorine-Treated Wheat-Starch Granules - the Influence of Surface Protein. *Journal of Cereal Science,* **3,** 279-293.

Greenwell, P. & Schofield, J.D. (1986). A Starch Granule Protein Associated With Endosperm Softness in Wheat. *Cereal Chemistry,* **63,** 379-380.

Gunstone, F., Harwood, J. & Padley, F. (1994). *The Lipid Handbook.* London: Chapman and Hall.

Hargin, K. & Morrison, W. (1980). The distribution of acyl lipids in the germ, aleurone, starch and non-starch endosperm of four wheat varieties. *J. Sci. Food Agric.*, **31**, 877 - 888.

Herman, J., Remon, J. & De Vilder, J. (1989). Modified starches as hydrophilic matrices for controlled oral delivery. I. Production and characterisation of thermally modified starches. *International Journal of Pharmaceutics*, **56**, 51 - 63.

Hindle, M. & Byron, P. (1995). Size distribution control of raw materials for dry powder inhalers using the aerosizer with the aero-disperser. *Pharmaceutical Technology*, 64 - 78.

Ho, T. (1991). *Polarity control for synthesis.* New York: Wiley.

Holm, J., Bjorck, I., Eliasson, A., Asp, N., Larsson, D. & Lundquist, I. (1983). Digestibility of amylose-lipid complexes in vitro. *Starch*, **35**, 294 - 297.

Hopper, M.L., King, J.W., Johnson, J.H., Serino, A.A. & Butler, R.J. (1995). Multivessel supercritical fluid extraction of food items in total diet study. *Journal of Aoac International*, **78**, 1072-1079.

Humbert-Droz, P., Mordier, D. & Doelker, E. (1982). *Pharm. Acta Helv.*, **57**, 136.

Imam, S. (1989). A tightly bound Mr 55000 polypeptide in cornstarch associated with the amylose portion of the granule. *Journal of Cereal Science*, **9**, 231 - 236.

Imberty, A., Chanzy, H., Perez, S., Buleon, A. & Tran, V. (1988). The Double-Helical Nature of the Crystalline Part of a-Starch. *Journal of Molecular Biology,* **201,** 365-378.

Ingram, J. & Lownthal, W. (1966). Mechanism of action of starch as a tablet disintegrant 1. factors affecting the swelling of starch grains at 37. *J. Pharm. Sci.,* **55,** 614 - 617.

Jarosz, P. & Parrott, E. (1984). Effect of lubricants on tensile strength of tablets. *Drug Development and Industrial Pharmacy,* **19,** 259 - 273.

Jeffree, C. & Read, N. (1991a). Ambient and low temperature scanning electron microscopy. In *Electron microscopy of plant cells.* ed. Hall, J. & Hawes, C. pp. 313 - 413. London: Academic Press.

Jeffree, C. & Read, N. (1988). Common artifacts associated with biological material examined by low temperature scanning elctron microscopy. In
Institute of physics conference series. ed. Dickinson, H. & Goodhew, P. pp. 17 - 18.

Jeffree, C. & Read, N. (1991b). Low temperature scanning electron microscopy in biology. *Jornal of microscopy,* **161,** 59 - 72.

Jenkins, J.P.J., Cameron, R.E. & Donald, A.M. (1993). A Universal Feature in the Structure of Starch Granules From Different Botanical Sources. *Starch-*
Starke, **45,** 417-420.

Karehill, P., Borjesson, E., Glazer, M., Alderborn, G. & Nystrom, C. (1993). *Drug Development and Industrial Pharmacy,* **19,** 2143.

Kawabata, A., Takase, N. & Miyoshi, E. (1994). Microscopic observation and X-ray diffractometry of heat/moisture treated starch granules. *Starch/Starke,* **46,** 463 - 469.

Khankari, R. & Hontz, J. (1997). Binders and Solvents. In *Handbook of pharmaceutical granulation technology.* ed. Parikh, D. pp. 59 - 72. New York: Marcel Dekker, Inc.

Lehrman, L. (1929). The fatty acids associated with rice starch, *Journal of the American Chemical Society,* **51,** 2185 - 2188.

Lehrman, L. (1932). The fatty acids associated with cassava starch *Journal of the American Chemical Society,* **54,** 2527 - 2530.

Lehrman, L. (1930). The fatty acids associated with wheat starch, *Journal of the American Chemical Society,* **52,** 808 - 811.

Lehrman, L. (1942). The nature of the fatty acids associated with starch. The adsorption of palmitic acid by potato and defatted corn and rice starches. *Journal of the American Chemical Society,* **64,** 2144 - 2146.

Lenaerts, V., Moussa, I., Dumoulin, Y., Mebsout, F., Chouinard, F., Szabo, P., Mateescu, M.A., Cartilier, L. & Marchessault, R. (1998). Cross-linked high amylose starch for controlled release of drugs: recent advances. *Journal of Controlled Release,* **53,** 225-234.

Lerk, C., Bolhuis, G. & Smedena, S. (1977). *Pharm. Acta Helv.,* **52,** 39.

Liu, H. & Lelievre, J. (1993). A Model of Starch Gelatinization Linking Differential Scanning Calorimetry and Birefringence Measurements. *Carbohydrate Polymers,* **20,** 1-5.

Lordi, N. (1994). "Starch" monograph. In *Handbook of Pharmaceutical Excipients.* ed. Wade, A.a.W., PJ. pp. 491 - 493. London: The Pharmaceutical Press.

Lund, D. (1984). Influence of Time, Temperature, Moisture, Ingredients, and Processing Conditions On Starch Gelatinization. *Crc Critical Reviews in Food Science and Nutrition,* **20,** 249-273.

Malvern Instruments Ltd., U. (1993). Diffraction Training: Windows diffraction training manual.

Manners, D. (1989). Recent developments in the understanding of amylopectin structure. *Carbohydrate Polymers,* **11,** 87 - 112.

Manudhane, K., Contractor, A., Kin, H. & Shangraw, R. (1969). Tabletting properties of a directly compressible starch. *Journal of Pharmaceutical Sciences,* **58,** 616 - 620.

McDonald, A., Stark, J., Morrison, W. & Ellis, R. (1991). The composition of starch granules from developing barley genotypes. *Journal of cereal science,* **13,** 93 - 112.

Mikus, F., Hixon, R. & Rundle, R. (1946). The complexes of fatty acids with amylose. *Journal of the American Chemical Society,* **68,** 1115 - 1123.

Miller, B., Derby, R. & Trimbo, H. (1973). A pictorial explanation for the increase in viscosity of a heated wheat starch-water suspension. *Cereal Chemistry,* **50,** 271 - 280.

Mitchell, J.P. & Nagel, M.W. (1996). An assessment of the API Aerosizer(R) for the real-time measurement of medical aerosols from pressurized metered-dose inhaler (pMDI) systems. *Aerosol Science and Technology,* **25,** 411-423.

Mitrevej, A., Faroongsarng, D. & Sinchaipanid, N. (1996). Compression behavior of spray dried rice starch. *International Journal of Pharmaceutics,* **140,** 61-68.

Mitrevej, A., Sinchaipanid, N. & Faroongsarng, D. (1996). Spray-dried rice starch: Comparative evaluation of direct compression fillers. *Drug Development and Industrial Pharmacy,* **22,** 587-594.

Mitrevej, A. & Varavinit, S. (1988). Modified rice starch for direct compression. In *12th Asian Congress of Pharaceutical Sciences, Federation of Asian Pharmaceutical Associations.* Bali, indonesia.

Mollenhauer, H. (1988). Artifacts caused by dehydration and epoxy embedding in transmission electron microscopy. In *Artifacts in biological electron microscopy.* ed. Crang, R. & Klomparens, K. pp. 43 - 64. New York & London: Plenum.

Mondero Perales, M., Munoz-Ruiz, A., Velasco Antequera, M., Munoz Munoz, N. & Jiminez-Castellanos Ballesteros, M. (1996). Comparative tabletting and microstructural properties of a new starch for direct compression. *Drug development and industrial pharmacy,* **22,** 689 - 695.

Morgan, K.R., Furneaux, R.H. & Larsen, N.G. (1995). Solid-State Nmr-Studies On the Structure of Starch Granules. *Carbohydrate Research,* **276,** 387-399.

Morrison, W. & Coventry, A. (1985). Extraction of lipids from cereal starches with hot aqueous alcohols. *Starch/Starke,* **37,** 83 - 87.

Morrison, W. & Gadan, H. (1987). The amylose content of starch granules in developing wheat endosperm. *Journal of Cereal Science,* **5,** 263 - 275.

Morrison, W.R. (1981). Starch Lipids - a Reappraisal. *Starke,* **33,** 408-410.

Muller, F. & Augsburger, L. (1994). The role of the displacement time waveform in the determination of heckel behaviour under dynamic conditions in a compaction simulator and a fully instrumented rotary tablet machine. *Journal of Pharmacy and Pharmacology,* **46,** 468 - 475.

Mussulman, W. & Wagoner, J. (1968). Electron microscopy of unmodified and acid modified corn starches. *Cereal Chemistry,* **45,** 162 - 171.

Myer, L.J.D., Damian, J.H., Liescheski, P.B. & Tehrani, J. (1992). Supercritical Fluid Extraction Versus Soxhlet Sample Preparation - a Comparative-Study For Extraction and Analysis of Organics in Solid Matrices. *Acs Symposium Series,* **488,** 221-236.

Ndife, M., Sumnu, G. & Bayindirli, L. (1998). Differential Scanning Calorimetry Determination of Gelatinization Rates in Different Starches due to Microwave Heating. *Lebensm. Wiss. Technol.,* **31,** 484 - 488.

Nierle, W., Kersting, H., Burmann, D. & Burman, I. (1998). Changes of Physical Properties of Wheat gluten and Starch as a Function of Removing Some Attending Substances. *Starch/Starke,* **50,** 493 - 499.

Nikuni, Z. (1978). Studies on starch granules. *Starch/Stärke,* **30,** 105 - 111.

Niven, R. (1993). Aerodynamic particle size testing using a time of flight aerosol beam spectrometer. *Pharmaceutical technology,* 72 - 78.

Olkku, J. & Rha, C. (1978). Gelatinisation of starch and wheat flour - a review. *Food Chemistry,* **3,** 293 - 317.

Oostergetel, G.T. & Vanbruggen, E.F.J. (1993). The Crystalline Domains in Potato Starch Granules Are Arranged in a Helical Fashion. *Carbohydrate Polymers,* **21,** 7-12.

Parrott, E. (1989). Comparative evaluation of a new direct compression excipient, Soludex(TM) 15. *Drug Development and Industrial Pharmacy,* **15,** 561 - 583.

Patel, N. & Hopponen, R. (1966). Mechanism of action of starch as a disintegrating agent in aspirin tablets. *Journal of Pharmaceutical Sciences,* **55,** 1065 - 1068.

Perales, M.C.M., MunozRuiz, A., Antequera, M.V.V., Munoz, N.M. & Ballesteros, M. (1996). Comparative tableting and microstructural properties of a new starch for direct compression. *Drug Development and Industrial Pharmacy,* **22,** 689-695.

Rees, J. & Rue, P. (1978). Time dependent deformation of some direct compression excipients. *Journal of Pharmacy and Pharmacology,* **30,** 601 - 607.

Rees, J. & Tsardaka, K. (1994). Some effects of moisture on the viscoelastic behaviour of modified starch during powder compaction. *European journal of Pharmaceutics and Biopharmaceutics,* **40,** 193 - 197.

Ring, S. (1995). Stiff tests for designer starches. *Chemistry in Britain,* **4,** 303 - 307.

Rizvi, S., Daniels, J., Benado, A. & Zollweg, J. (1986). Supercritical fluid extraction: Operating principles and food applications. *Food Technology,* 57 - 64.

Sair, L. (1964). *Methods in Carbohydrate Chemistry,* **4,** 283.

Sakr, A., Elsabbagh, H. & Emara, K. (1974). STA-Rx(R) 1500 Starch: a new vehicle for the direct compression of tablets. *Arch. Pharm. Chemi. Sci. Ed.,* **2,** 14 - 24.

Schoch, T. (1942). Non-carbohydrate substances in the cereal starches. *Journal of the American Chemical Society,* **64,** 2954 - 2956.

Schweizer, T., Reimann, S., Solms, J., Eliasson, A. & Asp, N. (1986). Influence of drum drying and twin screw extrusion cooking of wheat carbohydrates. II. Effect of lipids on physical properties , degredation and complex formation of starch in wheat flour. *Journal of Cereal Science,* **4,** 249 - 260.

Seguchi, M. (1984). Comparison of Oil-Binding Ability of Different Chlorinated Starches. *Cereal Chemistry,* **61,** 244-247.

Seguchi, M. (1985). Model Experiments On Hydrophobicity of Chlorinated Starch and Hydrophobicity of Chlorinated Surface Protein. *Cereal Chemistry,* **62,** 166-169.

Shangraw, R., Wallace, J. & Bowers, F. (1981). Morphology and functionality in tablet excipients for direct compression: part II. *Pharmaceutical Technology,* 44 - 60.

Shangraw, R.F. & Wallace, J.W. (1981). Sem Study of the Role of Morphology On the Functionality of Pharmaceutical Tabletting Excipients. *Acta Pharmaceutica Suecica,* **18,** 99-99.

Shen, M. & Eisenberg, A. (1966). Glass transitions in polymers. *Solid State Chemistry,* **3,** 407 - 481.

Silverio, J., Svensson, E., Eliasson, A. & Olofsson, G. (1996). Isothermal microcalorimetric studies on starch retrogradation. *Journal of thermal analysis,* **47,** 1179 - 1200.

Stark, J. & Lynn, A. (1991). Starch granules large and small. *Biochemical Society Transactions.*

Stark, J.R. & Yin, X.S. (1986). The Effect of Physical Damage On Large and Small Barley Starch Granules. *Starch-Starke,* **38,** 369-374.

Strickland, W., Nelson, E., Busse, L. & Higuchi, T. (1956). The physics of tablet compression. IX. Fundamental aspects of tablet lubrication. *J. Am. Pharm. Assoc. Sci. Ed.,* **45,** 51 - 55.

Stute, R. (1990). Eigenschaften und Anwedungsmoglichkeiten von Erbsenstarken, *Starch/Starke,* **42,** 178 -184.

Sulaiman, B.D. & Morrison, W.R. (1990). Proteins Associated With the Surface of Wheat-Starch Granules Purified By Centrifuging Through Cesium-Chloride. *Journal of Cereal Science,* **12,** 53-61.

Swinkels, J.J.M. (1985). Composition and Properties of Commercial Native Starches. *Starke,* **37,** 1-5.

Taylor, J.R.N. & Robbins, D.J. (1993). Factors Influencing Beta-Amylase Activity in Sorghum Malt. *Journal of the Institute of Brewing,* **99,** 413-416.

Taylor, T. & Nelson, J. (1920). Fat associated with starch. *Journal of the American Chemical Society,* 1726 - 1738.

Telloke, G.W. (1985). Chlorination of Cake Flour and Its Effect On Starch Gelatinization. *Starke,* **37,** 17-22.

Tester, R.F. & Morrison, W.R. (1990). Swelling and Gelatinization of Cereal Starches .1. Effects of Amylopectin, Amylose, and Lipids. *Cereal Chemistry,* **67,** 551-557.

Theiwes, H. & Steeneken, P. (1997). The glass transition of starch and the sub Tg endotherm of amorphous and native potato starch at low moisture content. *Charbohydrate Polymers,* **32,** 123 - 130.

Thiery, J. (1967). Mis en evidence des polysaccharides sur coupes fines en microscopie electronique. *Journal de microscopie,* **6,** 987 - 1018.

Vasanthan, T. & Hoover, R. (1992a). A comprative study of the composition of lipids associated with starch granules from various botanical sources. *Food Chemistry,* **43,** 19 - 27.

Vasanthan, T. & Hoover, R. (1992b). Effect of defatting on starch structure and physicochemical properties. *Food Chemistry,* **45,** 337 - 347.

Washburn, E. (1921). A method of determining the distribution of pore sizes in a porous material. *Proc. Natl. Acad. Sci.,* **7,** 115 - 116.

Webb, P. & Orr, C. (1997). *Analytical methods in fine particle technology.* Norcross: Micromeritics instrument Corporation.

Wells, J. & Aulton, M. (1988). Preformulation. In *Pharmaceutics, the science of dosage form design.* ed. Aulton, M. pp. 224. New York: Churchill Livingstone.

Whistler, R. & Hilbert, G. (1944). Extraction of Fatty substances from starch. , **66,** 1721 - 1722.

Whistler, R. & Thornburg, W. (1957). Development of starch granules in corn endosperm. *Journal of Agricultural Food Chemistry,* **5,** 203 - 207.

Whistler, R. & Turner, E. (1955). Fine structure of starch granule sections. *Journal of Polymer Science,* **18,** 153 - 156.

Wootton, M. & Bamunuarachchi, A. (1978). Water binding capacity of commercial produced native and modified starches. *Starch/Starke,* **30,** 306 - 309.

Wray, P. (1992). The physics of tablet compaction revisited, *Drug Development and Industrial Pharmacy,* **18,** 627 - 658.

Wurster, D., Peck, G. & Kildsig, D. (1982). A comparison of the moisture adsorption-desorption properties of corn starch, USP and directly compressible starch. *Drug development and Industrial Pharmacy,* **8,** 343 - 354.

York, P. (1988). The design of dosage forms. In *Pharmaceutics, the science of dosage form design.* ed. Aulton, M. pp. 1. New York: Churchill Livingstone.

Youngquist, R., Hughes, D. & Smith, J. (1969). Effect of chlorine on starch-lipid interactions. *Cereal Science Today,* **14,** Abstract 40.

Zeleznak, K. & Hoseney, R. (1987). The Glass Transition in Starch. *Cereal Chemistry,* **64,** 121 - 124.

Zobel, H.F. (1988). Molecules to Granules - a Comprehensive Starch Review. *Starch-Starke,* **40,** 44-50.

Zosel, K. (1981). Process for the decaffination of coffee. In *US Patent.*

Zou, W., Lusk, C., Messer, D. & Lane, R. (1999). Fat contents of Cereal Foods: Comparison of Classical with Recently Developed Extraction Techniques. *Journal of AOAC International,* **82,** 141 - 150.

Zuurman, K., Maarschalk, K.V. & Bolhuis, G.K. (1999). Effect of magnesium stearate on bonding and porosity expansion of tablets produced from materials with different consolidation properties. *International Journal of Pharmaceutics,* **179,** 107-115.

APPENDIX 1

MEDFILES PHARMA REPORT

MedFiles Pharma

Colorcon Inc.
Attn. to Dr Irv Lash
415 Moyer Boulevard
West Point, PA
USA

August 5th 1999

Ref: Tableting studies of starch-based powders

Dear Dr Lash,

Enclosed, please, find the report on the recent study of the starch-based powders, marked as "Sample 7/23/99".

The study was performed according to earlier procedure. The results showed that the sample material had rather good tableting characteristics.

If you have any questions regarding the present study or any other item please do not hesitate to contact us.

Best regards,

Jukka Ilkka
Reserch Scientist
MedFiles Pharma Ltd.

Oy MedFiles
Pharma Ltd
ammonkatu 10
P.O. Box 1450
70501 KUOPIO
Finland
158 17 288 1200
158 17 288 1249
E-mail
la@medfiles.fi
Krnro
rade Reg. No
639.610
Kotipaikka
istered office
Kuopio

Jukka Ilkka, M.Sc. (Pharm.)
Product Development
Pharmaceutical R & D

MedFiles

MEDFILES PHARMA Ltd
Sammonkatu 10
P.O.BOX 1450
FIN-70501 KUOPIO, Finland

Telephone +358 17 288 1245
Mobile +358 50 353 7254
Telefax +358 17 288 1239
E-mail: jukka.ilkka@medfiles.fi

288 1245
7254
1239
E-mail: jukka.ilkka@medfiles.fi

File RESULT050899
Sheet DBFsw

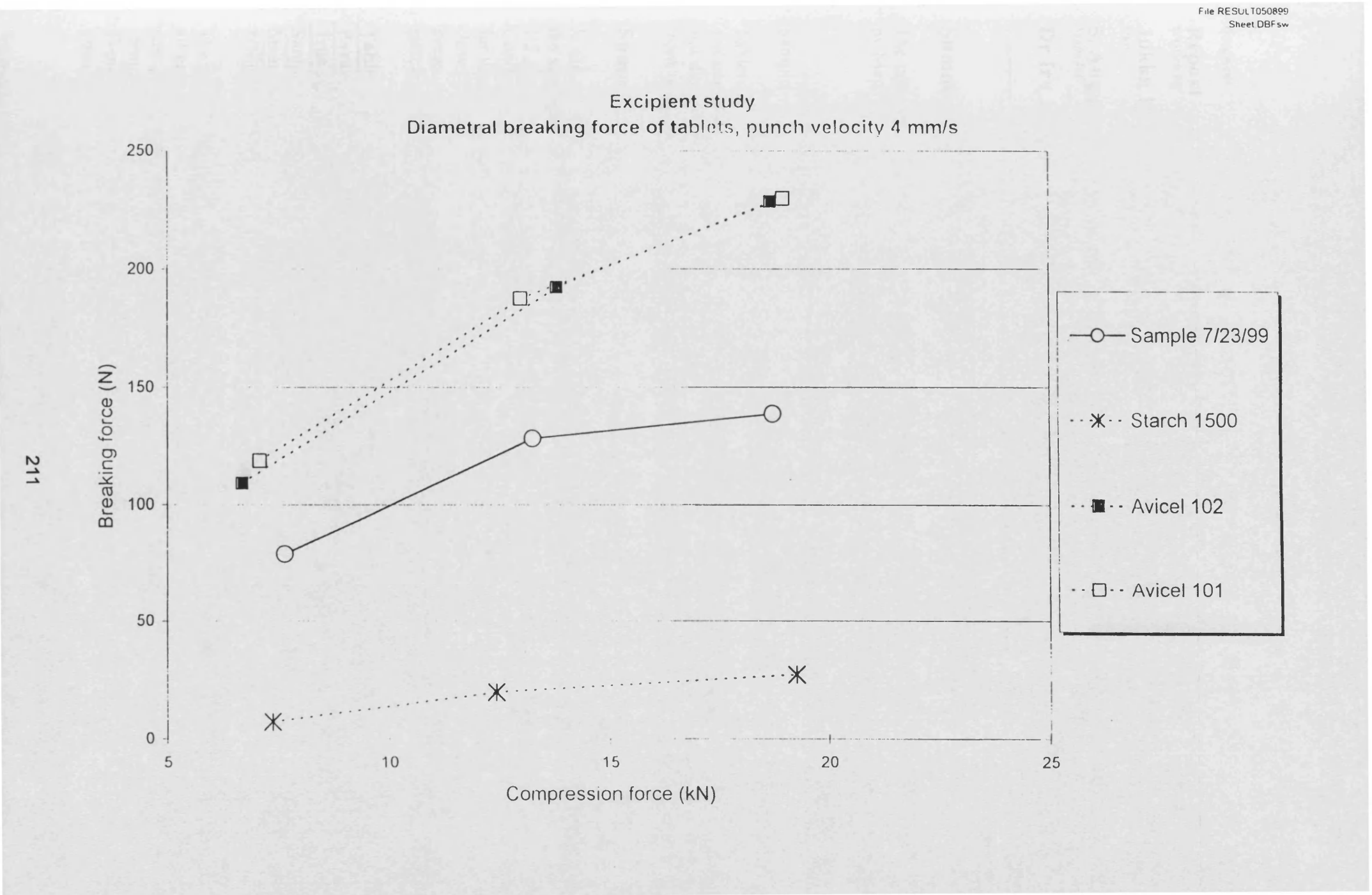

Document

Report on tableting studies (compaction simulator) on *starch-based materials*

Written by

Jukka Ilkka, Research Scientist, MedFiles Pharma Ltd

Date

5. August, 1999

Made for

Dr Irv Lash/Dr Dev Mehra, Colorcon Inc.

Summary of materials and methods

The tableting studies were performed according to previously described protocol (see earlier studies by MedFiles Pharma). The sample was starch-based powder marked as,

Sample 7/23/99.

Sample was used as received from the supplier.

Tablets were compressed in various conditions altering the punch velocity between 4 and 300 mm/s and compression force between 7 and 19 kN. The tablets were checked for the weight, dimensions and diametral breaking force. Mean yield pressure was determined using the Heckel analysis. Data from tablet compression at 13 kN/300 mm/s was used for Heckel analysis.

Summary of results

In the visual examination the sample was found as white free flowing powder. Particle density of the sample (Table 1) was comparable to density of common starches, which is ranging around 1.45-1.5 g/cm^3.
Compression behaviour of the sample was evaluated by Heckel analysis. The mean yield pressure for the sample was low indicating relatively soft material, which is deforming mainly by plastic flow (Table 1). According to yield pressure densification behaviour of the sample is similar to pregelatinised starch and microcrystalline cellulose. Typical yield pressure values for pregelatinised starch are ranging between 70-90 MPa and for microcrystalline cellulose between 60-80 MPa.

Table 1. Some physical parameters of the samples.

Parameter	Sample 7/23/99
True particle density	1.492 g/cm^3
Sample weight for tableting	0.146 g
Mean yield pressure	53 MPa*

*Obtained from compaction at 13 kN/300 mm/s

The sample showed good tableting characteristics. Firm and intact compacts were obtained with in all process conditions (Table 2 and Figs). Compared with the pregelatinised starch the mechanical strength of the sample tablets was clearly greater in all conditions. Although, the strength of the sample tablets decreased with increasing tableting speed adequate quality of the tablets remained. Typical values for Starch 1500, Avicel PH101 and PH102 are included in the graphs. Values obtained from earlier studies.

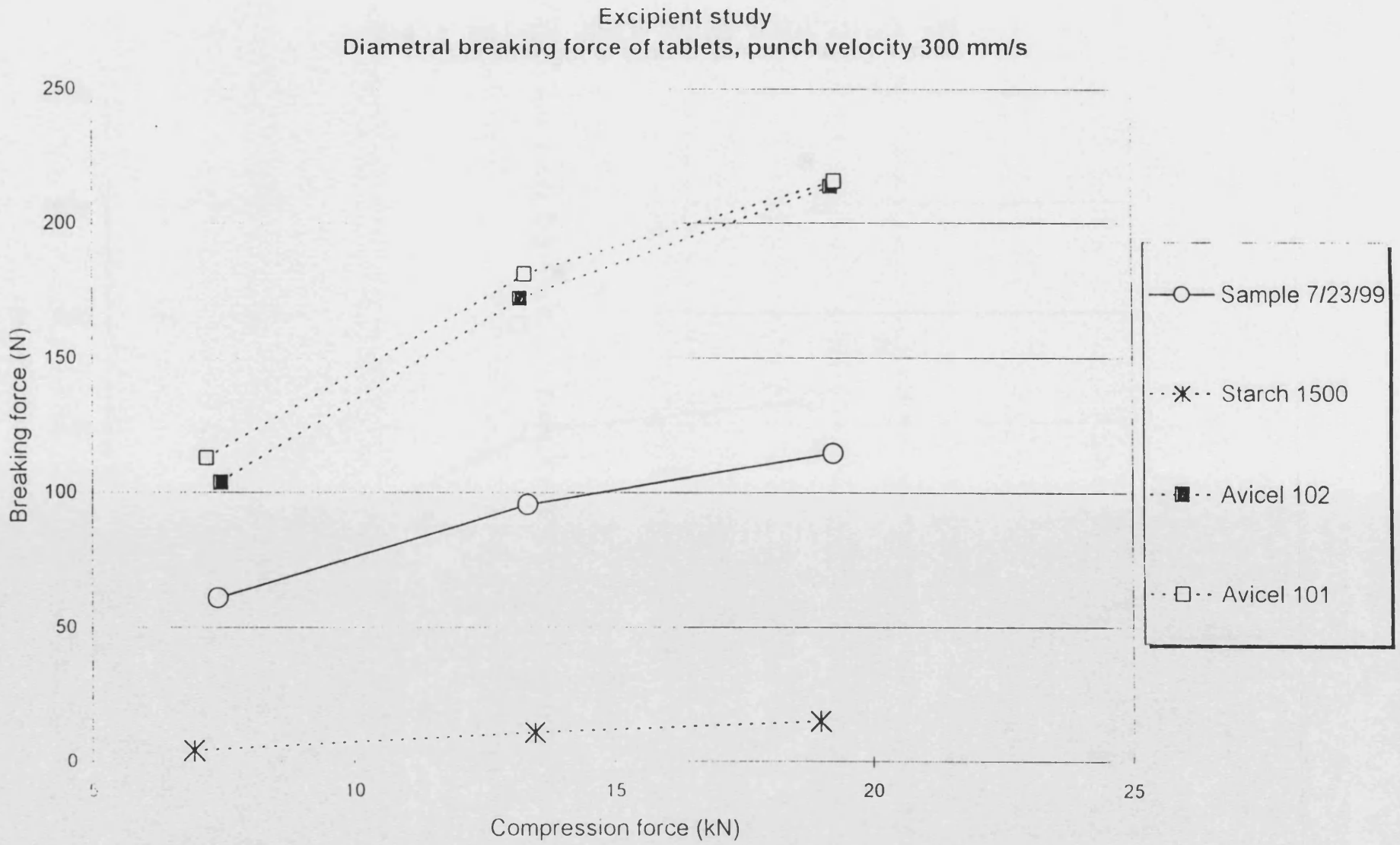

File RESULT050899
Sheet TSsw

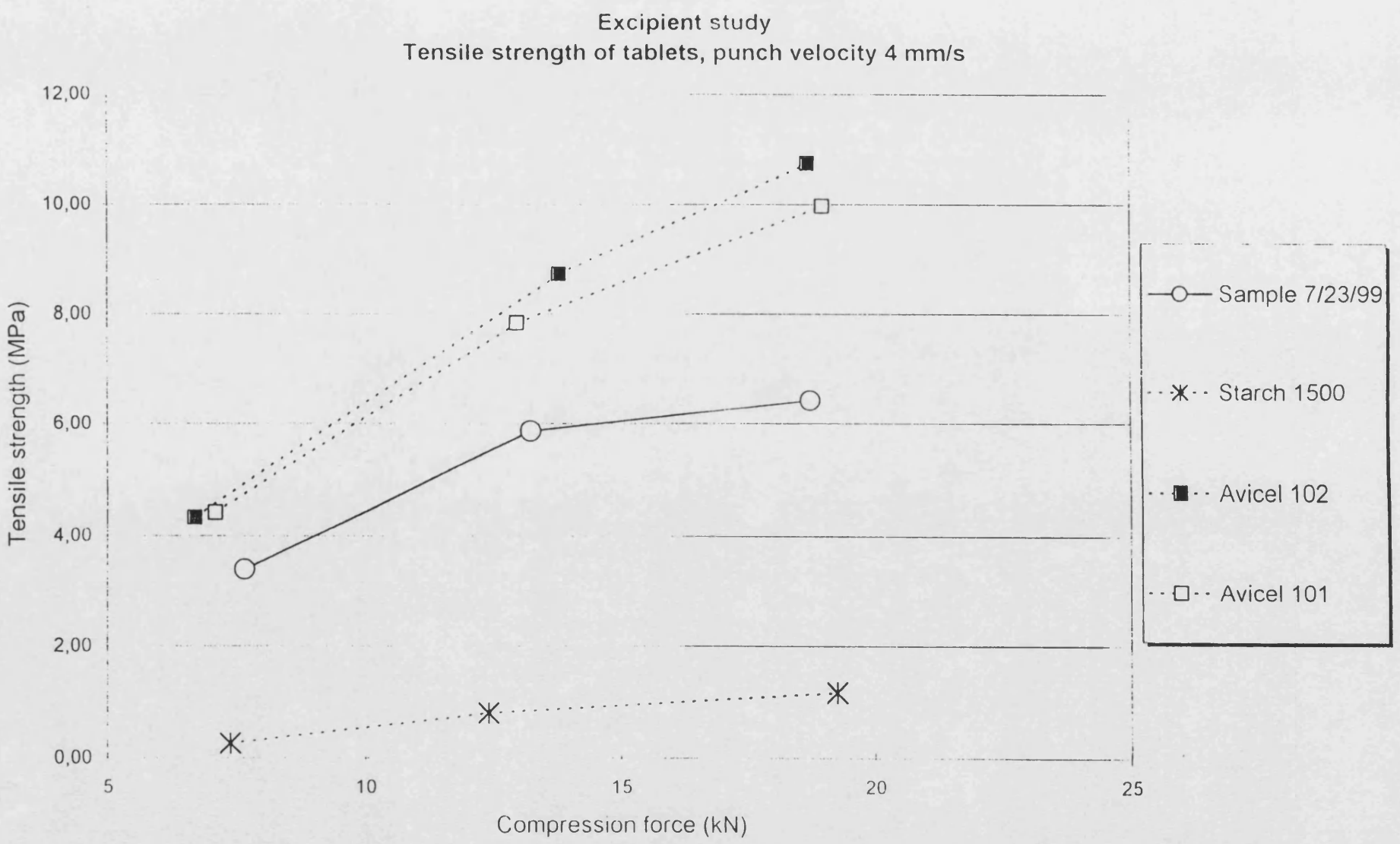

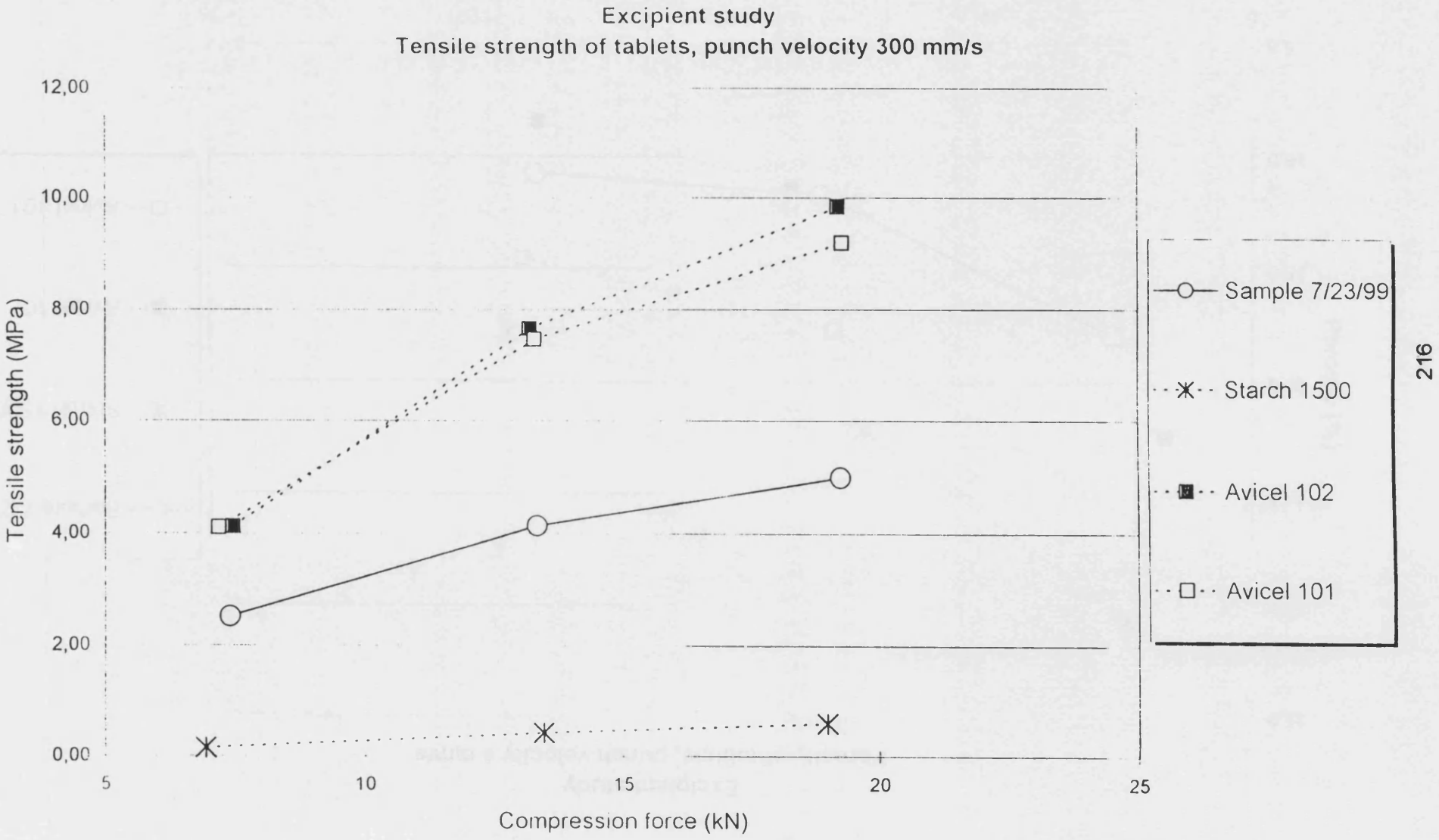
Excipient study
Tensile strength of tablets, punch velocity 300 mm/s
12,00
10,00
8,00
6,00
4,00
2,00
0,00
Tensile strength (MPa)
5
10
15
20
25
Compression force (kN)
Sample 7/23/99
Starch 1500
Avicel 102
Avicel 101
216

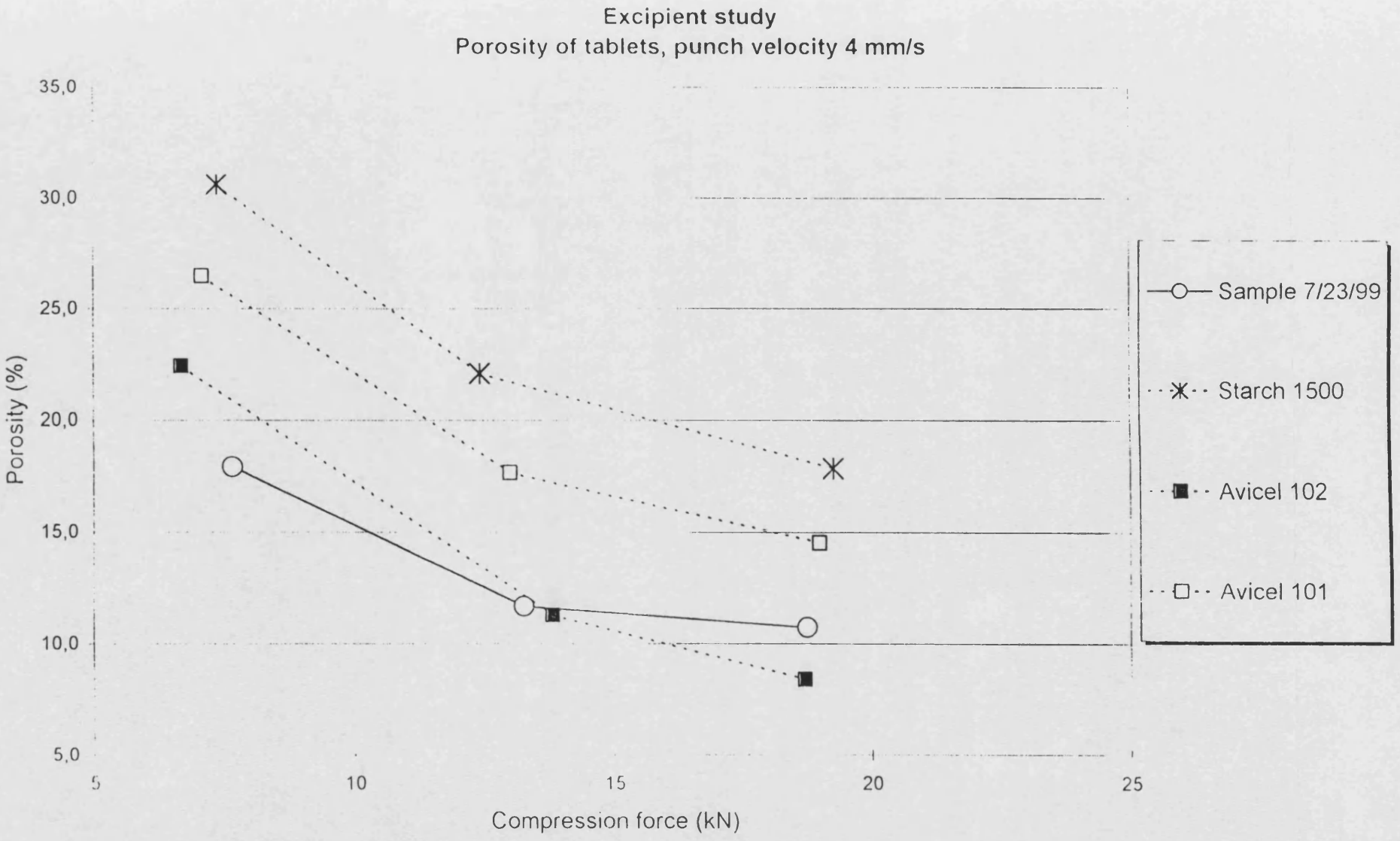
Excipient study
Porosity of tablets, punch velocity 4 mm/s
35,0
30,0
25,0
20,0
15,0
10,0
5,0
Porosity (%)
5
10
15
20
25
Compression force (kN)
Sample 7/23/99
Starch 1500
Avicel 102
Avicel 101

File RESULT050899
Sheet POR01

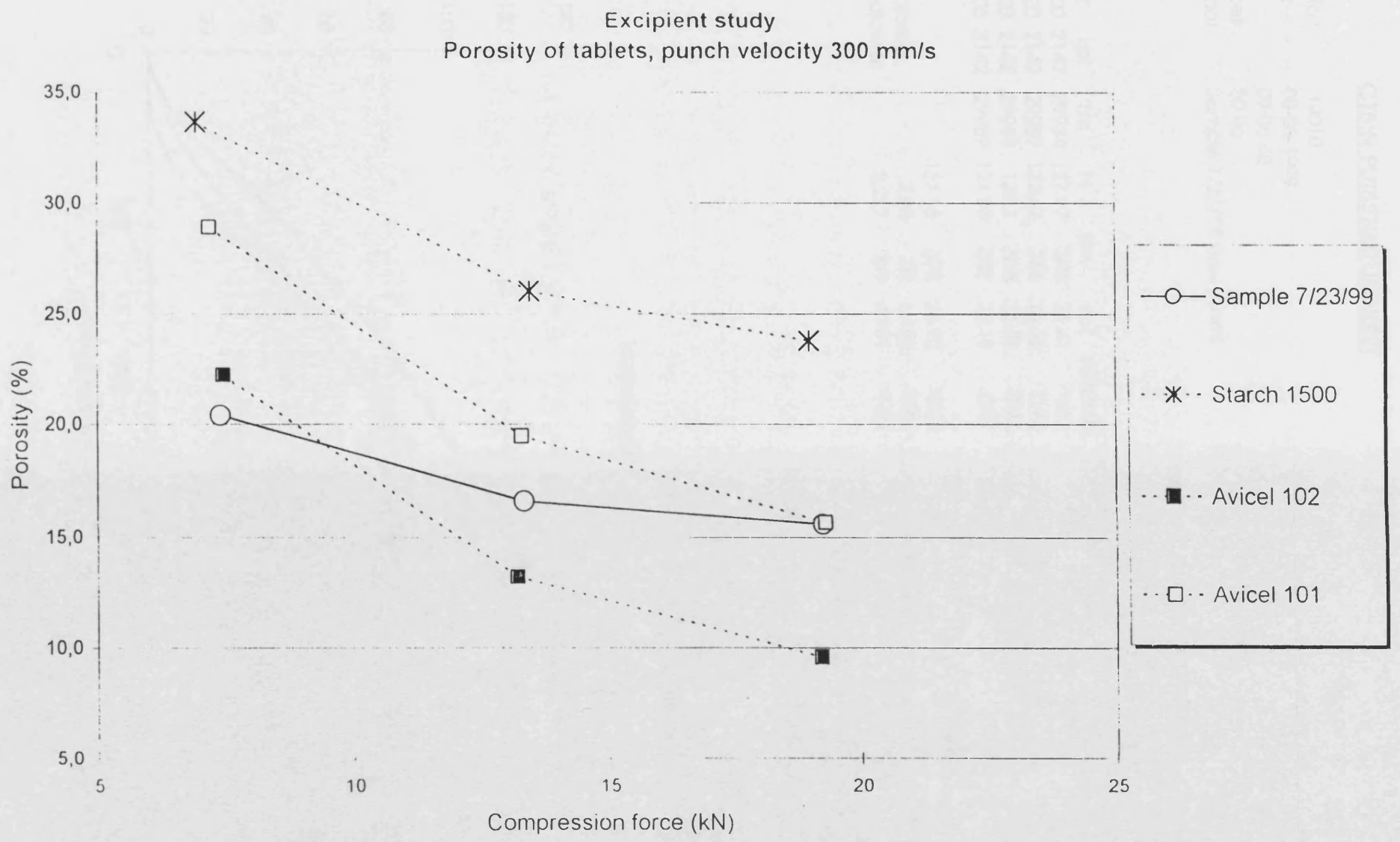

CT5:N PURISTUSTULOKSET

Tiedosto : 14010
Päivä : 08-05-1999
Aika : 09:06:48
Load cell : 50 kg
Lisätiedot : Sample 7/23/99 slow 13 kN

	Hz	kpl	ms	N	µm	mJ	mm/min
1	1000	2142	29934	127.17	343	23.41	0.84
2	1000	2142	29989	132.67	366	26.35	0.85
3	1000	2142	29989	127.1	393	25.79	0.85
4	1000	2142	29989	124.98	397	24.15	0.87
ka:				127.98	375	24.92	0.85
keskihajonta:				2.85	22	1.192	0.01
suht. hajonta:				2.227	5.9	4.781	1.02

Voimakäyrät

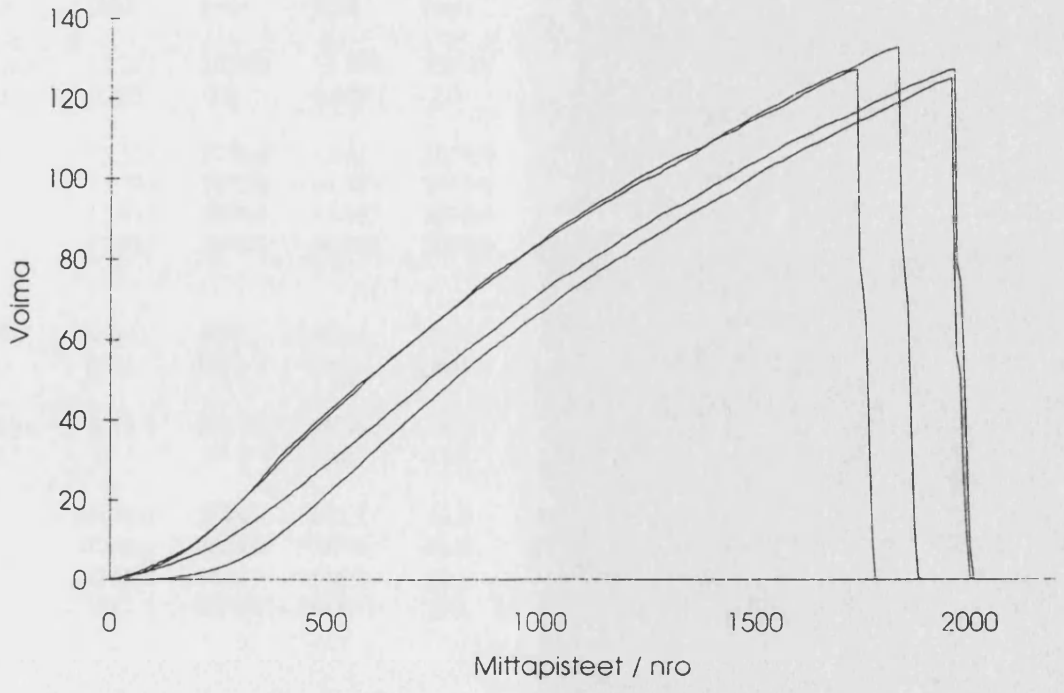

Compaction simulator statistical report:

Experiment	Person	ComTyp	MeasCyc	Date	Material
S9414008	Jilkka	single	4 ms	03.08.99	Sample_7/23/99 SLOW 7 kN

Tab No	Fupmax [kN]	FupmaxT [ms]	Flomax [kN]	FlomaxT [ms]	hmin [um]	hminT [ms]	Fejmax [kN]	FejmaxT [ms]	ConTime [ms]
mean	7.657	2072.0	6.237	2072.0	1287.2	2077.0	0.137	2869.0	334.0
std	0.248	0.0	0.227	0.0	2.4	2.0	0.025	62.7	2.3
1	7.404	2072.0	6.029	2072.0	1287.3	2076.0	0.099	2792.0	332.0
2	7.694	2072.0	6.319	2072.0	1283.8	2076.0	0.149	2892.0	332.0
3	7.984	2072.0	6.519	2072.0	1288.3	2080.0	0.149	2852.0	336.0
4	7.544	2072.0	6.079	2072.0	1289.5	2076.0	0.149	2940.0	336.0

Tab No	Wup [mJ]	Wlo [mJ]	Wexp [mJ]	Weje [mJ]	Wfri [mJ]	Wu [mJ]	Wnet [mJ]	Wanet [mJ]
mean	2345.2	1917.3	85.4	58.8	427.9	246.0	2013.8	1831.9
std	49.2	42.7	5.2	7.4	13.4	10.0	46.1	45.2
1	2284.5	1869.5	87.4	64.5	415.0	233.0	1964.1	1782.1
2	2351.3	1933.3	91.2	49.6	418.0	244.2	2015.9	1842.1
3	2404.4	1968.0	79.0	65.2	436.5	250.6	2074.8	1888.9
4	2340.7	1898.6	84.0	56.2	442.0	256.3	2000.4	1814.6

Compaction simulator statistical report:

Experiment	Person	ComTyp	MeasCyc	Date	Material
S9414010	Jilkka	single	4 ms	03.08.99	Sample 7/23/99 SLOW 13 kN

Tab No	Fupmax [kN]	FupmaxT [ms]	Flomax [kN]	FlomaxT [ms]	hmin [um]	hminT [ms]	Fejmax [kN]	FejmaxT [ms]	ConTime [ms]
mean	13.251	2074.0	11.249	2074.0	1202.6	2079.0	0.213	3464.0	381.0
std	0.402	2.3	0.305	2.3	2.8	2.0	0.101	622.1	3.8
1	13.321	2076.0	11.411	2076.0	1204.5	2080.0	0.361	4152.0	384.0
2	13.791	2072.0	11.581	2072.0	1205.4	2076.0	0.181	3812.0	380.0
3	12.911	2076.0	11.101	2076.0	1201.1	2080.0	0.181	3068.0	384.0
4	12.981	2072.0	10.901	2072.0	1199.5	2080.0	0.131	2824.0	376.0

Tab No	Wup [mJ]	Wlo [mJ]	Wexp [mJ]	Weje [mJ]	Wfri [mJ]	Wu [mJ]	Wnet [mJ]	Wanet [mJ]
mean	3195.4	2611.9	147.6	16.3	583.5	342.7	2705.1	2464.3
std	56.1	37.7	2.9	11.1	24.4	11.8	44.9	38.0
1	3179.0	2584.3	151.1	10.0	594.7	344.3	2683.7	2433.2
2	3276.4	2664.0	147.0	30.0	612.5	358.5	2770.9	2517.0
3	3178.8	2615.4	148.2	20.3	563.4	336.2	2694.4	2467.2
4	3147.2	2584.0	144.1	4.9	563.2	331.6	2671.5	2439.9

Compaction simulator statistical report:

Experiment	Person	ComTyp	MeasCyc	Date	Material
S9414004	Jllkka	single	0.1 ms	03.08.99	**Sample 7/23/99 FAST 13 kN**

Tab No	Fupmax [kN]	FupmaxT [ms]	Flomax [kN]	FlomaxT [ms]	hmin [um]	hminT [ms]	Fejmax [kN]	FejmaxT [ms]	ConTime [ms]
mean	13.344	35.8	11.619	35.9	1208.2	36.4	0.219	75.9	11.1
std	0.146	0.1	0.155	0.1	9.8	0.4	0.037	0.3	0.2
1	13.559	35.7	11.849	35.9	1218.3	36.8	0.219	76.3	11.3
2	13.309	35.8	11.559	35.9	1214.5	36.0	0.179	75.7	10.9
3	13.239	35.8	11.509	36.0	1197.8	36.1	0.209	75.6	11.1
4	13.269	35.7	11.559	35.9	1202.2	36.8	0.269	76.0	11.1

Tab No	Wup [mJ]	Wlo [mJ]	Wexp [mJ]	Weje [mJ]	Wfri [mJ]	Wu [mJ]	Wnet [mJ]	Wanet [mJ]
mean	3650.2	2899.9	224.0	128.6	750.3	433.4	2992.8	2675.9
std	63.4	40.3	55.3	32.2	23.6	16.7	18.3	26.4
1	3657.6	2908.8	263.4	99.0	748.8	423.6	2970.6	2645.4
2	3558.4	2840.5	146.3	108.5	717.9	421.6	2990.6	2694.3
3	3695.7	2924.2	222.8	136.4	771.5	457.7	3015.2	2701.4
4	3689.3	2926.1	263.6	170.8	763.2	430.8	2994.9	2662.5

Compaction simulator statistical report:

Experiment	Person	ComTyp	MeasCyc	Date	Material
S9414006	Jllkka	single	0.1 ms	03.08.99	**Sample 7/23/99 FAST 19 kN**

Tab No	Fupmax [kN]	FupmaxT [ms]	Flomax [kN]	FlomaxT [ms]	hmin [um]	hminT [ms]	Fejmax [kN]	FejmaxT [ms]	ConTime [ms]
mean	19.253	35.9	18.327	36.1	1168.2	36.2	0.347	78.3	13.3
std	0.115	0.2	0.202	0.1	4.3	0.1	0.026	0.3	0.1
1	19.395	36.1	18.557	36.3	1173.6	36.3	0.317	78.7	13.3
2	19.295	35.8	18.367	36.0	1163.7	36.0	0.357	78.1	13.3
3	19.175	35.6	18.317	36.1	1169.3	36.2	0.337	78.2	13.3
4	19.145	35.9	18.067	36.1	1166.2	36.1	0.377	78.1	13.2

Tab No	Wup [mJ]	Wlo [mJ]	Wexp [mJ]	Weje [mJ]	Wfri [mJ]	Wu [mJ]	Wnet [mJ]	Wanet [mJ]
mean	4316.6	3389.9	532.5	216.2	926.7	511.7	3272.4	2857.4
std	60.4	91.5	37.1	14.0	42.9	17.5	72.0	101.1
1	4346.7	3480.2	492.6	236.8	866.4	486.7	3367.3	2987.6
2	4335.9	3408.3	539.6	206.6	927.6	518.4	3277.8	2868.6
3	4357.1	3408.7	580.1	208.4	948.4	527.3	3249.7	2828.6
4	4226.9	3262.4	517.8	212.8	964.5	514.2	3194.8	2744.5

Table 2. Physical parameters obtained from tableting studies.

Sample	velo (mm/s)	Fup (kN)	DBF (N)	DBW (mJ)	TS (MPa)	Poro (%)	El.rec. (%)	hmin (µm)	heje (µm)	diam (µm)	m (g)	Wnet (mJ)
7/23/99	4	7,66	79	10,72	3,39	17,91	15,54	1287	1487	9981	0,1425	2014
	4	13,25	128	24,92	5,86	11,66	16,04	1203	1396	9965	0,1435	2464
	4	18,75	138,4	27,7	6,41	10,72	17,56	1173	1379	9963	0,1432	2959
	300	7,41	60,8	6,82	2,52	20,39	19,00	1295	1541	9984	0,1433	2231
	300	13,34	95,5	15,77	4,14	16,62	21,85	1208	1472	9968	0,1429	2993
	300	19,25	114,1	20,66	5,00	15,60	25,00	1168	1460	9955	0,1431	3272

Abbreviations:

Velocity:	punch velocity in mm/s
Force:	peak upper punch force in kN
DBF:	diametral breaking force of tablets in N
DBW:	diametral breaking work of tablets in mJ
TS:	tensile strength of tablets in Mpa
Poro:	porosity of compacts after ejection in %
El.Rec:	elastic recovery of tablets in %
hmin:	minimum height of compacts under compression in µm
heje:	height of compacts after ejection in µm
diam:	diameter of compacts after ejection in µm
m:	weight of compacts in g
Wnet:	net compression work in mJ

APPENDIX 2

GC/MS ANALYSIS OF STARCH 1500 AND NATIVE MAIZE STARCH EXTRACTS

Appendix 2: GC/MS analysis of Starch 1500 and native maize starch extracts

Solvent System	Compounds identified	Match(%)
DF48-Me-01 (U)	Hexadecanoic Acid, methyl ester	97
	9,12 Octadecadienoic acid, methyl ester	99
DF48-Me-02	Hexadecanoic Acid, methyl ester	83
	Hexadecanoic Acid	74
	9,12 Octadecadienoic acid, methyl ester	91
	9,12 Octadecadienoic acid	91
DF48-99-01 (M)	Hexadecanoic Acid, methyl ester	95
	Hexadecanoic Acid, ethyl ester	99
	Octadecanoic Acid, methyl ester	99
	9,15 Octadecadienoic acid, methyl ester	99
	9,12 Octadecadienoic acid, ethyl ester	98
	Octadecanoic Acid, ethyl ester	98
DF48-99-01 (U)	Hexadecanoic Acid, ethyl ester	95
	9, Octadecenoic acid, ethyl ester	95
	Octadecanoic Acid, ethyl ester	95
DF48-99-02 (M)	Pentadecanoic acid, 14-methyl ester	98
	Hexadecanoic Acid, ethyl ester	96
	10,13 Octadecadienoic acid, methyl ester	99
	9,12 Octadecadienoic acid, methyl ester	99
	9,12 Octadecadienoic acid, ethyl ester	99
DF48-99-03 (M)	Hexadecanoic Acid, methyl ester	53
	Hexadecanoic Acid, ethyl ester	53
DF48-96-03 (M)	Hexadecanoic Acid, methyl ester	97
	9, 12 Octadecadienoic acid, methyl ester	99
DF48-96-01A	Hexadecanoic Acid	83
	9,12 Octadecadienoic acid, methyl ester	93
	9,12 Octadecadienoic acid	87
DF48-96-02A	Hexadecanoic Acid	74
	9, Octadecenoic acid, methyl ester	86
	9,12 Octadecadienoic acid, methyl ester	91
DF48-85-01 (M)	Hexadecanoic Acid, methyl ester	99
	9,12 Octadecadienoic acid, methyl ester	91
	Octadecanoic Acid, methyl ester	90
DF48-70-01 (M)	Hexadecanoic Acid, methyl ester	93
DF48-60-01 (M)	9,12 Octadecadienoic acid, methyl ester	87
	Tetradecanoic acid, methyl ester	94

APPENDIX 3

UNMODIFIED STARCH 1500 PARTICLE SIZE ANALYSIS DATA

Appendix 3: Unmodified Starch 1500 partcle size analysis data

Range 145 - 200μm

S1500 (1)	S1500 (2)	S1500 (3)	S1500 (4)	S1500 (5)
0.172	0	0.3778	0.1419	0
0	0.1306	0.1614	0	0
0.1007	0	0	0.1561	0
0.4156	0.1293	0.0769	0.2496	0.0133
0	2.1444	0.1658	0	0.1217

Range 90.2 - 145μm

S1500 (1)	S1500 (2)	S1500 (3)	S1500 (4)	S1500 (5)
21.4324	0.0956	25.4734	20.0752	9.7293
1.3816	17.9555	21.1191	0.0822	10.2885
18.6126	1.5354	8.9195	20.4518	6.1468
23.4946	20.4889	18.2064	21.8795	10.9277
10.4454	33.2686	20.6982	8.2147	18.8028

Range 70.2 - 90.2μm

S1500 (1)	S1500 (2)	S1500 (3)	S1500 (4)	S1500 (5)
20.0862	5.8944	20.3352	20.3262	15.0882
10.8228	16.956	19.0156	6.0223	13.5122
19.9594	12.0966	17.2183	15.6882	15.0785
16.9782	19.4181	18.559	20.3527	16.6909
17.3556	18.099	20.419	14.6906	16.7195

Range 50.1 - 70.2μm

S1500 (1)	S1500 (2)	S1500 (3)	S1500 (4)	S1500 (5)
21.961	16.4187	20.0522	22.917	17.3712
20.5237	19.6969	20.763	23.451	15.4595
23.025	21.878	22.664	16.0446	20.5098
17.8191	21.903	19.7492	22.352	20.85
22.952	16.7069	21.85	19.4307	18.1983

Range 20 - 50.1μm

S1500 (1)	S1500 (2)	S1500 (3)	S1500 (4)	S1500 (5)
23.3099	40.8553	20.6985	23.4598	31.3094
39.0373	26.4038	25.3869	43.4747	32.3185
25.8572	38.2268	32.8622	27.2135	33.084
25.6305	23.8205	25.8482	22.5082	30.8053
36.0339	18.7431	23.2141	36.2924	29.8905

Range 0.5 - 20μm

S1500 (1)	S1500 (2)	S1500 (3)	S1500 (4)	S1500 (5)
13.0388	36.735	13.0621	13.0794	26.5021
28.234	18.8526	13.5538	26.9703	28.4211
12.4408	26.2631	18.3356	20.7668	25.1757
15.6617	14.2403	17.543	12.6002	17.6698
13.2135	11.0379	13.652	21.3717	16.2669

APPENDIX 4

DEFATTED STARCH 1500 PARTICLE SIZE ANALYSIS DATA

Appendix 4: Defatted Starch 1500 partcle size analysis data

Range 145 - 200μm

DF48-Me-02	DF48-96-03	DF48-96-01	DF48-60-01	DF48-Pr-02	DF48-Bu-01	DF48-He-03
0	0	0	0	0	0	0
0	0	0	0	0	0	0
0	0	0	0	0	0	0
0	0	0	0	0	0	0
0	0	0	0	0	0	0

Range 90.2 - 145μm

DF48-Me-02	DF48-96-03	DF48-96-01	DF48-60-01	DF48-Pr-02	DF48-Bu-01	DF48-He-03
7.0866	12.8654	23.6345	17.2253	6.6555	12.5229	3.2574
13.9833	7.531	19.4539	15.5036	9.5651	12.3143	3.5151
18.5469	6.4324	15.6971	11.8308	16.8572	11.9462	1.1463
15.672	1.4609	6.0192	12.8641	21.5572	11.0363	0
21.6823	13.5662	6.1569	24.0613	13.3643	7.9511	24.0819

Range 70.2 - 90.2μm

DF48-Me-02	DF48-96-03	DF48-96-01	DF48-60-01	DF48-Pr-02	DF48-Bu-01	DF48-He-03
17.6521	19.5859	22.771	21.623	16.891	18.3716	13.2145
20.3552	18.5968	22.422	20.1062	17.4907	19.4405	14.0811
21.3413	16.272	21.3862	19.3112	21.636	18.7569	11.6085
20.8982	12.762	17.2845	21.4233	22.646	20.0121	10.9726
21.701	19.2882	17.86622	19.6463	18.7939	16.4894	21.527

Range 50.1 - 70.2μm

DF48-Me-02	DF48-96-03	DF48-96-01	DF48-60-01	DF48-Pr-02	DF48-Bu-01	DF48-He-03
21.8832	24.053	23.623	23.087	24.68	21.879	19.6434
22.926	25.069	26.074	23.304	22.047	22.776	20.4563
23.859	21.962	26.542	22.66	25.716	24.931	18.986
23.418	20.3338	25.925	23.806	25.425	25.097	20.152
22.621	22.878	23.922	19.6502	20.552	23.527	19.7164

Range 20 - 50.1μm

DF48-Me-02	DF48-96-03	DF48-96-01	DF48-60-01	DF48-Pr-02	DF48-Bu-01	DF48-He-03
30.5072	26.7315	21.5797	27.3877	36.0065	28.5756	37.6172
27.0582	29.7604	24.7084	27.3595	34.4104	27.6988	35.36
25.0902	31.1972	27.7951	30.3807	26.1549	28.9199	38.6003
26.877	35.371	35.3308	27.983	22.1492	30.8786	40.7239
23.9635	25.7045	33.8618	24.9576	32.9922	35.7454	21.9421

Range 0.5 - 20μm

DF48-Me-02	DF48-96-03	DF48-96-01	DF48-60-01	DF48-Pr-02	DF48-Bu-01	DF48-He-03
22.8752	16.7644	8.3927	10.6768	15.7674	18.6511	26.2671
15.6766	18.9811	7.342	13.7264	16.4875	17.7704	26.5872
11.1632	24.136	8.5795	15.8178	9.6352	15.446	29.6587
13.1359	30.1623	15.134	13.923	8.2226	12.9756	28.1518
10.0311	16.5629	18.1924	11.6842	14.2967	16.2872	12.7332